ENGINEERING RESEARCH INSTITUTE
UNIVERSITY OF MICHIGAN
ANN ARBOR

THEORETICAL STUDY, DESIGN AND CONSTRUCTION OF C-W MAGNETRONS FOR FREQUENCY MODULATION

FINAL REPORT

Technical Report No. 3
Electron Tube Laboratory
Department of Electrical Engineering

BY

H. W. WELCH, JR.

J. R. BLACK

G. R. BREWER

G. HOK

Approved By:

W. G. Dow

Project M694

For

CONTRACT NO. W-36-039 sc-32245
SIGNAL CORPS, DEPARTMENT OF THE ARMY
DEPARTMENT OF ARMY PROJECT NO. 399-13-022
SIGNAL CORPS PROJECT NO. 112B-0

May 27, 1949

TABLE OF CONTENTS

PERSONNEL OF UNIVERSITY OF MICHIGAN ELECTRON TUBE LABORATORY

Name	Title	Approximate Time with Project	
Scientific and Engineering Personnel			
*W. G. Dow	Professor of Electrical Engineering	35 months	Supervisor
*H. W. Welch	Research Physicist	35	Full time
*J. R. Black	Research Engineer	29	Full time
*G. Hok	Research Engineer	17	1/4 time
*G. R. Brewer	Research Assistant	16	1/2 time
R. S. Buritz	Research Engineer	12	Full time
R. K. Brown	Research Engineer	13	1/2 time
R. Callahan	Research Associate	12	1/2 time
C. K. Birdsall	Research Assistant	4	1/4 time
L. W. Holmboe	Research Engineer	6	1/3 time
H. C. Early	Research Engineer	2	Full time
Service Personnel			
*V. R. Burris	Machine Shop Foreman	25	Full time
*R. F. Steiner	Assembly Technician	19	Full time
*Jane Merithew	Draftsman	31	3/4 time
*D. L. McCormick	Instrument Maker	4	1/4 time
*E. A. Kayser	Instrument Maker	2	1/4 time
*T. J. Keith	Instrument Maker	1	1/4 time
*J. Mossar	Technician	6	1/4 time
*S. Spiegelman	Secretary	5	1/4 time
C. F. Crable	Technician	12	1/3 time
N. H. Brown	Technician	4	Full time
F. R. Arams	Technician	5	1/4 time
G. F. Knowles	Machinist	5	1/5 time
G. Sabadash	Machinist	13	1/2 time
R. Spooner	Secretary	9	1/4 time
M. Wisusik	Secretary	13	1/4 time
Others		12	1/2 time or less

* Starred personnel are the present staff of the electron tube laboratory.

ABSTRACT

The problems involved in frequency modulation of magnetrons by means of the magnetron type space charge swarm have been investigated. The technique of making impedance measurements on hot magnetrons has been used extensively. Experimental results agree very well with the theoretical analysis. This work, which is summarized in the present report, has been discussed in detail in Technical Report No. 1 issued by the project entitled "Space-Charge Effects and Frequency Characteristics of C-W Magnetrons Relative to the Problem of Frequency Modulation."

The interdigital magnetron has been used as a basic structure for the development of frequency modulation magnetrons in this laboratory. Operation in the zero order mode is desired. Technical Report No. 2 entitled "Operation of Interdigital Magnetrons in the Zero Order Mode" discussed in detail principles of design and resulting performance of tubes of several basically different designs constructed in this laboratory. This work is summarized in the present report. The techniques used in construction of interdigital tubes are described in considerable detail.

Three frequency modulation magnetron designs have been studied. Preliminary tests have been made on an oscillating model of one of these designs. The results of this development are not complete, but are presented in their present form.

A general outline of the procedure used and the facilities of the laboratory are discussed. The principles of tubes, based on the interdigital principle, which might be applicable to magnetron amplifier, signal generators and high power magnetrons, are given brief attention. Suggestions are offered for the direction to be taken in future research in this field. Complete drawings for one model and assembly drawings of all tubes designed in this laboratory are given.

ACKNOWLEDGMENTS

The frequent contacts with representatives of Evans Signal Laboratory have been very valuable to the personnel of the Electron Tube Laboratory. Special thanks should be given to Dr. J. E. Gorham, Mr. G. R. Kilgore, Mr. J. F. Hull and Mr. Phillip Cohen.

The work of the project is continuing under Contract No. W-36-039 sc-35561.

THEORETICAL STUDY, DESIGN AND CONSTRUCTION OF C-W MAGNETRONS FOR FREQUENCY MODULATION

FINAL REPORT

I. INTRODUCTION

1. Purpose

The purpose of this report is to summarize the progress in the University of Michigan Electron Tube Laboratory during the period from July 1, 1946 through April 30, 1949, on Contract No. W-36-039 sc-32245 for the Signal Corps. This contract stipulates that the program of work should consist essentially of two parts as follows:

Part 1. A study of problems involved in the development of r-f tubes and associated r-f circuits for communication equipment, the requirements of which are, in general, outlined in the following paragraph. The results of this study are to be reported to the Signal Corps, listing the problems involved and suggesting steps to be taken in further research.

The technical and operational characteristics to be used as a basis for the above work are as outlined below:

> a. Carrier Frequency Range and Stability. The equipment shall require one r-f oscillator tube for both transmitter and receiver which shall be tunable for at least the range from 2000 to 2400 megacycles. The frequency stability with respect to all phenomenon tending to shift frequency shall be comparable with that of the most stable cavity which may be possible without unduly complicating the size and weight of the equipment. The temperature range to be covered will be -40° centigrade to +60° centigrade.

b. Modulation. The type of modulation utilized in the equipment shall be frequency modulation which is sufficiently wide and linear to accommodate the intelligence modulation band of 0 to 5 megacycles with distortion of all types as small as possible. (These distortion products shall be in the order of one-tenth of one per cent or less for at least the first one-half megacycle of the intelligence band).

c. Operation. The transmitter power output shall be sufficient to provide signal-to-noise ratios in the order of 50 to 80 db in the receiver when operating over a line-of-sight transmission path 50 miles long. Sufficient margin for propagation difficulties shall be included in this power output. (This margin may be in the order of 30 to 50 db.) All vacuum tubes shall be capable of at least 1000 hours of operation.

d. System Requirements. The resulting equipment shall be as simple and light-weight as possible, as well as very efficient in respect to power consumption. The antenna radiating and receiving apparatus shall be capable of being mounted on a sectional mast which shall have a total height of at least 50 feet. This antenna system shall have provision for connection with the transmitting and receiving equipment at the base and shall allow full duplex operation (4-wire circuit with discrimination between transmitted and received signals of the order of 70 db) with the simplest antenna system possible (the antenna apparatus shall not exceed in complexity a three- to four-inch diameter sectional mast and one forty-eight-inch diameter reflector, or equivalent, except for diversity reception facilities). Diversity reception facilities preferably utilizing some form of radio carrier frequency mixing shall be included in the equipment.

Part 2. Basic research on tube and correlated circuit problems.

The basic findings resulting from investigations under Part 1 are to serve as a guide in the choice of problems.

Initial objectives of the Tube Research program are to be:

a. Achievement of a more satisfactory understanding of the nature and causes of frequency pushing in magnetron oscillators.

b. Attainment of means for controlling the frequency of magnetrons by building them with amplifier properties to permit the frequency to be controlled by external low power stable frequency sources.

Initial objectives of the Circuit Research program are to be:

a. Study of existing magnetrons by making "hot impedance measurements" whereby the r-f impedance of the tube is measured as a function of d-c voltage (cathode heated and the applied d-c voltage too low to initiate oscillation).

b. Devising of a working combination of magnetron power tubes, magnetron or other reactance tubes, and monitoring tubes susceptible of either frequency or amplitude modulation at a frequency stability suitable for communicating purposes.

The actual procedure which has been followed in conducting this research is outlined in detail in Section 2 which follows. The program has been essentially within tne limits outlined above, conditioned partly by the findings resulting from study of existing knowledge of the subject and partly by the desire to maximize in usefulness the capabilities of personnel, equipment and funds available to the project. In order to limit the scope of research the program has been limited to include primarily problems pertaining to frequency modulation and frequency control of magnetrons. The choice of a magnetron-type oscillator as a prime source of power is based on the belief of the University of Michigan research staff that it has greater possibilities of maximum efficiency than other microwave devices, that there is probably more room for new ideas based on the magnetron principle, and that the Michigan research staff is better qualified to work with magnetrons than other microwave tubes. This thought was, of course, more or less in mind at the instigation of the project.

Magnetrons constructed for use in research have been entirely of the interdigital type. This emphasis has been partly based on belief that the interdigital magnetron holds more possibility of an incorporated frequency modulation and control system and partly because there is more opportunity and more need for improvement of this type magnetron than with vane magnetrons or

with split anode magnetrons. The conditions which must be placed upon the resonant circuit and interaction space design of interdigital magnetrons to favor operation in the zero order mode have been studied in considerable detail. Several tubes have been built. The best performance observed to date is 500 watts output at 75 per cent efficiency.

An electronic system of modulation is necessary for the obvious reason that the desired modulation band is five megacycles. Any other type of system would have excessive inertia. Emphasis has been upon the placement of an electronic modulating reactance directly within the oscillator resonant circuit. This is as opposed to the system in which a separate reactance tube is coupled to the oscillator structure.

Electron beam type of reactance modulation using the cyclotron resonance has been investigated by other laboratories in various types of magnetrons. Use of properties of the magnetron type space charge cloud of cylindrical geometry has, on the other hand, been more or less limited to split anode structures and load impedance modulation devices. The interdigital magnetron, because of the cylindrical geometry of its resonant circuit, is particularly adaptable to use with space charge reactance of cylindrical geometry. The properties of this type of space charge have been studied in this laboratory by making impedance measurements on conventional magnetrons in which a space charge cloud is present. The voltage applied to the magnetron is kept less than the value necessary to support oscillation. The effect of variation in voltage and magnetic field on resonant wavelength and unloaded Q of the magnetron is observed. These effects are related by theoretical analysis to properties of the space charge. A basic understanding of the space charge cloud is thus obtained, making possible intelligent

design of magnetrons for frequency modulation incorporating such a scheme for changing reactance.

Frequency stabilization of a frequency modulated prime source of power (as opposed to a low level source with amplifier) necessarily involves a monitoring system with a stable reference. The resonant circuit of the prime source cannot have a high loaded Q since low Q, of the order of 100 in this case, is required to allow frequency modulation. If electronic frequency control is furnished on the prime source (as is certainly the case if frequency modulation is possible) the problem of stabilization by a monitoring system is one of associated circuitry which has been proven practical in several instances.

The laboratory facilities for construction and testing of magnetrons have been built up to a point where the facilities compare very favorably with other experimental electron tube laboratories in this country. This has been accomplished as much as possible with the aid of University funds, equipment and facilities.

Much of the theoretical and experimental work has been carried on more or less simultaneously, depending upon the availability of time and equipment. In the following pages, an attempt is made to summarize the material logically, separating theory from experiment. The most important results having to do with frequency characteristics of c-w magnetrons and with design of interdigital magnetrons for operation in the zero order mode are discussed in detail in two separate technical reports.(1) The first of

---

(1) Technical Report No. 1, "Space-Charge Effects and Frequency Characteristics of C-W Magnetrons Relative to the Problem of Frequency Modulation", H. W. Welch.

Technical Report No. 2, "Operation of Interdigital Magnetrons in the Zero Order Cavity Mode", H. W. Welch and G. R. Brewer.

these was published in November, 1948. The second appears concurrently with the present report.

The principles discussed in these reports have been applied to the design of two frequency modulation magnetrons. Initial magnetron performance tests have been made on one of these, but no data on electronic frequency control have been obtained at the writing of this report.

The work of this project is continuing under a new contract, No. W-36-039 sc-35561, so some of the material presented herein pertains to unfinished developments.

2. Outline of Procedure

In a research project of any magnitude and time duration, several more or less independent activities must be carried on simultaneously with occasional concentrated effort on one activity or the other. The purpose of this section is to outline in a general way the procedure used in approaching the problems defined for the project.

a. Survey of Existing Knowledge Pertaining to the Problem: The first step in this phase of the activity was to estimate on the basis of the technical and operational characteristics mentioned in Section I the approximate specifications of a magnetron which would be suitable to use with the equipment. This being done, a survey of available literature in the form of wartime government reports, magazine articles, and other postwar publications was made with emphasis on papers related to design problems in c-w magnetrons and theoretical and experimental analysis of frequency modulation of magnetrons. A fairly complete bibliography of references was given in Technical Report No. 1. Several laboratories working on similar problems were visited and arrangements made to obtain recent progress reports. Through these

reports and subsequent personal contacts with engineers from other laboratories, knowledge of current developments was kept up to date.

b. Construction and Improvement of Laboratory Facilities: This activity includes the building up of a satisfactory machine shop, assembly equipment, and microwave test facilities. A lack of space in the initial location of the laboratory delayed the installation of part of the machine shop and brazing equipment until late 1947. During this period the facilities of the Physics Department machine shop were used and all brazing was done in a hydrogen bottle. Most of the microwave test equipment was constructed in the Michigan Laboratory because of the unavailability at the outset of the project of commercially manufactured equipment in the desired frequency range. War surplus equipment was obtained where possible. After installation in the new Electrical Engineering Building in late 1947, the time spent on improvement of laboratory facilities was very small.

c. Theoretical and Experimental Analysis of Resonant Circuit Geometries Applicable to Interdigital and Frequency Modulation Magnetrons: In order to provide immediate familiarity with the various modes possible in the interdigital magnetron, demountable brass models approximating the structure to be used were built and subjected to extensive measurements before final designs for operable tubes were settled upon. A simplified theory of the zero order mode was developed. This study included an analysis of the effect of the cathode circuit upon performance which was more detailed than any previous work on this subject. As a result, several possible schemes for frequency modulation suggested themselves. Brass models were built to test experimentally some of the principles involved, and two of these were subsequently used as the basis for design of frequency modulation magnetrons.

d. Theoretical and Experimental Study of Characteristics of Magnetron Space Charge: The emphasis in this activity was on study of effects on frequency. In order to accelerate the program, initial measurements were conducted on 10 cm commercially available c-w magnetrons. Most of the effort was aimed toward an improved understanding of effects of magnetron space charge in a non-oscillating structure. Theory was developed to explain quantitatively hot impedance measurements of this type. This theory was applied to the results of experiments made on tubes built in this laboratory, with good agreement at low r-f voltage. High r-f voltage measurements and measurements on oscillating magnetrons were subject only to explanation which was partially quantitative and partially qualitative. The results of all of this work were discussed in Technical Report No. 1.

e. Design and Construction of Magnetrons to be Used for Research: Three basically different interdigital magnetrons were designed on the basis of the survey of existing knowledge and analysis of the r-f circuit. These tubes served several purposes; as subjects of research on space charge characteristics, as a check on scaling and resonant circuit theory, as a guide in developing construction techniques, and as basis for subsequently designed frequency modulation magnetrons. Two basically different frequency modulation magnetrons were designed. The study of the performance of these tubes will be the subject of future activity.

3. Limiting Specifications

In order to get an idea of the general electronic properties of a tube which would fit into a system as described in the technical objectives of the contract, an estimate has been made of the power output which will be necessary. Using this figure, one can approximate the various voltages,

currents, etc., which determine the nature of the equipment to be built around the tube, for test as well as use purposes.

The power output needed is determined by the following factors:

a. Distance between transmitter and receiver
b. Assumptions made about the transmission characteristics of the path between transmitter and receiver
c. Type of antennas used
d. Signal-to-noise ratio desired in the receiver
e. Practical limitations on size and weight of equipment

It will be seen that a compromise is necessary between the third and last requirements and the other three.

The calculations are made assuming figures for antenna gain distance noise level, etc., commensurate with the figures listed in the technical objectives and other known limitations.

The initial assumptions are:

a. 20 mc bandwidth f-m receiver, 5 mc band out of second detector at 50 db signal-to-noise ratio.
b. 50-mile transmission path.
c. antenna 5 feet in diameter.(1)
d. 6 db transmission margin in r-f systems of transmitter and receiver.
e. no margin over "free space" transmission.
f. frequency about 2000 megacycles.

The receiver input noise is assumed to be 12 db above the theoretical minimum. The resulting noise power present at the receiver input is found to be

Noise power present at receiver input = 132×10^{-14} watts

In order for peak signal amplitudes to equal peak noise amplitudes the signal power must be a factor of 10 greater than the noise power. Threshold is defined as where the peak signal amplitude is equal to twice the maximum

---

(1) Recommended antenna size was increased after initial calculations indicated that power requirements were near to marginal values.

peak noise amplitude. The threshold power is proportional to the square of the amplitude. Therefore:

$$\text{Required input signal at threshold for f-m} = (2)^2 \times 132 \times 10^{-13}$$
$$= 528 \times 10^{-13} \text{ watts.}$$

After taking into account the noise reduction factor due to an f-m detector the resulting signal-to-noise ratio at threshold, for an f-m receiver

$$\frac{\text{Signal}}{\text{Noise f-m}} = 25.8 \text{ db}$$

All calculations leading to the above mentioned figures are based on the method outlined by Murray G. Crosby.(1)

The desired signal-to-noise ratio is 50 db. Thus, an additional 24.2 db or 263 times threshold power is required. Therefore:

$$\text{Power required at receiver input for 50 db signal-to-noise ratio} =$$
$$= 263 \times 528 \times 10^{-13}$$
$$= 13.9 \times 10^{-9} \text{ watts.}$$

6 db power loss is allowed for design compromises in the receiver and 3 db loss in the receiver r-f transmission circuit. Therefore:

$$\text{Power delivered by receiving antenna for 50 db signal-to-noise ratio} =$$
$$= 8 \times 13.9 \times 10^{-9}$$
$$= 111 \times 10^{-9} \text{ watts.}$$

Assuming parabolas 5 feet (1.52 meters) in diameter (D) at both receiver and transmitter, λ = .146 meters and path length, L, of 50 miles,

---

(1) Crosby, Murray G., "Frequency Modulation Noise Characteristics", Proc. IRE, April 1937.

Ratio of transmitted to received power

$$\frac{P_T}{P_r} = \frac{2.8\,\lambda^2 L^2}{D^4}$$

$$= 7.2 \times 10^{11}$$

Power delivered to the transmitting antenna is, therefore,

$$P_T = 7.2 \times 10^{11} \times 1.11 \times 10^{-11}$$

$$\cong 8 \text{ watts.}$$

A 3 db loss is assumed in the transmitter r-f transmission circuit. Power delivered by the transmitting tube is 16 watts for free space transmission at 50 miles.

Received field strengths at microwave frequencies may be expected to be subject to fades up to a maximum of about 30 db below free space values; it is therefore desirable to provide a transmitting tube with a power output in excess of that required for free space transmission. If a 30 db margin is assumed, this makes the power requirement 16,000 watts, an impractical value for a system as "simple and light-weight as possible", as specified in the system requirements.

500 watts is considered a practical tube power output suitable for use in the system desired. For a tube power output of 500 watts

Excess power available over free space requirement

= 500/16 = 31.2 or 14.9 db.

A total of 12 db loss was assumed for design compromises and r-f transmission loss. Therefore, the maximum possible transmission margin over free space requirements for a 500-watt tube would be 15 + 12 or 27 db.

Based on this result and consideration of other conditions imposed by the system requirements, the following desirable properties are tentatively

set up for magnetrons designed by the Michigan Laboratory.

a. Frequency, tunable from 2000 to 2400 mc
b. Approximate power output, 500 watts
c. Frequency modulatable, 5 megacycle rate; 10 megacycle deviation from center frequency
d. Minimum amplitude modulation
e. Frequency stability, .01 per cent after 5 minute warm-up period for 4 hours operation
f. Plate voltage, 2000 to 3000
g. Plate current, .5 ampere to 1 ampere
h. Cooling: air

Boundary specifications for the proposed magnetron are given in Table 1. These values are not to be taken as a range for a particular tube, but satisfactory tubes are expected to fall within the ranges given.

TABLE 1

Boundary Tube Specifications

Filament voltage	6-15 volts
Filament current	10-20 amperes
Frequency range	2000-2400 mc
Typical Operation	
Filament voltage	6-15 volts or less
Anode voltage	2000-3000 volts
Anode current	.4-.6 amperes
Power output	300-700 watts
Efficiency	40-60 per cent
Maximum Ratings	
Peak anode current	1.2-1.8 amperes
Average anode current	.5-.7 amperes
Anode dissipation	400-800 watts
Cooling*	Forced air

* Note: Tubes built for experimental purposes are all water-cooled for simplicity in structure.

II. BASIC THEORY

4. Characteristics of Magnetron Space Charge

The analysis of magnetron space charge has been given in detail in Technical Report No. 1, Sections 5 and 6. The results will be summarized here. Two types of properties are studied; these are:

Type 1. Properties having to do with the distribution of angular velocity, field, potential and charge density and definition of the space charge boundary.

Type 2. Properties having to do with the propagation of electromagnetic waves in the space charge distribution so defined.

The properties of the first type are analyzed for two important cases.

Case I. This case concerns space charge as it is assumed to exist in a non-oscillating or static magnetron. In this case, a steady state condition is assumed in which the electrons have no initial radial velocity and no radial velocity throughout the space charge cloud (i.e., no radial currents). Individual electrons follow, therefore, circular trajectories around the cathode. The angular velocity, field, potential and charge density are functions of radius. The resulting picture is a rotating cylinder of space charge with different layers of the cylinder traveling at different velocities and having different densities.

Case II. This case concerns space charge as it is assumed to exist under conditions where all electrons in the region considered are moving around the interaction space of the magnetron synchronous with an angular velocity determined by properties of the magnetron resonant circuit. This angular velocity in the case of the fundamental mode of oscillation of the magnetron is given by

$$\omega_n = \frac{\omega_o}{n} \tag{1}$$

$\omega_o = 2\pi f_o = 2\pi$ resonant frequency of magnetron

$n = \frac{N}{2} = \frac{1}{2}$ number of anode segments in the magnetron

Space charge of this type, called synchronous space charge, exists if two conditions are satisfied. An r-f voltage of the proper frequency must be imposed upon the magnetron anodes; and the d-c potential on the magnetron must be high enough that the outermost electrons of the static magnetron space charge (Case I) shall have attained at least synchronous velocities. Electrons which tend to revolve at higher velocities will be slowed to synchronism by the r-f field in regions where they tend to go against the field, moving outward until the energy abstracted from the d-c field just balances that given to the r-f field. In regions where they tend to take energy from the r-f field, the electrons are accelerated and sent inward by the action of the steady magnetic field. Thus, synchronous magnetron space charge tends to form in spokes outside a region of static magnetron space charge.

A sketch showing these two types of space charge as they might appear is given in Figure 4.1. Analysis shows that the condition for which electrons in the spokes can just reach the anode is just the condition defined by Hartree for initiation of magnetron-type oscillation. The analysis also shows that the density of the static magnetron space charge is considerably greater than the density of the synchronous magnetron space charge. The ratio of densities might be of the order of 2 to 1 to 10 to 1 in typical magnetrons.

Other results defining the various distributions, voltages for which space charge reaches the anode for the two cases, voltage for which outermost

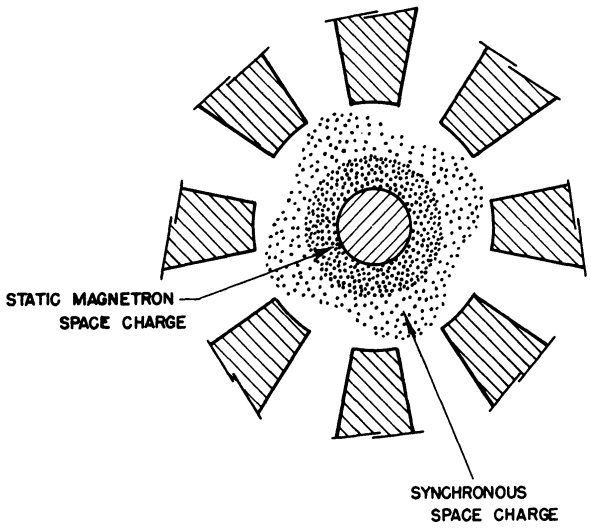

FIG. 4.1
PICTORIAL REPRESENTATION OF SPACE CHARGE WITHIN INTERACTION SPACE.

electrons in the static magnetron space charge reach synchronism, and boundary of static space charge as a function of anode potential and magnetic field are presented graphically in Technical Report No. 1. Curves are plotted in dimensionless variables. Some of these, showing distributions in the two types of space charge, are shown in Figure 4.2. The validity of some of the theoretical results is borne out by results of experiments described briefly in Section 12 of the present report.

Properties of the Type 2, that is properties having to do with the propagation of electromagnetic waves in the space charge distribution, are of great importance to understanding of the problems of frequency modulation with magnetron-type space charge. For the purposes of this analysis, the space charge cloud, as defined by analysis of the properties of Type 1, is considered in the manner that we consider a free electron gas. Small signal strengths are assumed although experimental evidence indicates that certain of the properties are not altered by the presence of large signals.

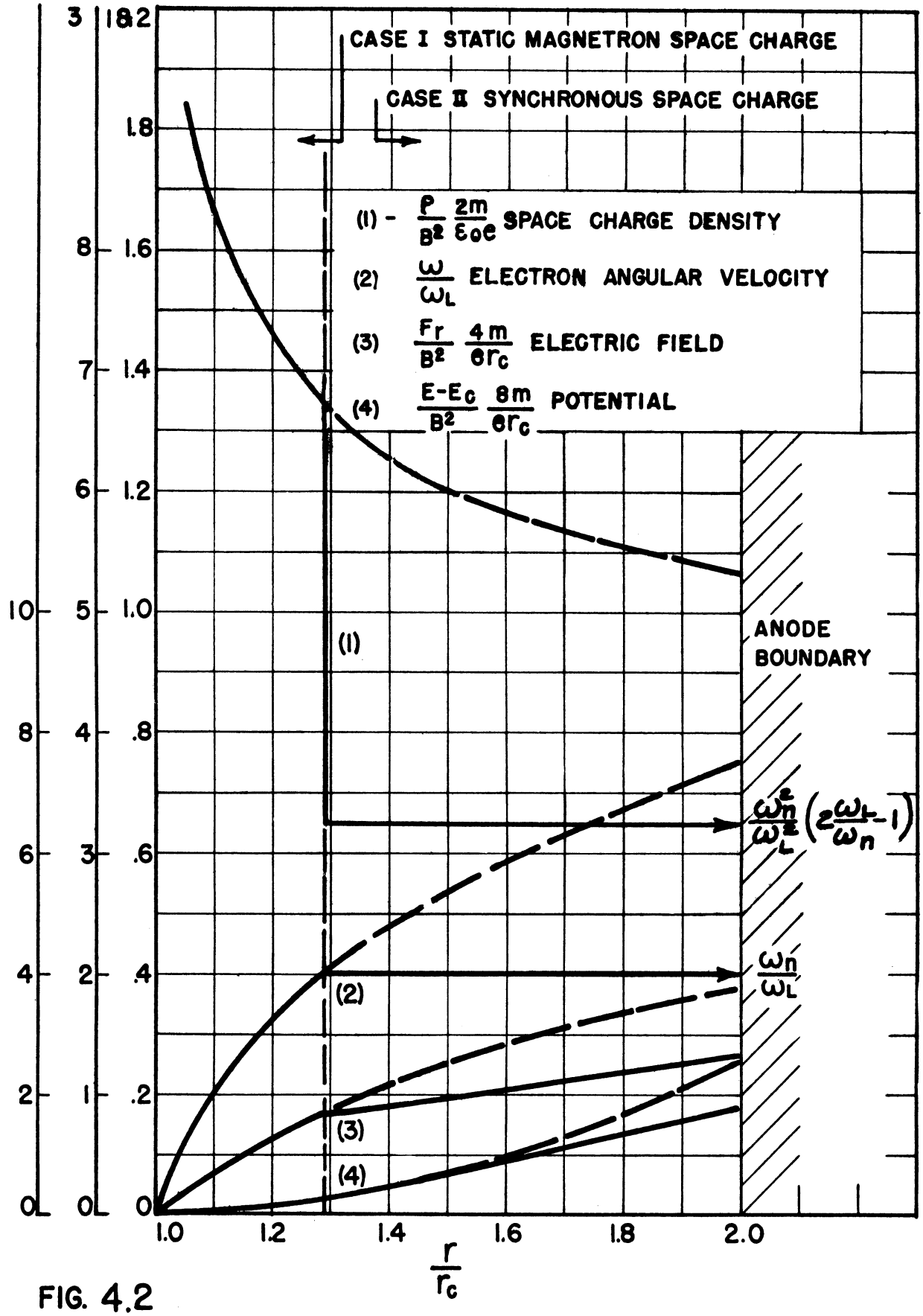

FIG. 4.2
CASES I AND II. DISTRIBUTION IN TYPICAL MAGNETRON AS HARTREE CLOUD REACHES THE ANODE FOR $\omega_n/\omega_L=4$

NOTE:
DOTTED CURVES ARE CONTINUATION OF STATIC DISTRIBUTION

If large signals are used, the losses introduced by cathode bombardment become measurable. There is no damping term included in the usual treatment of a free electron gas because complete energy transfer occurs in collisions between electrons. In this sense, the free electron gas is not comparable to a conductor because in the former the mean free path is practically infinite and collision damping is negligible. Collision damping makes the conductivity finite.

The space charge in the magnetron is considered as an atmosphere of determined density and boundary given by the results of analysis of the properties of Type 1. In this case, it is immaterial what system of coordinates is used for the force equations. It is only necessary to discover what happens to an electromagnetic wave at the boundary of the space charge and within the space charge atmosphere. For this purpose the equations of force on the electron are solved for velocity in the presence of the electromagnetic field. The velocity multiplied by the charge density gives the resultant r-f current. A complex conductivity can be defined which is a function of space charge density, frequency, and the steady magnetic field in which the space charge is circulating. The space charge density, when developed in the magnetron, is itself a function of magnetic field and radius. The dielectric constant of the medium is in turn defined in terms of the complex conductivity. This is the significant result for the purposes of this analysis. The dielectric constant so obtained depends on the orientation of the magnetic field and results are given for propagation perpendicular to the steady magnetic field and parallel to the steady magnetic field. The first case applies to the space charge as usually located within the multianode magnetron. The second case applies to magnetron-type space charge present in a coaxial line with wave propagation in the axial direction.

If the dependence of the static magnetron space charge on radius is omitted, these results are as follows:

For propagation perpendicular to the magnetic field

$$\epsilon_r = 1 - \frac{1}{2} \frac{\left(\frac{\omega_c}{\omega_f}\right)^2 \left(\omega_f^2 - \frac{\omega_c^2}{2}\right)}{\left(\omega_f^2 - \frac{\omega_c^2}{2}\right) - \frac{\omega_c^2}{2}(1 \pm 1)} \qquad (2)$$

For propagation parallel to the magnetic field:

$$\epsilon_r = 1 - \frac{1}{2} \frac{1}{\frac{\omega_f}{\omega_c}\left(\frac{\omega_f}{\omega_c} \pm 1\right)}$$

where

ϵ_r = relative dielectric constant of space charge cloud

$\omega_c = \frac{Be}{m}$ (cyclotron angular frequency)

B = steady magnetic field

$\frac{e}{m}$ = charge to mass ratio of an electron

ω_f = $2\pi f$ where f is frequency of wave incident upon space charge

These results are shown graphically in Figure 4.3. The double-valued dielectric constant is not a new concept since similar results are obtained in analysis of the ionosphere.(1) The electromagnetic field may be considered made up of two circularly polarized waves of right and left hand polarization; the two polarizations having different orientations with respect to the static magnetic field. This causes one polarization to propagate differently than the other, resulting in two values of effective dielectric constant.

---

(1) Mimno, H. R., "The Physics of the Ionosphere", Review of Modern Physics, Vol. 9, No. 1, pp. 1-68, January 1937.

There are three regions of interest in the graphs of Figure 4.3. For values of ω_f/ω_c less than .36, the relative dielectric constant is negative in Figure 4.3a and negative or large positively in Figure 4.3b. An electromagnetic wave will not propagate in a region of negative dielectric constant, so total reflection occurs at the space charge boundary. The presence of this type of space charge in a coaxial structure such as a magnetron would therefore increase the capacitance between elements. A large positive dielectric constant as given in Figure 4.3b will have the same effect for a different reason, of course. On the other hand, for values of ω_f/ω_c greater than 1.36, the relative dielectric constant in both cases is positive but less than unity. The presence of such a space charge in a coaxial structure would therefore reduce the capacitance between elements. The region between $\omega_f/\omega_c = .36$ and $\omega_f/\omega_c = 1.36$ contains several anomalies. Very little experimental data are available in this region except in the immediate vicinity of the cyclotron resonance, $\omega_f/\omega_c = 1$. In this region, the analysis based on dielectric constant is probably in error since the electrons oscillate with very large amplitudes and the damping term is no longer insignificant. The reason for this is that the natural frequency with which the electrons traverse a circular orbit in the magnetic field coincides with the impressed electromagnetic frequency. Electrons therefore move in phase with the impressed voltage and are continually accelerated. This case has been analyzed in detail by Lamb and Phillips,[1] under the rather restricting limitation that the thickness of the sheath of electrons

---

(1) Lamb, W. E., Jr., and Phillips, M., "Space Charge Frequency Dependence of Magnetron Cavities", Journal of Applied Physics, Vol. 18, pp. 230-238, February 1947.

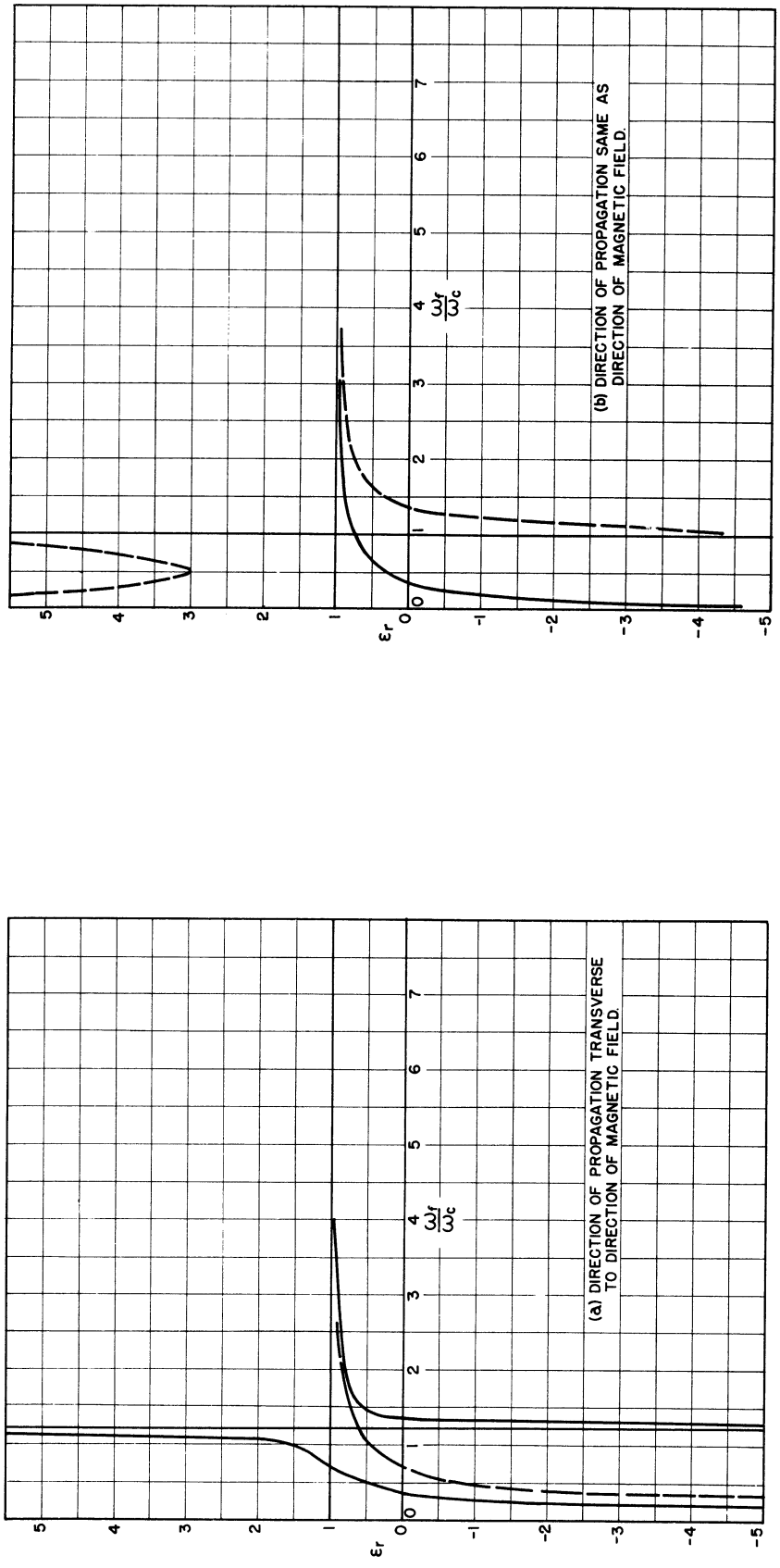

FIG. 4.3 DIELECTRIC CONSTANT OF MAGNETRON SPACE CHARGE AS FUNCTION OF ω_f / ω_c

surrounding the cathode shall be very small compared to the cathode diameter. The effects of electron beams near the cyclotron resonance have been analyzed and used experimentally by several groups.

The validity of this theory is also borne out by the experiments discussed in Section 12 of this report. Detailed discussion is given in Technical Report No. 1, Section 6.

5. Frequency Characteristics of Magnetrons Related to Space Charge; Origin of Noise in Magnetrons

The analysis described in the last section yields results which immediately provide a qualitative picture of several characteristics of the magnetron related to its oscillation frequency or resonance frequency. It has already been mentioned that the voltage required for initiation of oscillation can be calculated using the concept of a synchronous space charge. Voltages calculated in this manner agree quite well with experimentally observed values. Frequency pushing, or variation of oscillation frequency with magnetron anode current, can also be explained qualitatively on basis of the synchronous space charge. The frequency at which oscillation is initiated is always lower than the cold resonance frequency of the magnetron. This is the case because oscillations tend to start at the lowest anode voltage, corresponding to the lowest angular frequency of the rotating swarm of electrons, for which circuit losses can be accounted for by energy conversion of the electrons. The frequency of the current induced in the magnetron anodes by the spokes of the electron swarm is less than the resonant frequency of the magnetron; the magnetron as a result presents a positive reactance. The spokes, therefore, tend to lag behind the r-f voltage wave as they progress around the interaction space between cathode and anode. An anode voltage is

raised, increasing plate current, the spokes tend to speed up, coming more nearly in phase with the traveling electromagnetic wave. At the same time, oscillation frequency increases so that a smaller positive reactance is presented corresponding to a reduced phase angle between r-f voltage and current. The total change in frequency is of the order of magnitude of resonant frequency multiplied by $1/Q_L$, where Q_L is the loaded Q of the magnetron. The Q, however, is not the determining factor in the amount of pushing to be expected. Other factors, including the shunt impedance presented by the magnetron and the operating d-c voltage, have an effect on the pushing. The relation of these factors which will give a quantitative evaluation of frequency pushing on a particular magnetron is still undetermined.

Space charge effects on frequency contours in the Rieke diagram are related to the synchronous space charge in practically the same sense as frequency pushing. Essentially, frequency of oscillation produced is related to the power output of the magnetron. The power output is determined in turn by the load conductance. Oscillation frequency would supposedly be determined by load susceptance; however, due to the effect which produces pushing, oscillation frequency is also dependent upon load conductance. This effect is observed in Rieke diagrams of magnetrons, where it is seen that lines of constant frequency do not coincide with lines of constant load susceptance. In the case of klystrons, the frequency contours are straight lines inclined at an angle to the constant susceptance lines. However, in the case of the magnetron the relationship is not so definite.

The most important effects of the magnetron space charge on frequency insofar as this project is concerned are those due to the static magnetron space charge rather than the effects due to the synchronous space

charge. These effects are of two types. The resonant frequency of the magnetron cavity will decrease due to an increase in the capacitance between anodes as the diameter of the space charge swarm is increased when the dielectric constant of the swarm is negative. The resonant frequency of the magnetron cavity will increase due to a decrease in capacitance between anodes as the diameter of the space charge swarm is increased when the dielectric constant of the swarm is positive and less than unity. The diameter of the space charge swarm is increased in either case by increasing anode voltage on the magnetron. The swarm in the first case has the same effect on frequency as would be produced by a conducting surface replacing the swarm. The magnitude of the frequency change to be expected in the two cases differs. The capacitance which is affected is that between anode and cathode which is a small percentage, usually of the order of 4-6 per cent, of the total effective circuit capacitance. In the second case, where the dielectric constant is positive, but less than unity, the maximum conceivable effect would be a complete cancellation of the capacitance between anode and cathode. This would cause a change in resonant frequency of 2 to 4 per cent. However, in the first case, where the dielectric constant is negative, the capacitance between anode and cathode can be increased indefinitely (in theory), thus producing large percentage variation in frequency. Practically speaking, the magnitude of this change is probably limited where high r-f voltages are present as the swarm nears the anode. The linearity would certainly not be good for large frequency shifts. It is expected, however, that frequency shifts will be obtained with a good linearity in a range of 1 to 3 per cent.

The diameter of the space charge swarm is limited if a voltage at which oscillations may be initiated is reached, or if the magnetic diode cut-

off (Hull voltage) is reached. In the first example, synchronous space charge is formed which has a relative dielectric constant very near unity and effects on frequency are primarily of the type mentioned in the discussion of frequency pushing. In order to prevent initiation of oscillation in a structure to be used for frequency modulation, anode structures must be specially designed. This problem is discussed in Section 8. In the second example, the space between anode and cathode is filled with space charge and additional effects due to further increase in voltage are of a secondary nature. In both cases, d-c plate current is drawn.

The cyclotron resonance effect which occurs for a sharply defined value of magnetic field is also usable in frequency modulation devices. The natural resonance of the individual electrons can introduce quite large reactive currents into the resonant system causing frequency shifts which have been observed to be of the order of 1 per cent. This resonance can occur either in oscillating magnetrons, in which case the efficiency is affected, or in non-oscillating structures in which the observed resonant frequency is shifted. This resonance effect has been observed in experimental work in the Michigan Laboratory, but it is not intended under the present program that it will be used to produce modulation.

The origins of noise in magnetrons have been the subject of much investigation, theoretical and experimental. One interesting point arises in this connection from the analysis of the assumptions and results arising from the investigation of the magnetron space charge. The solutions obtained in the simple steady state analysis of the static magnetron and synchronous magnetron space charge require that electrons which reach the anode, either at the magnetic diode cut-off or at the voltage for initiation of

oscillation, have the minimum amount of kinetic energy of angular velocity required for existence in a stable state at the anode radius. Thus, plate current must exist at higher voltages. If current initiates at lower voltages the electrons must have a smaller minimum kinetic energy and thus smaller angular velocities. If this is the case, they must have been slowed down by some mechanism in their transit to the anode. The only significant mechanism by which the electrons can be decelerated is in a transfer of energy from the d-c field to some electromagnetic field. Since noise voltages are experimentally observed to exist in pre-oscillating magnetrons and static magnetrons operating below cut-off, it is logical to assume that the production of these voltages is the mechanism by which electrons give up their energy and therefore reach the anode at lower than predicted values of d-c voltage. Conversely, it is necessary, if noise is produced, that plate current be drawn. This is true simply because if noise energy is to be produced by the system, then energy must be given to the system by the power supply. The noise probably originates in the cathode as thermal noise, etc., and is amplified by the process of continuous interchange of energy between the d-c field and the noise through the medium of the electron swarm. On the basis of these ideas, it is suggested that experiments designed to cast light on the origins of noise produced by magnetrons should be made on non-oscillating structures and correlated carefully with the d-c current drawn by the magnetron. It is also possible that an amplifier could be constructed employing the principle of interaction between layers of magnetron space charge traveling at different velocities similar to the already constructed electron-wave tube.

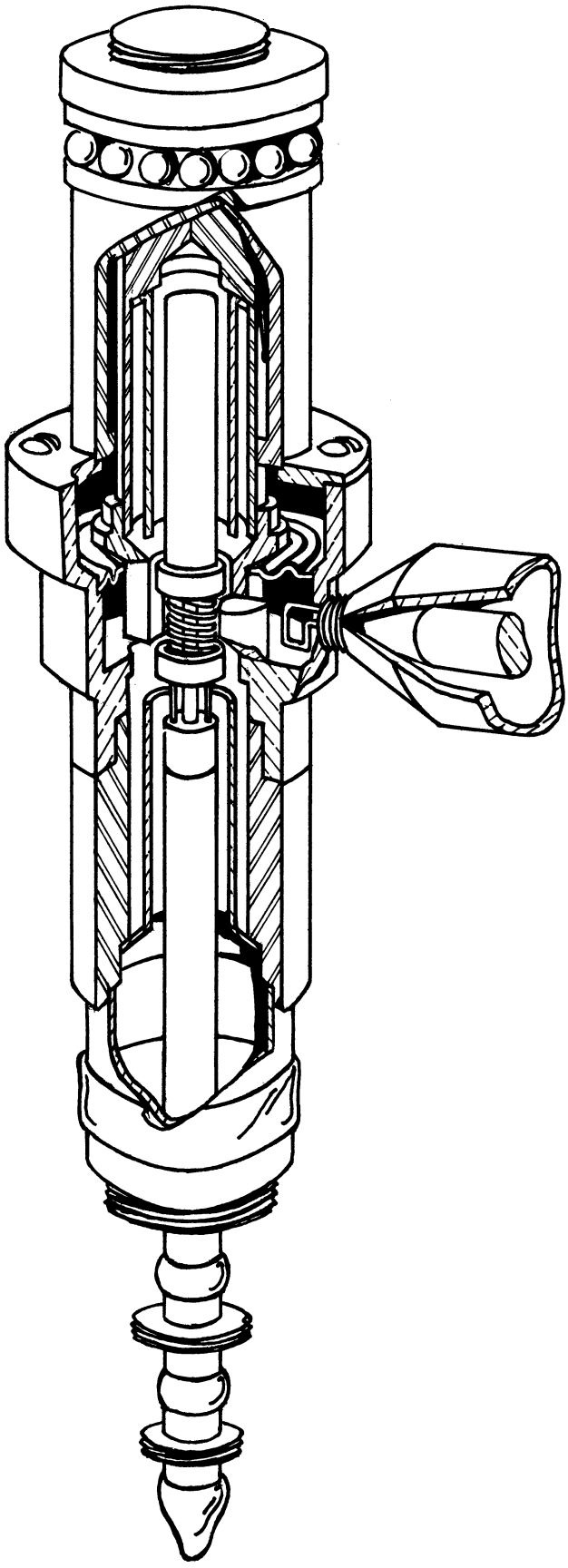

FIG. 6.1 SECTIONAL VIEW
INTERDIGITAL MAGNETRON

6. R-f Circuit of Interdigital Magnetron

a. The Cavity: The principal resonant element of an interdigital magnetron of the type shown in Figure 6.1 is a toroidal cavity, loaded at the center by a set of N interlocking "fingers". The region of the toroid can be thought of as a cylindrical cavity operating in the TM$_{\ell 10}$ mode. The electric and magnetic field configurations of such a cavity, in the modes most often encountered, i.e., the zero order mode ($\ell = 0$) and the first order mode ($\ell = 1$), are shown in Figure 6.2. It is seen that in the desired zero order mode the only electric field component present is directed longitudinally, parallel to the axis of the cavity, while the magnetic fields encircle the center. There is no variation of the fields with angular position ϕ or the longitudinal directions, Z.

In the higher order modes, there is variation in the electric and magnetic fields with angle ϕ but as before, no variation in the Z direction. The fields in the first order mode are more concentrated toward the center of the cavity, in close proximity to the teeth, as contrasted with the zero order mode where they are more evenly distributed throughout the cavity. We may form a rather rough analogy between the higher order fields and the zero order fields modulated by a factor cos ($\ell\phi$) where ℓ is the mode number. Then there will exist nodal lines crossing the cavity; at each such line the fields vanish. The magnetic field will be expected to be oriented in the ϕ direction in such a manner that the maximum flux emerges between the teeth between which the voltage nodal line extends. This is shown in Figure 6.2.

The electric field lines in the interaction space corresponding to the zero and first order cavity modes are shown in Figure 6.2. It is seen that for the zero order mode the interaction space fields are similar to

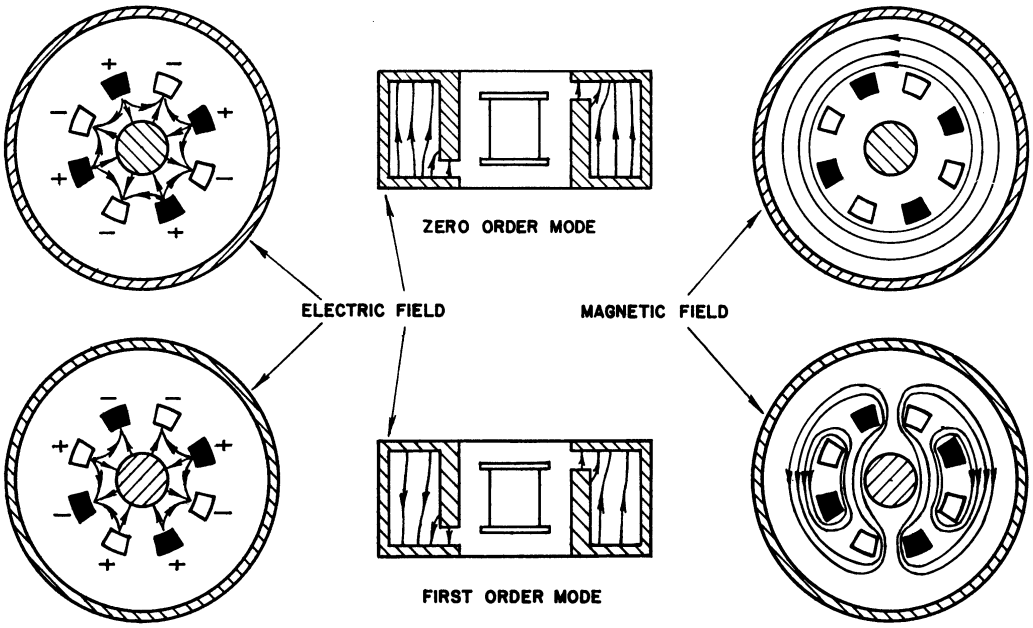

FIG. 6.2 FIELD CONFIGURATION IN ZERO AND FIRST ORDER MODES.

those present for a vane or hole and slot type magnetron when operated in the π mode. In this cavity mode (TM010), alternate teeth are necessarily of opposite polarity with 180° phase difference between them. In higher order modes these fields can again be considered as similar to the zero order field modulated by the factor cos $(\ell\phi)$ so that there will be ℓ nodal lines around the cavity.

This field configuration in the cavity prompts one to consider it as a radial transmission line with the output terminated in a conducting surface at radius R_c. It is found[1] that the impedance looking into such a transmission line is

$$Z_{in} = -j \frac{hZ_{oa}}{2\pi R_a} \frac{\sin(\theta_a - \theta_c)}{\cos(\psi_a - \theta_c)} \qquad (6.1)$$

---

(1) Ramo and Whinnery, "Fields and Waves in Modern Radio", John Wiley and Sons, pp. 354 and 406.

where the functional relationships between ψ, Z_{oa}, θ, and $\frac{2\pi R}{\lambda}$ are given by a set of curves in Report No. 2.

The condition for resonance in the cavity is then

$$j \frac{\lambda}{2\pi c C_A} = Z_{in} \tag{6.2}$$

That is, the capacitive reactance of the teeth, assumed a lumped capacitance, is considered equal to the impedance seen looking outward into the cavity from the boundary at outer edge of teeth. This method of analysis is obviously most accurate when the thickness of teeth is small compared with the depth $(R_c - R_a)$ of the cavity. From a knowledge of C_A, the tooth or anode capacitance, and the cavity dimensions, the resonant wavelength of any such cavity can be calculated. Formulae for the tooth capacitance are presented in Report No.2, having been derived from parallel plate relations and the capacitance of concentric squares, together with correction terms for the fringing field.

b. The Cathode Circuit: It is seen from Figure 6.1 that the cathode support structure forms a coaxial line from the cavity, terminated in a choke and by-pass combination. In the experimental measurements of this tube, use is made of brass models in which the choke and by-pass is represented by a shorting slug in the cathode line. In this case the impedance Z, seen looking from the edge of the cavity into the line is

$$Z_1 = Z_o \tan \frac{2\pi}{\lambda} \zeta_1 \tag{6.3}$$

and

$$Z_2 = Z_o \tan \frac{2\pi}{\lambda} \zeta_2$$

where ζ_1 and ζ_2 are the lengths of line from edge of cavity to shorting plugs.

In actual tubes where the choke and by-pass is used in the cathode line, if Z_3 is the impedance formed by the choke and by-pass in series:

$$Z_2 = Z_o \frac{Z_3 \cos \beta\zeta + jZ_o \sin \beta}{Z_o \cos \beta\zeta + jZ_3 \sin \beta} \qquad (6.4)$$

c. The Complete Circuit: While, as stated previously, the principal resonant element of an interdigital magnetron is a toroidal cavity with interlocking "fingers", in any consideration of the complete r-f circuit of such a tube, the effect of the cathode support line must be included. This can be understood by reference to Figure 6.3 in which an equivalent circuit is shown in comparison with a schematic representation of the tube. The desired mode in the cavity involves a field configuration in which the electric field vectors are parallel to the axis of the cavity, resulting in opposite polarity, at any given instant of time, on opposite ends of the cavity.

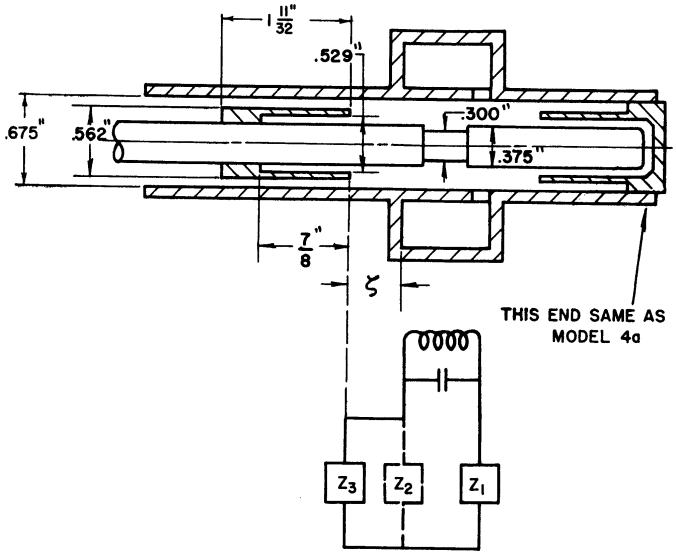

FIG. 6.3 SCHEMATIC AND EQUIVALENT CIRCUIT OF INTERDIGITAL MAGNETRON.

This type of operation results in a voltage between each side of the cavity and the cathode support and, therefore, in very close coupling between the coaxial transmission lines, formed on each side of the cavity by the cathode support structure, and the cavity itself. In the equivalent circuit of

Figure 6.3, Z_1 and Z_2 represent the impedances, at the edge of the cavity, presented by the cathode lines. These impedances were evaluated in terms of the length of line and terminating impedance in the previous section.

In higher order cavity modes there is an angular distribution of voltage around the fingers so that on the average there are no fields which can effect coupling between cavity and cathode lines.

In order to demonstrate the existence of the close coupling between cavity and cathode line for the zero order cavity mode and lack of it in higher order cavity modes, a brass model of an interdigital tube has been constructed in which the cathode structure was represented by a coaxial line shorted at equal distances on either side of the center line of the cavity. The variation in resonant wavelength of the system with distance to the short was measured for the zero and first order modes. As predicted, these measurements show very little effect on first order mode wavelength, but a considerable effect on zero order mode wavelength as the distance is changed, demonstrating the relative amounts of coupling between cathode line and cavity in the two modes.

As a result of the voltage across the cavity end of the cathode lines, power can flow down the line and in the case of the filament end of the cathode, can escape through the glass seal to be radiated from the external cathode structure. This radiation loss appears as a resistive component in impedance Z_2 and it is obviously desirable to minimize this loss. As shown in Report No. 2, this can be done by making Z_2 a very high impedance. An equation is derived in Report No. 2 from which can be obtained the proper design of a choke and by-pass combination to make Z_2 very large. If we consider the emitting surface of the cathode as a neutral point, in order

for the voltage between this point and each tooth to be the same, it is necessary to make Z_1 very large also; that is, Z_1 is made a very high reactance.

The effect of improper choke and by-pass design is to place a low resistance component in Z_2; in extreme cases, this may be great enough to prevent oscillation in the desired mode by lowering the Q to an immeasurably low value. By making Q measurements on a tube which has an improperly designed choke and by-pass, it is possible to determine the ratio of the power dissipated through the cathode line to that coupled to the load through the coupling loop. This ratio has been found to be as high as 82 per cent in brass models of which the Q was measurable.

7. Problems in Design of Interdigital Magnetrons for Zero Order Mode Operation

The design of interdigital magnetrons for zero order mode operation is a special problem because of the important part played by the cathode circuit. Factors affecting interaction space design are no different from those used in other types of magnetrons insofar as achieving maximum electronic efficiency is concerned. However, limitations imposed by heat dissipation, resonant cavity design, and mode separation must be considered in the special relationships they have to the interdigital magnetron operation.

The problem of heat dissipation is mainly one of getting heat out of the fingers. For this purpose, fingers should be made short and thick. Making the fingers short limits the length of the anode and therefore the length of the cathode, which in turn limits available emitting area. Making the fingers thick affects the capacitance and therefore resonant circuit design. The present method of tuning, for which one set of anode fingers is supported by a monel diaphragm, complicates somewhat the cooling problem for this anode set.

Factors which are believed to affect mode wavelength separation are discussed in Technical Report No. 2. The evidence of experiments performed in this laboratory on four tube models indicates that mode separation is proportional to a factor $C_A \frac{R_c}{\frac{R_a + r_a}{2}}$. Here C_A is the capacitance between anode sets, R_c is the outer cavity radius, R_a the inner cavity radius and r_a the anode radius; $\frac{R_a + r_a}{2}$ is therefore the mean anode radius. Voltage separation of modes is further dependent on the number of anodes, large N giving the best separation.

The resonant circuit must be designed to meet all of these requirements. Essentially, the anode capacitance is determined by choice of N, r_a, tooth thickness and tooth length. The outer cavity radius is then calculated using the method outlined in Section 6. The choke and by-pass combination is then designed to have optimum effectiveness in the center of the tuning range by the method also discussed in Section 6. The importance of various factors affecting design has been studied by use of brass models and by designing and building three basically different operating magnetrons. Assembly drawings for all models are given in Appendix C. The design parameters for these tubes are listed in Table 7.1. The model 1 magnetron, none of which was completed, is exactly like model 2 except that no cathode chokes are provided. Model 3A is like model 3 except for outer cavity radius. This combination of model 3 and 3A was very useful in giving a wide range in wavelength over which the effectiveness of the choke and by-pass combination could be tested. Cathodes for models 1 to 3 were obtained from Litton Engineering Laboratories. The model 4 magnetron which uses cathodes built here was intended to serve as a basis for the design of frequency modulation magnetrons. However, the mode separation is not good and the present by-pass

TABLE 7.1

Design Parameters Used in Magnetrons Constructed at University of Michigan

Magnetron	r_a cm	r_c cm	$\frac{r_a}{r_c}$	L cm	R_a cm	R_c cm	h cm	ℓ cm	d cm	N	C_A $\mu\mu$f	λ cm	E_o volts	B_o gauss	E volts	B gauss
Model 2	.665	.27	2.46	.660	1.18	2.22	1.54	1.27	.259	8	3.35	15	1230	376	5000	1000
Model 3	.45	.27	1.66	.660	.900	1.90	.95	.834	.117	12	4.96	16	220	349	2500	2000
Model 3A	.45	.27	1.66	.660	.900	1.52	.95	.834	.117	12	4.96	13	335	430	2500	2000
Model 4	.665	.381	1.75	.300	.925	1.71	1.03	.875	.130	16	4.52	14	355	286	2500	900

design does not allow operation in the zero order mode. The basic design for frequency modulation tubes may necessarily be patterned more on the lines of model 3.

8. Frequency Modulation of C-W Magnetrons(1)

The approach used by this laboratory to the problem of frequency modulation is to develop a structure with a single resonant cavity containing two magnetron anode structures. One anode structure, of the interdigital type, serves the usual functions as a capacitive element in the resonant circuit and as a multianode structure which forms the electromagnetic field with which the magnetron space charge interacts to produce oscillations. The other anode structure, not necessarily of the interdigital type, serves simply as a capacitive element in the system. The capacitance in this element is varied by varying dimensions of a magnetron type space charge swarm. A separate cathode is used for the modulation anode so that the swarm diameter can be controlled by a voltage independent of the voltage on the oscillator section.

For the greatest effect on frequency, the magnetic field in the modulator structure must be adjusted to give a space charge swarm of negative dielectric constant as discussed in Section 5. If a multianode structure is used in the modulator section, the number of anodes is restricted, since it is undesirable for this structure to oscillate. In order to prevent oscillation and still have magnetic field large enough to give negative dielectric constant, the number of anodes is determined by the following relationship

$$\frac{r_a}{r_c} < \frac{1}{\sqrt{1 - \frac{1.44}{N}}} \qquad (8.1)$$

(1) See Sections 8 and 9 of Technical Report No. 1 for details.

$$\frac{r_a}{r_c} = \frac{\text{anode radius}}{\text{cathode radius}}$$

N = number of anode segments

In practical cases at the frequency and power level being considered, the number of anodes is limited, preferably, to less than 4. In this case, $r_a/r_c = 1.25$.

Assembly drawings for two magnetrons, model 5 and model 6, which have been designed along these lines are given in Appendix F. A third possibility is discussed in Section 13. These three designs represent three avenues of development based on the interdigital magnetron principle which are represented in Figure 8.1.

In Figure 8.1a, the principle used in the model 5 is illustrated. In this case, the strong coupling to the cathode line is utilized to introduce the reactance of the space charge into the system. In Figure 8.1b, the principle of model 6 is illustrated. Here the cavity of the interdigital magnetron is extended axially to provide space for a second set of anodes. The interdigital structure is modified to permit support of the center post in the cavity. The number of anode segments in the oscillator section is 16, in the modulator section, 4. In Figure 8.1c, the cavity is extended laterally to permit introduction of a second anode set. Again the modulator section has four anode segments. This tube has not been developed beyond the brass model stage, although it has some desirable features such as ease of cooling, tuning possibilities and possibilities for use with glass envelope tubes. One model 6 has been constructed and operated without the modulator cathode. Parts for model 5 have been constructed but will not be assembled until the model 4 interdigital tube, upon which the model 5 design is based, is made to operate satisfactorily.

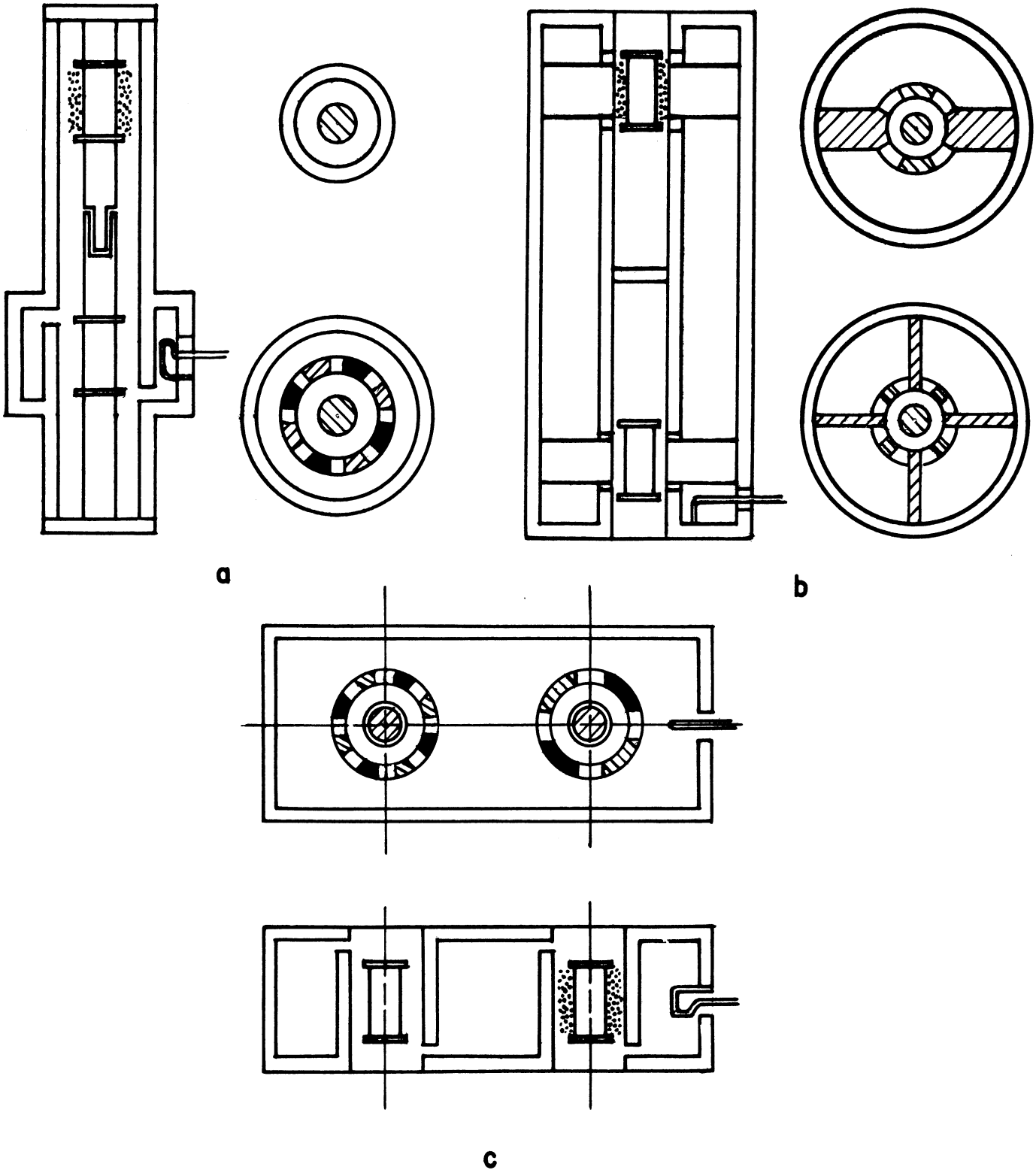

FIG. 8.1 BASIC GEOMETRIES FOR FREQUENCY MODULATION MAGNETRONS DEVELOPED IN THE UNIVERSITY OF MICHIGAN ELECTRON TUBE LABORATORY.

NOTE: MODULATING SPACE CHARGE INDICATED BY DOTS.

Techniques, such as spiral beam modulation and other uses of the cyclotron resonance which have received emphasis in other laboratories, are not being considered. The use of dielectric properties of the magnetron space charge has not been developed to its maximum usefulness and it is believed that the combination of this technique with geometries based on the interdigital magnetron principle will yield frequency modulation over bandwidths heretofore unattained, possibly as much as 3 to 5 per cent. The linearity which can be achieved may be good only for bandwidths of the order of 1 per cent. Experimental information on operable models will give more basis for analysis of this problem and better knowledge of the limitations.

III. EXPERIMENTAL RESULTS

9. Measurements on R-f Circuit of Interdigital Magnetrons

The theoretical characteristics of the r-f circuit of an interdigital magnetron have been given in Section 6. In this section experimental verification of these statements and formulae will be presented.

a. The Cavity: In order to determine the field configurations and resonant wavelength in the cavity, brass models were made with dimensions adjustable. Small holes were placed around the surfaces through which probes could be inserted to measure the relative intensity of the electric field at various points. An indication of the magnitude of the r-f voltage as a function of angular position in the interaction space was obtained by means of a rotating probe replacing the cathode. The results of these various experiments are presented below.

The formulae and curves used in the calculation of resonant wavelength of an interdigital cavity are presented in detail in Report No. 2 and will not be repeated here. However, Table 11.1 in Section 11 summarizes the results of measurements on several cavities and compares the computed wavelength value with that obtained experimentally. It is seen that in some cases the agreement between experimentally measured resonant wavelengths and calculated values is good and in others there is some variance. This agreement or lack of agreement is dependent on the relative thickness of teeth as compared with cavity diameter, for reasons explained in Section 6a. This table includes only the zero order cavity mode; for results of work on the higher order cavity modes, reference is made to Report No. 2.

Figure 9.1 shows the variation in resonant wavelength of the cavity as the outer cavity diameter is changed, for the first and zero order modes.

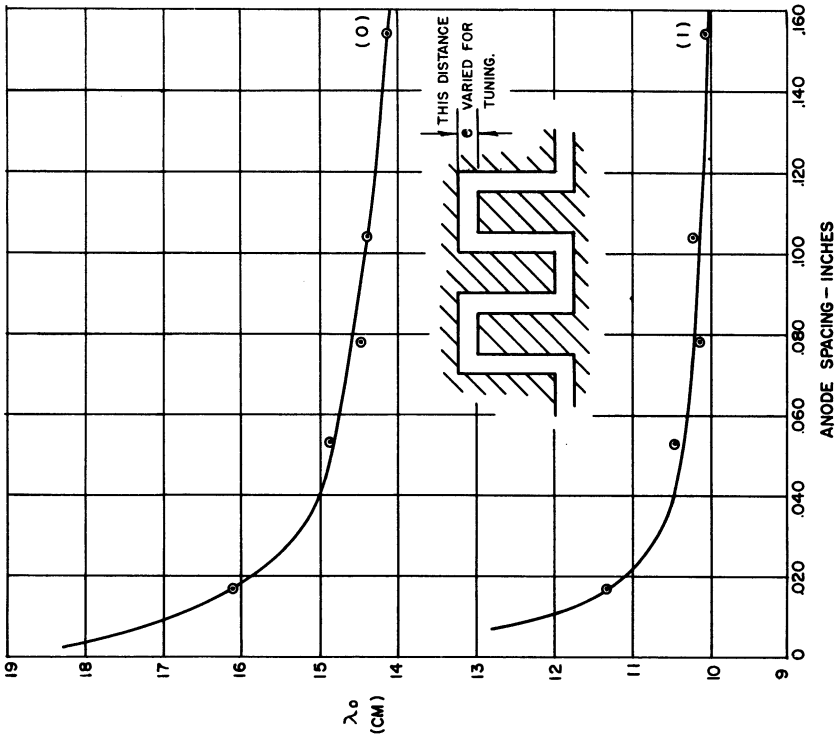

FIG. 9.2 TYPICAL TUNING CURVES OF ZERO AND FIRST ORDER MODES.

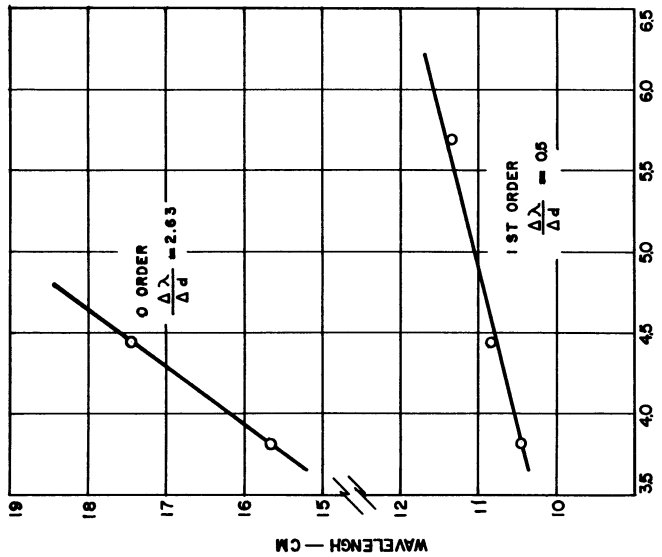

FIG. 9.1 EFFECT OF CAVITY DIAMETER ON RESONANT WAVELENGTH OF ZERO AND FIRST ORDER MODES.

The difference in slope between the lines corresponding to the first and zero order modes can be readily understood when the field patterns shown in Figure 6.2 are examined. It is seen that the fields in the first order mode are concentrated more toward the center of the cavity, encircling the teeth so that less effect of the outer conducting surface will be present.

The tuning of the interdigital cavity is accomplished by varying the distance between the ends of the fingers and the end walls of the cavity. When the teeth are of the same cross-section along their length, the principal effect on capacitance (C_A) will be the change in end spacing so that the capacitance variation with anode spacing would be expected to be approximately a rectangular hyperbola. This limits the tuning range to the region of small anode spacings and is shown to be true by the typical tuning curves of Figure 9.2. In order to increase the tuning at large anode spacings, various modifications have been tried. For example, tapering the back surfaces of the teeth will result in a tuning curve which is similar to that of 9.2 except the flat portion slopes downward, resulting in increased tuning range.

b. The Cathode Circuit: In Section 6 of this report the conditions for resonance in the system were given and the importance of the cathode circuit as a wavelength determining factor was emphasized. Figure 9.3 shows a comparison between the measured resonant wavelength of a brass model of an interdigital tube as function of cathode line length and the value calculated from the resonance relation of Equation (6.3). It is seen that the agreement is very good, providing confirmation of the equivalent circuit shown in Figure 6.3.

An experiment was also performed in order to determine whether a choke and by-pass could replace the shorting plugs in a brass model and yield

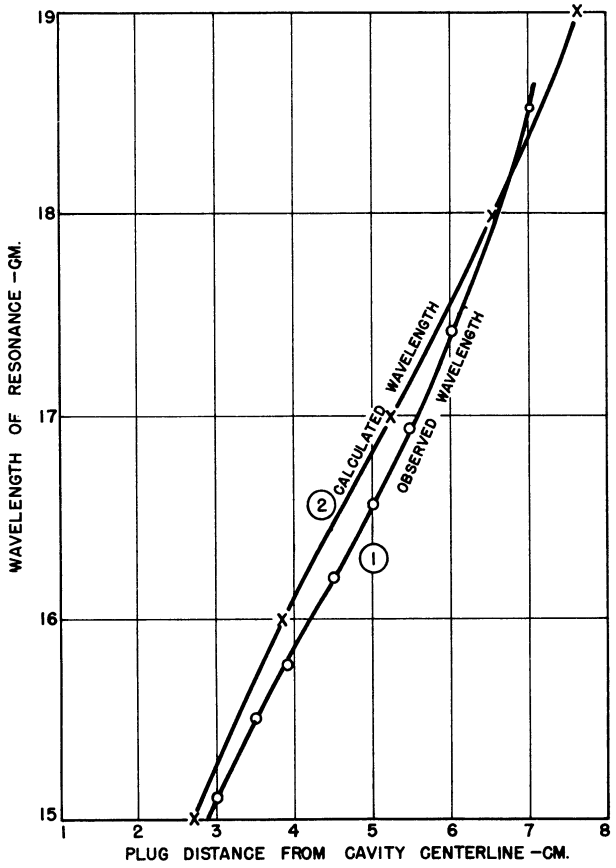

FIG. 9.3
COMPARISON OF CALCULATED AND OBSERVED
EFFECT OF CHOKE LENGTH

the same agreement. It was found that this is possible and that a properly designed choke and by-pass is equivalent to the shorting plugs over a wide range of wavelength even though the choke and by-pass are designed for only a fixed wavelength.

Most of the experimental observations concerning the effect of the cathode line were made in the course of a study of the frequency modulation possibilities by means of the cathode line so that these data will be presented in Section 13.

10. Construction of Interdigital Magnetrons

Assembly techniques employed by the Michigan Tube group will be discussed below. In Section 14, the special methods used in the construction of the novel model 5 and model 6 f-m tubes will be treated separately. The constructional methods employed by this laboratory have necessarily been of the "laboratory" type and are not necessarily the best suited for mass production. The Michigan group has, however, kept in mind at all times techniques and methods for mass production of these tubes, a problem which is felt to be of great importance.

In order to eliminate the problem of cathode construction in the early stages of this project, thoriated tungsten cathodes were purchased from the Litton Engineering Laboratories and employed in the first three models. As the facilities of the laboratory improved, a rugged tungsten cathode was built here and employed in all of the later tubes. A cathode of the thoria dispenser type will probably be used in future models.

Table 10.1 gives the history of the 19 tubes which underwent construction at this laboratory. Of the 19 total tubes starting construction, 8 were completed and operated successfully. Neglecting three tubes (serials No. 1, 4 and 11) which were lost due to an incorrectly calibrated thermocouple, dropping on the floor when partially constructed and lost in the first braze, the record is a shrinkage of 50 per cent which is felt to be quite good considering some of the tubes were constructed simultaneously with the construction of laboratory facilities.

a. Materials Used in Tube Assembly

Solder: All solder employed in the construction of the tube body (tube, except for the cathode) is gold-copper (37% Au, 63% Cu) solder except

TABLE 10.1

Serial No.	Model No.	Assembled	History	Operated	Present Condition
1	1	May 1947	Overheated glass to point of collapse in bake out.	No	Unusable
2	1	June 1947	Long history on pump with cathode slumping troubles. Rebuilt vacuum pump and tipped off 10/6/47. Tip-off seal cracked in cleaning bath.	No	Unusable
3	3	October 1947	Leak in diaphragm. Appeared due to extensive bake on pumps.	No	Unusable
4	3	October 1947	Accidental damage caused by visitor before glassing cathode	No	Unusable
5	3	November 1947	Completed and operated in pulsed condition. Arc-over due to misaligned choke prevents c-w operation. Tube lost trying to repair.	Yes	Unusable
6	3	January 1948	Leak developed in diaphragm due to oxidation caused by extended bake out.	No	Unusable
7	3	February 1948 March	Output seal cracked. Serial No. 8 was pumped while this was repaired. Tipped off pumps March 1948. Tip off seal cracked with filament lit before data could be obtained.	No	Unusable
8	3	February 1948	Extensive tests made on this tube. Over 500 watts c-w have been obtained at greater than 70% efficiency.	Yes	Usable

Serial No.	Model No.	Assembled	History	Operated	Present Condition
9	3A	May 1948	Operated and tested hot. Test and x-ray showed misaligned cathode. Cathode realigned but leak appeared in diaphragm in second bake out on pumps.	Yes	Unusable
10	3A	June 1948	Brazed in new furnace. Leak appeared in output seal. Attempts to repair leak failed.	No	Unusable
11	2	July 1948	Lost in brazing due to faulty brazing jig.	No	Unusable
12	2	July 1948	New assembly technique was tried on this tube and it was lost in brazing.	No	Unusable
13	2	August 1948	Leak developed while on the pump due to a faulty diaphragm.	No	Unusable
14	2	October 1948	Leak appeared due to faulty braze. Easier to build new tube than repair present one.	No	Unusable
15	2	November 1948	Operated for several days. Output seal cracked in setting up an experiment.	Yes	Unusable
16	2	December 1948	Operated but was lost on test bench due to cathode failure from back bombardment while operating in wrong mode.	Yes	Unusable
17	4	January 1949	Operated	Yes	Usable
18	4A	February 1949	Operated	Yes	Usable
19	6	April 1949	Operated	Yes	Usable

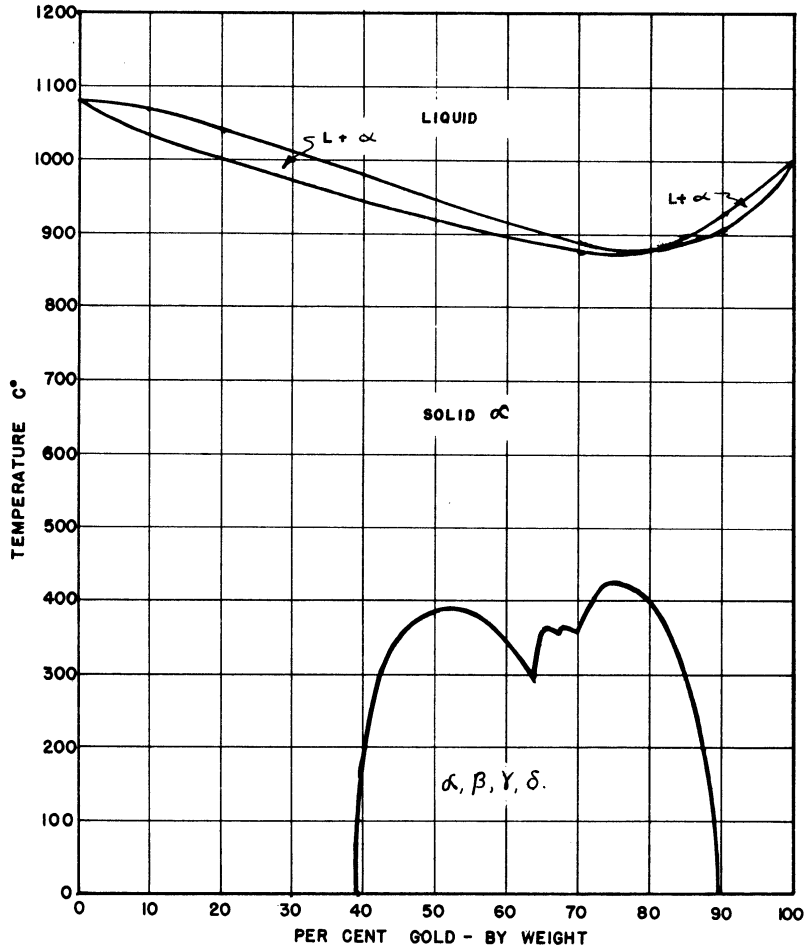

FIG. 10.1 GOLD-COPPER CONSTITUTION DIAGRAM
(FROM AMERICAN SOCIETY FOR METALS 1939)

for the eutectic BT silver solder (melts at 778°C) braze joining the output assembly to the cavity.

Gold-copper was chosen because it allows one to make several successive brazes on the tube without the danger of previous brazes letting go. The constitution diagram of gold-copper, Figure 10.1, shows that a solid solution forms from 0 to 40 per cent gold by weight. Between 40 and 89 per cent gold, several phases may occur while only a solid solution forms above 89 per cent. It is best to keep out of the 40-89 per cent region since this solder is rather brittle and also there is a possibility of leaks occurring along the crystalline boundaries. For the sake of economy, it is best not to work in the 89-100 per cent region. One is, therefore, limited by the above considerations to the 0-40 per cent region. The melting point varies about 80°C as the solder varies from 37 per cent to 10 per cent gold. Using 37 per cent gold solder and brazing at 1070°C the solder dissolves

some of the copper body and forms approximately a 10 per cent gold solder whose melting point is about 1070°C. A second braze is possible using 37 per cent gold solder and a brazing temperature of 1060°C. Other brazes can be made at 10°C lower temperature steps with 1000°C being the lower limit of the braze. If purely mechanical and electrical brazes are required with no vacuum requirements imposed, the brazes can be successfully made down to 970°C.

The above technique is important in research work where expensive and complicated fixtures cannot be justified due to the small number of tubes constructed of each model.

BT silver solder (eutectic) is employed for brazing the output assembly to the tube body. This was chosen because of its lower melting temperature which enables one to easily replace the output seal if it becomes damaged.

Pure platinum solder is employed on the cathode structure where high temperatures are encountered.

Copper brazes are made wherever two pieces having melting temperatures above Cu are joined and where the temperature problem is not severe.

Copper: Oxygen Free High Conductivity (OFHC) copper is employed entirely in all of these tubes. Due to its low oxide content, it is permissible to braze this type of copper in a hydrogen atmosphere and still maintain a dense non-porous leak-proof body.

Steel: Steel is necessarily used inside the vacuum envelope due to magnetic circuit considerations. Hot rolled SAE 1020 is used since there is less chance of axial leaks forming in the rolling process with this material than there would be for cold rolled steel. No leaks have been discovered to date in steel parts.

The steel is copper plated before brazing to provide high electrical conductivity and ease of brazing. A Rochelle salt-cyanide bath is employed for copper plating to a depth of approximately 0.0005 inch thick.

Monel: The diaphragm was constructed of 0.007 inch sheet Monel which is an excellent material for diaphragm use in vacuum tubes. It is vacuum tight, easily brazed, non-corrosive, and retains strength and some springiness after the brazing operations.

Kovar: The glass to metal seals are Kovar to 7052 Corning glass and all seals were made by the laboratory personnel on a Litton type "F" glass blowing lathe. The Kovar was first cut to length, polished with Axolite (320 grit), degreased, annealed in H_2 atmosphere at 1100°C for 10 minutes and then glassed.

Cleaning Solutions:

Copper bright dip:

H_2SO_4 - 8 parts
HNO_3 - 4 parts
H_2O - 1 part

The above solution is used to clean copper parts.

Oakite No. 32:

Oakite No. 32 diluted 1:1 with water is used hot to clean Kovar and parts constructed of different materials which would ordinarily plate one on another by electrolytic action in a cleaning bath. Kovar requires mechanical rubbing between dips to clean.

Hydrochloric Acid:

50% HCl is used to clean steel parts.

Sodium Cyanide:

Solution (5 oz/gal) is used for cleaning steel parts before copper plating.

Sodium Hydroxide:

Electrolytic cleaning of tungsten and molybdenum using carbon electrodes and 11 volts a-c.

Anodic Cleaning, using iron cathodes, is used for degreasing very dirty parts.

Carbon Tetrachloride is used hot for degreasing.

Distilled Water, Alcohol and Ether are used for rinsing and drying parts.

Copper Plate:

Steel pole pieces are plated by means of a Rochelle salt copper cyanide bath.

b. Tube Body Construction

Drawings referred to in this section are given in Appendix D of this report.

Anodes (Dwg No. A-5003, A-5004): The anodes are turned and milled from OFHC copper with the critical tolerances held to $\pm$.001 inch. The hobbing technique would be a most useful method for producing these parts in large numbers.

Cavity (Dwg No. A-9010): The cavities are turned out of OFHC copper bar. In the early models the hole for the output seal was tapped with a 3/8-24 thread. In later models this is left as a smooth bored hole into which the output assembly is snugly fitted. In production, the upper support portion (non-evacuated section) above the diaphragm could be eliminated from the cavity and incorporated in the tuner piece, thus greatly simplifying this part.

Chokes (Dwg No. A-9006 and A-9014): The chokes are turned out of solid bar OFHC copper since no tubing is kept in stock. In production these probably could be easily made in two parts, a tube and a washer brazed together.

Pole Pieces (Dwg No. A-9007 and A-9013): The pole pieces are turned from hot rolled steel, cleaned and copper plated. The plated (.0005 inch thick) pole pieces are stored in a "hot" box until assembly.

Diaphragm (Dwg No. A-9016): The diaphragm is made out of .007 inch monel metal stamped in single face to rubber pad dies. A typical die is shown in Figure 10.2. The material is first formed (Figure 10.2a) with the center slug in the base on an 80-ton hand press. It is judged that approximately 60 tons is required in the forming operation. After forming, the center slug is removed from the base and the trim and piercing operation is carried out (Figure 10.2b). The die is designed so the rubber comes down first, clamping the formed monel piece to prevent its slipping while it is trimmed and pierced.

The above die lends itself admirably to experimental work since it is simple and cheap to build. The diaphragms have proved to be quite satisfactory for experimental work, giving a total travel of .15 inch. None have failed as yet due to fatigue; however, it is estimated that the maximum number of cycles any diaphragm has as yet undergone is only about 50.

A compound die would probably be better for producing large numbers of these tubes.

Output Assembly (Dwg No. A-7001): The output assembly employed in these tubes was chosen because of simplicity and ease of production. In later tubes, we hope to use a ceramic-to-metal output seal. The present seal has held up with outputs exceeding 500 watts when working into a reasonably flat line.

The outside taper (Dwg No. A-7001-1, Appendix D) is turned from OFHC copper using a boring tool shaped to form the correct taper (30°). The

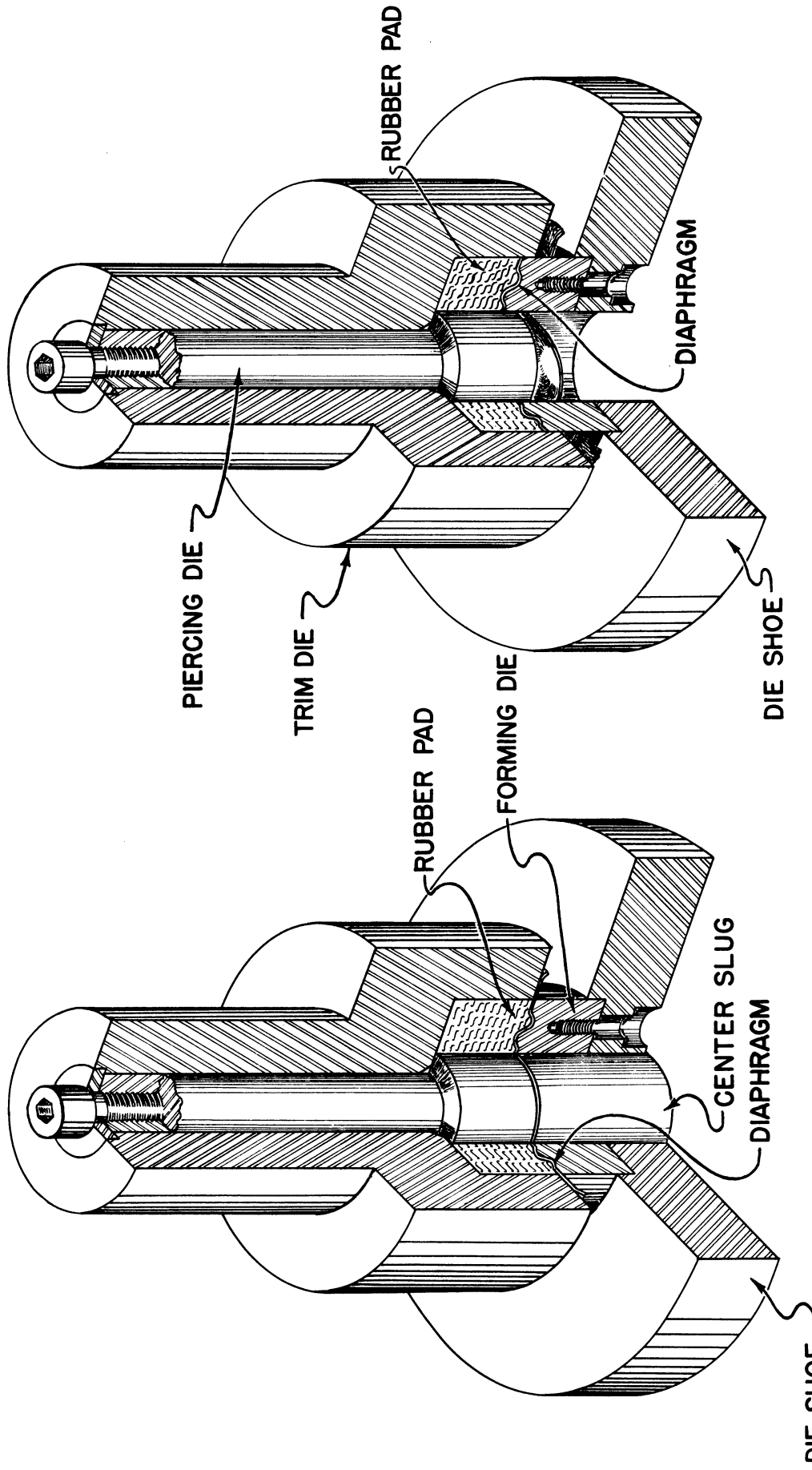

FIG. 10.2 DIAPHRAGM DIE

outside Kovar piece (Dwg No. A-7001-2) is cut, polished, cleaned in Oakite solution, annealed and brazed to the outside taper in a H_2 atmosphere using gold-copper solder. This braze is made in the hydrogen brazing bottle so it can be watched carefully and cooled immediately after the solder flows. Prevention of overheating keeps the solder from alloying deep into the crystal boundaries of the Kovar which would cause stress and finally a crack through the Kovar when subjected to a few temperature cycles. This is due to the large difference in the coefficient of expansion of the Kovar and the solder.

The inside taper (Dwg No. A-7001-3) is turned from OFHC copper and brazed to the inside Kovar piece (Dwg No. A-7001-4) with gold-copper solder using the precautions taken with the outside taper braze. A ring of .020 inch solder is placed on the inside and outside of the joint for this braze.

The processes in the glassing operation are shown in Figure 10.3. First, the outside Kovar is oxidized and a slight taper made on the glass (Figure 10.3a) so it will fit snugly all around inside the Kovar and extend inside approximately 3/16 inch. The Kovar is heated at its end with the glass lathe running full speed so that the glass is thrown out firmly against the Kovar when soft. The glass is blown and pulled slightly to form a wall of even thickness and then cut to length after cool (Dwg B, Figure 10.3b). A glass bead is formed on the inside Kovar piece centered 5/8 inch from the end. The Kovar is first oxidized and then a 1/4-inch long glass tube is slid into place where it is melted onto the metal (Figure 10.3c and Figure 10.3d).

The inner and outer tapers are then glassed together as shown (Figure 10.3, e and f) by paddling the outside glass onto the center bead. Care is taken to produce a fairly sharp bend in the seal which tends to reduce strain on the seal. By blowing and pulling the glass wall, thickness

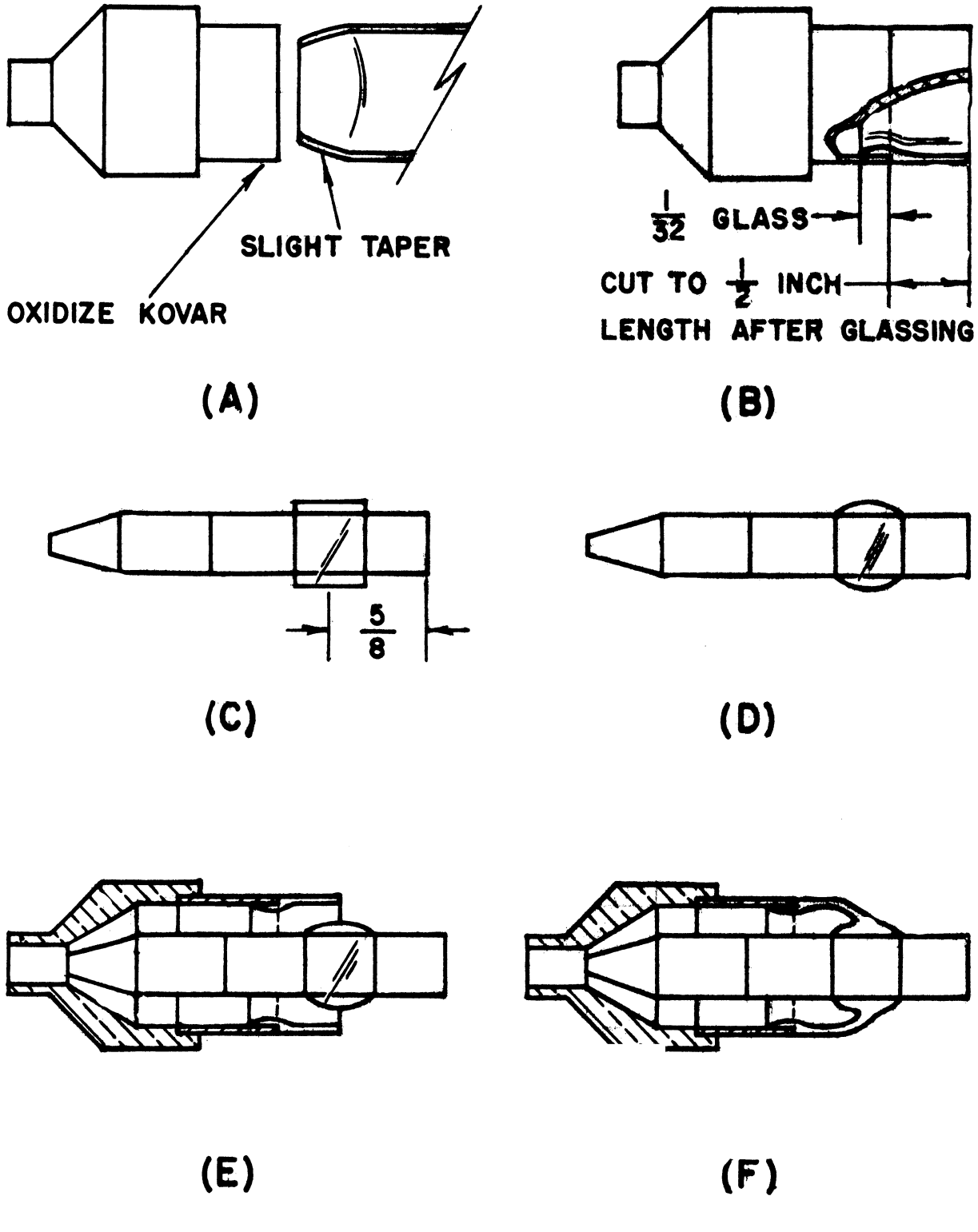

FIG. 10.3 OUTPUT ASSEMBLY GLASSING OPERATION

is evened. The pieces are aligned axially by means of jigs. The glass diameter is kept slightly less than the outer diameter of the outside Kovar. The seal is then annealed in an oven.

The coupling loop (Dwg No. 7001-5) is made of OFHC copper, turned to the proper diameter and then rolled to form a flat band. The part is ready for bending when the material is milled off the edges of the rolled flat section. The loop is bent in a jig which holds the dimensions of this part quite accurately. A torch is applied to the copper to keep it in the annealed state while bending. The loop is cleaned in bright dip.

The formed loop is joined to the output assembly by tin soldering the loop to the inner conductor and brazing with phos-copper to the outer conductor. A small piece of pure tin is placed in the hole of the inner conductor before the loop is placed into position. When the loop is phos-copper soldered to the outer conductor the tin will melt forming a good electrical connection to the inner conductor. Care is taken in brazing with phos-copper to make sure that most of the phosphorus is driven out of the solder. This raises its melting point to approach that of copper and insures against this joint melting when the output assembly is silver soldered to the tube body. The presence of the high vapor pressure tin within the tube gives no trouble since it is well hidden and remains fairly cool.

In another method of assembly the above mentioned technique using tin permits a simplification in the bending and construction of the loops by allowing one to braze one end of the loop directly to the bottom of the cavity with gold-copper solder at the time the main body is brazed. Thus, only one bend is required to form the loop and the phos-copper braze is eliminated. The tin braze of the center conductor is made at the time the output assembly is silver soldered to the tube body.

c. Assembly of Tube Body

The tube bodies are assembled in four steps:

1st Braze: Brazing Kovar sleeve (Dwg No. 9015), cathode pole piece (Dwg No. A-9007), cathode choke (Dwg No. A-9006), cavity anode (Dwg No. A-5004), cavity (Dwg No. A-9010), diaphragm (Dwg No. A-9016) and the diaphragm anode (Dwg No. A-5003) together in one operation.

2nd Braze: The tuner screw (Dwg No. A-9013) and tuner choke (Dwg No. 9014) are gold-coppered together at the same time the first braze is made.

3rd Braze: Here the tuner slug and choke assembly of the second braze are gold-copper brazed to the main assembly of the first braze.

4th Braze: This operation consists of brazing the output assembly (Dwg No. A-7001) into the main tube body, thus completing the tube body.

The first braze is made in a hydrogen furnace on a pre-oxidized stainless steel jig which holds all of the parts in accurate alignment. The jig is pictured in Figure 10.4 and consists of three main parts. The choke and pole piece are held in alignment by means of the larger bottom section. A small cap fits over the top of the bottom section of the jig and holds the anodes concentric to each other and concentric to the main body of the tube. The output hole is aligned with reference to the anode teeth by means of scribe lines on the cavity and cavity anode. The spacing between the teeth is held by means of stainless steel wires of the correct diameters placed between the teeth. In order to clearly picture this jig, it has been divided into two sections in Figure 10.4. In actual use all the parts are placed on the jig and brazed together in one operation.

The usual precautions are taken to insure cleanliness of the parts before assembly and cotton gloves are worn in the assembly operation. Gold-

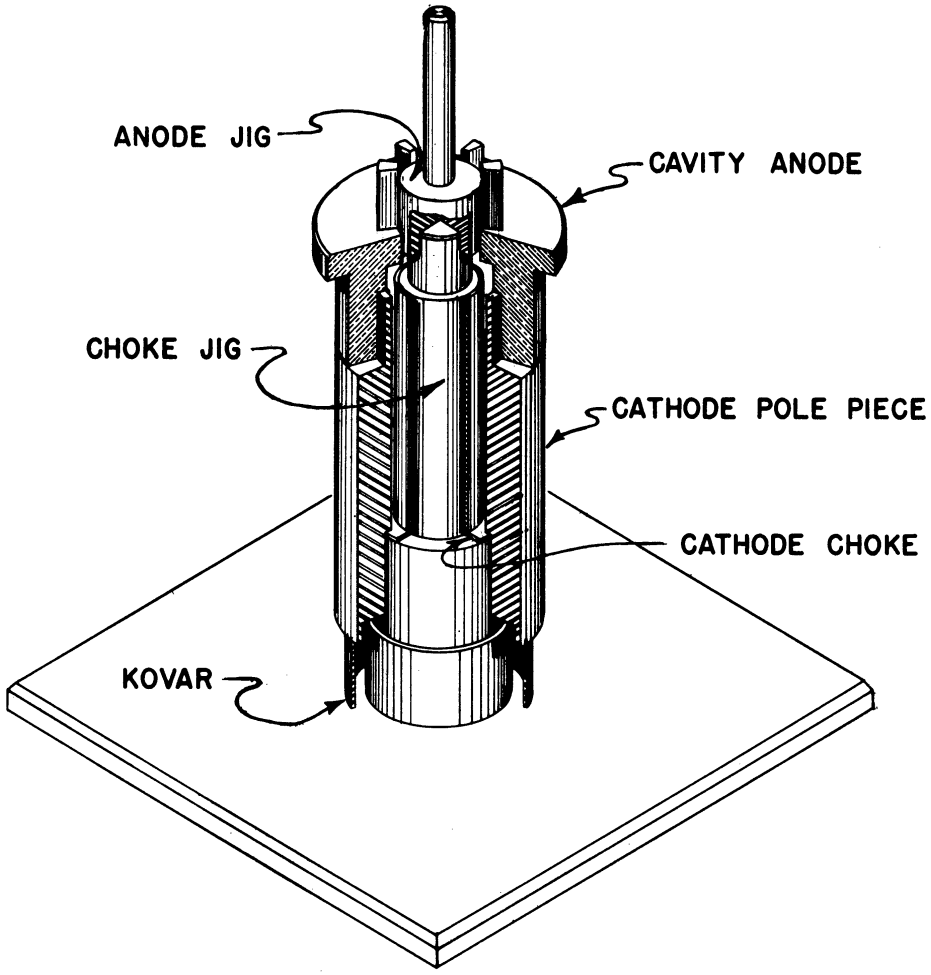

FIG. 10.4 A LOWER ASSEMBLY OF 1ST. BRAZE JIG

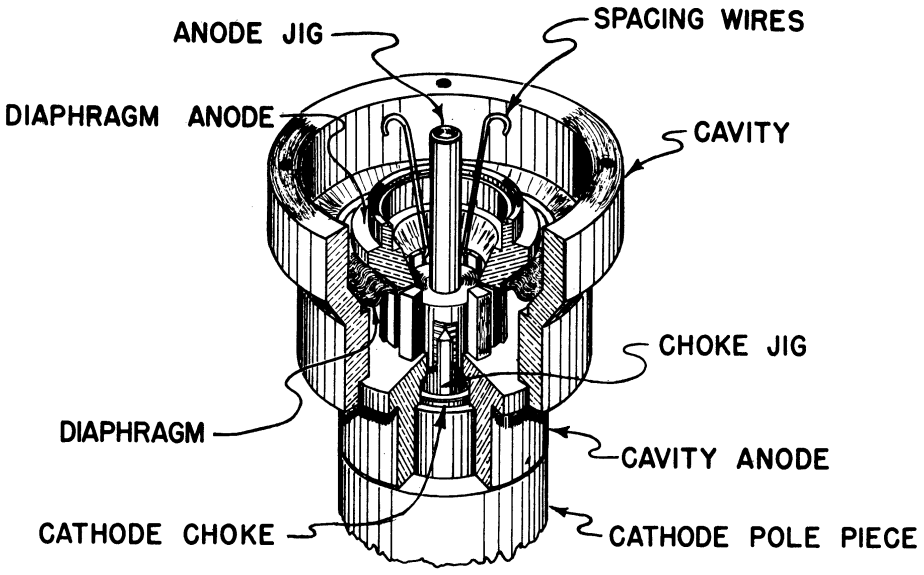

FIG. 10.4 B UPPER ASSEMBLY OF 1ST. BRAZE JIG

copper solder is used entirely for this braze which is done in the hydrogen furnace at 1030°C for 12 minutes. The tube is then stored in a hot box until its next brazing operation.

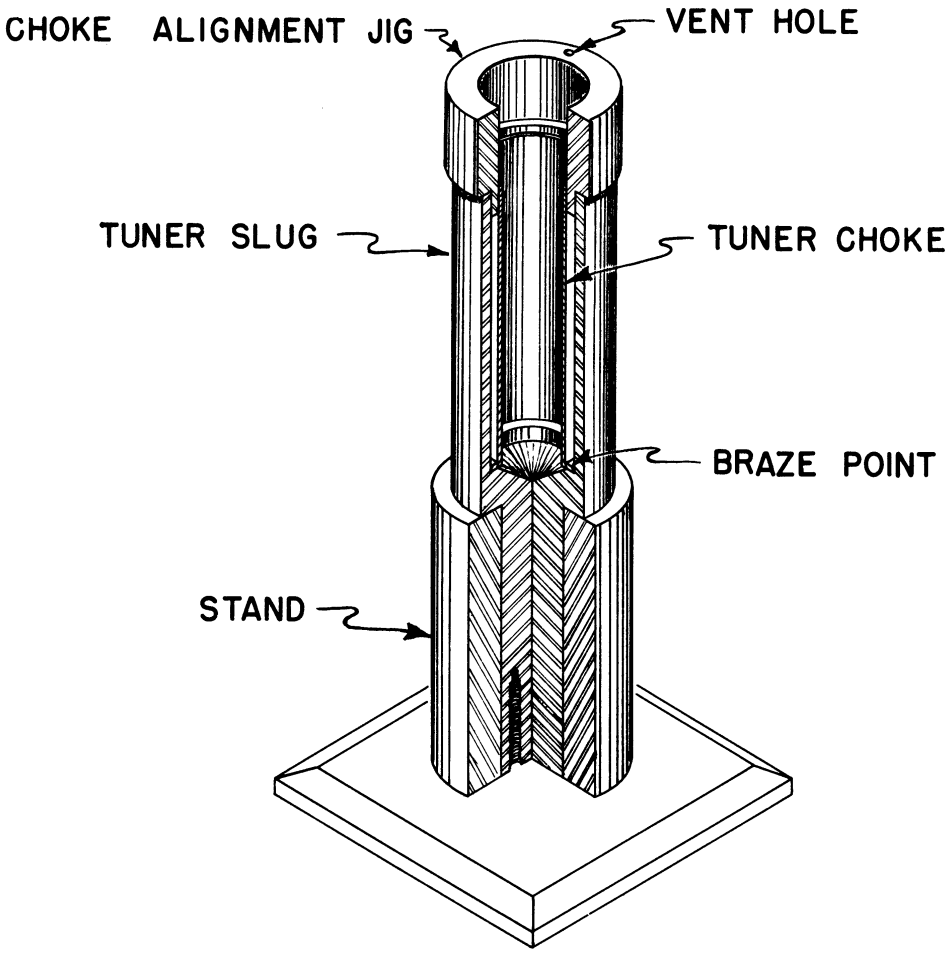

FIG. 10.5 2 ND. BRAZE JIG

The second braze is made in the furnace at the time of the first braze. It consists of brazing the tuner choke to tuner slug. A small ring-type jig holds the free end of the choke concentric with the slug and is shown in Figure 10.5. Holes drilled in the ring provide adequate entrance for hydrogen to the otherwise sealed-off space between the choke and slug. After brazing, the assembly is stored in the hot box until used in the third braze.

The third braze joins the sub-assemblies of the first two brazes together. This is done in the hydrogen furnace with gold-copper solder at

1020°C for 10 minutes. No jig is required for this braze since it is done in an upright position and the parts fit snugly. Gold-copper must be used for this braze because of its proximity to the upper anode which gets hot enough to melt silver solder during bake-out on the pumps. .

The fourth braze, done in the hydrogen brazing bottle (Figure 10.6), solders the output assembly to the main body of the tube. The lower melting silver solder (BT) is used for this braze allowing one to remove easily the output seal for replacement in case of damage. The output assembly is aligned by means of scribe lines so that the loop is oriented vertically in the tube with the inner conductor side facing downward. An .080-inch diameter molybdenum filament is used for heating the parts and is wound so that it is only about 1/8 inch distant from the cavity. A heat shield of 1/8-inch transite is placed over the output seal to keep direct radiation from the filament from the glass seal. The tube is first flushed with hydrogen before the brazing to make sure no oxidation takes place inside the tube. Heat shock to the output seal is reduced by gradually increasing the filament temperature until the solder flows, whereupon the filament temperature is immediately reduced.

A glass seal is made inside and outside the cathode Kovar ring and glass tubulation sealed on for leak testing with a G.E. helium mass spectrometer leak detector. After testing for leaks, the tube (without the cathode) is sealed to the pumps where it is "pre-evacuated". This pre-evacuation procedure, due to the large diameter and constriction-free tubulation, quickly removes the major high vapor pressure materials which might have found their way into the structure and greatly shortens the final pumping time. The entire tube is baked at 425°C until the vacuum reaches 5×10^{-6} mm/Hg and then

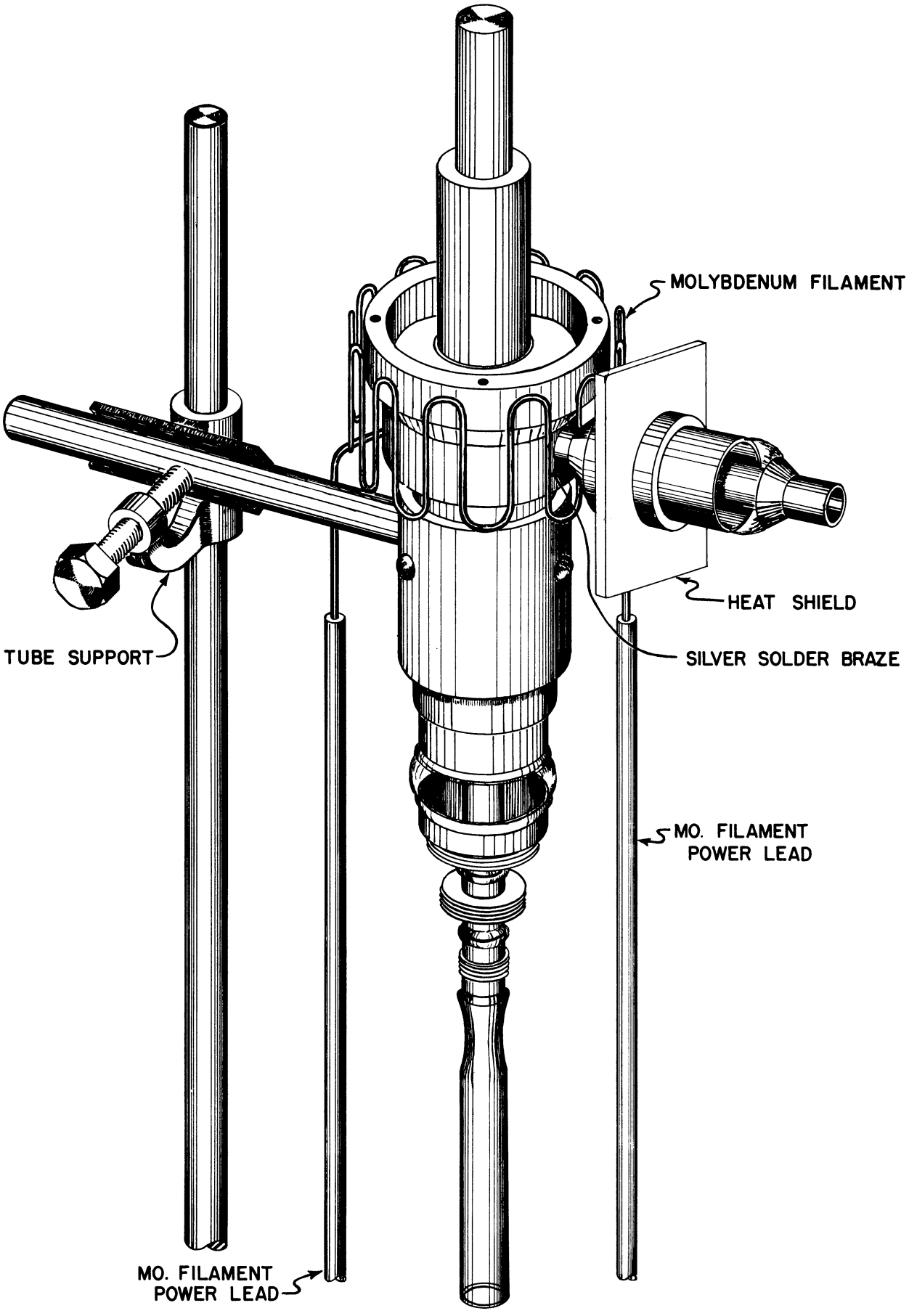

FIG. 10.6 4TH BRAZE - OUTPUT ASSEMBLY TO TUBE BODY

only the metal portion is baked at 625°C until the above vacuum is obtained. The tube is then ready for insertion of the cathode.

d. Construction of Cathode Parts

Drawings for the cathode used in model 4 magnetron are given in Appendix E of this report. It is a pure tungsten center-tapped bifilar filament. Temperature limited emission characteristics are shown in Figure 10.7.

Filament (Dwg No. A-8003-14): The filament is wound on a stainless steel jig (Figure 10.8) with grooves cut on it to take the tungsten wire. The filament is set by baking in a hydrogen atmosphere at 1000°C for 4 minutes and then removed from the jig using alcohol as a lubricant.

Center Support (Dwg No. A-8003-3): The center support is ground from .110-inch tungsten rod on an internal grinder set up especially for external grinding of this part. The slot is ground into the top by means of a small wheel set up in a milling machine.

Upper End Hat (Dwg No. A-8003-1): The upper end hat is turned from molybdenum rod. Especial care is taken to keep the top surface of this piece parallel with the under surface.

Lower End Hat (Dwg No. A-8003-2): The lower end hat is turned and drilled from molybdenum rod.

Upper Cathode (Dwg No. A-8003-8): The upper cathode is turned and drilled from molybdenum rod. The large hole is drilled to decrease the weight of this structure.

Slug (Dwg No. A-8003-13): The slug is turned and drilled from monel. The two outer holes are fitted with beryllia insulator sleeves held in place by prick punching the edges of the monel.

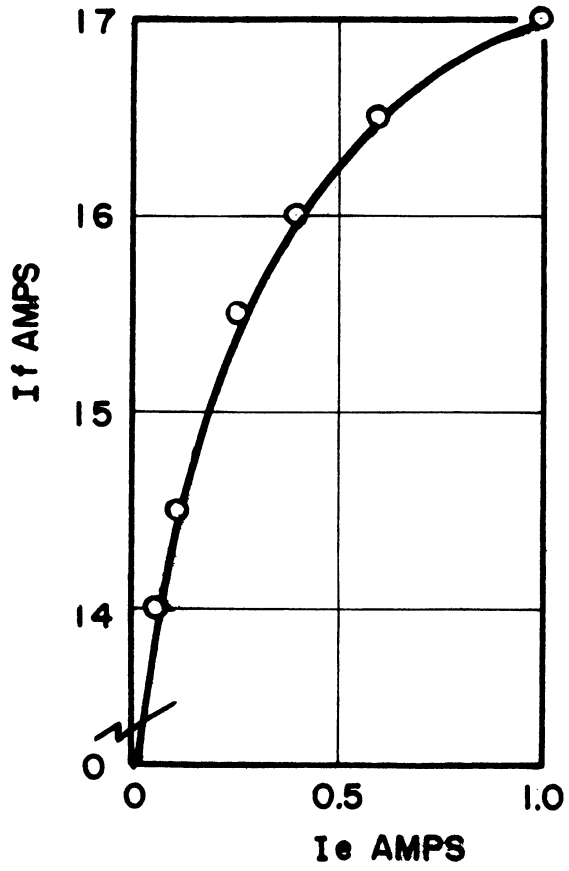

FIG. 10.7
EMISSION CURRENT VS. FILAMENT CURRENT MODEL 4 CATHODE TEMPERATURE LIMITED

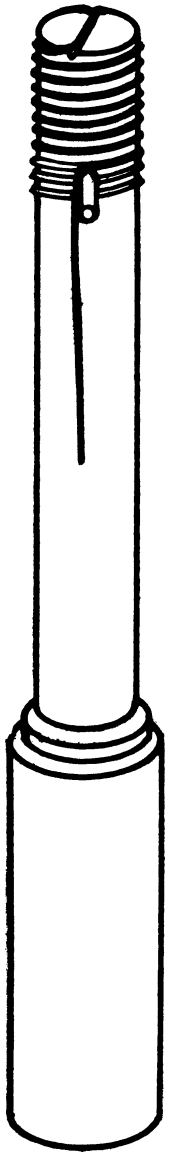

FIG. 10.8
FILAMENT FORMING JIG

Stem (Dwg No. A-8003-12): The stem is cut and drilled out of 3/8-inch Kovar tubing. Ten holes are drilled in this part to allow pumping of the tube. One end is polished inside and out with Aloxite No. 320 grit cloth.

Cup (Dwg No. A-8003-7): The cup is turned out of a drawn Kovar cup and polished with Aloxite No. 320 grit cloth.

Lugs (Dwg No. A-8003-9): Two lugs are cut and polished with Aloxite cloth from 3/8-inch Kovar tubing.

Connectors (Dwg No. A-8003-4,5,6): The connectors are turned from copper and threaded to take special parts designed to screw to the connectors furnishing good electrical contacts to the cathode and protecting the glass seals.

Leads (Dwg No. A-8003-10,11): .050-inch nickel leads are bent on jigs to shape. Molybdenum leads .040-inch diameter are later spot welded to these to carry the heater current to the filament.

e. Assembly of Cathode

The filament, center conductor and upper end hat are arc welded together in a hydrogen atmosphere using a carbon electrode. The parts are held in position by jigs shown in Figure 10.9. The stand is made of stainless steel and holds the center support vertical. A small cylinder of molybdenum slides between the filament and center support accurately holding the filament in alignment. A split spacer of molybdenum clamped between the two end hats holds the top end hat perpendicular to the center support. The arc is maintained long enough so the metal flows down into the slot anchoring the filament to the center support.

The next step is platinum soldering the upper cathode part to the filament sub-assembly. This is done in the hydrogen brazing jar where

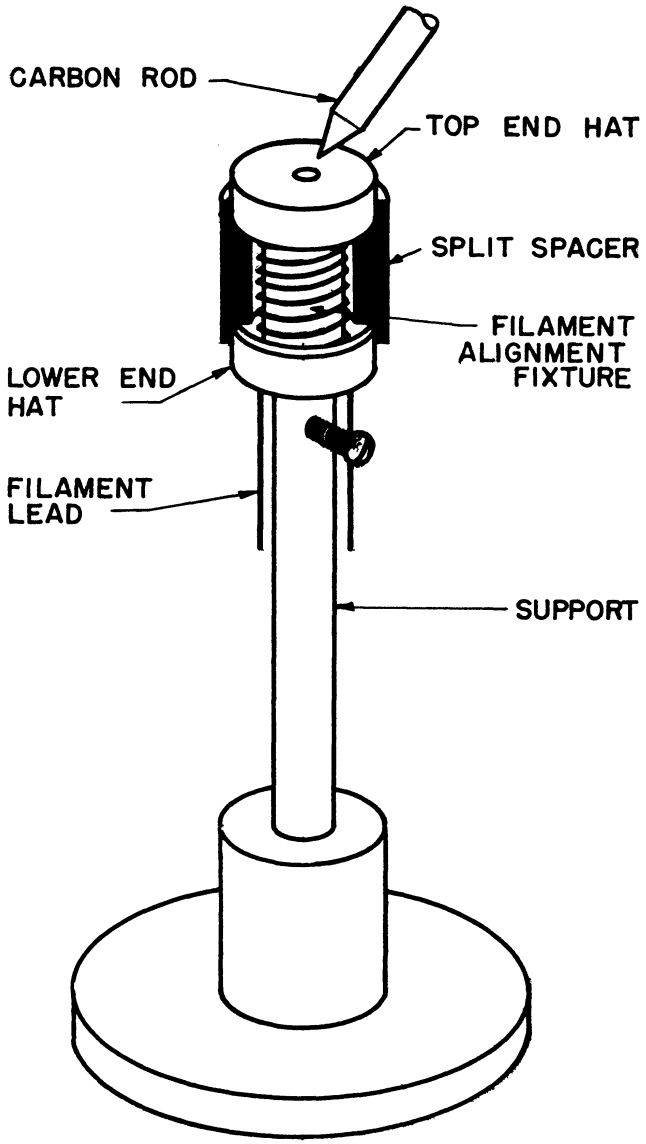

FIG. 10.9

TOP END HAT WELDING JIG

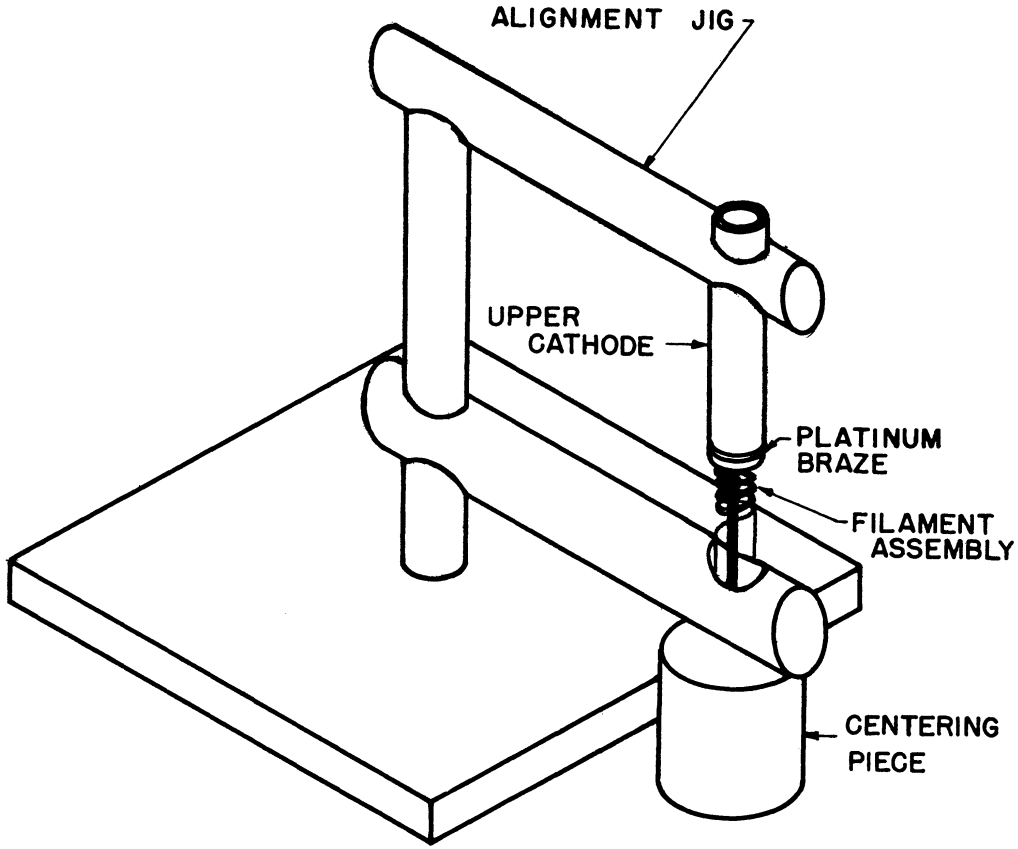

FIG. 10.10

UPPER CATHODE BRAZING JIG

platinum melting temperatures can be obtained. The parts are shown aligned by the jig in Figure 10.10. The jig is made of stainless steel and has two holes having a common axis machined in it. The upper cathode is held in the top hole while the filament sub-assembly is held in the bottom holes by means of a stainless steel slug. One turn of .015-inch Pt wire is placed at the joint and it is heated by means of an .080-inch diameter molybdenum filament spaced very close to the joint.

The lower end hat is then platinum soldered in the hydrogen brazing jar using the molybdenum split jig employed for aligning the upper end hat. This jig correctly spaces the end hats and holds the lower end hat perpendicular to the center support.

The connectors and leads are gold-copper brazed to the lugs in a stainless steel jig shown in Figure 10.11.

Figure 10.12 shows the stainless steel jig used for gold-copper brazing the upper connector and cup to the stem. The brazing of the lugs and stem is done in the hydrogen brazing jar where the solder can be carefully watched so the parts can be immediately cooled after the solder has run.

Inside-outside glass beads are next put on both ends of the lugs, on the cup and on the stem. Glass tubulation is sealed to the lower end of the bottom lug and a tip-off constriction formed in it near the lug. .040-inch molybdenum wires are next spot welded to the nickel leads before lugs are glassed to each other and to the stem. No glass is required for this glassing operation other than that already in the beads. This stem assembly is annealed in the annealing oven and later cleaned in Oakite No. 32 solution.

The monel slug and filament assembly are then copper brazed to the stem assembly. These two brazes are done simultaneously. Care is taken to have the molybdenum filament leads align with those of the filament.

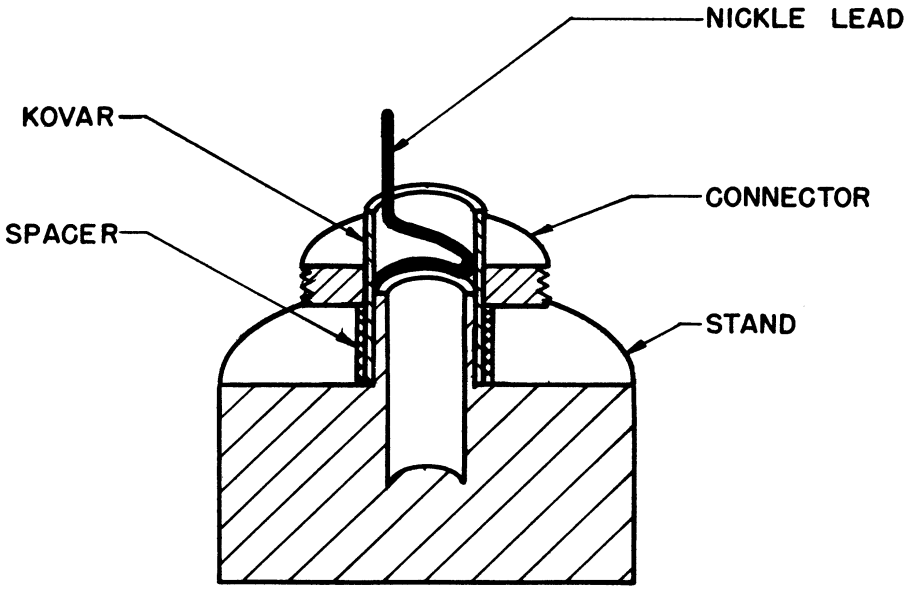

FIG. 10.11

CONNECTOR TO LUG BRAZING JIG.

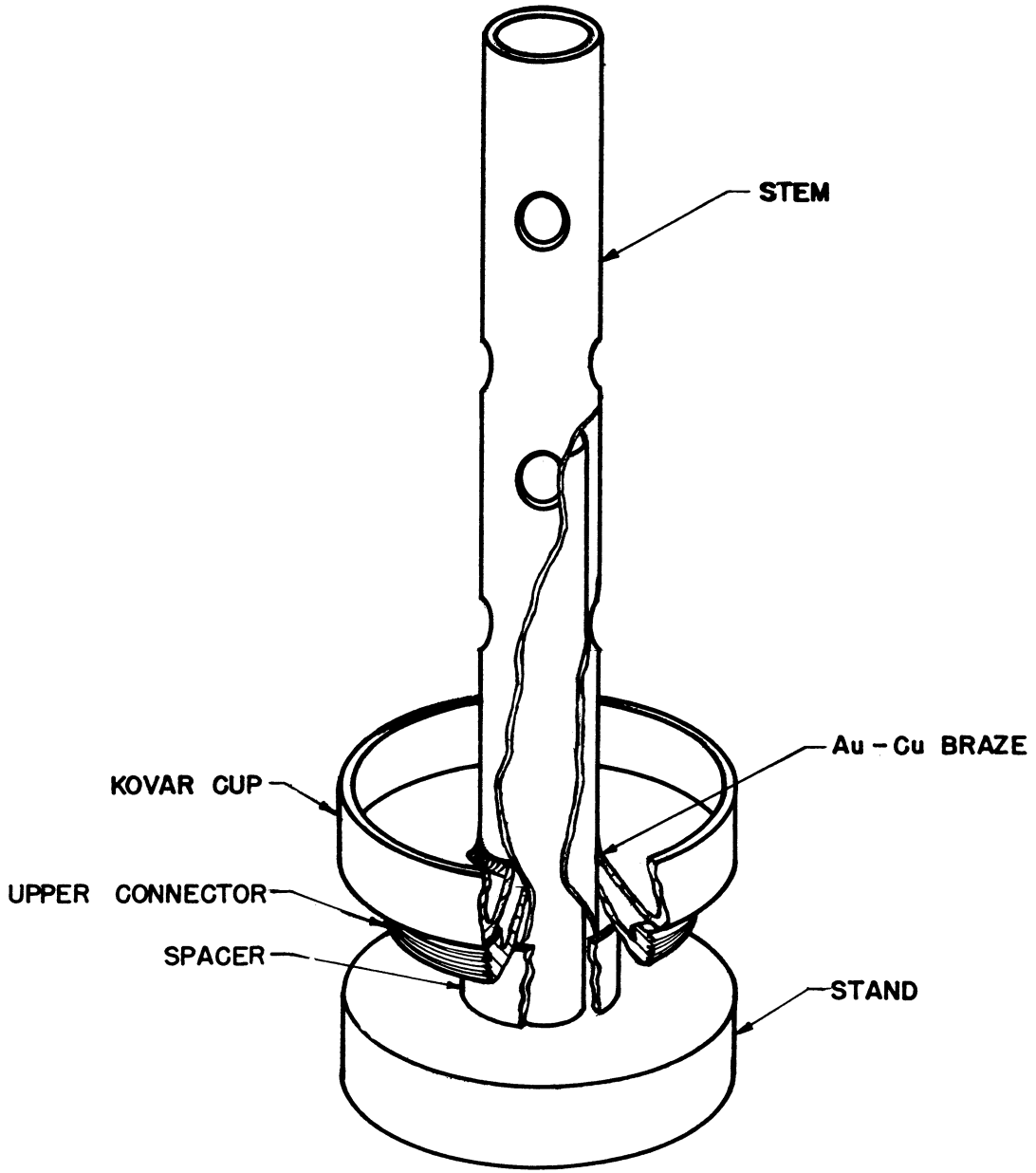

FIG. 10.12

CUP TO STEM BRAZING JIG

The leads are next arc welded to the filament in the hydrogen atmosphere carbon arc welder. The filament leads are aligned in the holes of the lower end hat by means of small glass beads which were hand drawn to size from a small glass tube. The beads are formed to just slide over the tungsten wire and fit snugly inside the lower end hat hole. The tungsten filaments are then arc welded to the molybdenum leads and the glass beads removed by means of hydrofluoric acid.

The cathode is cleaned, rinsed in alcohol, dried and lighted in a hydrogen atmosphere for final clean-up before sealing in the tube. The cathodes are stored in the hot box until used.

f. Assembly of Cathode to Tube Body

The tuner pole piece and yoke (Dwg No. A-9012 and A-9011) are silver soldered together by means of a hand torch and screwed to the tube cavity. The tube is held in the glass lathe by the tuner pole piece in a four-jawed chuck. It is centered accurately in the chuck by means of a special indicator shown in Figure 10.13. A test indicator is mounted on a lever bar and is calibrated to measure the end movement of the bar in thousandths of an inch. The bar can extend into the tube enabling one to indicate the anode fingers and align them accurately in the lathe.

The cathode is held by its stem in a wooden collet and is aligned by heating and bending the glass stem. A standard dial indicator is used to test the alignment of the cathode. The depth of cathode insertion is gaged by means of the jigs shown in Figure 10.14. The stop which is screwed onto the middle connector of the cathode is adjusted to length by means of an accurately measured jig. This sets the stop to a predetermined distance (distance from the center of the cavity to the lower outside edge of the cavity, plus three inches) from the center of the filament. This operation is shown

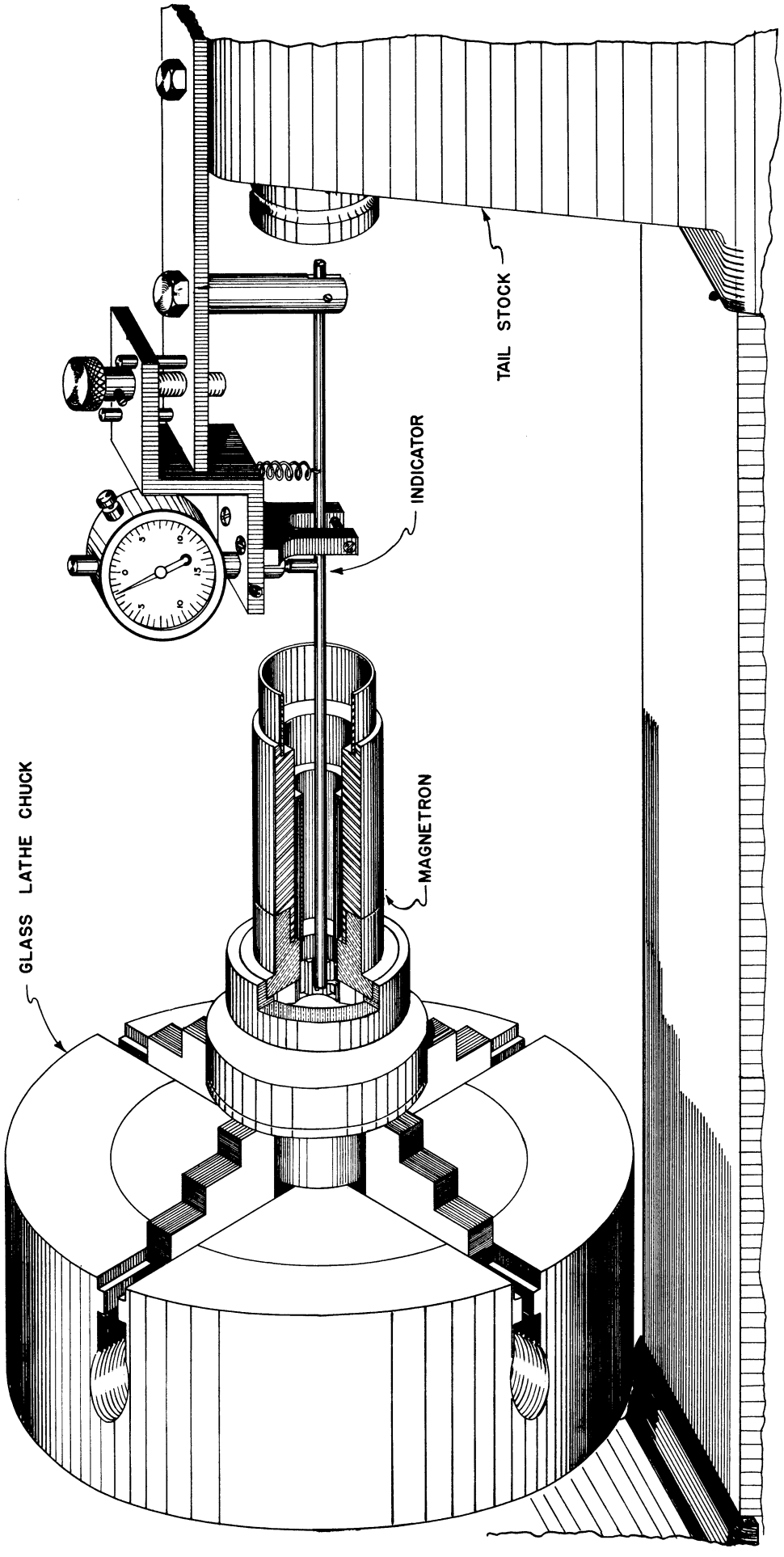

FIG. 10.13 TUBE ALIGNMENT JIG

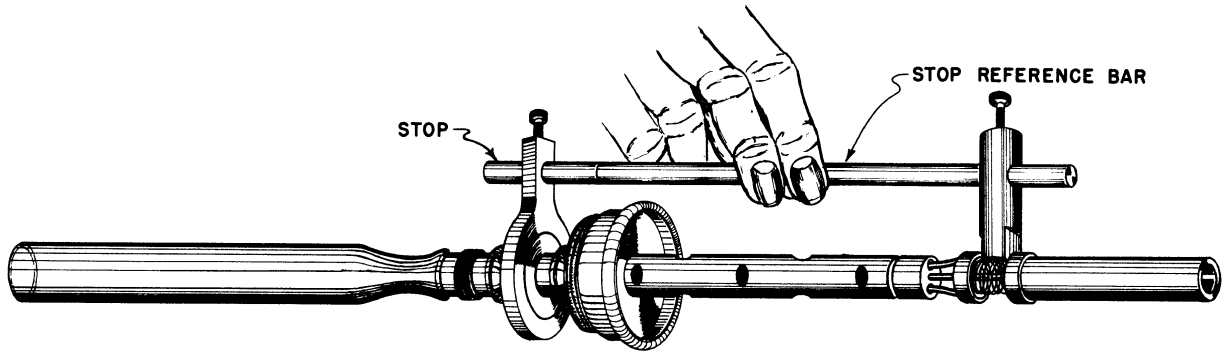

A

FIG. 10.14 STOP ADJUSTMENT

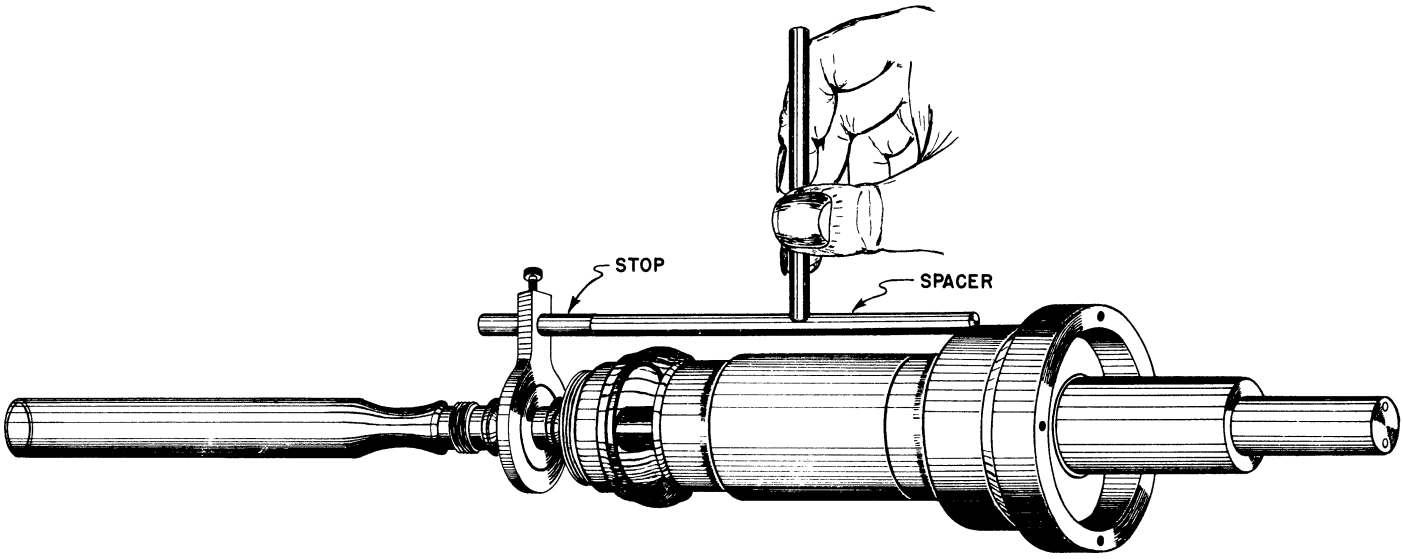

B

FIG. 10.14 CATHODE GLASSING DEPTH FIXTURE

in Figure 10.14, part A. When glassing the cathode to the tube body the cathode is inserted until the stop just hits a spacer (three inches long) placed between the stop and the bottom end of the cavity (Figure 10.14b). Thus the cathode is aligned concentrically and axially with the tube.

Nitrogen which has been passed over methanol is used to flush the tube before glassing and is also used for blowing. The alcohol in the nitrogen unites with any oxygen remaining in the tube, thus preventing oxidation of the tube and cathode during glassing.

g. Evacuation Procedure

The evacuation procedure given below is used successfully for tubes having thoriated tungsten filaments.

1. Seal the tube to vacuum system stem down, vertical position. A carbon heat shield is placed over stem to keep the tip-off flame away from the lower Kovar-glass seal.

2. Pump until ion gauge reading is less than .2 microampere (approximately 3×10^{-6} mm Hg).

3. Heat entire tube in large oven at 425°C for 2 hours or until ion gauge reads .2 microampere. Determine temperature with two thermocouples, one on tube body and one on glass seal.

4. Heat metal body of tube 7 to 8 hours at 625°C in small electric oven.

5. Turn filament up slowly to 20 amperes after ion gauge reading gets below .1 microampere (approximately one hour).

6. After 5 hours of heating and again just before end of run, flash the filament to 26 amperes for 30 seconds and then run at 23 amperes for 2 minutes.

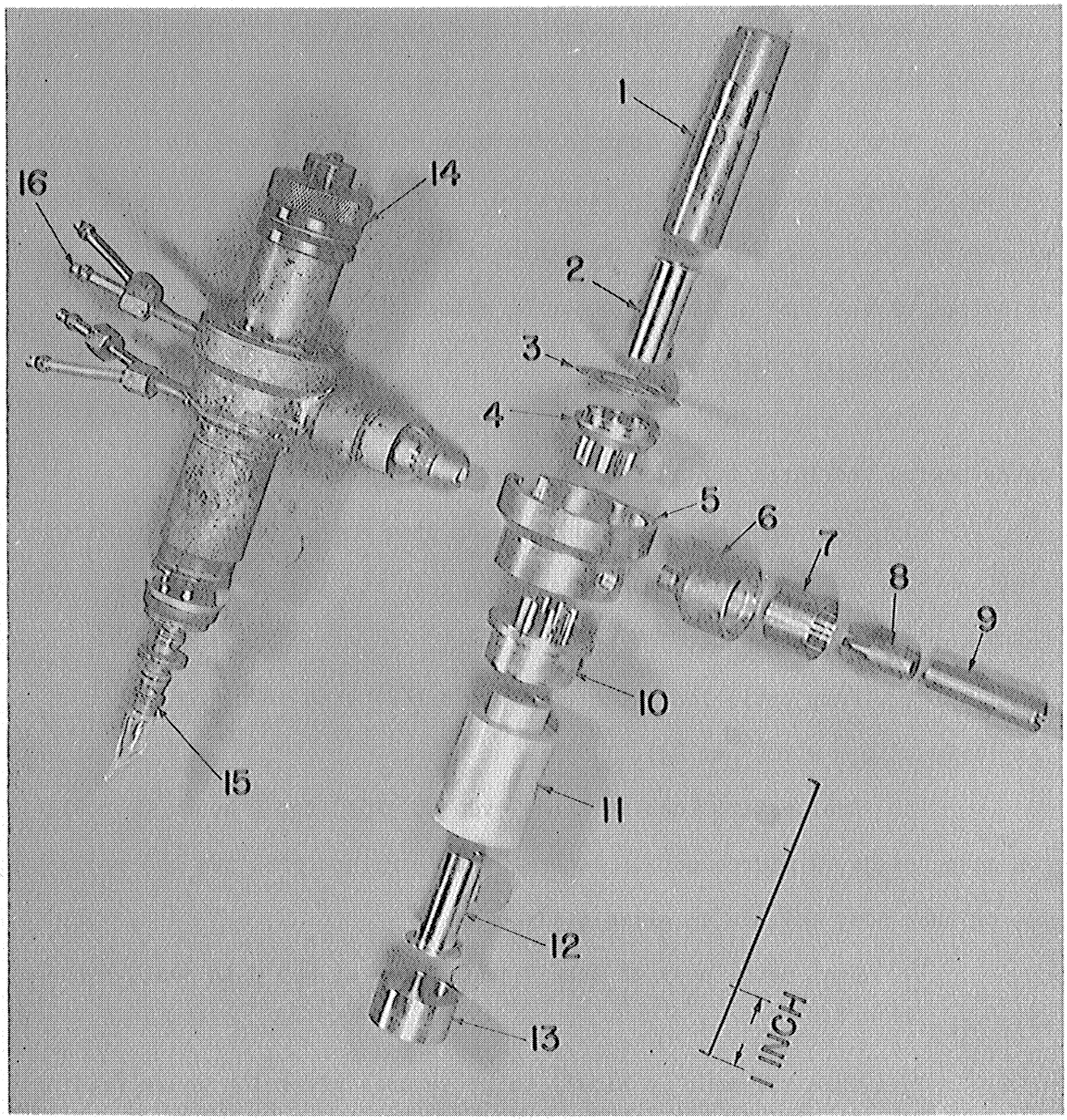

Figure 10.15 Interdigital Magnetron and Parts

1. Tuner screw
2. Tuner choke
3. Diaphragm
4. Diaphragm anode
5. Cavity
6. Outside taper
7. Outside Kovar
8. Inside taper
9. Inside Kovar
10. Cavity anode
11. Cathode pole piece
12. Cathode choke
13. Kovar sleeve
14. Tuner pole piece assembly
15. Cathode assembly
16. Water cooling tubes

7. Turn off filament and remove small oven; bake whole tube in large oven at 425°C for 3 hours.

8. Turn oven off, heat metal body to 625°C for 2 hours, filament at 20 amperes, ion gauge reading should be down to about .05 microampere (between 10^{-6} and 10^{-7} mm Hg).

9. Remove oven, flash filament to 26 amperes for 5 seconds, 5 times, 2 minutes apart; hold at 18 amperes between flashes; then run at 20 amperes for 30 minutes.

10. Run plate voltage for 1-1/2 hours. Set filament at I_f = 18 amperes and set plate voltage so that approximately 300 watts is dissipated in the anode.

11. Spark with Tesla coil to remove points of cold emission.

12. Flash and season as in step No. 9.

13. Seal off pumps while tube is still hot. Gradually heat glass so any gas given off is pumped out. Flame anneal tip-off.

h. Final Assembly

Copper tubes for cooling the tube are soft soldered to the lower end of the cavity and to the upper anode. A thrust ball bearing assembly (Nice No. 1005) is placed over the tuner screw and the tuning nut (Dwg No. A-9004) is screwed onto the tuner screw. The tube is now ready for insertion into the magnet and for operation.

A photograph of an assembled magnetron and parts is given in Figure 10.15.

11. Performance Tests on Interdigital Magnetrons

The details of performance results are discussed in Technical Report No. 2, Section 7. The experimental results agree very well with predicted performance. Of the seven interdigital tubes which have been operated, three are still operable. The results may be summarized as follows.

a. Model 2 Magnetrons: Two model 2 magnetrons were operated. Maximum observed efficiency was 22.5 per cent. Predicted efficiency is 32 per cent. Mode jump current was low. Tuning range of these tubes was from 15.5 cm to 17.5 cm. One tube was lost before any measurements other than wavelength were made. Apparently the cause was destruction of the cathode from excessive back heating during moding.

b. Model 3 Magnetrons: Two model 3 magnetrons were operated. One was restricted to pulse operation because a misaligned by-pass sleeve caused arc-over when steady voltage was applied. The other has been operable for a year and a half. Maximum observed efficiency is 72 per cent at 500 watts c-w output. Predicted efficiency is 70 per cent. Operable tuning range of this tube is from 16.4 cm to 19.5 cm. Back heating is very slight; mode jump current is high over high efficiency portion of the tuning range. This tube has been used in measurements on space charge clouds and cyclotron resonance.

c. Model 3A Magnetron: One model 3A magnetron was operated. The cathode was slightly misaligned, causing intermittent shorts on the long wavelength end of the tuning range. Maximum observed efficiency was 42 per cent at 100 watts c-w output. Operable tuning range on this tube was from 14.9 cm to 16 cm. The results on this tube combined with the results on model 3 give a broad picture of the performance of the cathode choke and by-pass combination.

d. Model 4 and Model 4A Magnetrons: One model 4 and one model 4A tube have been operated. Neither tube will oscillate in the zero order mode. Oscillations were obtained in the first and second order modes at 7 cm and 10 cm. Model 4 and model 4A are different in the axial spacing of the by-

pass sleeve from the anode base. Cold tests show that the by-pass is not spaced closely enough to the cathode. This is being corrected on a second revision. Both tubes oscillate in the first and second order modes. Less than fifty watts output is observed. Extensive quantitative measurements have not been made because efficiency is poor. Both tubes are still operable.

e. General Results: Table 11.1 summarizes the results on four models. Measured wavelength is from 3 to 6 per cent greater than predicted wavelength. This is in part due to neglect of the effect of capacitance to cathode in the calculation, and in part due to over-simplified approach to the equivalent circuit. This latter is especially the case for the model 3A tube. In this tube, the tooth thickness is nearly equal to the radial cavity thickness (outer cavity radius - inner cavity radius) so the assumption that the capacitance is lumped is probably not valid.

Predictions based on interaction space design, such as Hartree voltage and electronic efficiency, check very well with results.

Effect of the cathode line on the performance of all tubes agrees with theoretical analysis. Both model 2 and model 3 exhibit a maximum efficiency at a point in the tuning range corresponding to maximum impedance of the cathode line. These facts were discovered first by experience and later by analysis.

Factors influencing mode separation are fairly well indicated by the experience with four models. Factors affecting mode jump current appear to be shunt impedance, interaction space design, cathode emission and mode separation. In a given magnetron, for instance, mode jump current can generally be increased by increasing shunt impedance, emission and mode separation. The function of all factors depending on interaction space design is not yet clear, although it is fairly certain that, in a given tube,

TABLE 11.1

Summary of Performance of Magnetrons Built at University of Michigan

Magnetron	λ_o (cm)		Mode	E_o	B_o	E	B	B/B_o	$\frac{E_{Hartree}}{E_o}$		Q_o	Q_L	η_e(%)	η_c(%)	η(%)	
	calc.	meas.		volts	gauss	volts	gauss		calc.	meas.	meas.	meas.	calc. max.	calc.	calc. max.	meas.
Model 2	15	15.6	$n=\frac{N}{2}=4$	1130	360	4400	900	2.5	4.0	3.9	503	251	75	48	36	22.5
Model 3	16	17.0	$n=\frac{N}{2}=6$	196	329	2500	2100	6.4	11.8	12.7	510	120	92	76	70	72
Model 3A	13	14.6	$n=\frac{N}{2}=6$	266	383	2400	2100	5.5	9.0	9.4	--	--	89	55 est.	48 est.	43 at 15.8 cm
Model 4	14	14.6	$n=\frac{N}{2}=8$	327	274	2100 calc.	1000 assumed	3.7	6.4	--	98	58	84.5	41	34	--

higher voltage, lower current operation demands higher shunt impedance.

12. Experimental Study of Magnetron Space Charge

Experimental measurements on the space charge have been designed to determine the effect of the space charge on resonant circuit characteristics under various conditions of magnetic field, anode potential and r-f voltage. Most of the measurements were completed before the theory outlined in Sections 4 and 5 was fully developed. However, the magnetic fields used were widely enough separated to yield results falling in regions of both positive and negative dielectric constant.

The measurements taken are of four types as outlined below.

a. Impedance Measurements at Constant Magnetic Field and R-F Voltage, Anode Potential as Variable Parameter: Data of this type have been recorded on QK59 magnetrons obtained commercially. Unloaded Q, resonant wavelength and input conductance are measured as a function of anode potential using a constant r-f voltage and magnetic field. For the same magnetic field, the same kind of data are then obtained for other r-f voltages. High r-f voltage is obtained by using a second magnetron for a signal generator. An attenuator is placed between the signal generator magnetron and the magnetron under investigation. This attenuator serves both as protection for the signal generator magnetron and as a means of varying the r-f voltage. Typical data of this type are shown in Figure 12.1. These experiments illustrate: (1) sharp rise in Q and drop in conductance just before tube starts oscillating as electrons contribute energy to balance losses in the system; (2) wavelength shift with voltage as electron swarm of negative dielectric constant expands; (3) lowering of the entire Q curve as r-f voltage is increased due to increased losses caused by back bombardment.

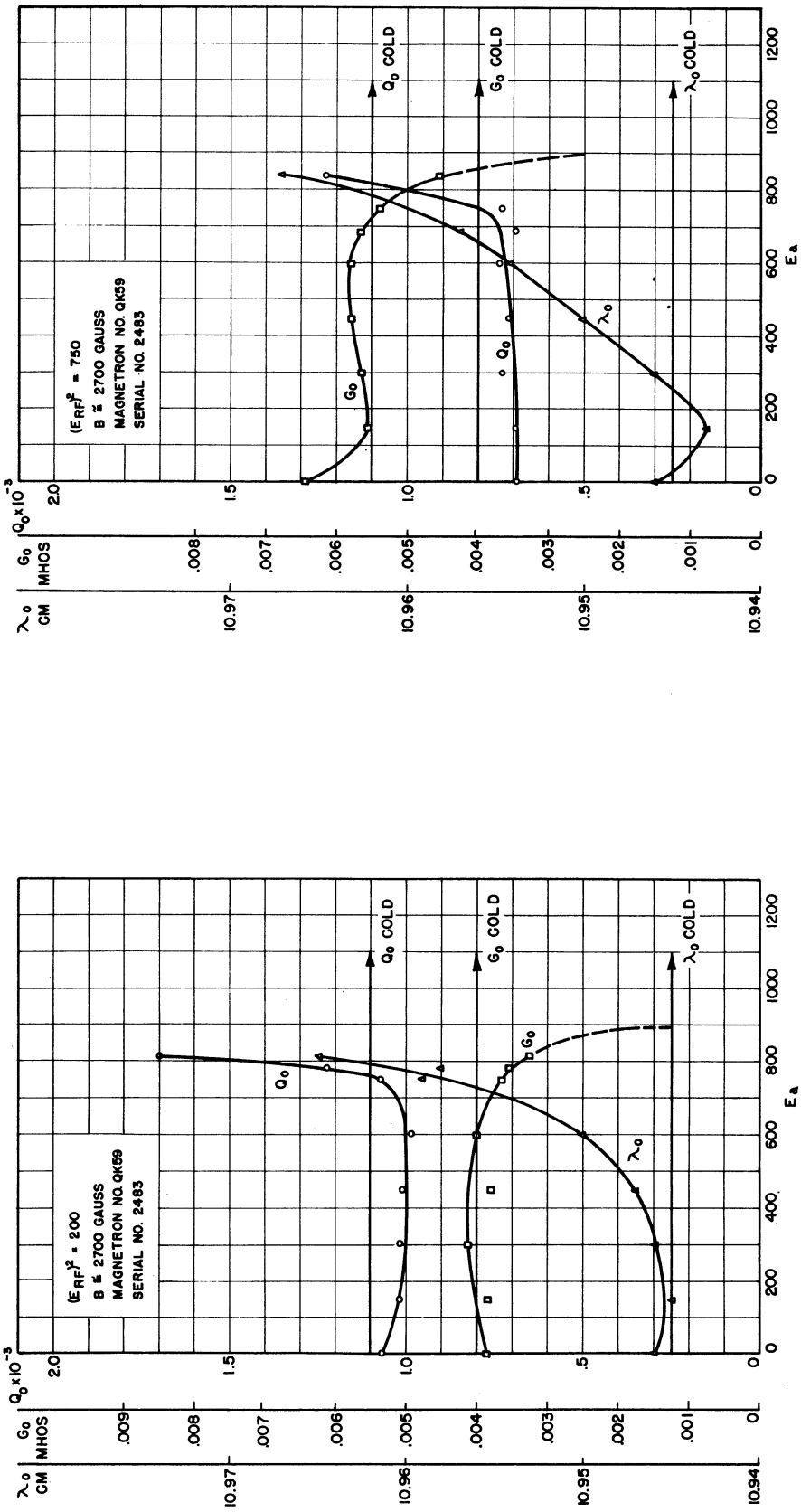

FIG. 12.1b

FIG. 12.1a

FIG. 12.1 Q_0, λ_0, G_0 OF HOT MAGNETRON AS A FUNCTION OF PLATE VOLTAGE FOR VARIOUS RF VOLTAGES

b. Impedance Measurement at Constant Magnetic Field and Anode Potential, R-F Voltage as Variable Parameter: Data of this type have also been recorded on QK59 magnetrons at anode potentials about half of the value necessary to start oscillation. Data are recorded just as in (a). The anode voltage selected is about half of the voltage necessary for oscillation. Typical curves are given in Figure 12.2 This experiment shows that when r-f voltage exceeds a moderate value, losses increase rapidly due to back bombardment, and that resonant wavelength is not materially affected. Plate current is negligible in both (a) and (b).

c. Resonant Wavelength Measurement at Low R-F Voltage for Different Magnetic Fields, Anode Potential as Variable Parameter: Data of this type have been recorded on a model 3 magnetron. Resonant wavelength and input

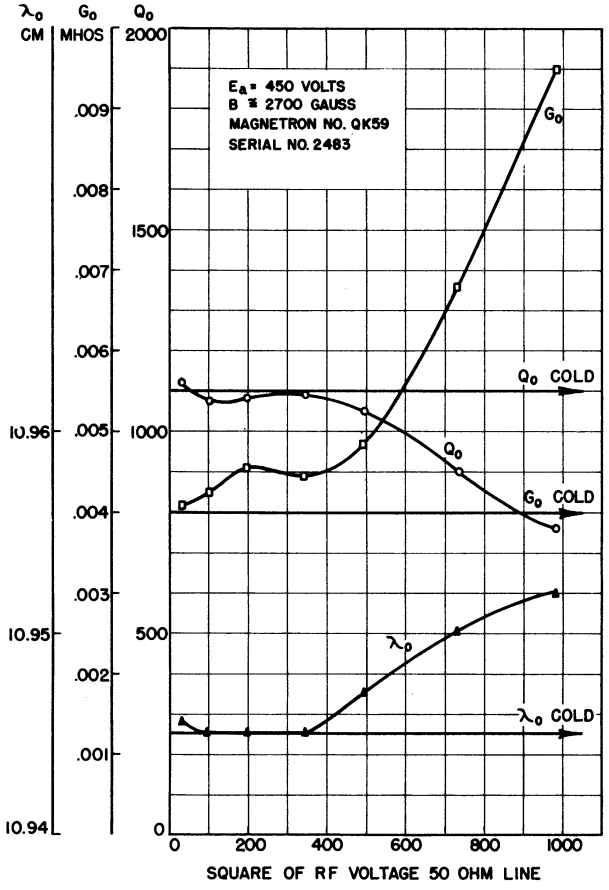

FIG. 12.2-Q_0, λ_0, G_0 OF HOT MAGNETRON AS FUNCTION OF RF VOLTAGE FOR PLATE VOLTAGE

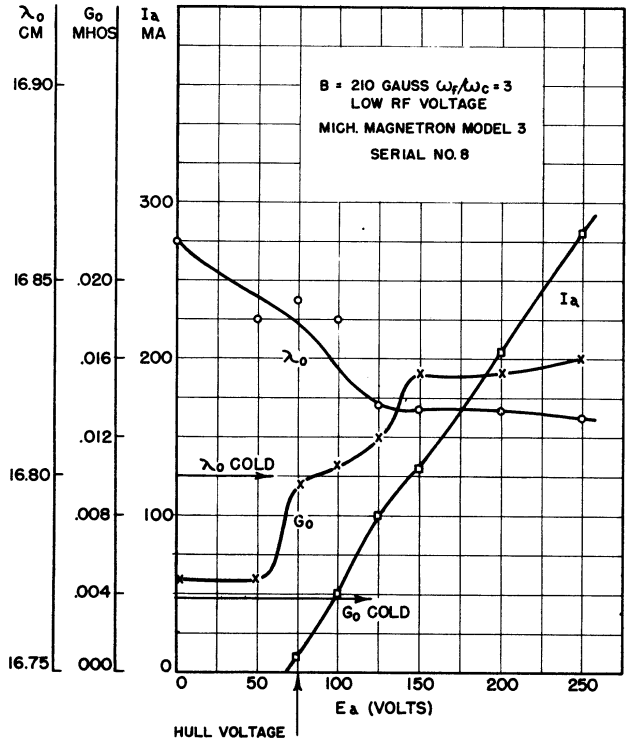

FIG. 12.3a

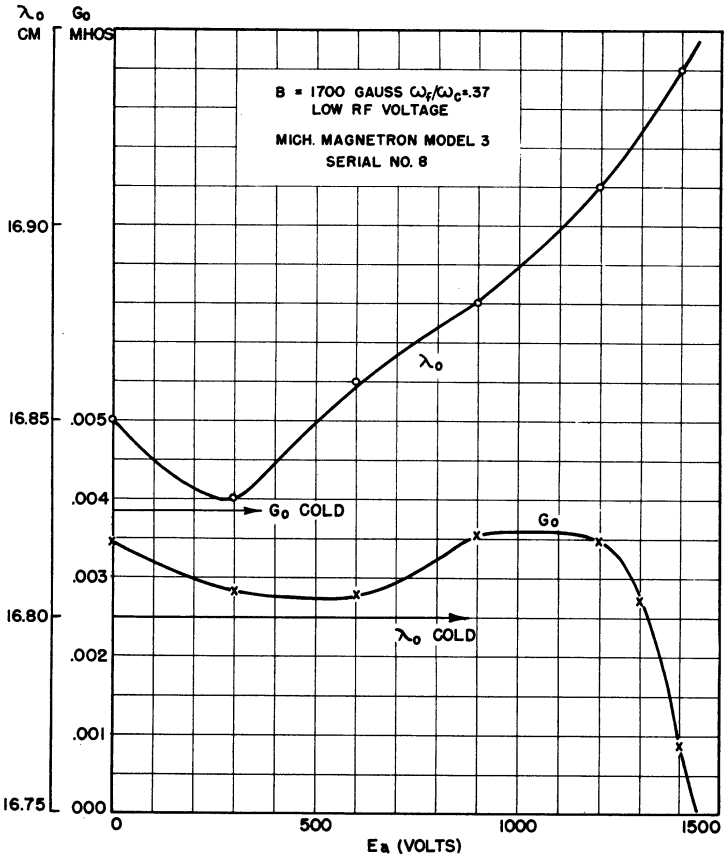

FIG. 12.3b

FIG. 12.3 λ_o AND G_o OF HOT MAGNETRON AS FUNCTION OF PLATE VOLTAGE

conductance only were measured. The primary purpose was to find the effect of magnetic field on wavelength shift with applied d-c voltage. Typical data are shown in Figure 12.3. Calculated values of the wavelength shift to be expected in these experiments agree very closely with the observed values. In the case illustrated by Figure 12.3a, the dielectric constant of the space charge is positive. The calculated shift in wavelength up to the Hull voltage is .021 cm. The observed value is .025 cm. Anode current (I_a) is drawn above this point and the space is filled with electrons so that no further shift in wavelength is to be expected unless due to changing cloud density. In the case illustrated by Figure 12.3b, the dielectric constant of the space charge is negative. The calculated wavelength shift is .095 cm. The observed value is 0.11 cm. The wavelength shift is limited in this case to the value corresponding to the voltage at which oscillation begins.

d. Resonant Wavelength Measurement at Low R-F Voltage and Constant Cloud Radius, Magnetic Field as Variable Parameter: Cloud radius is kept constant by keeping the ratio E/B^2 (anode voltage to square of the magnetic field) constant. Data have been recorded on a model 3 magnetron in the vicinity of the cyclotron resonance. A typical curve is given in Figure 12.4. This illustrates the effect of the resonances of the individual electrons. More data are needed in this region to give a clear picture of the electron behavior. Reference to Figure 4.3 will show that very complex behavior is expected in the region of the cyclotron resonance.

The major importance of these experiments is that they conform to the ideas based on the effective relative dielectric constant of space charge swarms, and show that the simple solution for the magnetron space charge based on the rotating swarm hypothesis with no radial velocities is sufficiently accurate to predict quantitatively the results of certain experiments.

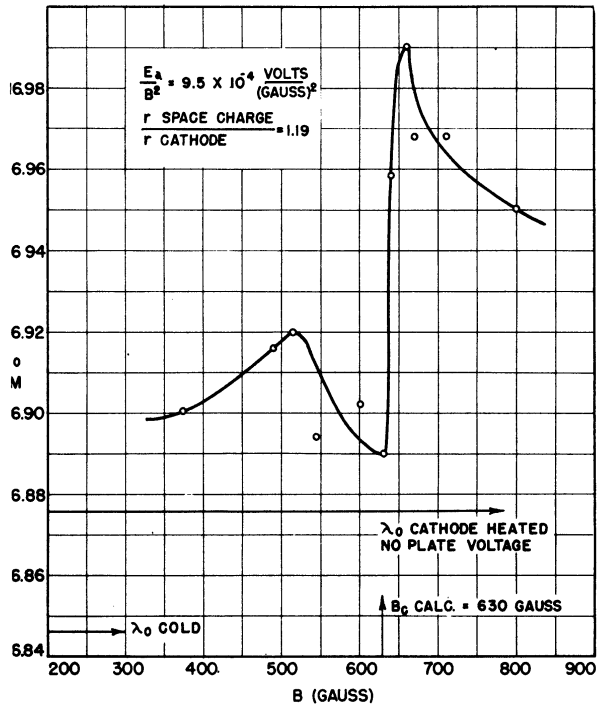

FIG. 12.4 DATA ON CYCLOTRON RESONANCE. λ_0 AS A FUNCTION OF MAGNETIC FIELD FOR HOT MAGNETRON. RADIUS OF SPACE CHARGE BOUNDARY CONSTANT.

This last statement is based on the fact that the boundary of the swarm which must be calculated to determine the wavelength shift is known only through measurement of anode voltage. In order to relate this boundary to anode voltage, it is necessary to use the space charge density within the swarm. This density is determined on the basis of the rotating swarm hypothesis. We are thus provided with a rather firm basis for design of frequency modulation magnetrons. The effects of high r-f voltage are not yet calculable, but these experiments indicate that, although losses will increase, it may be possible to operate at a constant loss on the plateau of a curve similar to 12.1b and thus achieve a minimum of amplitude modulation.

13. Measurements on R-F Circuit of F-M Magnetrons

As has been pointed out previously, one of the advantages of the interdigital magnetron is the possibility of obtaining frequency modulation by means of varying the reactance coupled into the cavity from the cathode line. This effect has been used in the design of an f-m interdigital magnetron. Two other forms of interdigital magnetrons designed for frequency modulation have also been studied. All of these designs involve frequency modulation by means of expanding a cylindrical space charge cloud in a region of the r-f circuit of the tube where the change in reactance can be coupled with the oscillating section to produce a change in frequency. Measurements made on brass models of these tubes are discussed below.

a. Model 5: It has been shown by means of Figure 9.3 that the reactance coupled into the cavity by means of the cathode line can be used to give a considerable resonant wavelength shift. This effect has been used in the design of an f-m interdigital magnetron, shown together with its equivalent circuit in Figure 13.1. It is seen that the cathode circuit is a coaxial line approximately one wavelength long with the oscillator cathode inserted in one end and a modulator cathode in the other end so that their emitting surfaces are at high r-f voltage points. The cavity is placed at one high voltage point and the modulator anode at the other. The voltage distribution along the cathode line is shown in Figure 13.2, which demonstrates the correct placement of modulator anode, etc. The model used in these measurements is shown in Figure 13.3. The tuning is achieved by varying the impedance Z_1 presented at the cavity by varying the diameter of a rotating space charge cloud at the voltage maximum point. As was discussed briefly in Section 5, it can be shown that under certain conditions of applied magnetic field relative to signal frequency used, the outer

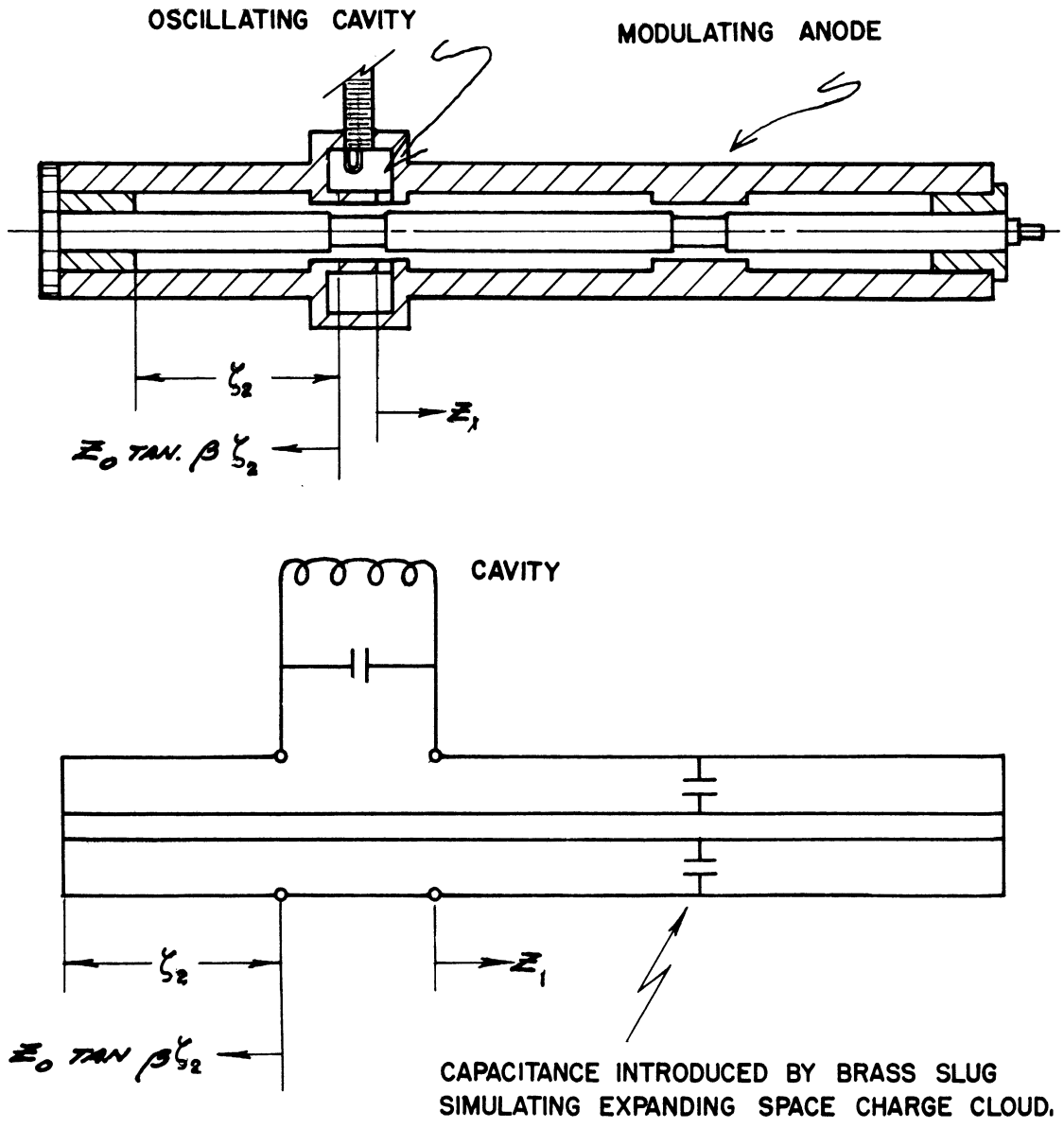

FIG. 13.1 EQUIVALENT CIRCUIT OF MODEL 5 F-M MAGNETRON.

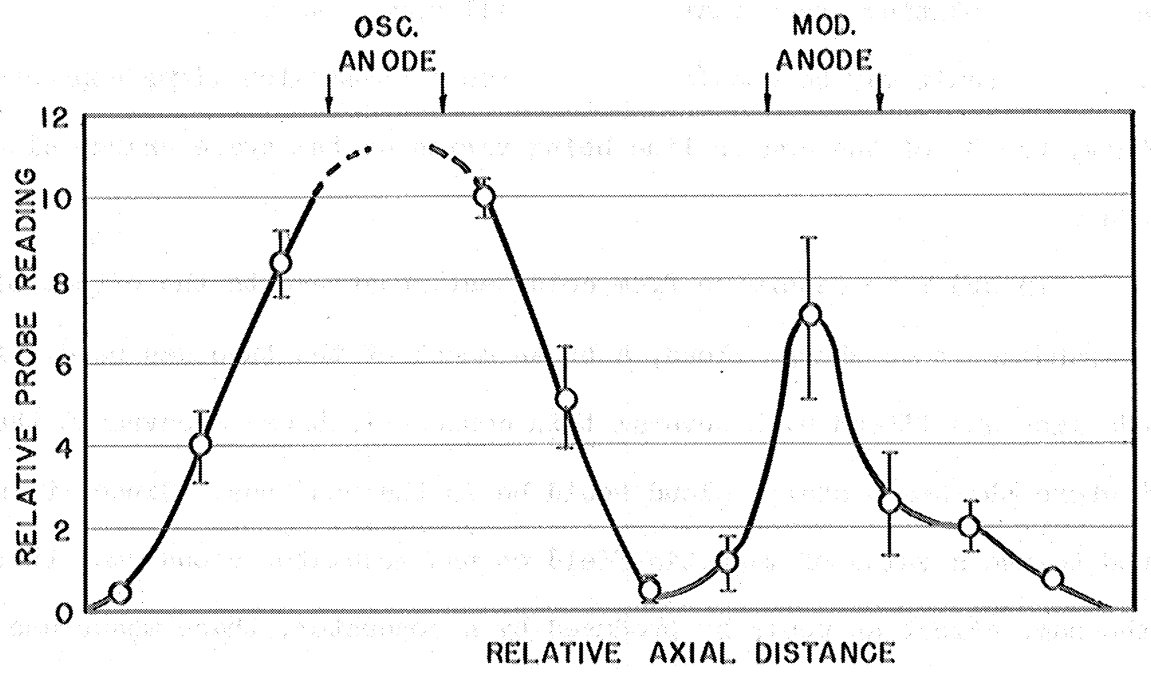

FIG. 13.2
AXIAL DISTRIBUTION OF FIELD
IN COLD TEST MODEL 5 EM. MAGNETRON

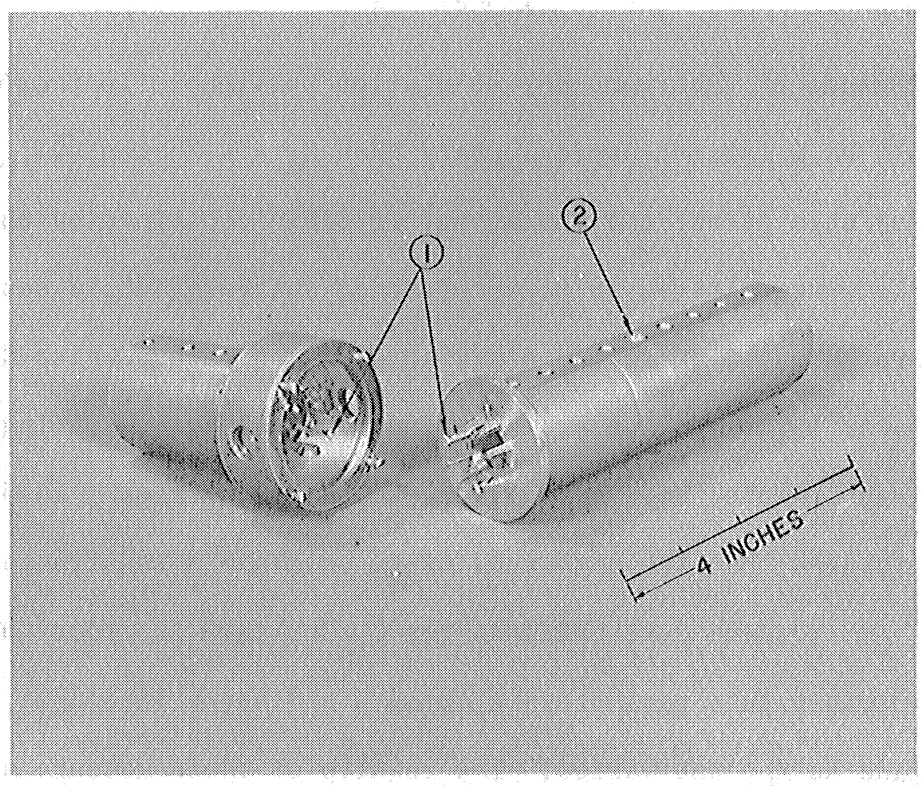

Figure 13.3 Brass Model of Model 5 Magnetron with Tapered Tooth Structure
(1) Oscillator Anodes
(2) Modulator Anodes

surface of a rotating space charge cloud will appear as a conducting sheet. Thus, this circuit may be considered as three transmission lines connected together, the Z_o of the center line being varied as the space charge cloud expands.

In order to determine from cold test measurements the effect of this expanding space charge cloud, a brass model of the tube was used. The cathode line was fitted with several thin concentric brass sleeves at the point where the space charge cloud would be in the hot tube. Since it is planned to use a value of magnetic field on the modulator cloud such that it has the same effect as would be produced by a conductor, these measurements should duplicate actual electronic performance.

The condition for resonance in the system is

$$\frac{\lambda^2}{2\pi cL} - \frac{\lambda}{Z_o \tan \frac{2\pi}{\lambda}\zeta_2 + Z_1} - 2\pi c C_A = 0 \qquad (13.1)$$

Thus the magnitude of the frequency modulation obtainable is proportional to ζ_2 and should be a maximum approximately when $Z_1 = - Z_o \tan \frac{2\pi}{\lambda}\zeta_2$. In order to check this effect and the amount of tuning obtained by the use of the concentric brass sleeves in place of space charge cloud, a set of measurements were taken of $\Delta\lambda$ versus diameter of brass sleeve, with distance ζ_2 as parameter. The results are shown in Figure 13.4. Plotting the value of $\Delta\lambda$ for given diameter versus ζ_2, curves 1 and 2 of Figure 13.5 are obtained. It is seen that the magnitude of $\Delta\lambda$ obtainable is affected by changes in ζ_2. No data were obtained for $\zeta_2 > 5$ cm. In order to determine the effect on other tube parameters such as Q and shunt impedance, Q measurements were made as ζ_2 was varied. The results of these measurements are shown in curve 3 of Figure 13.5. It is seen that from a standpoint of Q,

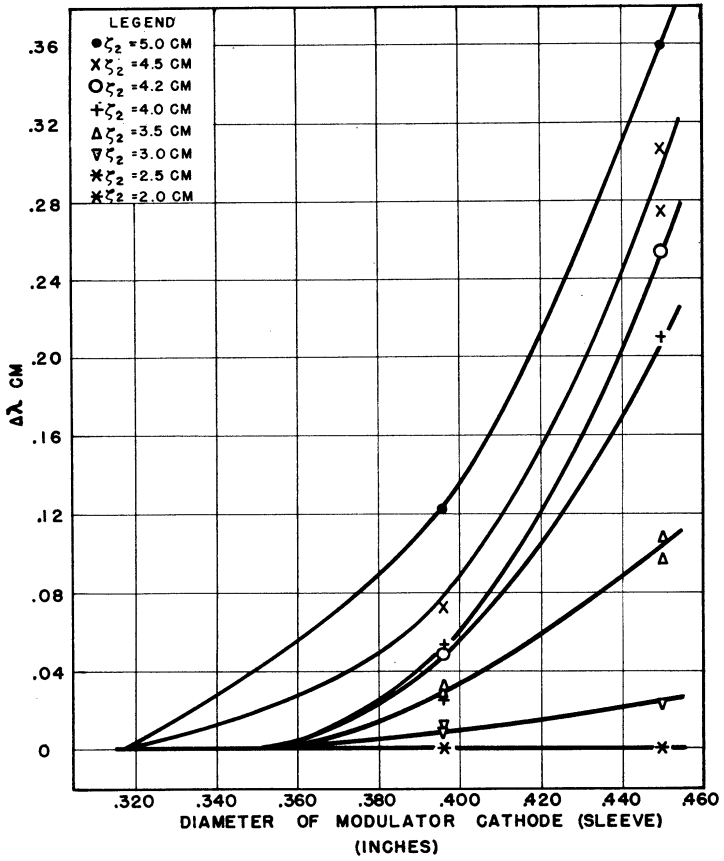

FIG. 13.4
SHIFT IN RESONANT WAVELENGTH OF BRASS MODEL 5 FM MAGNETRON WITH CHANGE IN CATHODE SLEEVE DIAMETER MODULATOR. DISTANCE FROM END OF FINGER TO SHORTING PLUNGER AS PARAMETER (ζ_2)

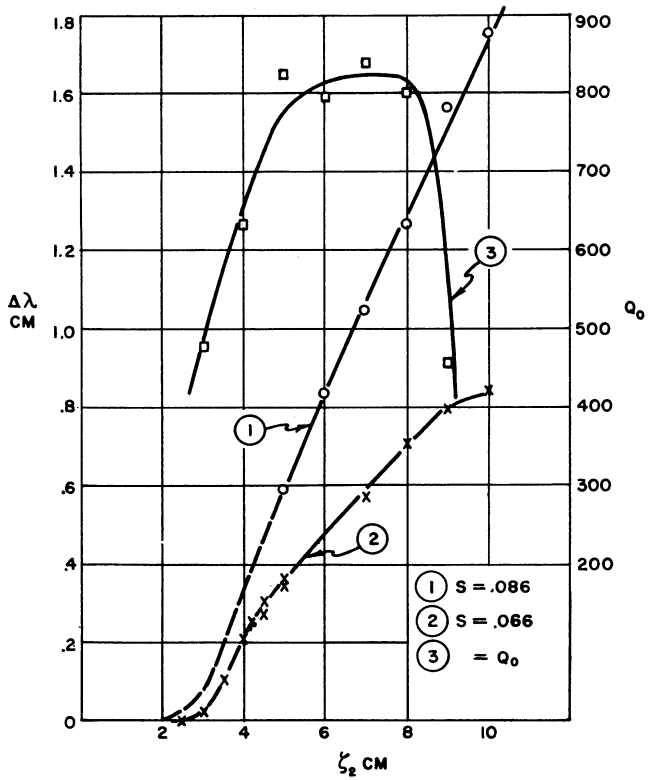

FIG. 13.5 $\Delta\lambda$ VS ζ_2 FOR TWO THICKNESSES OF BRASS SLEEVE (S) SIMULATING SPACE CHARGE CLOUD.

the circuit should be satisfactory for ζ_2 as great as 8 cm, giving a value of $\Delta\lambda$ as great as 1.25 cm. Of course, for such large shift this analysis is not exact but should seem to indicate the variables which must be considered in the design of a structure of this kind for maximum frequency modulation. Using the data of Figure 13.4 of $\Delta\lambda$ versus diameter of space charge cloud, together with the known Hull relation between diameter of space charge cloud and voltage applied, the magnitude of $\Delta\lambda$ versus voltage can be computed. This was done and reasonable linearity of $\Delta\lambda$ versus modulating voltage can be obtained up to $\Delta\lambda \simeq .06$ cm. Consideration of the properties of the space charge cloud and the capacitance change of concentric condensers reveals that the linearity should be limited to regions where the edge of the cloud is not close to the modulating anode. This is so since the capacitance change is greater per unit change in radius as the anode is approached, and also the change in radius with voltage is greater as the anode is approached.

Parts have been machined for an operating model 5, but assembly has not been completed for reasons discussed in the next section.

b. Model 6: The model 6 magnetron uses a novel type of resonant cavity which stems essentially from the interdigital principle. As shown by Figure 13.6, the model 6 f-m magnetron consists of a coaxial cavity which is electrically one wavelength long, loaded at each high voltage point by a set of radial vanes, the ends of which penetrate into slots in the inner conductor. One set of vanes is intended for use for frequency modulation, the capacitance between vane and inner conductor being changed by the expanding space charge cloud. The other set of vanes is intended as the oscillator section. The cathodes are inserted inside the center conductor.

In order to determine the capacitance introduced by each of the vanes, a series of measurements were made of cavity length versus resonant

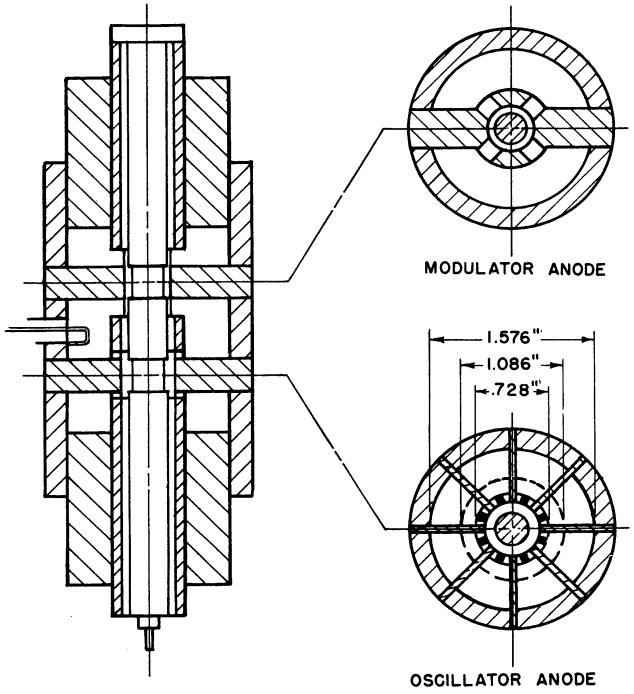

FIG. 13.6 MODEL 6 COAXIAL FM MAGNETRON

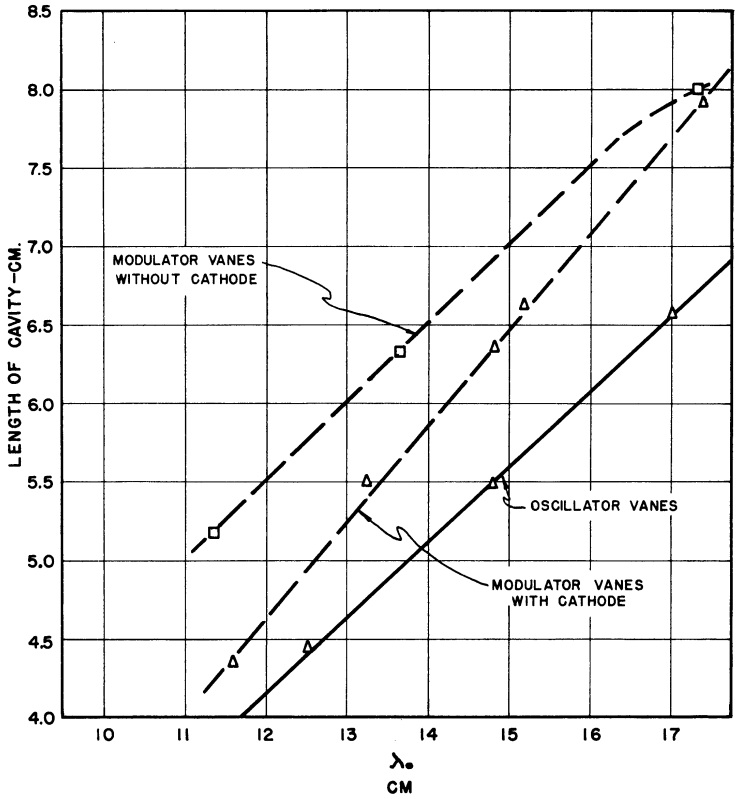

FIG. 13.7

LENGTH OF CAVITY vs. RESONATE WAVELENGTH FOR COAXIAL CAVITY LOADED BY OSCILLATOR AND MODULATOR VANES. MODEL 6 F-M MAGNETRON.

wavelength for only oscillator vanes, with each shorting plunger symmetrically spaced from the vanes. These readings were repeated as each pair of vanes was added, allowing an accurate determination of the capacitance per vane as 0.33 $\mu\mu$f. The capacitance of the modulator vanes was also determined in this way with and without the cathode in place. Since the modulator vanes are intended to change the circuit capacitance, the area of vane exposed to cathode is greater and spacing of end of vane to cathode is less than the oscillator vanes so that while very slight effect of the presence of the cathode on oscillator circuit resonance is noted, an appreciable effect is seen for the modulator vanes. The results of these measurements are shown in Figure 13.7 which enables the design of a tube of this type to be made for any desired wavelength.

In the search for a suitable output coupling system for this cavity, several designs of probes and loops were tried. It was found that for effective coupling, the output wire must be connected directly to the inner conductor of the coaxial line forming the cavity. In order to find the proper position along the line to place the coupling for desirable Q and circuit efficiency values, measurements of external Q and circuit efficiency versus length of line from shorting plunger on oscillator end to the point of coupling were taken. From such data, the optimum position was chosen. One of the brass models used in these experiments is shown in Figure 13.8. This model is the basis for the model 6 tube as finally constructed (see next section).

Some idea of the amount of frequency modulation to be expected is given by reference to Figure 13.7. The insertion of the cathode causes approximately a 10 per cent shift in wavelength corresponding to a 20 per cent

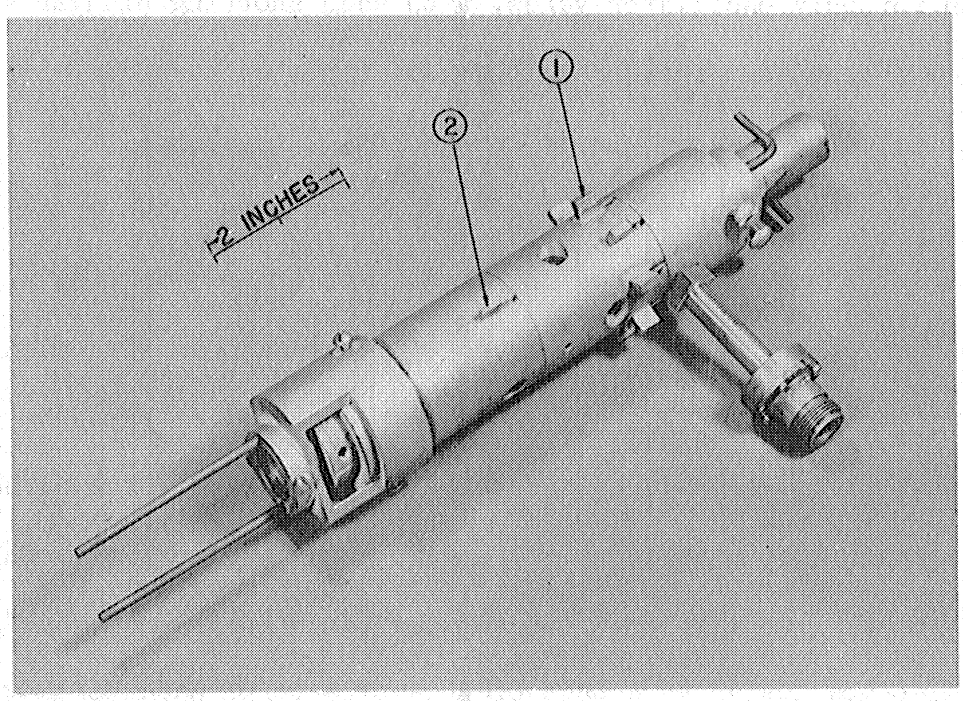

Figure 13.8 Brass Model of Model 6 Magnetron Used in Cold Tests
(1) Oscillator anodes; (2) Modulator anodes

change in capacitance. The capacitance to cathode is easily changed 25 per cent by the presence of the space charge swarm. The frequency modulation can therefore be expected to be 2.5 per cent or greater.

There are several factors in the design of a tube of this type which were brought out in the cold testing. First, by reference to the end view shown in Figure 13.6, it is seen that the outer vanes can resonate of themselves, as does a vane magnetron; in this case, the inner conductor slots and bars will act only to increase the lumped capacitance across the ends. Such a resonance was observed and it was found necessary to reduce the outer to inner conductor diameter ratio so as to shorten the vanes. In this way, the resonant wavelength of the vane mode was reduced to below eight centimeters, far from the desired operating wavelength of the tube.

The other factor to be considered is the rather low unloaded Q of this type of structure. The measured values of Q_o on a brass model averaged

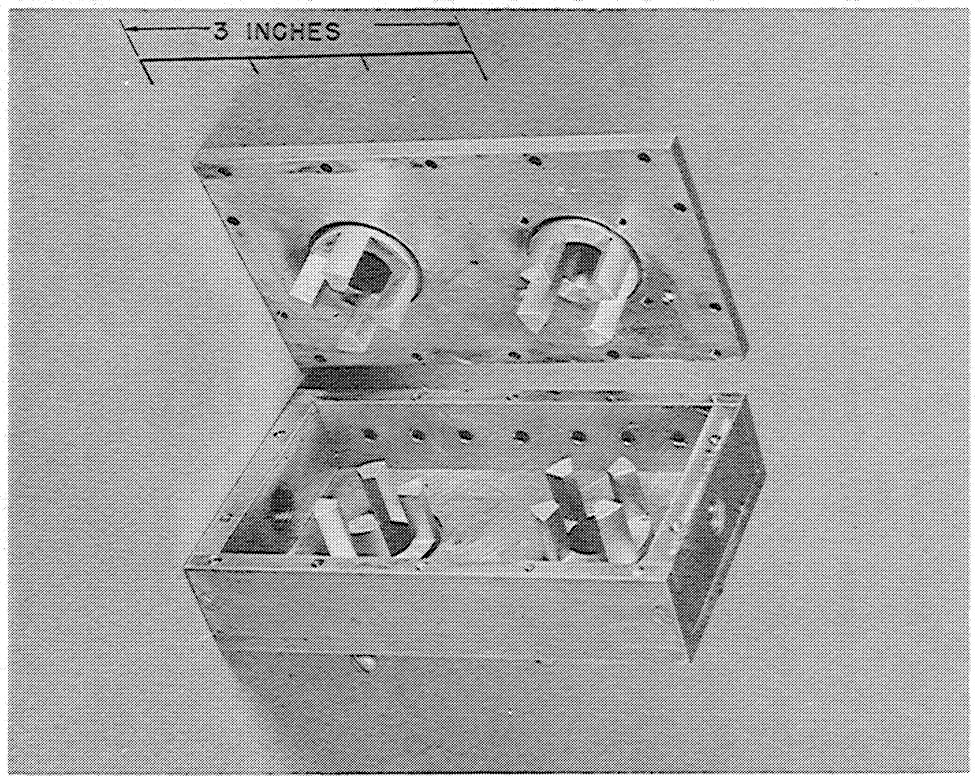

Figure 13.9 Brass Model of Rectangular Cavity F-M Magnetron

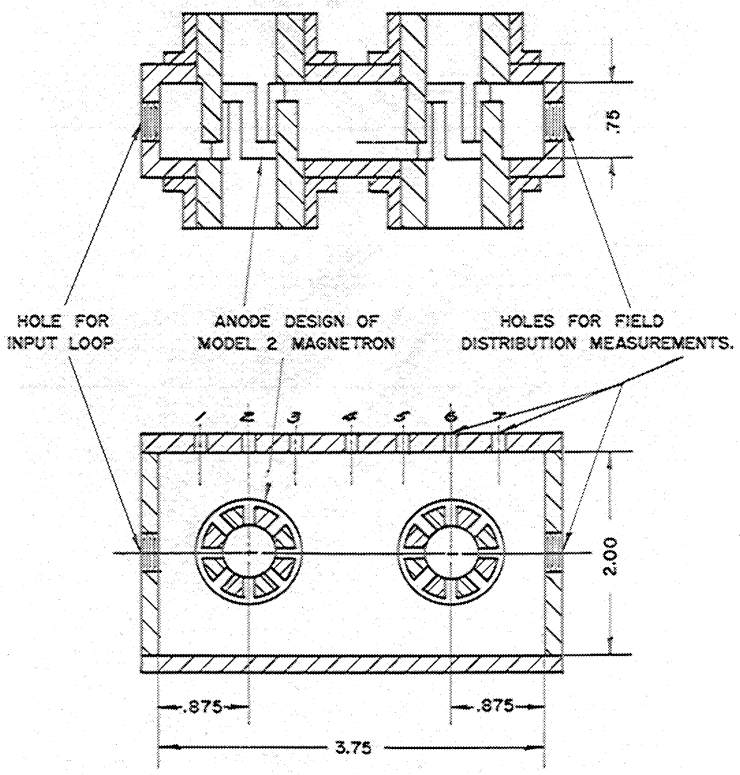

FIG. 13.10 RECTANGULAR CAVITY MAGNETRON
DIMENSIONS IN INCHES

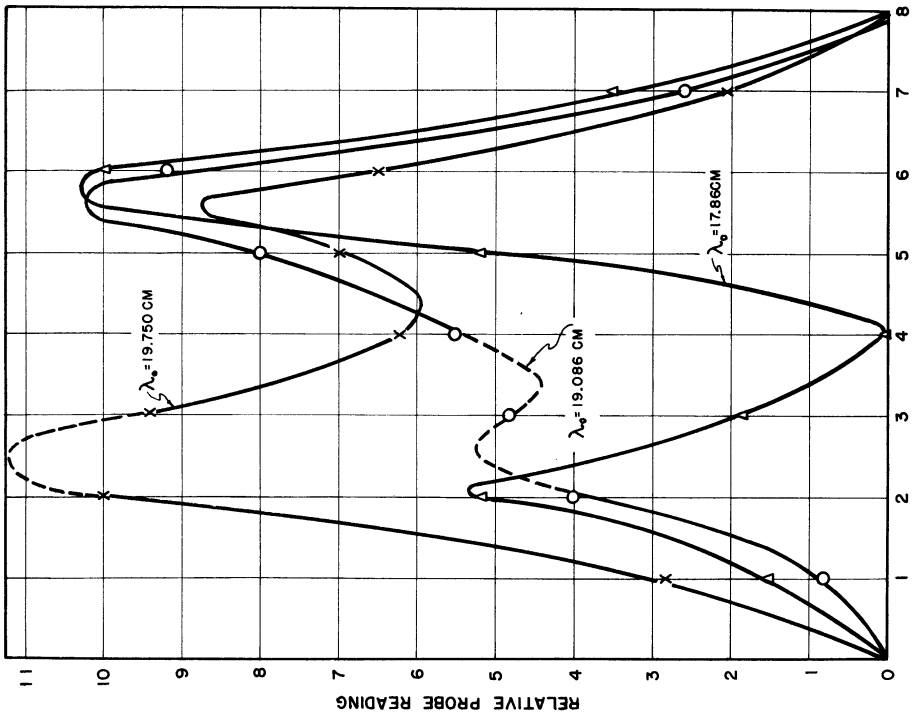

FIG. 13.12
RESONANCES FOR WHICH MAXIMA ARE LOCATED AT ANODE POSITION. CAVITY OF FIG. 8.2 ANODES IN PLACE

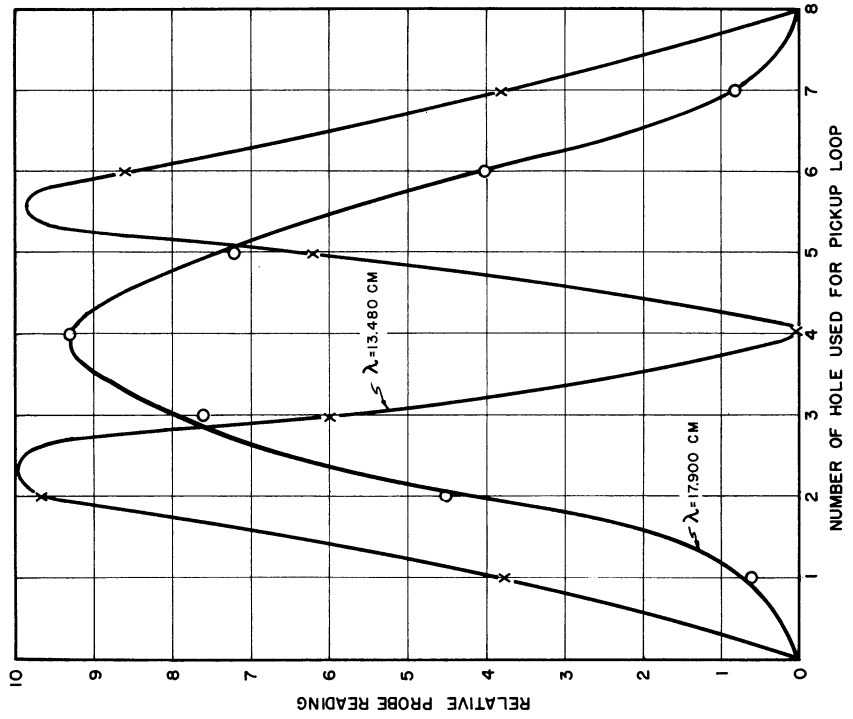

FIG. 13.11
FIRST AND SECOND ORDER MAJOR CAVITY RESONANCES IN RECTANGULAR CAVITY MAGNETRON. ANODES NOT IN PLACE

about 260. On a soldered copper model, this may be expected to be somewhat higher but this type of structure has an inherently large surface to volume (i.e., energy storage volume) ratio so that normal Q_o values of the order of 700-1000 would probably not be obtained.

A tube of the model 6 design has been constructed without the modulator cathode and is discussed in the next section.

c.: The third design of f-m magnetron consists of two interdigital tooth structures placed at the voltage maxima of a rectangular, electrically-one-wavelength-long cavity. The arrangement is shown in Figure 13.9. Measurements of the intensity of the fields at various positions along the line were made on the model with dimensions as given in Figure 13.10. The field patterns corresponding to the one-wavelength and one-half-wavelength modes in the cavity without tooth structures are shown in Figure 13.11; they are seen to be symmetrical as expected. Figure 13.12 shows the pattern for the one-wavelength mode with teeth in place. It is seen that the originally symmetrical pattern of Figure 13.11 has been distorted and concentrated near the teeth. Three modes seem to be present, two of which are probably due to approximately the same field distribution (at approximately 19 cm). The third mode at 17 cm is another field distribution which has the same general form when investigated at the limited number of points made available at the holes.

This structure is planned to produce frequency modulation in much the same way as the previous two designs. One of the interdigital structures would be used as a modulator where an expanding space charge cloud would change the capacitance and therefore the resonant wavelength of the cavity. The other set of segments will act as oscillator.

14. Construction and Performance of Frequency Modulation Magnetrons

Assembly drawings of models 5 and 6 f-m magnetrons are shown in Figures 14.1 and 14.2. To date, model 6 has been constructed and operated and parts have been machined for model 5. Both tubes have two cathodes and two sets of anodes; one set is to be used for the generation of radio frequencies while the other set is to be used to provide modulation. Cold tests on duplicate brass models of these tubes were described in the last section.

Model 5: The assembly drawing of model 5 is given in Figure 14.1.

The oscillator anode structure, end pole pieces, chokes and output assembly are the same as model 4. Since efforts to make the model 4 tube oscillate in the zero order mode have thus far been unsuccessful, assembly of model 5 has been delayed. Parts have been constructed and assembly will be completed as soon as the oscillator design is corrected. The modulator anode is simply a smooth bore anode. The upper cathode structures are designed to form an r-f short between the two cathodes and are to be spaced by means of lava beads (not shown in the assembly drawing).

It is planned to braze the body of this tube together in four operations. The first operation will consist of brazing the oscillator anodes, cavity, pole piece, output loop and choke together using a brazing fixture similar to that discussed and shown in Section 10 of this report.

The second braze will join the center pole piece, modulator anode, modulator pole piece, Kovar and choke together.

The third braze will join the sub-assemblies of the first two brazes together.

The fourth braze will silver solder the output assembly to the tube body.

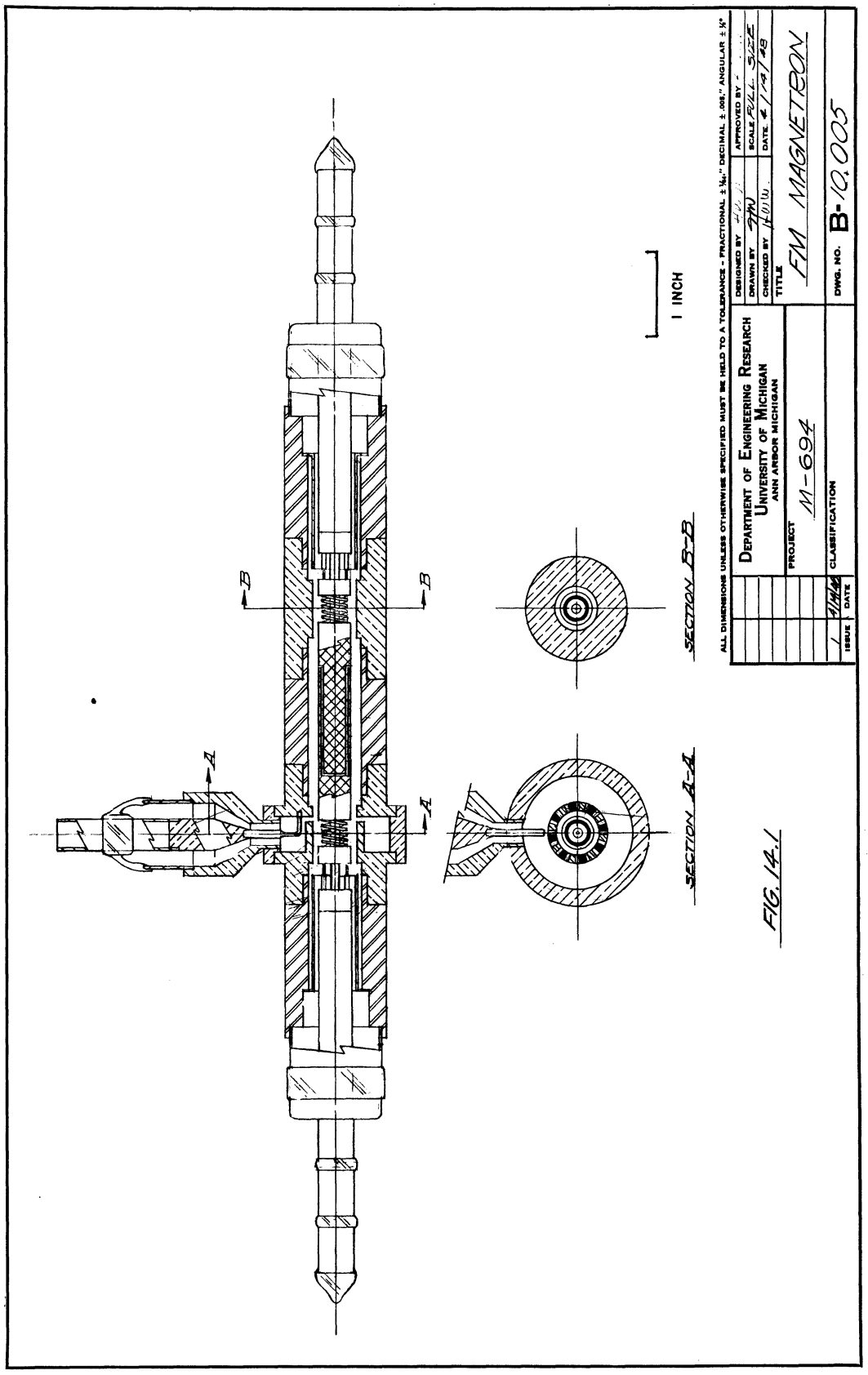
B
B
A
A
1 INCH
SECTION B-B
SECTION A-A
ALL DIMENSIONS UNLESS OTHERWISE SPECIFIED MUST BE HELD TO A TOLERANCE - FRACTIONAL ± 1/64" DECIMAL ± .005" ANGULAR ± 1/2°
DESIGNED BY
DRAWN BY FMW
CHECKED BY
APPROVED BY
SCALE FULL SIZE
DATE 4/14/48
DEPARTMENT OF ENGINEERING RESEARCH
UNIVERSITY OF MICHIGAN
ANN ARBOR MICHIGAN
TITLE FM MAGNETRON
PROJECT M-694
ISSUE 1
DATE 4/14/48
CLASSIFICATION
DWG. NO. B-10,005

FIG. 14.1

Care must be taken in cathode assembly to insure alignment of the upper end hats with that of the filaments and stem.

Model 6: The tube body of model 6 is brazed together in five main steps, using gold-copper solder except for the output seal assembly braze to the tube body. The vanes (part 8) for the oscillator anode are stamped out of sheet OFHC copper by means of a die and brazed with gold-copper solder to the cavity body (part 1). The vanes are held in place by means of a slotted stainless steel jig similar to those used to braze the vanes in a vane magnetron. The anode pieces (parts 3 and 7) and Kovar rings are brazed to their respective pole pieces (parts 2 and 6) at the same time the vanes are brazed to the cavity body. Jigs hold the anodes in alignment with the pole pieces for this braze. The anodes are turned and milled from OFHC copper and look quite similar to those of an interdigital magnetron. At the same firing of the above brazes, the two copper rings (parts 4) are brazed to the center pole piece (part 5). The above brazes are made in a hydrogen furnace at 1065°C.

The oscillator anode-pole piece assembly is next brazed to the cavity body assembly and the center pole piece assembly is brazed to the oscillator anode. Scribe lines on the oscillator pole piece and cavity body align the oscillator anode with respect to the oscillator vanes. Two stainless steel jigs fitting into each end of the center pole piece align this part with respect to the tube body. The above braze is made at 1055°C.

Modulator vanes (part 11) are next brazed to the cavity body being held in a stainless steel jig and aligned with respect to the oscillator vanes by means of scribe lines on the cavity body and on the modulator vane jig. This braze is made at 1040°C.

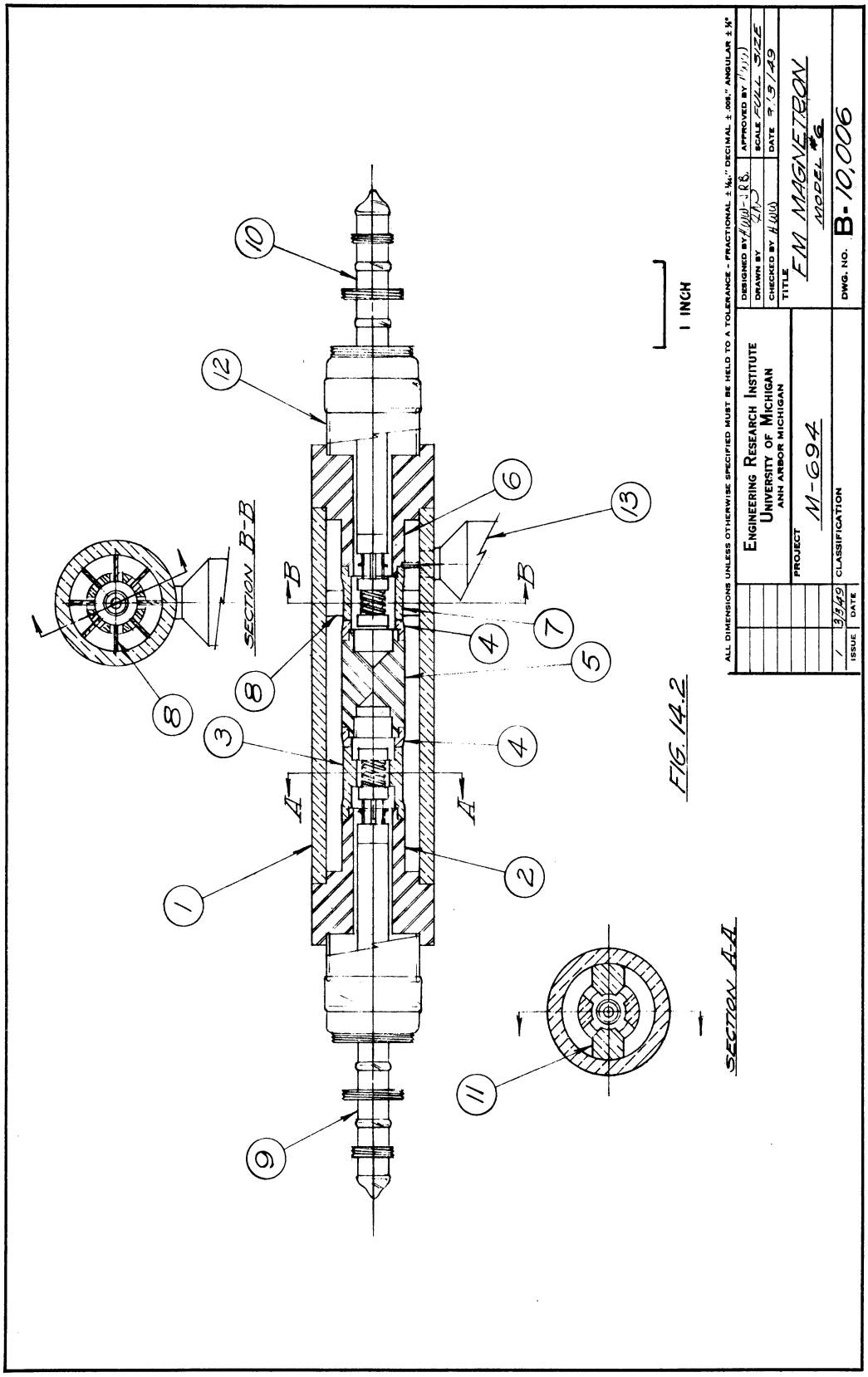
SECTION B-B
SECTION A-A
1 INCH
ALL DIMENSIONS UNLESS OTHERWISE SPECIFIED MUST BE HELD TO A TOLERANCE - FRACTIONAL ± 1/64," DECIMAL ± .005," ANGULAR ± 1/2°
ENGINEERING RESEARCH INSTITUTE
UNIVERSITY OF MICHIGAN
ANN ARBOR MICHIGAN
PROJECT M-694
DESIGNED BY
DRAWN BY
CHECKED BY
TITLE EM MAGNETRON MODEL #6
APPROVED BY
SCALE FULL SIZE
DATE 7/9/49
ISSUE 1
DATE 3/49
CLASSIFICATION
DWG. NO. B-10,006

FIG. 14.2

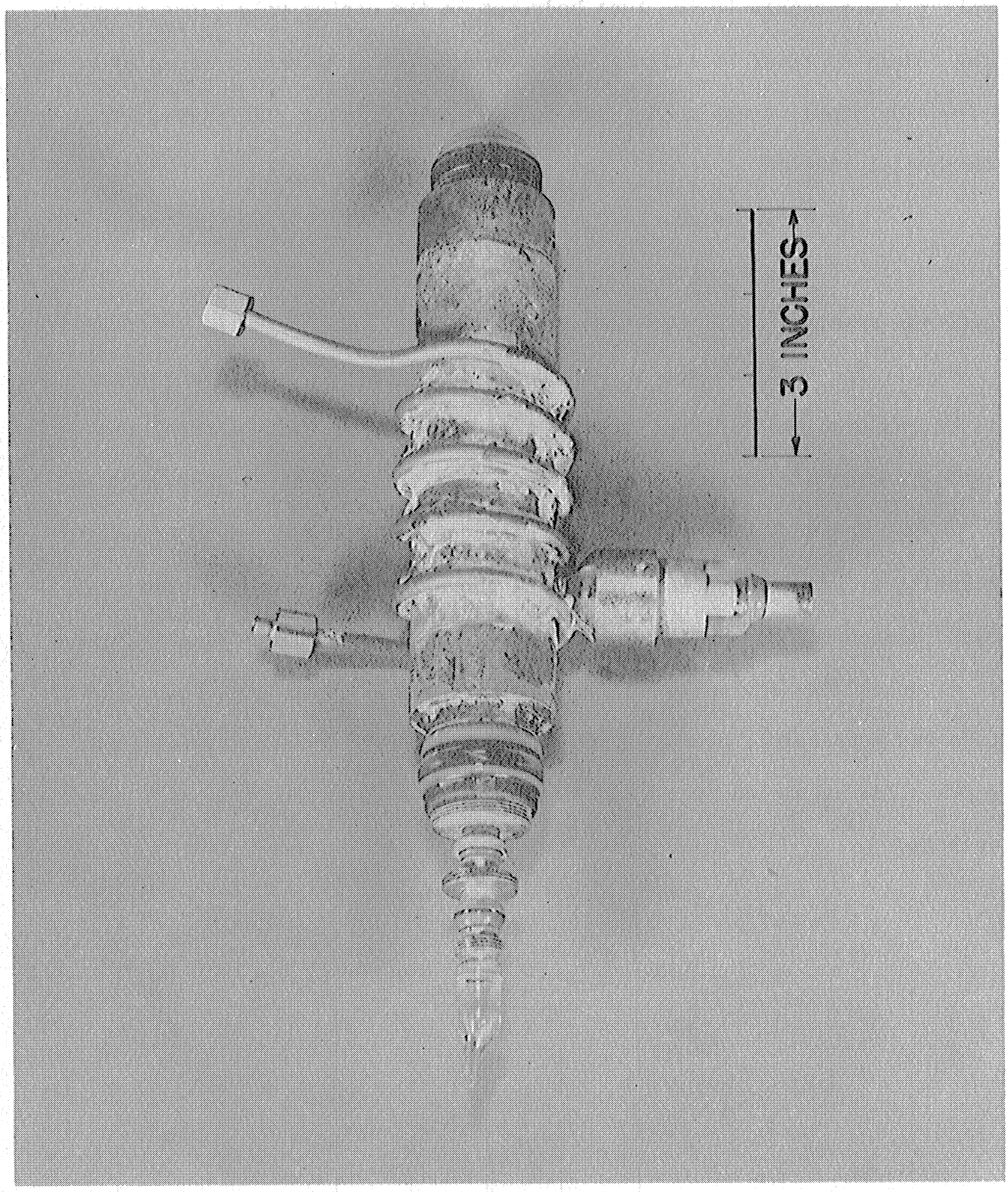

Figure 14.3 Model 6 Magnetron Assembled except for Modulator Cathode

The final gold-copper braze consists of brazing the modulator anode-pole piece assembly to the tube body and to the center pole piece assembly. The modulator anode is aligned with respect to the modulator vanes by means of scribe lines on the anode body and on the modulator pole piece. This braze is made at 1025°C.

The output assembly (part 13) which is similar to that discussed in part 10 of this section is then silver soldered to the tube body in the hydrogen brazing jar.

The cathodes are assembled and inserted into the tube using the technique discussed in Section 10. A steady rest is used on the Litton glass lathe to maintain alignment of the body when the cathode is glassed.

The tube body without the cathodes has 25 metal parts brazed in accurate alignment with each other and shows the ease in which such complicated structures can be constructed using the gold-copper solder technique as discussed in Section 10 of this report. The first attempt to build this tube was successful, producing a good hard tube with accurately aligned parts. The assembled tube is shown in Figure 14.3 without the modulator cathode.

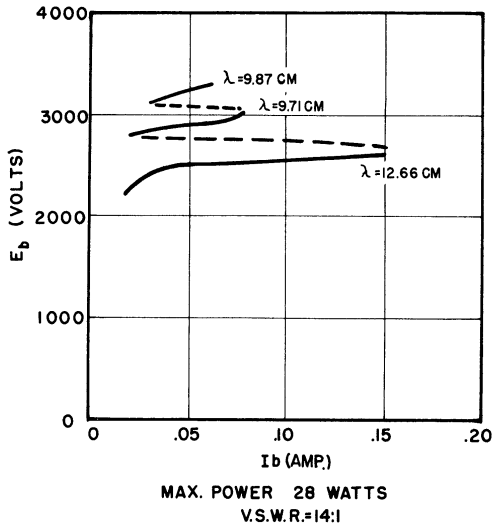

FIG. 14.4
VOLT AMPERE CHARACTERISTICS
ON FIRST MODEL 6 MAGNETRON

Initial tests on this tube have been made. Operation is obtained in the desired mode only by inserting a reflector in the test line. Under these conditions, weak oscillations are obtained at 12.7 cm. Some power is coupled out the cathode line. Without the reflector in the line, the tube oscillates in a higher order mode at 9.8 cm. A volt ampere characteristic copied from the oscilloscope screen is shown in Figure 14.4.

IV. MISCELLANEOUS RESULTS

15. Magnetron Amplifier Possibilities

The study of the properties of magnetrons as stable amplifiers of microwave power is included in the program for this project. At about the same time as this program was written, Dr. A. Nordsieck of the Columbia Radiation Laboratory in a letter to Lt. Col. H. Zahl pointed out the surprising fact that practically no attention has been given to the possibility of devising a magnetron amplifier despite the obvious desirability of such a tube. This letter was circulated as Appendix III to the minutes of the meeting of the R-F Power and Oscillator Tubes Subcommittee of the Vacuum Tube Development Committee, August 7, 1946. This section gives a brief discussion of this problem and attempts to indicate along what lines a solution can be sought. In addition, two tentative amplifiers are described.

The applications and the requirements for a magnetron amplifier as referred to in the program are similar to those of a Class-C power amplifier on lower frequencies. A small power applied to the input terminals determines the frequency of the output, but the relation between input and output voltage is not necessarily linear. The amplifier is primarily characterized by its power gain, power output, efficiency, and bandwidth.

It is well known that the magnetron oscillator and the traveling-wave amplifier are closely related. In a magnetron amplifier we would attempt to combine some of the most important features of both: the high power output and efficiency of the former with the high gain and possibly the broad frequency band of the latter.

An essential feature of the magnetron oscillator is the fact that the electrons may revolve a large number of times round the cathode before

they reach the anode. When we look at the magnetron as a traveling-wave tube, this means that its effective length is many times the circumference of its inter-electrode space. This indicates that the anode structure of a magnetron amplifier must differ considerably from the anode structure of the conventional magnetron. An additional reason is the difficulty of avoiding power transfer from the output point to the input point of a single-loop transmission line of cavities. Theoretically, the obvious solution then is to arrange the anode segments in a helical instead of circular fashion and to give the electrons a small axial velocity component. However, along a helix with a large number of turns the r-f field experienced by an electron will not be essentially different from the field along an axial arrangement of equal sections, each similar to a conventional magnetron anode.

The design of a magnetron amplifier along these lines offers a number of problems which are difficult but do not appear to be insoluble.

a. The Electron Optics of the Tube: The electrons should be given an axial velocity component in addition to their magnetron motion in a plane perpendicular to the axis, in such a way that this magnetron motion is disturbed as little as possible. Obvious methods of attack are (1) insertion of dummy cathodes or end hats such as to produce an axial component of the electric field (Figure 15.1); (2) shaping of the pole pieces so that the magnetic field diverges slightly in the direction of axial electron motion; or (3) a combination of both of these methods.

b. The R-F Circuit Design: Each section of the anode along the axis resembles a conventional magnetron anode, maybe a vane structure or an interdigital system. A certain regenerative effect is therefore inherent, but the electrons do not remain long enough in one section to cause instability.

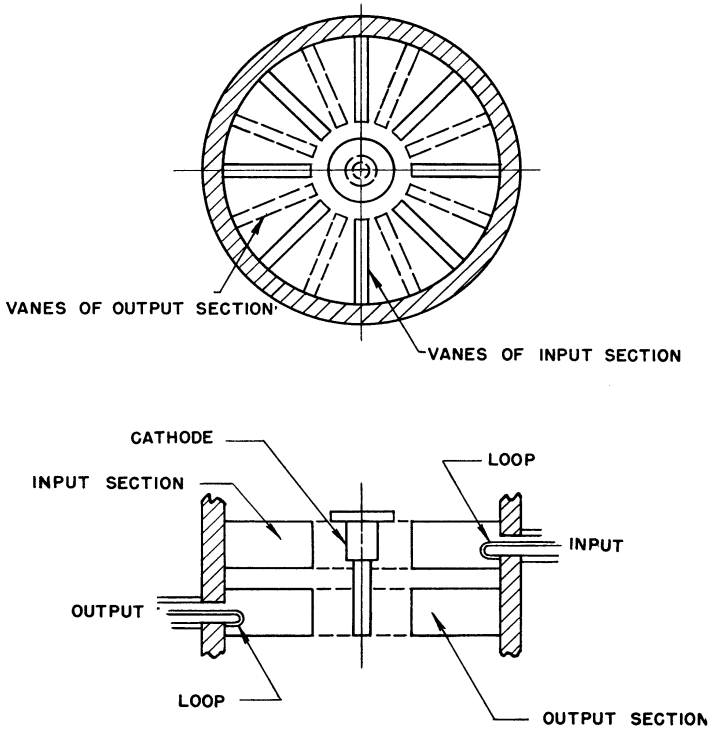

FIG. 15.1 PROPOSED VANE TYPE MAGNETRON AMPLIFIER DESIGN

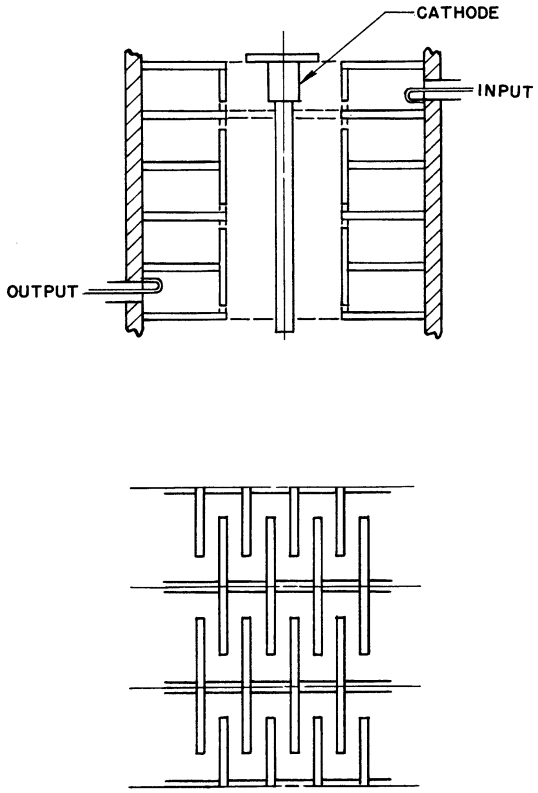

FIG. 15.2 PROPOSED INTERDIGITAL TYPE MAGNETRON AMPLIFIER DESIGN

The r-f voltage in the section becomes progressively higher toward the output end of the structure. It is therefore important that no power is fed back toward the input end and self-sustained oscillations are prevented from building up. This can be accomplished in two different ways: (1) by eliminating virtually all electro-magnetic coupling between the sections, so that they are coupled only by means of the electron stream; or (2) by forming a transmission line out of the sequence of sections and terminating this line in an impedance equal to the characteristic impedance of the line.

Figures 15.1 and 15.2 are rough sketches of magnetron amplifiers embodying these ideas. In the amplifier of Figure 15.1, only two anode sections are incorporated. They are of the multivane type, and the electro-magnetic coupling between the two systems is eliminated by turning one system 90 electrical degrees with respect to the other. The reason why a third section is not included is of course that such a section would necessarily have some coupling to one of the previous systems. It is possible, however, that if the coupling to the second section by the same method is made zero, the coupling to the first section can be made small enough for stability with a reasonable gain. Each section would be tuned to operate in the π-mode.

This type of amplifier would be expected to have an efficiency and a power output comparable to those of a magnetron oscillator but the small number of sections may make gain and stability low. It is a narrow-band amplifier. In the tube shown in Figure 15.2, the anode system is formed by a cylindrical wave guide with a number of circular irises each carrying a finger system like that of an interdigital magnetron. The input frequency is far below the resonance frequency of each cavity between two irises, so that the structure operates as a low-pass filter excited in its pass band. The load at the output end should be so adjusted that this filter is terminated

in its characteristic impedance, so that reflection of power toward the input is avoided. As in the traveling-wave tube, some attenuation along this artificial line may considerably improve the stability of the amplifier.

This is a broad-band device but there is some doubt as to the efficiency and power output obtainable. The phase difference between consecutive irises is considerably less than 180°. Consequently, the voltage between fingers attached to opposite sides of the same cavity is comparatively small.

These two examples do not exhaust the possibilities of circuit design for a magnetron amplifier along the lines discussed in this section. They only serve to illustrate the contention that specific designs can be worked out where these general ideas can be applied with a reasonable expectation of success.

16. Possible Developments Based on the Interdigital Magnetron Principle

During the course of development work on magnetrons involving the interdigital tooth structure, several other structures involving this method for producing the interaction fields have suggested themselves. Two of these will be described here.

a. Signal Generator: A set of interdigital anodes or fingers can be inserted in series in the high voltage end of the center conductor of a coaxial resonator to form a widely tunable magnetron signal source. A schematic drawing of such a tube is shown in Figure 16.1 in the form of a $\lambda/4$ or $3\lambda/4$ long coaxial line loaded by the capacitance of the fingers at one end and tuned by means of shorting plates moved along the line. The entire unit or possibly just the electronic portions could be contained in the vacuum. The former structure would involve the difficulty of transmitting the tuning motion into the vacuum with bellows, etc. The latter possibility

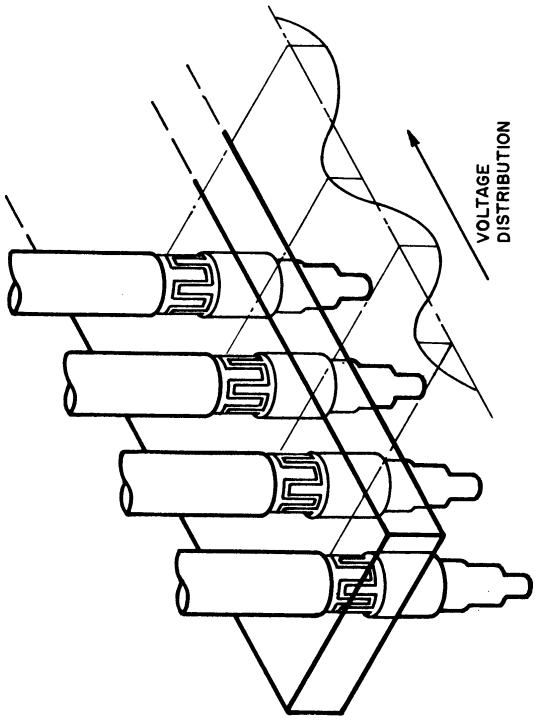

FIG. 16.2
PROPOSED HIGHPOWER
MAGNETRON

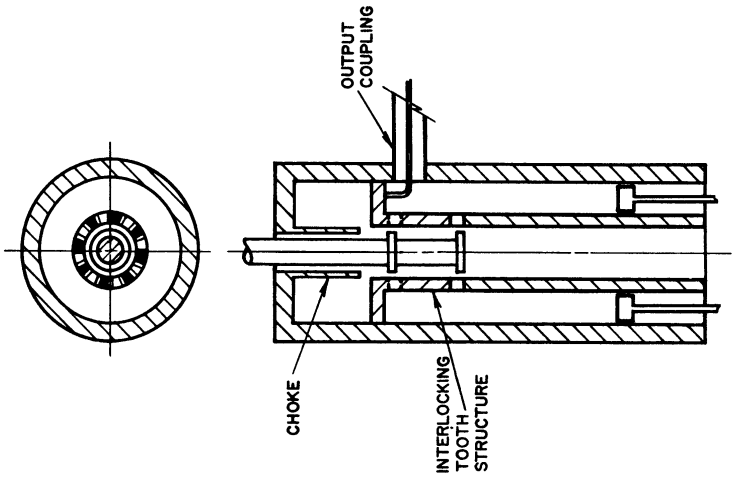

FIG. 16.1 PROPOSED COAXIAL
INTERDIGITAL MAGNETRON.

may allow the use of a "plug-in", vacuum-contained cathode and interdigital anodes, permitting easy and inexpensive replacement of expendable portions of the tube. This type of resonator would give relatively mode-free operation, the $\lambda/4$ length being advantageous in this respect over the $3\lambda/4$ cavity.

Any of the standard mechanical frequency modulation methods could be used with this tube or the cavity can be made $\lambda/2$ or λ long with interdigital anodes at both ends, allowing electronic frequency modulation by the use of an expanding space charge cloud inside one set of anodes, as described previously in this report.

It is believed that the advantages offered by the relative freedom from moding, wide tunability, and possible replacement of cathode and finger structure make this tube very well suited for use as a signal generator.

b. High Power Magnetron: The interlocking finger type of magnetron anode also lends itself to the construction of a high power magnetron. A set of anodes may be placed at each high voltage point along the length of a rectangular resonator as shown in Figure 16.2. Other types of resonators are of course possible. In this way presumably as much power as desired could be obtained by merely increasing the number of such anodes. Practically, however, moding difficulties would place an upper limit to the number used. Separate cathodes would be required for each set of anodes, as each would oscillate separately, contributing its share of the total power. This is advantageous since one of the major limiting factors in high power tubes is availability of cathode emission. Suggested possible applications of such a tube include use as a power source for a particle accelerator. The tube would be only slightly tunable.

The model with two anode sets built for the tests described in Section 13c could be used as a basis for development. Two anodes would produce a "push-pull" type of oscillation which might provide a simple way for easily doubling the output for the same anode voltage with existing interdigital anode designs.

V. LABORATORY FACILITIES

Most of the equipment and facilities of the Electron Tube Laboratory are shown in the drawings and photographs on the following pages. The laboratory is housed in three rooms on the third floor of the new Engineering Building and has a total floor space of about 2400 square feet. One room is devoted primarily to test equipment, one to assembly and processing equipment and one to the machine shop. Desk and work bench space is divided between the three rooms.

Each room has plug-in molding strips on the walls supplying 115 volts 60 cycle power. Outlet boxes conveniently arranged about the rooms supply a variety of outlets for 115 or 230 volts d-c, 230 volts 3ϕ 60 cycle power and 115 volts 3ϕ 60 cycle power. All combinations of these voltages can be connected to any outlet box by means of a master distribution panel located in each room. Water, air and gas are also conveniently furnished to the rooms.

17. Test Laboratory

A floor plan of the test laboratory is shown in Fig. 17.1 and a general view is shown in Fig. 17.2. Working space for four or five sets of apparatus is available plus space for computation and storage of equipment. Most of the microwave equipment was built by this laboratory, partly because of lack of availability shortly after the war, and partly because certain special purpose equipment was necessary.

The set-up in the center of the room (Fig. 17.2) is used for "hot impedance" testing in the investigation of properties of the magnetron space charge.

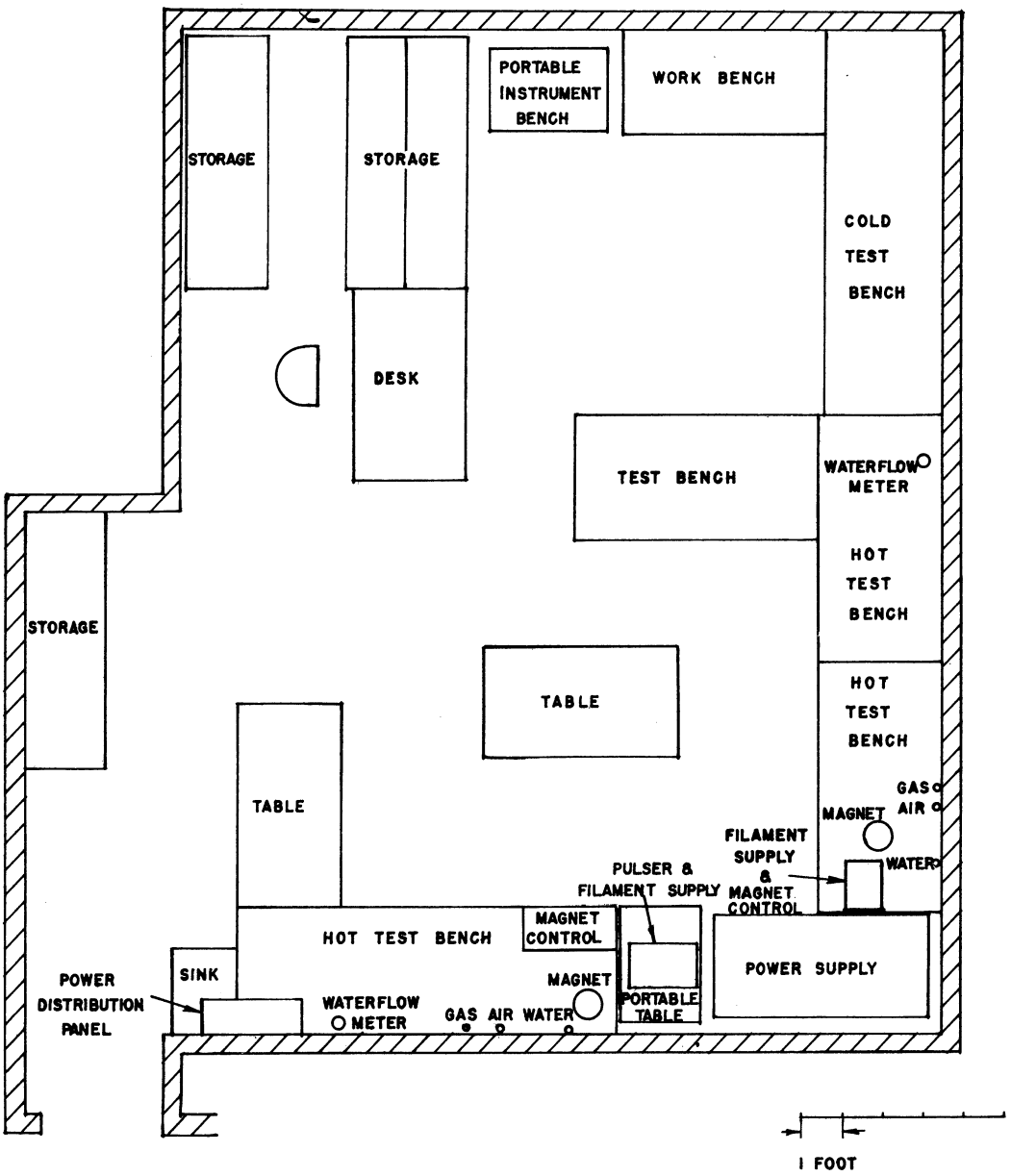

FIG. 17.1 TEST LABORATORY.

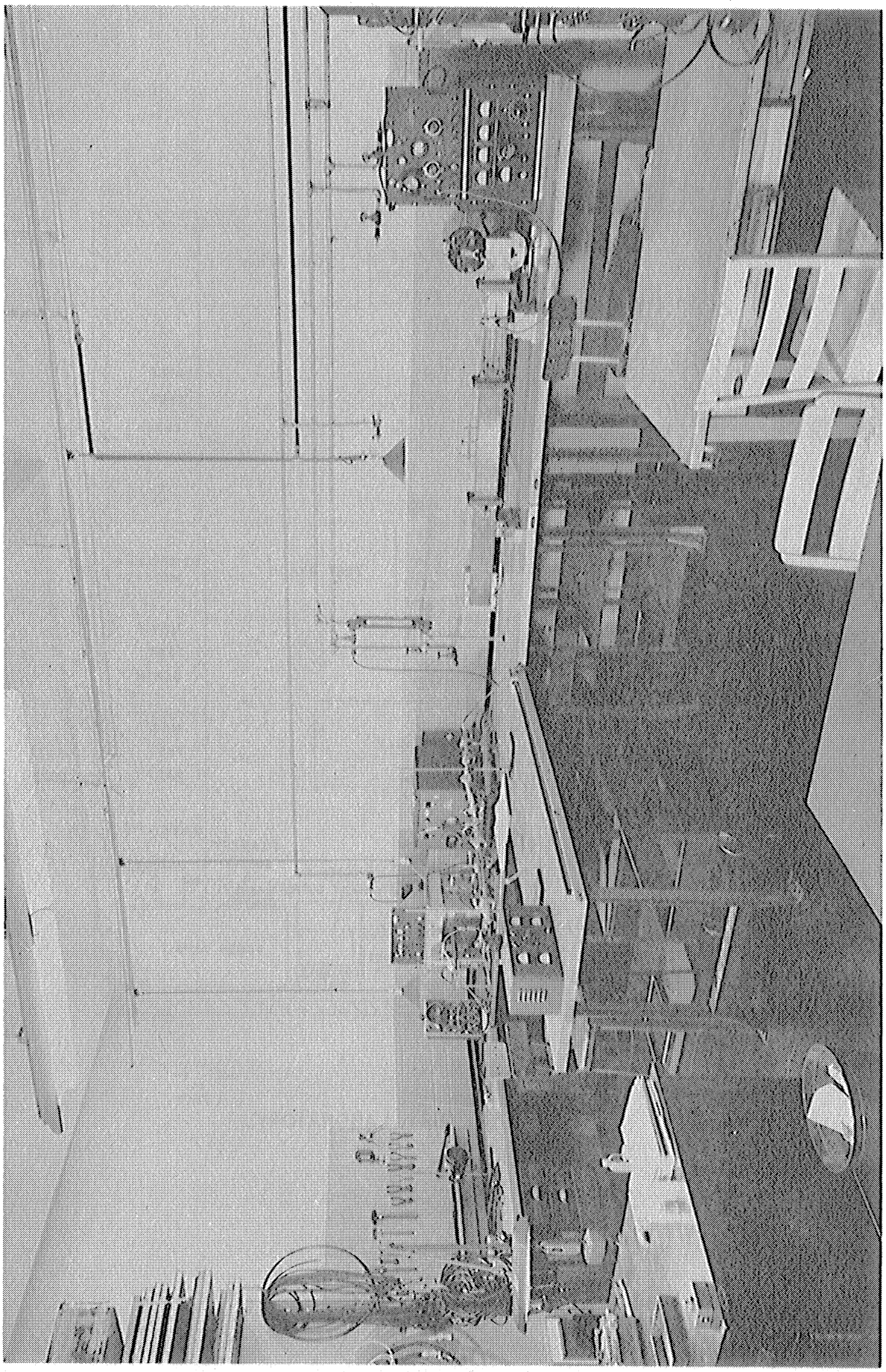

Figure 17.2 Test Laboratory

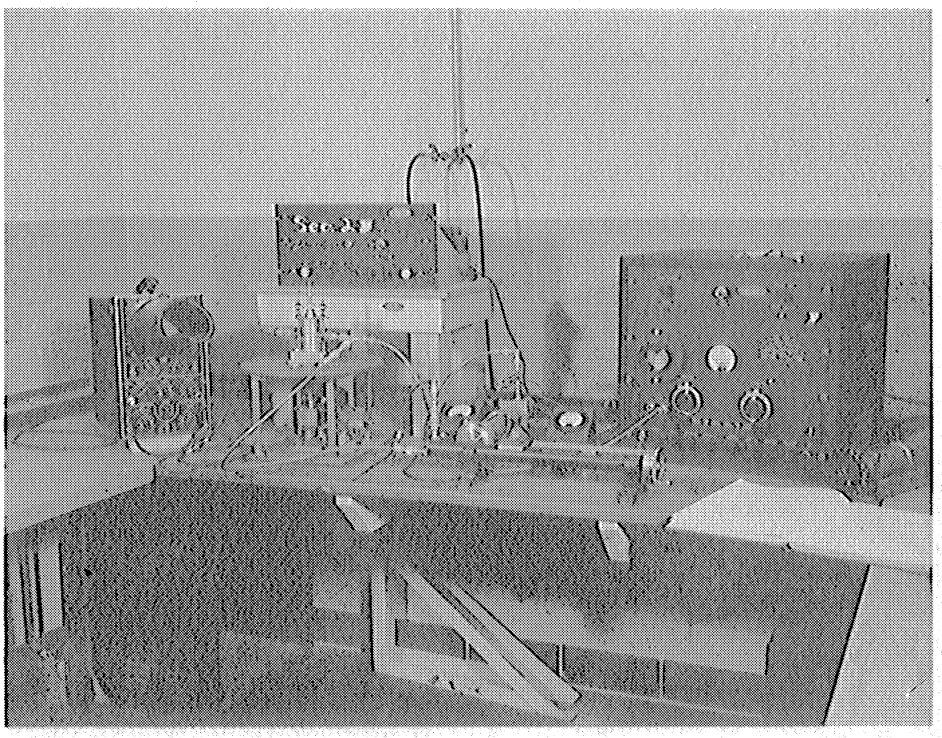

Figure 17.3 Rotating Probe Set

Fig. 17.3 is a close-up view of the rotating probe set shown in the corner of the room (Fig. 17.2). This instrument is used to measure field distributions in magnetron models. The set was designed and built at the University and has proved to be an extremely versatile and useful instrument. Dummy cathodes of various shapes containing a probe for picking up fields in the interaction space are held in place with a standard type N r-f fitting and are rotated on a bearing mounting by a synchronous motor. A crystal mounted in the rotating structure is used as a detector and leads are connected by means of a mercury cup to an oscilloscope where the output of the crystal is displayed. The whole assembly of probe, motor, mercury cup, etc., can be raised and lowered with respect to the magnetron model by means of a screw and worm gear adjustment.

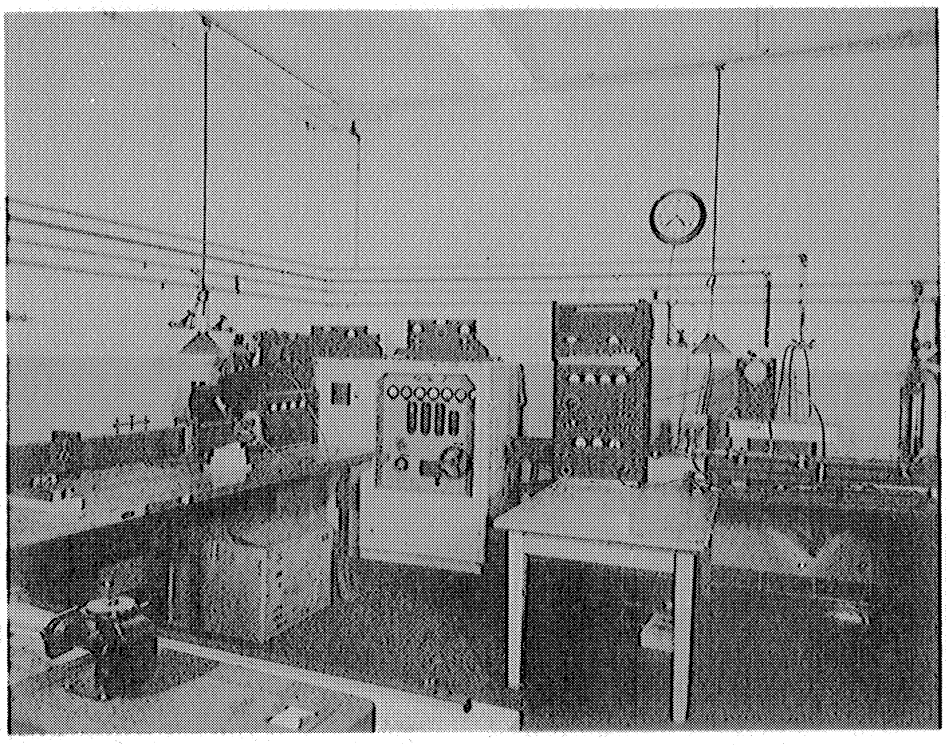

Figure 17.4 Hot Test Benches

Two hot test benches are shown in Fig. 17.4. One is equipped with 2x4 inch wave guide and associated water loads, dummy loads, slotted section, coax to wave guide matching section, probes, etc. This wave guide equipment was built at the laboratory to fit the special frequency range involved since suitable guide was not available on the market at the time.

The other hot test bench shown in Fig. 17.4 is equipped with a 1-5/8 inch coaxial line, with its associated tapers, slotted sections, dummy loads, water load, etc. This line and associated fittings was also constructed at this laboratory. Polystyrene washers act as spacers for the inner conductor and the line has a characteristic impedance of 49 ohms. Two adjustable carriages have been built to carry the wave guide and coaxial lines.

The coaxial line water load is shown in Fig. 17.5. The center conductor (part 7) tapers down to a small diameter and is surrounded by a glass

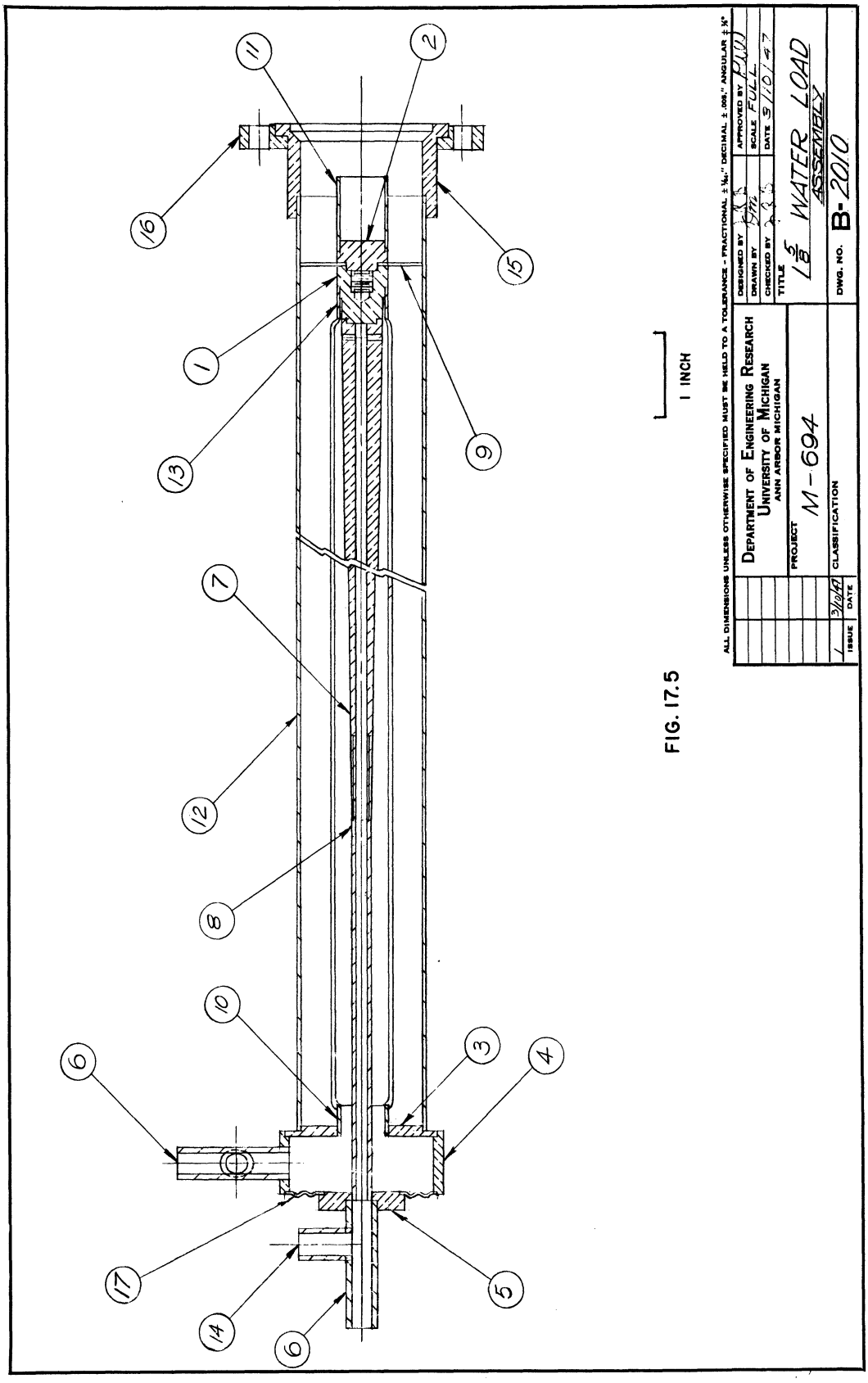
1
2
3
4
5
6
6
7
8
9
10
11
12
13
14
15
16
17
1 INCH
ALL DIMENSIONS UNLESS OTHERWISE SPECIFIED MUST BE HELD TO A TOLERANCE - FRACTIONAL ± 1/64" DECIMAL ± .005" ANGULAR ± 1/2°
DESIGNED BY
DRAWN BY
CHECKED BY
APPROVED BY LDW
SCALE FULL
DATE 5/20/47
TITLE 1 5/8 WATER LOAD ASSEMBLY
DEPARTMENT OF ENGINEERING RESEARCH
UNIVERSITY OF MICHIGAN
ANN ARBOR MICHIGAN
PROJECT M-694
DWG. NO. B-2010
CLASSIFICATION
1 ISSUE 3/047 DATE

FIG. 17.5

tube. Water flows through the inside of the taper, out through small holes into the space between the glass tube and the taper and out the end. The novel feature is that Kovar to glass seals are incorporated in this load eliminating water leak troubles. A monel diaphragm similar to that used in the tubes prevents fracture of the glass due to heat expansion. The voltage standing wave ratio of this load is less than 1.5 to 1 over the frequency range used. A flow meter measures the rate of water flow and two sensitive thermometers measure the rise in water temperature from which the power dissipated in the load can be determined.

An assembly drawing for the adjustable reflectors designed and built at the laboratory for use in the 1-5/8 inch coaxial line is shown in Fig. 17.6. The reflectors are used for matching purposes and for inserting a given standing wave ratio into the line. The reflector (Part 4) is 1/8" by 3/4" and can be inserted into the coaxial line until it just shorts to the center conductor. The assembly fits into a standard crystal or bolometer probe carriage as designed by M.I.T. for use on S-band slotted sections.

The large power supply shown in the corner of the room in Fig. 17.4 has variable output up to 15,000 volts at 7.5 K.V.A. The supplies on either side of this rectifier contain filament and magnet controls. The one to the right also contains a pulser which may be used for display of volt ampere characteristics on an oscilloscope and also for an emission tester. The pulser unit also can be used as a sixty-cycle modulator.

Two spectrum analysers are shown in Fig. 17.2, one by the rotating probe and one by the wave guide set-up. They are Model 1SS-4SE and Type 107 designed by M.I.T. and built by Sylvania.

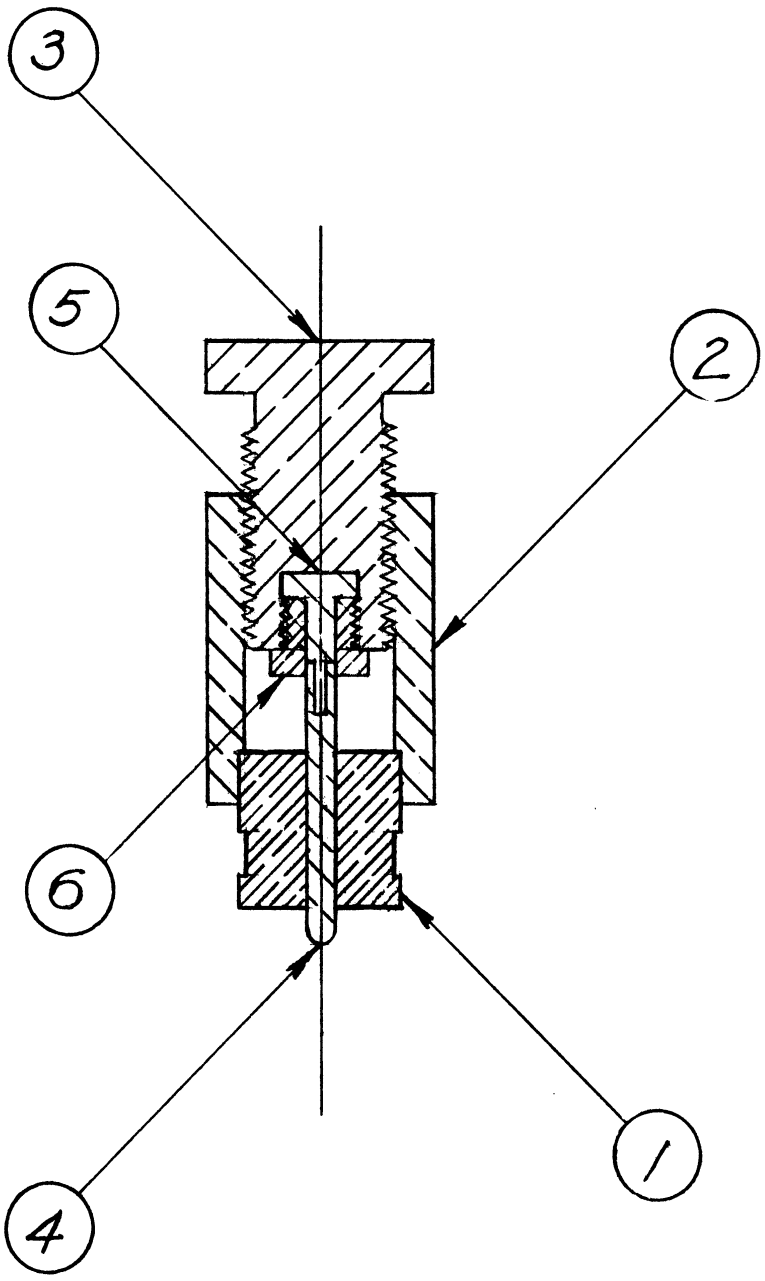

FIG. 17.6

ALL DIMENSIONS UNLESS OTHERWISE SPECIFIED MUST BE HELD TO A TOLERANCE - FRACTIONAL ± 1/64," DECIMAL ± .005," ANGULAR ± ½°

		DEPARTMENT OF ENGINEERING RESEARCH UNIVERSITY OF MICHIGAN ANN ARBOR MICHIGAN	DESIGNED BY H.W.W. DRAWN BY JM CHECKED BY H.W.W
		PROJECT M-694	TITLE ADJUSTABLE REFECTOR ASSEMBLY
	4/14/47	CLASSIFICATION	DWG. NO. A-2012
ISSUE	DATE		

APPROVED BY

SCALE FULL SIZE

DATE 4/14/47

Two signal generators using type 707B tubes have been built in this laboratory, one of which is pictured in Fig. 17.7. They cover a wave length range from 8 to 21 cm. and have a power output of approximately 75 milliwatts.

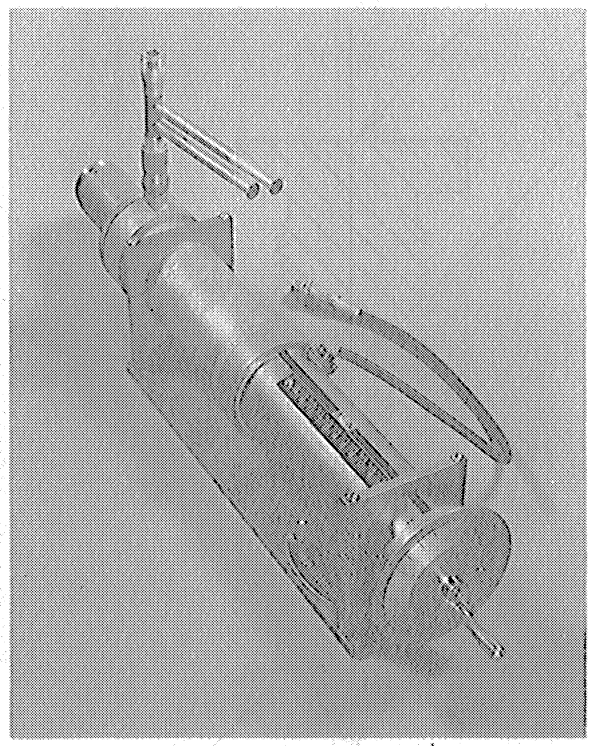

Figure 17.7 707B Oscillator

Three electro magnets have been constructed for operation at 220 volts d-c. Two have a maximum field of 2500 gauss across an air gap of 3/4 inch and one has a maximum field of 4400 gauss across an air gap of 3/4 inch.

A flux meter (Model F, Sensitive Research Company) is used to measure the magnetic flux of these magnets and has proved to be a versatile and useful instrument.

Three type 208 Dumont oscilloscopes, a Browning Laboratory Type P-4E Synchroscope, a Ferris Instrument Company Model 22A Signal Generator

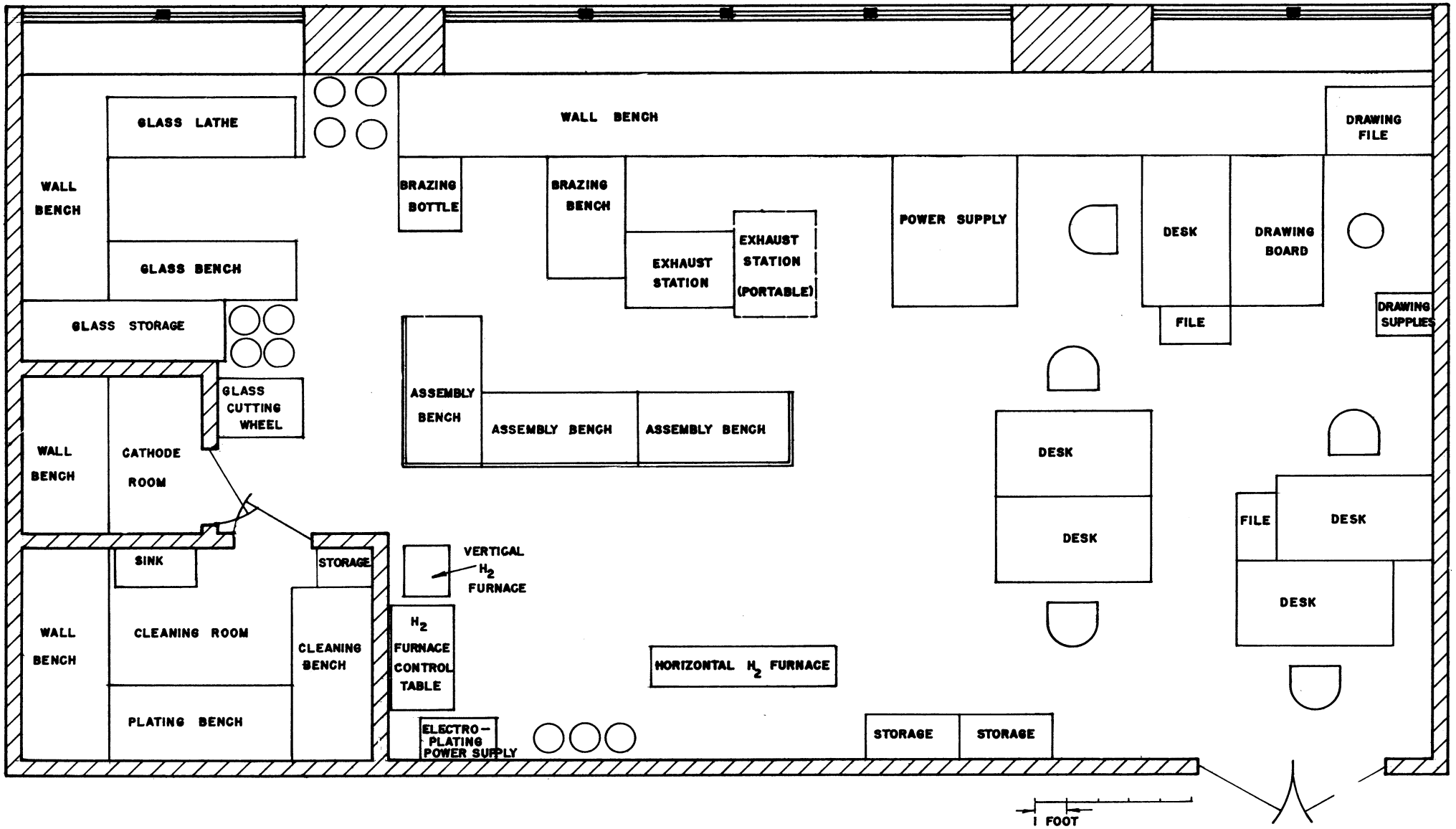

FIG. 18.1 ASSEMBLY LABORATORY.

(85KC to 25MC), a General Radio vacuum tube voltmeter Type 726A, an M.I.T. designed Thermistor Bridge type TBN-3EV, crystal and bolometer mounts and various pieces of microwave plumbing and instruments complete the equipment.

This laboratory also enjoys the position of being able to draw on the laboratory equipment and facilities of the entire University.

18. Assembly Equipment

The assembly room floor plan is shown in Fig. 18.1. This room contains a plating and cleaning room, a cathode room, processing equipment, storage space, work bench space and some desk space.

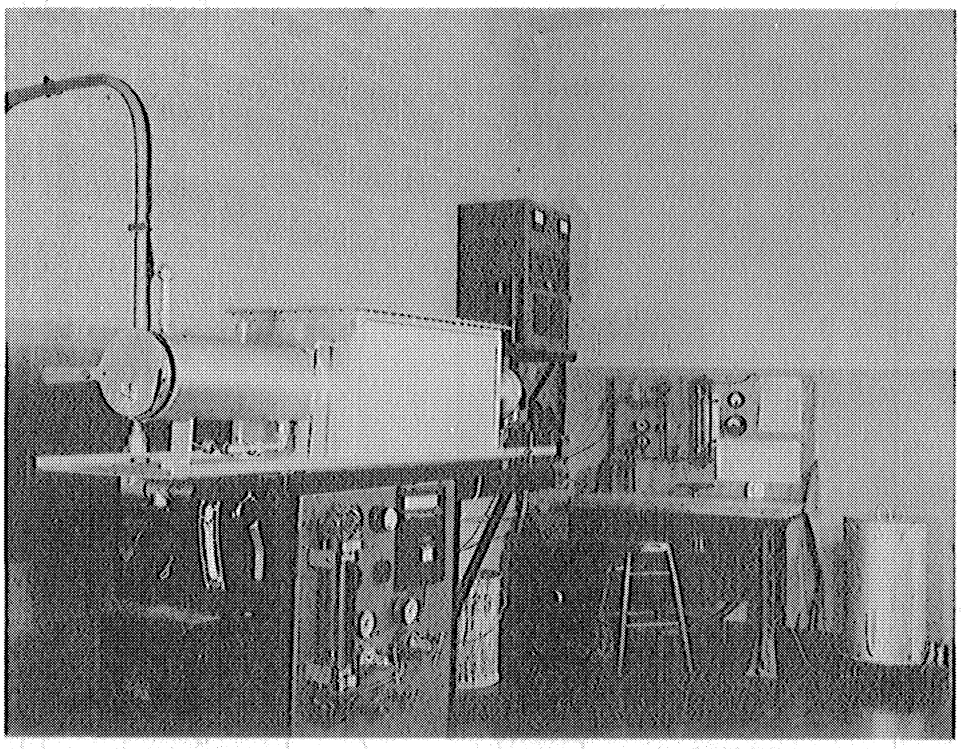

Figure 18.2 Hydrogen Furnaces

The hydrogen furnaces are shown in Fig. 18.2. The horizontal hydrogen furnace has a 5-1/4-inch manifold capable of attaining 1100°C and is automatically temperature regulated. A water jacket cooling section is shown on the near end, enabling continuous brazing operations. Its control board shows the hydrogen flowmeter, hydrogen and nitrogen pressure valves and the automatic temperature control unit.

The vertical hydrogen furnace shown in Fig. 18.2 on the floor to the right has a 7-inch manifold and will also attain 1100°C but is not automatically regulated. Continuous brazing operations cannot be made with this furnace; however, a water-cooled jacket enables two brazes to be made in a working day. The control bench for this furnace is shown to the left of the furnace.

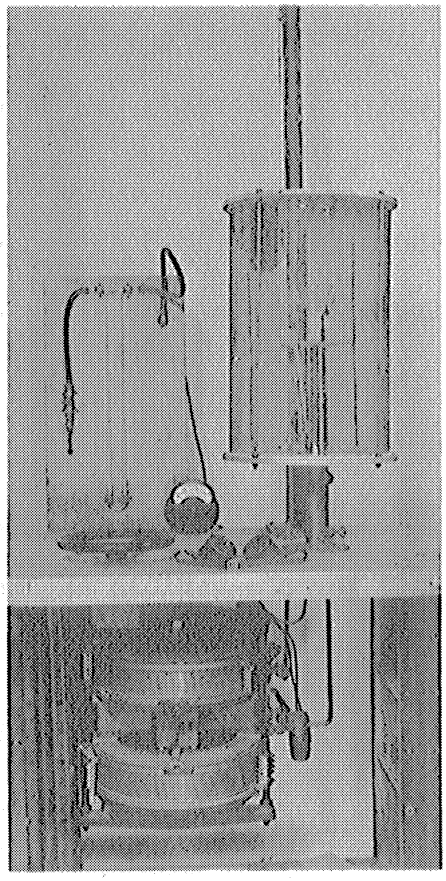

Figure 18.3
Hydrogen Brazing Bottle

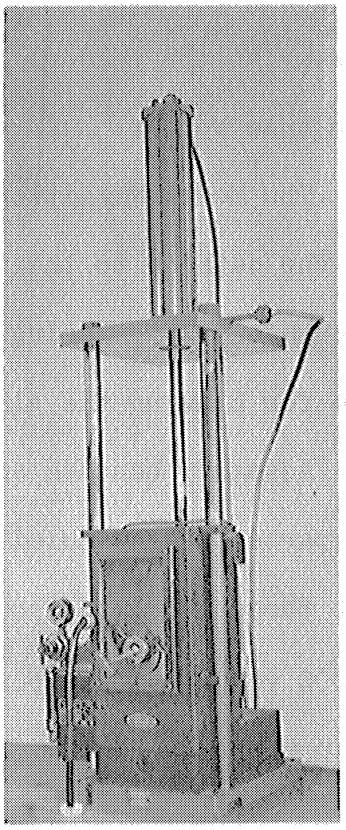

Figure 18.4
H_2 Atmosphere Arc Welder

Fig. 18.3 shows a view of the hydrogen brazing bottle in which temperature in excess of 1800°C can be reached on small parts. The parts are heated by radiation from a hot molybdenum filament which receives its power from the large variable transformer shown under the table. A mercury manometer for indicating hydrogen flow is pictured at the back of the table. The jar is raised and lowered on a ball bearing track and has a spring type "weightless" window sash type counterbalance. Currents up to 180 amperes are passed through the .080 inch molybdenum filaments to heat them.

The hydrogen atmosphere carbon arc welder is shown in Fig. 18.4. An arm holding the carbon electrode protrudes through a hole in the heavy glass window. An air cylinder controlled by a foot valve raises and lowers the hood over the parts to be welded. To the left is shown the hydrogen valves and flowmeter as well as a timer which controls the length of time the arc is on. Under the table (not shown in the picture) is a rectifier for supplying power to the welder. High melting temperature materials are joined together in this welder.

The Model F. Litton Glass Lathe is shown in Fig. 18.5 set up for glassing the cathode to the tube. Jigs and fixtures are used to align the parts accurately in glassing. Nitrogen which has been passed over alcohol is available for blowing the glass and prevents oxidation of tube parts.

Assembly benches and a portable power supply are shown in Fig. 18.6. The tube parts are assembled in jigs and prepared for the various assembly stages at these tables. The small portable rectifier in the foreground will supply 5000 volts at .5 amperes. This supply is used in tube processing as well as in the test room.

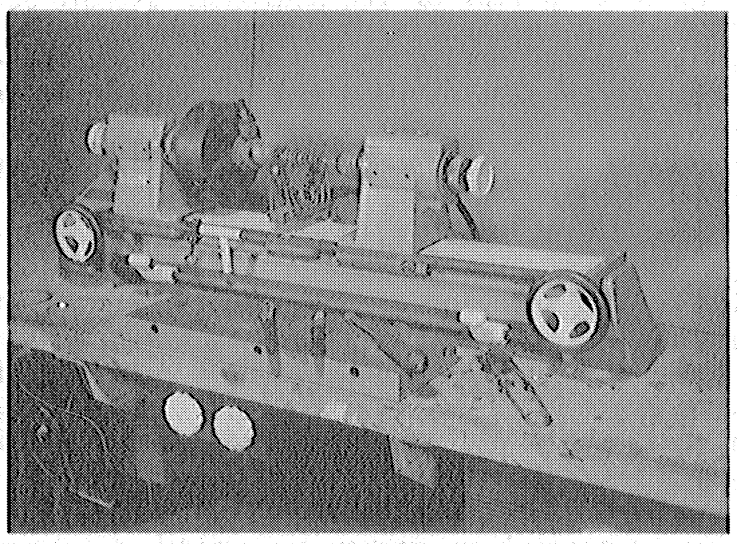

Figure 18.5 Litton Glass Lathe

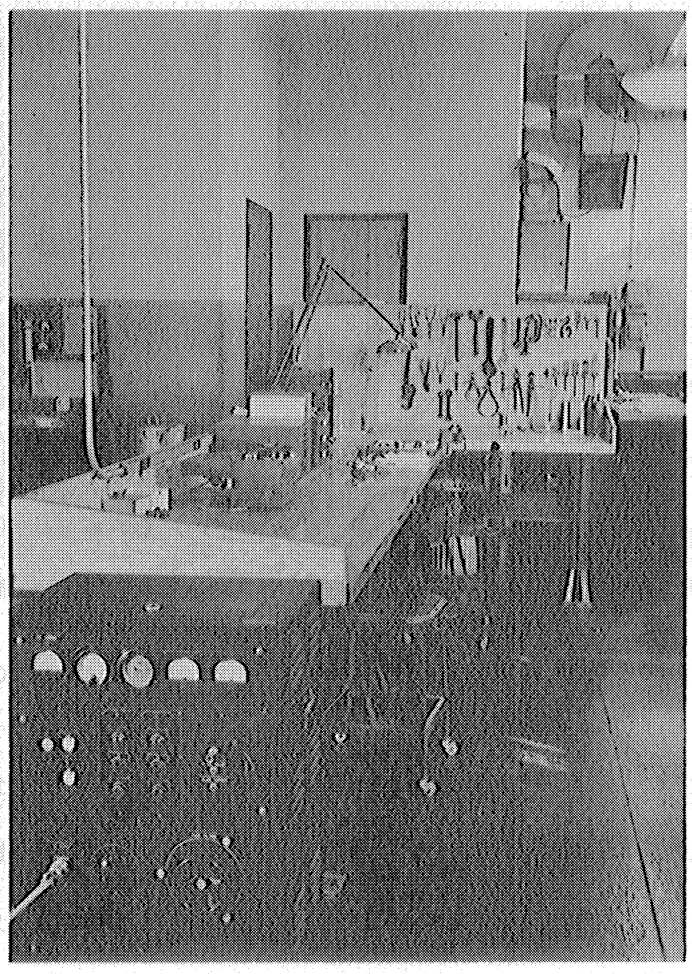

Figure 18.6 Tube Assembly Benches

The blower which is visible near the ceiling is an exhaust fan for the cleaning and electroplating room and the dust-free cathode room. These rooms are normally shut off from the rest of the laboratory. Air intake is supplied through dust filters.

A portion of the interior of the cleaning and electroplating room is shown in Fig. 18.7. Two cleaning baths, two electroplating tanks and a wash tank are visible in this picture. The rectifier for plating shown on the wall in Fig. 18.2 supplies 100 amperes at 6 volts.

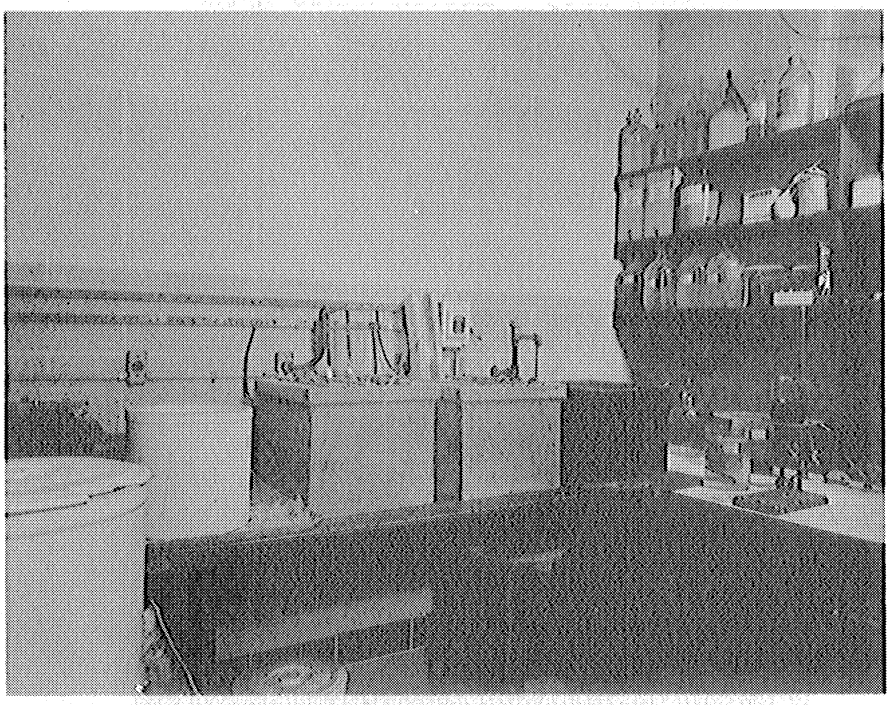

Figure 18.7 Cleaning and Electroplating Room

The evacuation station is pictured in Fig. 18.8 showing a tube sealed to the manifold. The upper right panel contains an automatically regulated ionization gage circuit and a thermocouple vacuum gage circuit. The upper left panel contains controls for the station; i.e., switches for the pumps,

oven, filament supply and a vacuum interlock as well as thermocouple meters and filament meters. The lower left panel contains controls for the ovens, filament and pumps. The large aluminum box below the upper panels is an oven which can be lowered over the tube to bake it at 425°C. A small portable oven can also be used to bake the metal portions of the tube to 625°C. An oil vapor diffusion pump having an activated charcoal baffle produces vacuums in the order of 5×10^{-7} mm Hg.

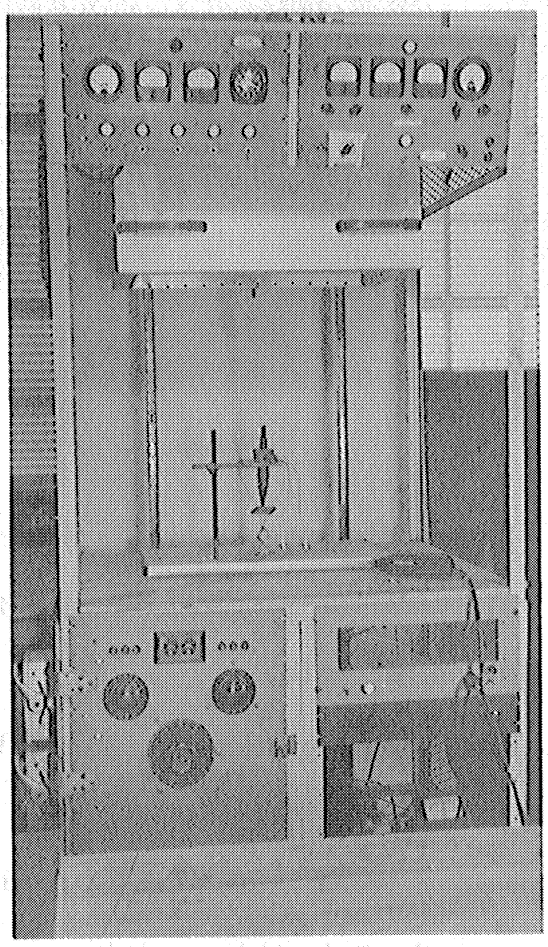

Figure 18.8 Vacuum Station

The glass cutting wheel shown in Fig. 18.9 is used to cut glass tubing to accurate lengths. Water is used as a coolant and to remove glass dust.

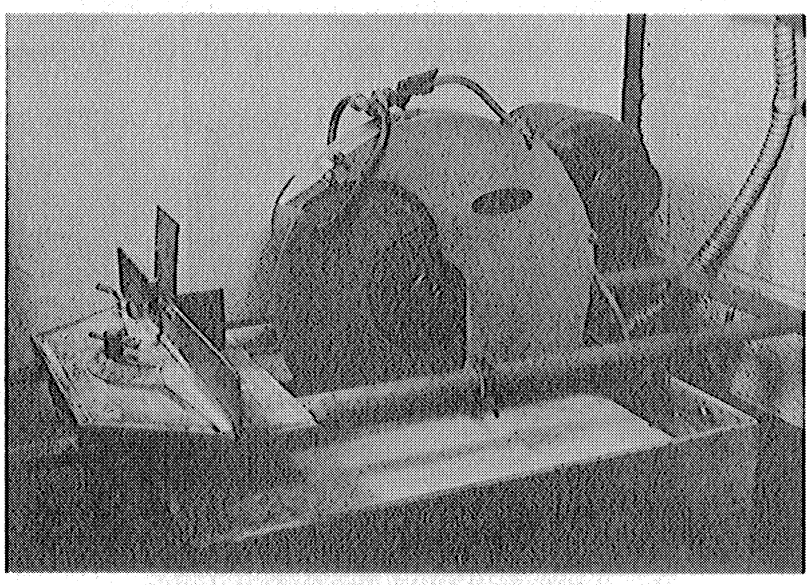

Figure 18.9 Glass Cutting Wheel

The "hot box" for storing tube parts is shown in Fig. 18.10. A 100 watt electric bulb maintains the temperature in this box well above the dew point, reducing oxidation of parts.

The 1 K.V.A. spot welder pictured in Fig. 18.11 is used for welding small parts.

The glass annealing ovens, spot welder, hand-brazing bench, and parts storage space are not shown in this report.

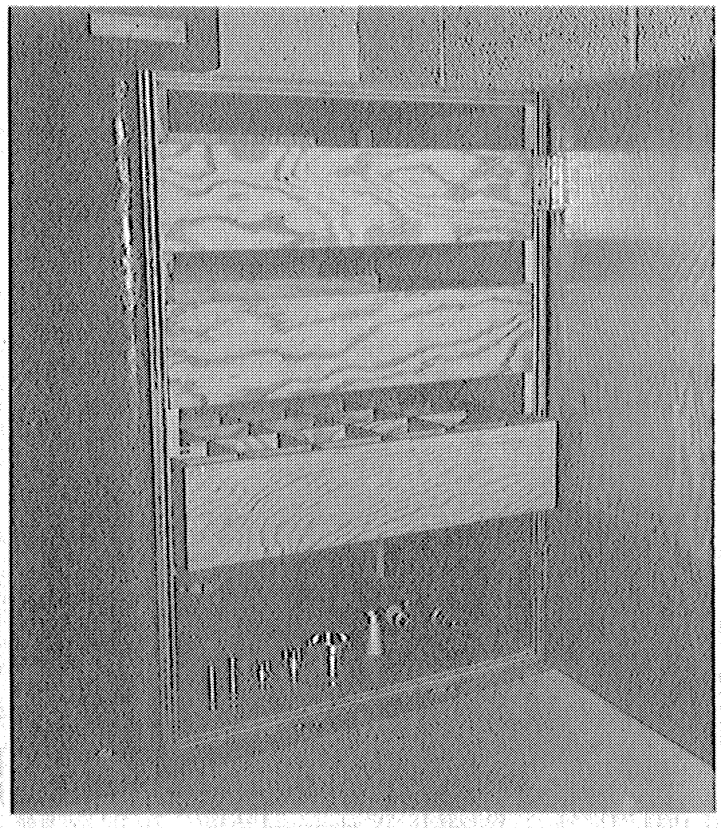

Figure 18.10 "Hot" Box

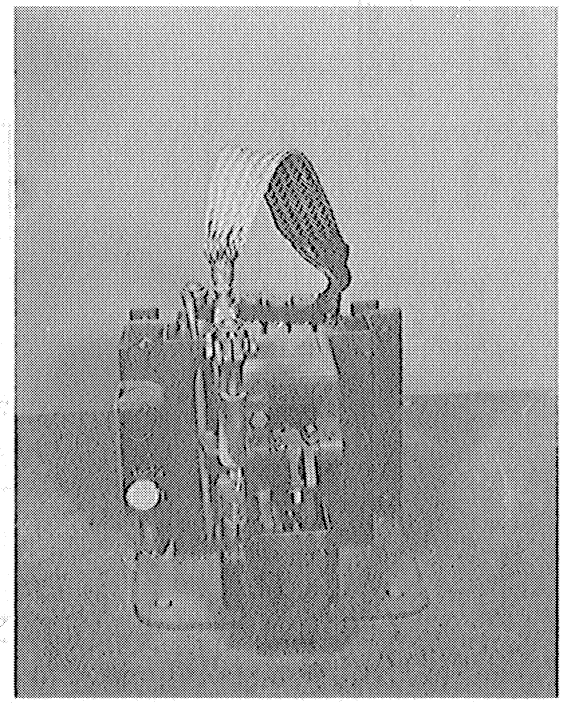

Figure 18.11 Spot Welder

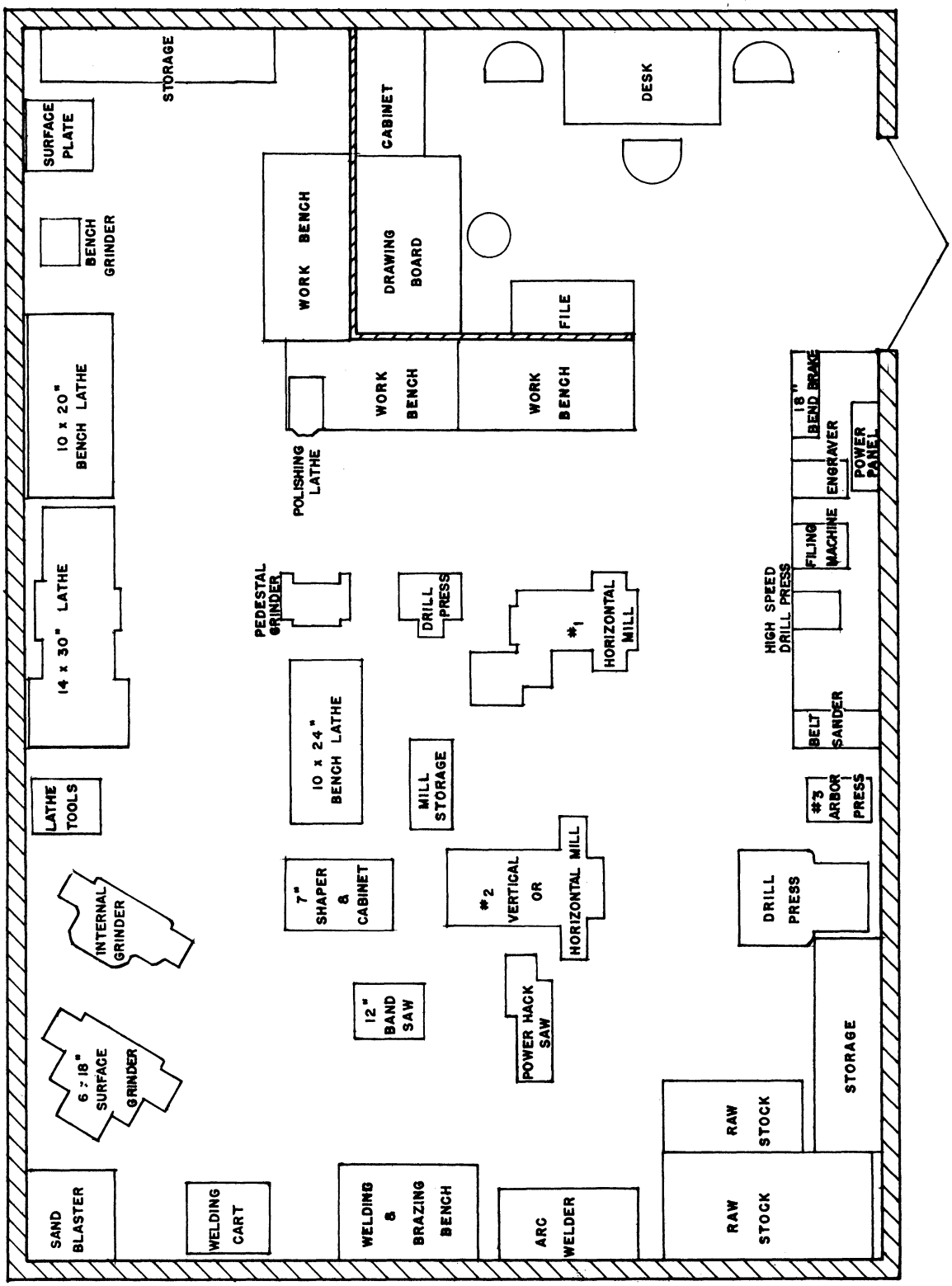

FIG. 19.1 MACHINE SHOP.

19. Machine Shop

The floor plan of the machine shop is shown in Fig. 19.1. Fig. 19.2 shows a portion of the hand bending brake, the engraving machine and the filing machine to the extreme left. Behind the filing machine is the soldering bench with the Prestolyte hand torch. The arbor press and the heavy duty Allen drill press can be seen on the left wall in front of a small tool storage cabinet. At the rear of the room is shown the stock rack and a 220 to 440 volt transformer hanging on the wall. The No. 2 Brown and Sharp universal mill with a Bridgeport attachment and the horizontal Cincinnati Mill No. 1 are shown to the right.

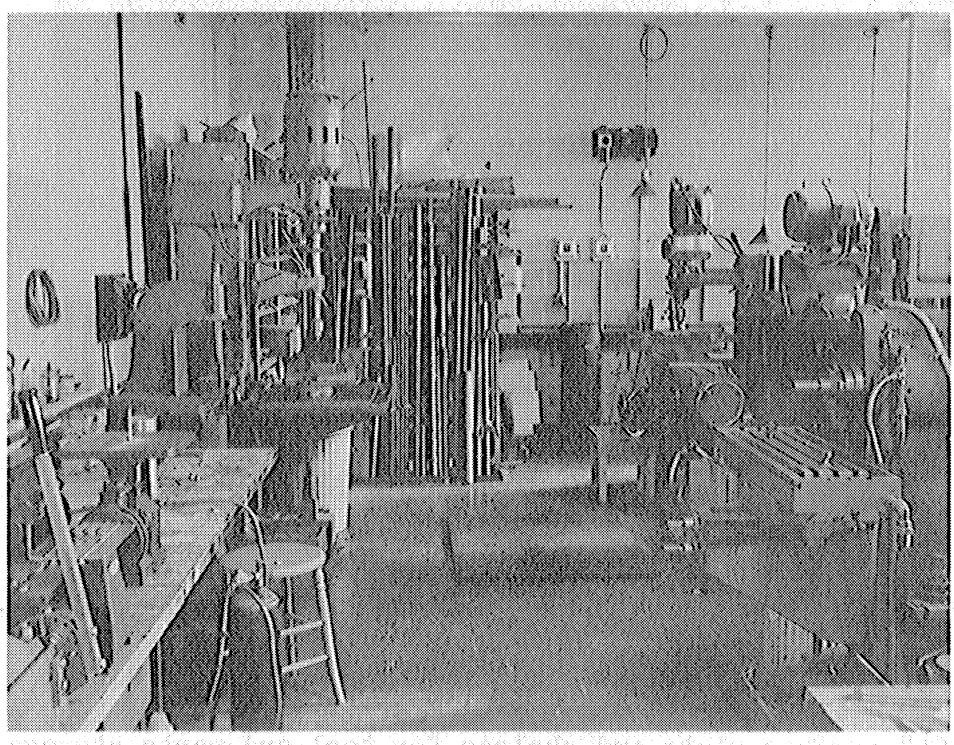

Figure 19.2 Machine Shop

Fig. 19.3 shows another portion of the machine shop. A Sheldon 10-inch lathe can be seen to the left with a bench grinder and metal band saw to its rear. The welding bench with the oxy-acetylene brazing equipment is shown at the rear wall. A portion of a Norton hydraulic surface grinder can be seen behind a Majestic internal grinder on the right hand side of the picture.

Figure 19.3 Machine Shop

Fig. 19.4 shows the 14-inch Hendy tool room lathe and a 9-inch Ames speed lathe to the right. Behind the Ames lathe can be seen a portion of a 24" x 24" surface plate and shelves for tool and parts storage.

Fig. 19.5 shows work bench space, a Shauer polishing lathe, a jeweler's lathe, a watchmaker's high speed drill press and a pedestal grinder.

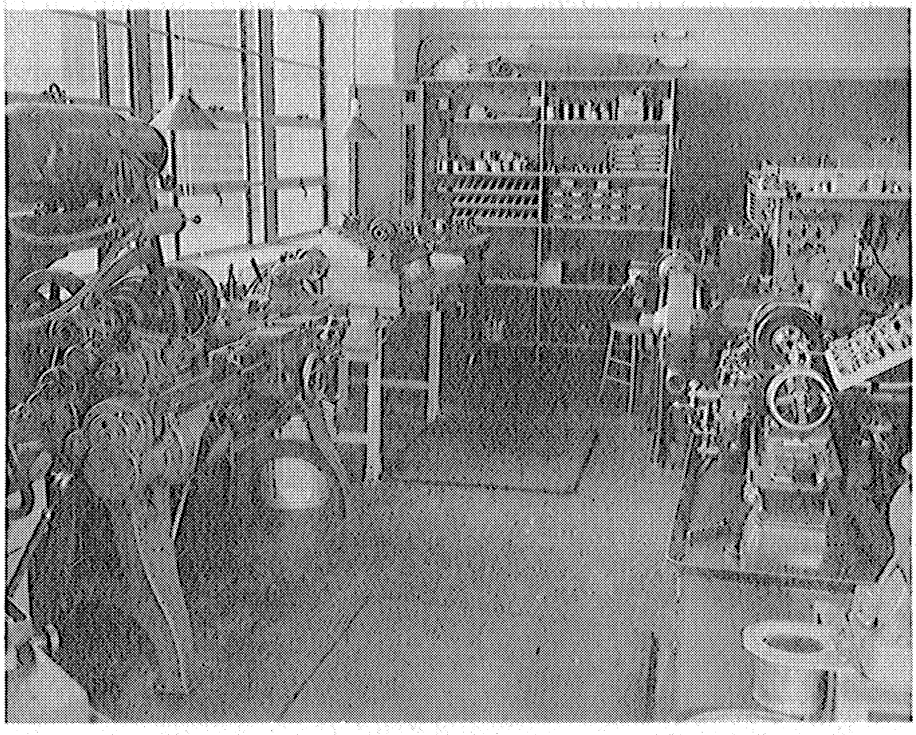

Figure 19.4 Machine Shop

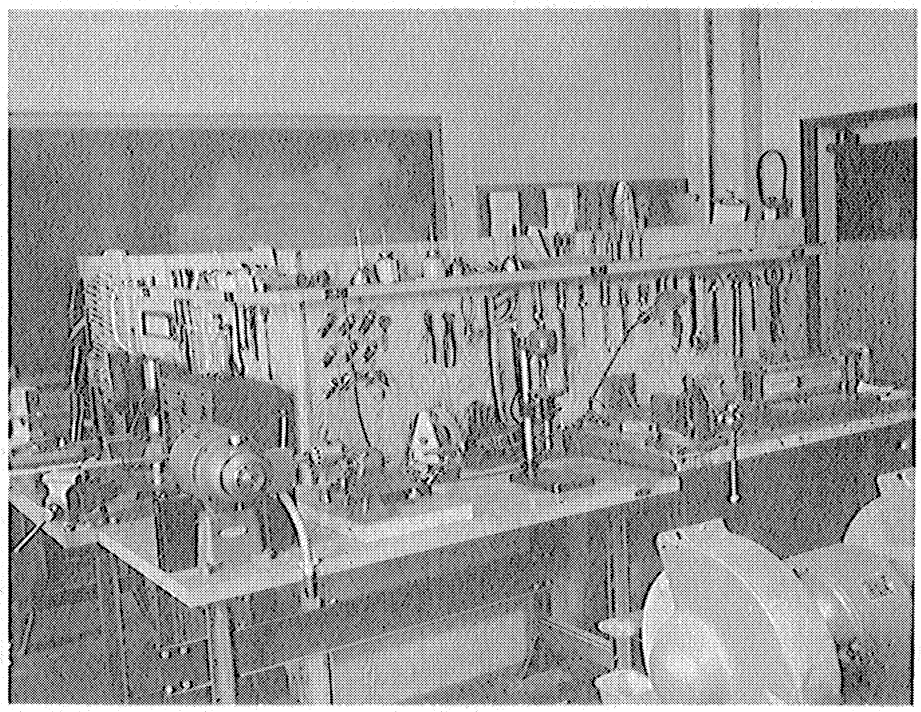

Figure 19.5 Machine Shop

Not shown in the pictures are a 7-inch Ammco shaper, a Mott sand blaster, a Walker-Turner 1/2-inch drill press, and a Toledo power hack saw. Precision measuring equipment such as Johanasson blocks, height gages, Sheffield visual indicator, angle plates, cubes, bench centers, micrometers, etc., complete the tool room equipment.

VI. CONCLUSIONS

20. Summary of Results

The results of the work done on this contract can be placed in four broad categories. These are the following:

a. Through theoretical and experimental analysis, an improved understanding of the space charge and its effects in the magnetron has been obtained.

b. Factors which influence the design of interdigital magnetrons for operation in the zero order mode have been evaluated by extensive analysis, experimental tests, construction and operation of tubes of varied design.

c. Using the results above as a basis, three new designs for frequency modulation magnetrons have been developed and preliminary experimental tests made.

d. It has been demonstrated that a relatively small research group in a University laboratory can over a long period of time carry on a broad program covering several phases of a problem. In this case, for instance, analysis of the space charge in the magnetron, study of various microwave resonant circuit geometries, design and construction of operating tubes, and evaluation of performance of these tubes have been carried out simultaneously.

Two technical reports have been prepared covering work done on categories a and b above. Eight operable magnetrons have been built and studied. Six of these were different in design. It should be pointed out that the major purpose for building a tube in a laboratory of this type is

to obtain and interpret research data on an individual tube. The gathering of statistical information on a number of tubes is more properly left to industrial laboratories or to agencies operating in cooperation with industrial laboratories.

The techniques used in construction, and research which is in progress but not considered ready for comprehensive presentation, are discussed in some detail in the present report. This includes the preliminary experiments on frequency modulation magnetrons. A complete report on problems specifically related to frequency modulation magnetrons will be presented when operating tubes are available and experimental tests have been made.

21. Proposed Future Activity

Several areas for investigation have been brought to light by the research on this project which have been relatively unexplored because enough time was not available. Also, emphasis has been on obtaining knowledge of basic principles of design for frequency modulation magnetrons, so that some of the more obvious practical problems have not been investigated with thoroughness.

It is recommended that the following fields should receive further attention.

a. Development of one or more of the proposed frequency modulation magnetron designs into a practically usable, tunable tube.

b. Development of a broader band choke and by-pass combination for the cathode line to increase usable tuning range in the zero order mode.

c. Development of an improved tuning method for interdigital magnetrons.

d. Further investigation of fundamentals of magnetron operation with particular emphasis on factors which determine optimum shunt impedance and influence mode jump current.

e. Experimental study of the properties of the magnetron space charge in the vicinity of the cyclotron resonance. This should be carried on at constant space charge swarm radius for values of magnetic field from that for which the dielectric constant of the space charge is definitely positive and less than unity to that for which the dielectric constant of the space charge is definitely negative.

f. Study of the relationship between pre-cutoff and pre-oscillatory anode currents and noise level in the magnetron.

g. Study of the possibilities of amplification of r-f energy in the magnetron space charge and the effect of this amplification on noise level.

h. Development of a tube for signal generator use based on ideas presented in Section 16.

i. Research and development on magnetron amplifiers based on the ideas presented in Section 15.

j. Development of a high-power interdigital structure with several anode sets in a multi-wave length cavity as proposed in Section 16.

k. Consideration of the problems which would be involved in development of a high power glass or ceramic envelope interdigital structure for use in an external cavity.

The primary effort of the University of Michigan group in the future on Contract No. W-36-039 sc-35561 will be to carry out the activity of part a. After the development of the frequency modulation magnetron has progressed to the extent that evidence of reasonably good operating characteristics is obtained on completed tubes, a report will be prepared giving the

basic principles of design and results and interpretation of experimental tests on the tubes. This should be accomplished within the coming year.

It is also certain that some attention will be given to the problems listed in parts b, c, d, and e on this contract. The extent of the work in any case will depend on how well it fits in with the primary program. Problems of developing a broad-band choke design, improving tuning methods and investigation of factors determining optimum shunt impedance will undoubtedly receive considerable attention. Any significant results will be the subject of technical reports issued by the laboratory.

APPENDIX A

Distribution of Activity of Personnel Employed by the Project

(The figures in this table are necessarily estimated since overlapping of function occurs in many cases. Vacation time is not included.)

Activity	Man Months	Per cent of Total Time	Per cent of Total Payroll
Research, design, technical reporting by senior staff	48	25.0	33.6
Research and testing by student research assistants	20	10.4	6.8
Engineering of equipment used in testing and processing. Development of assembly and processing techniques	28	14.6	18.6
Construction of apparatus used in testing and processing	12	6.25	4.9
Assembly and processing of tubes (not including machining of parts)	12	6.25	6.0
Machine and shop work	36	18.75	16.5
Drafting and illustrating	24	12.5	8.8
Secretarial	7	3.65	1.6
Miscellaneous Services	5	2.6	3.2

TABLE B.1

Distribution in Expenditure in Per Cent by Six Month's Periods

Six Month's Period	July-Dec 1946	Jan-June 1947	July-Dec 1947	Jan-June 1948	July-Dec 1948	Jan-June 1949	Per Cent of Total Expenditure
Personnel	51.7	37.4	48.6	55.7	59.0	57.0	50.3
Material and Apparatus	22.6	44.4	29.4	18.5	15.6	15.5	26.4
Travel	1.5	1.6	.4	1.4	0.0	1.5	1.0
Service Charge	23.0	16.0	21.0	23.9	25.4	24.5	21.6
Miscellaneous	1.2	.6	.6	.5	0.0	1.5	.7
Per Cent of Total Funds Expended During Interval	10.7	24.7	19.0	18.6	16.3	11.7	100.0

APPENDIX B

Distribution of Funds and Equipment Allocated to the Project

a. The approximate distribution and rate of expenditure of contract funds is indicated by the percentages in Table B.1 which faces this page. A complete inventory has of course been submitted to the contractor.

b. In addition to the funds furnished by the contractor, a number of items are being used in the test room on loan from the Evans Signal Laboratory. These are the following: two amplifiers for use with crystal or bolometer; two thermistor bridges with mounts; four oscilloscopes; two spectrum analyzers; two wave meters; one General Radio vacuum tube voltmeter; one synchroscope; one 2C38 oscillator cavity and miscellaneous 7/8-inch coaxial microwave plumbing.

c. Several pieces of equipment and facilities have been purchased or provided by the University for use in the electron tube laboratory. The equipment includes the following: a hydrogen atmosphere arc welder, K.V.A. spot welder, parts for hydrogen furnaces built in the laboratory; arbor press; Allen heavy duty drill press; Cincinnati No. 1-1/2 horizontal mill; Browne and Sharpe No. 2 horizontal mill; L.W. 5 x 5 power hack saw; Norton 6 x 18 hydraulic surface grinder; Majestic internal grinder; 14 x 30 Hendy lathe; 10-inch Ames bench lathe; Schauer polishing lathe; Walker Turner band saw with master speed ranger; Sheffield visual indicator; a set of Johannason gauge blocks and a Jones and Lamson 20-inch pedestal type optical comparator. Various meters and other test equipment belonging to the Department of Electrical Engineering are used from time to time as needed. A helium mass spectrometer leak detector and x-ray equipment is available for use by the project.

Facilities installed especially for the electron tube laboratory by the University include the following: plumbing for water cooling, water loads, laboratory sinks and the electroplating laboratory; two specially constructed rooms with forced air circulation for electroplating and cleaning, and cathode assembly; and electrical installation of machines, processing and test equipment and furnaces.

APPENDIX C

Assembly Drawings of Interdigital Magnetrons Constructed at University of Michigan

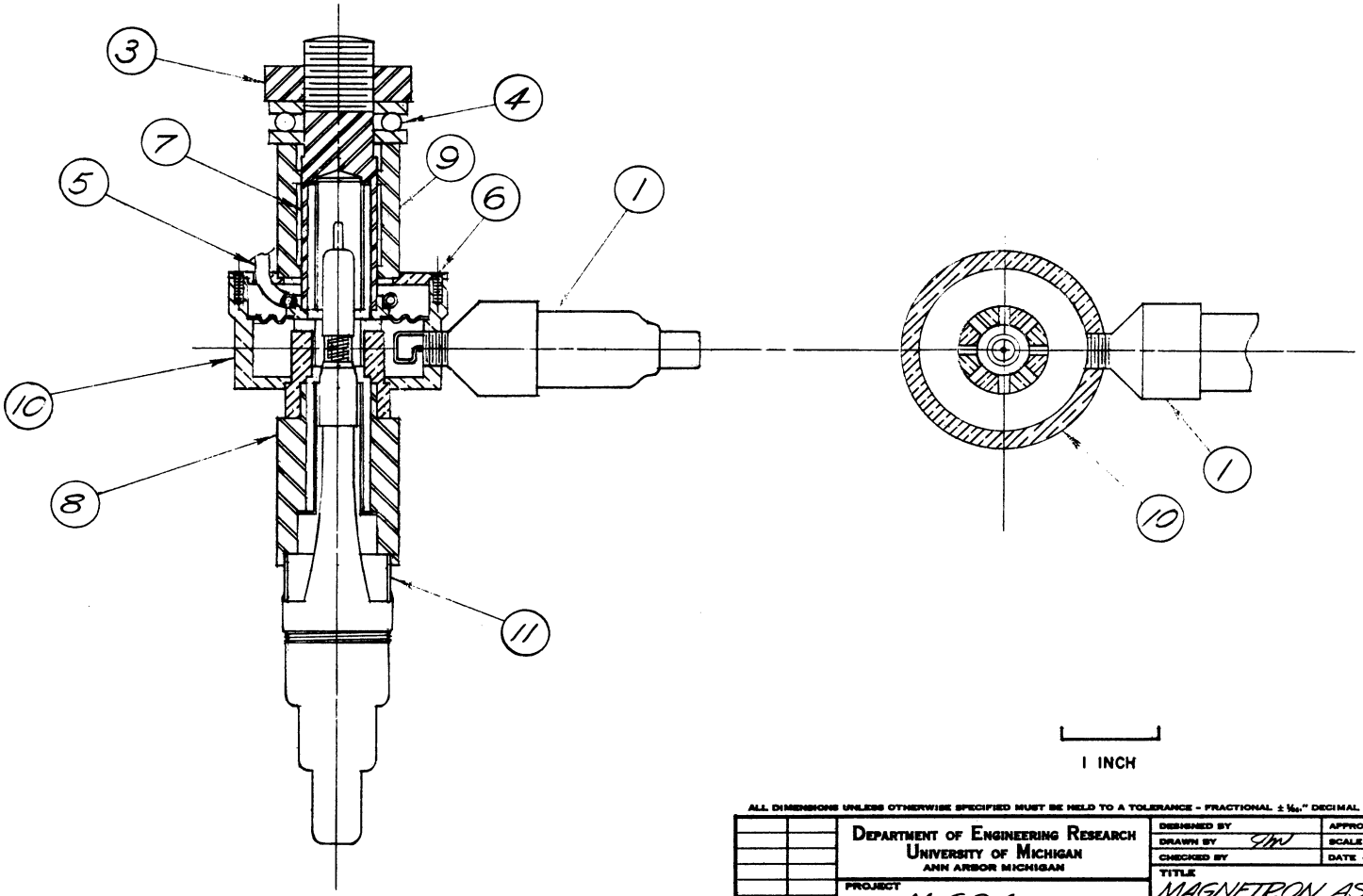

1 INCH

ALL DIMENSIONS UNLESS OTHERWISE SPECIFIED MUST BE HELD TO A TOLERANCE - FRACTIONAL ± 1/32," DECIMAL ± .005," ANGULAR ± ½°

		DEPARTMENT OF ENGINEERING RESEARCH UNIVERSITY OF MICHIGAN ANN ARBOR MICHIGAN	DESIGNED BY	APPROVED BY
			DRAWN BY GW	SCALE FULL SIZE
			CHECKED BY	DATE 9/15/47
		PROJECT M-694	TITLE MAGNETRON ASSEMBLY MODEL 2	
1	9/16/47	CLASSIFICATION	DWG. NO.	B-10,002
ISSUE	DATE			

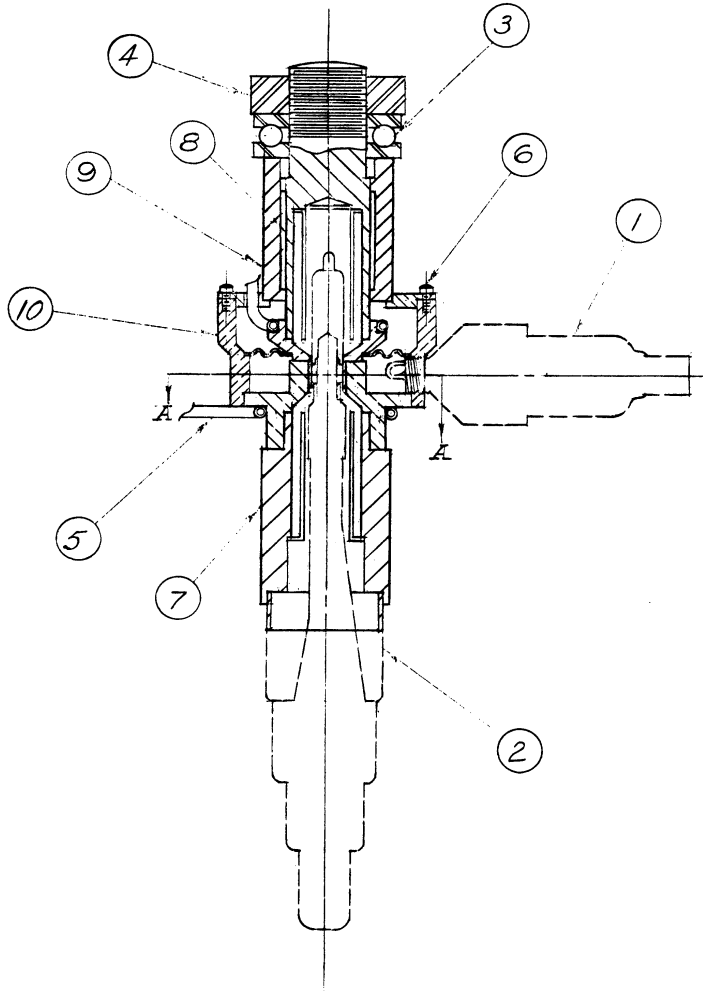

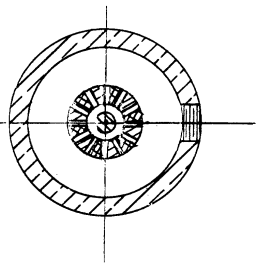

SECTION A-A

1 INCH

ALL DIMENSIONS UNLESS OTHERWISE SPECIFIED MUST BE HELD TO A TOLERANCE - FRACTIONAL ± 1/64" DECIMAL ± .005" ANGULAR ± 1/2°

		DEPARTMENT OF ENGINEERING RESEARCH UNIVERSITY OF MICHIGAN ANN ARBOR MICHIGAN	DESIGNED BY AWW, RSB; APPROVED BY AWW
			DRAWN BY JMS; SCALE FULL SIZE
			CHECKED BY AWW; DATE 5/9/47
		PROJECT M-694	TITLE MAGNETRON ASSEMBLY MODEL 3
1	5/9/47	CLASSIFICATION	DWG. NO. B-10,003
ISSUE	DATE		

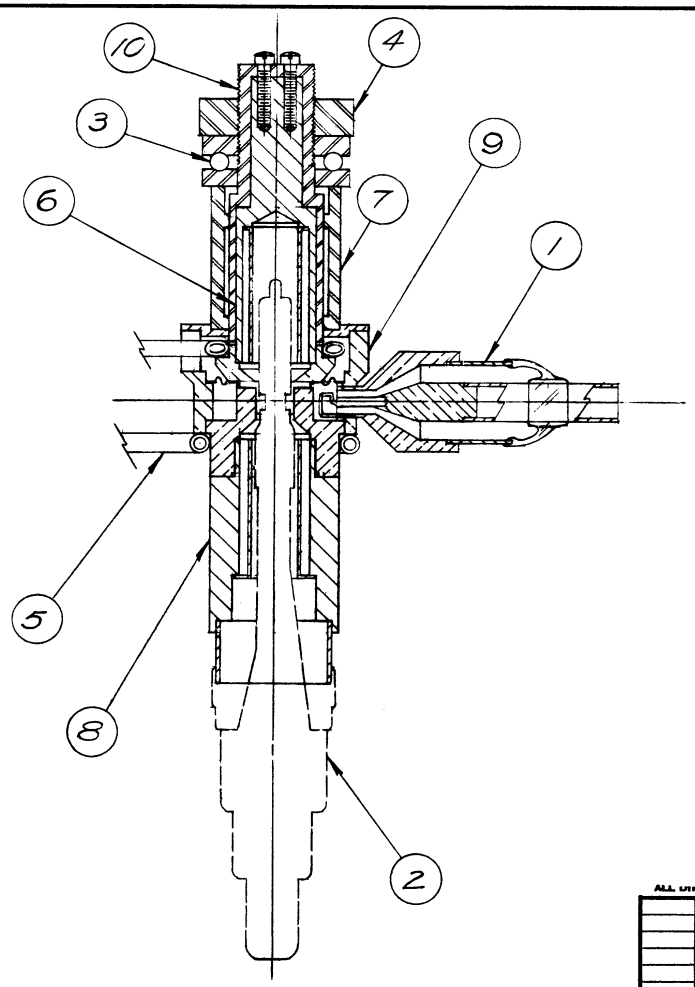

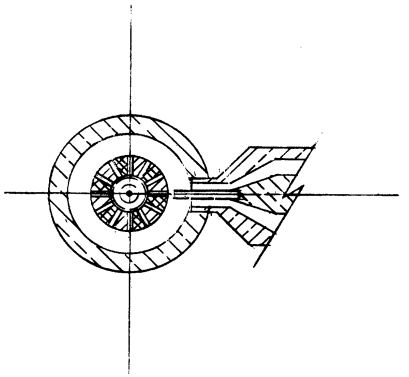

1 INCH

ALL DIMENSIONS UNLESS OTHERWISE SPECIFIED MUST BE HELD TO A TOLERANCE - FRACTIONAL ± 1/64" DECIMAL ± .005" ANGULAR ± ½°

		DEPARTMENT OF ENGINEERING RESEARCH UNIVERSITY OF MICHIGAN ANN ARBOR MICHIGAN	DESIGNED BY A.W.W	APPROVED BY H.WW
			DRAWN BY	SCALE FULL SIZE
			CHECKED BY J.B.S.	DATE 3/12/48
		PROJECT M-694	TITLE MAGNETRON ASSEMBLY MODEL 9A	
1	3/24/48	CLASSIFICATION	DWG. NO. B-10003A	
ISSUE	DATE			

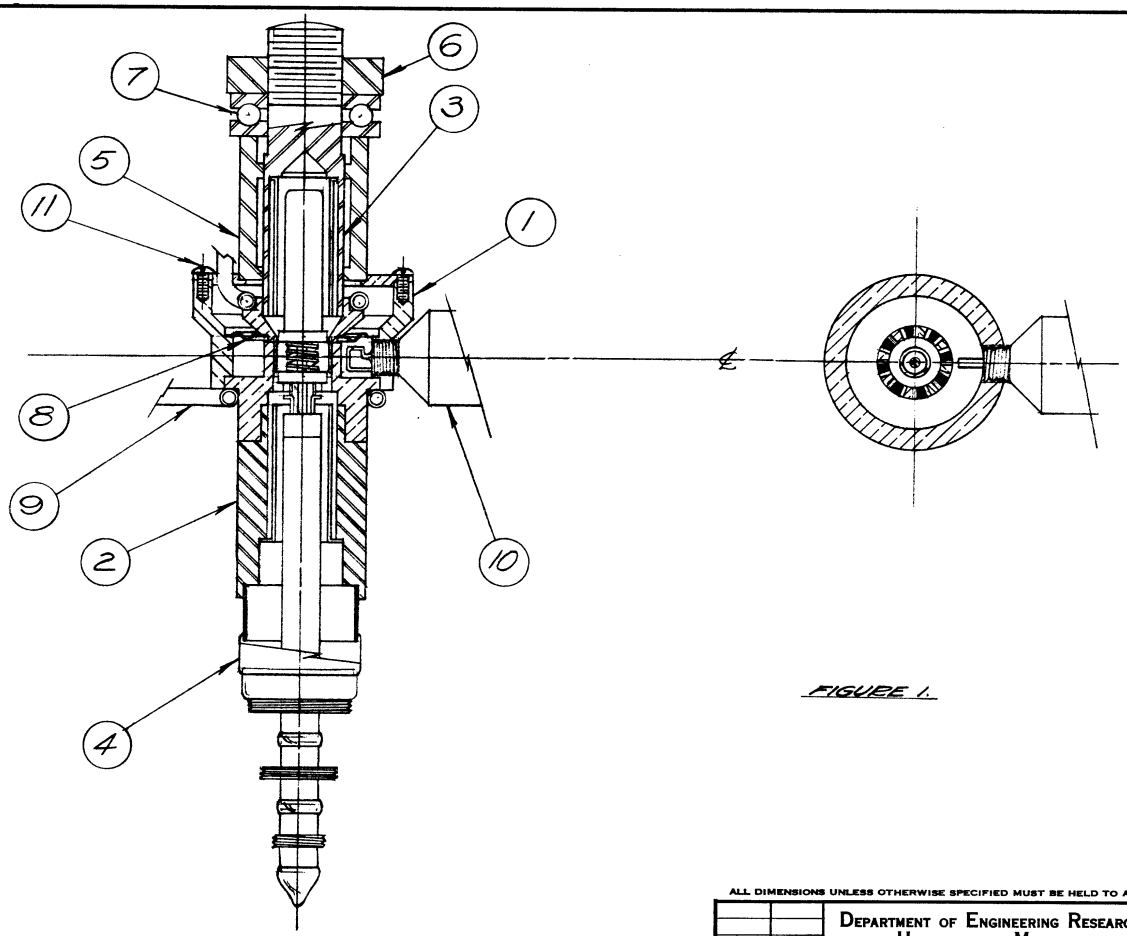

FIGURE 1.

1 INCH

ALL DIMENSIONS UNLESS OTHERWISE SPECIFIED MUST BE HELD TO A TOLERANCE - FRACTIONAL ± 1/64," DECIMAL ± .005," ANGULAR ± 1/2°

		DEPARTMENT OF ENGINEERING RESEARCH UNIVERSITY OF MICHIGAN ANN ARBOR MICHIGAN	DESIGNED BY H.W.W. J.R.B. / APPROVED BY H.W.W.
			DRAWN BY / SCALE FULL SIZE
			CHECKED BY H.W.W. / DATE 8/12/47
		PROJECT M-694	TITLE MAGNETRON ASSEMBLY MODEL #4
1	8/R/47	CLASSIFICATION	DWG. NO. B-10,004
ISSUE	DATE		

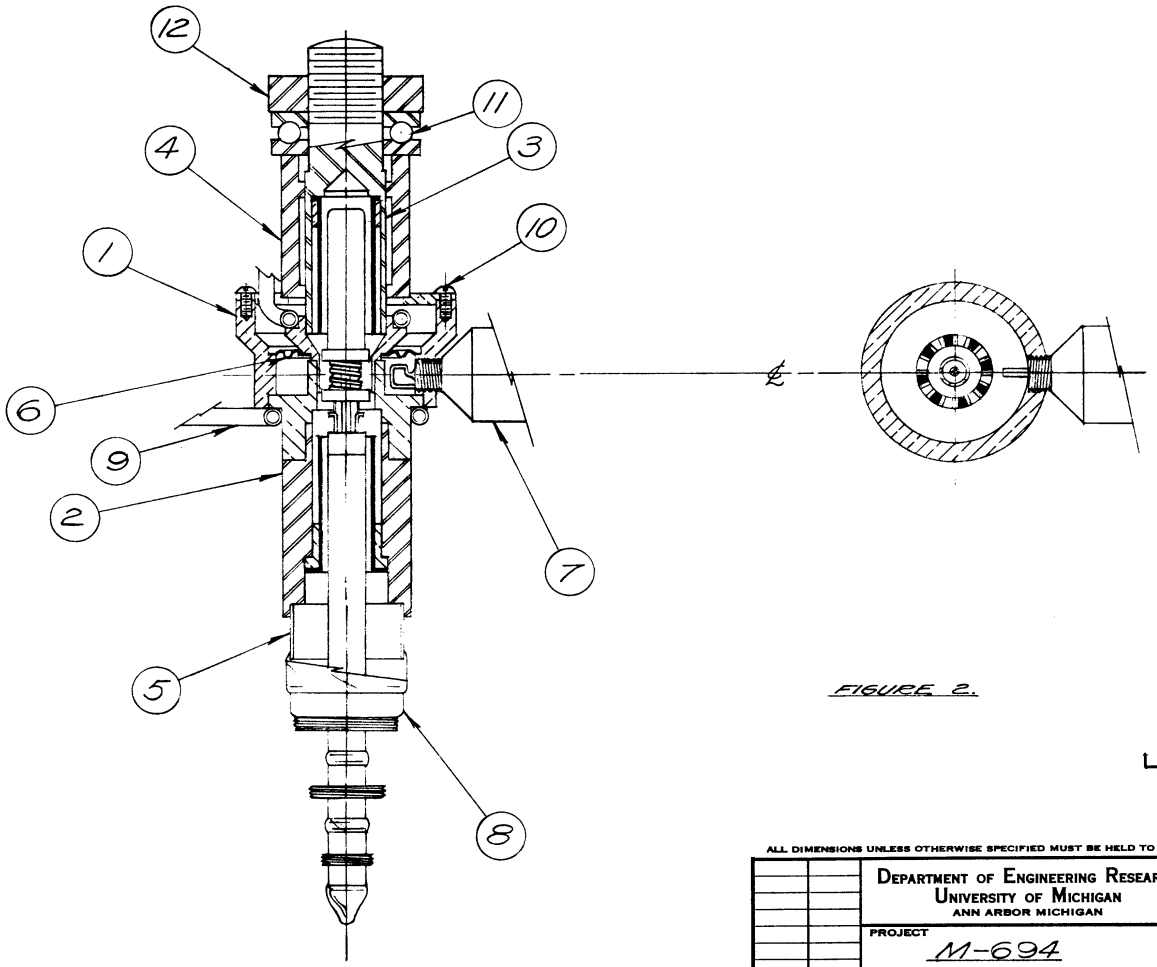

FIGURE 2.

1 INCH

ALL DIMENSIONS UNLESS OTHERWISE SPECIFIED MUST BE HELD TO A TOLERANCE - FRACTIONAL ± 1/64," DECIMAL ± .005," ANGULAR ± ½°

		DEPARTMENT OF ENGINEERING RESEARCH UNIVERSITY OF MICHIGAN ANN ARBOR MICHIGAN	DESIGNED BY H.W.W.	APPROVED BY H.W.W.
			DRAWN BY J. J	SCALE FULL SIZE
			CHECKED BY J.R.B.	DATE 9/15/47
		PROJECT M-694	TITLE MAGNETRON ASSEMBLY MODEL #4A	
1	8/14/47	CLASSIFICATION	DWG. NO. B-10,004 A	
ISSUE	DATE			

APPENDIX D

Parts and Sub-Assemblies for Model 3

Interdigital Magnetron

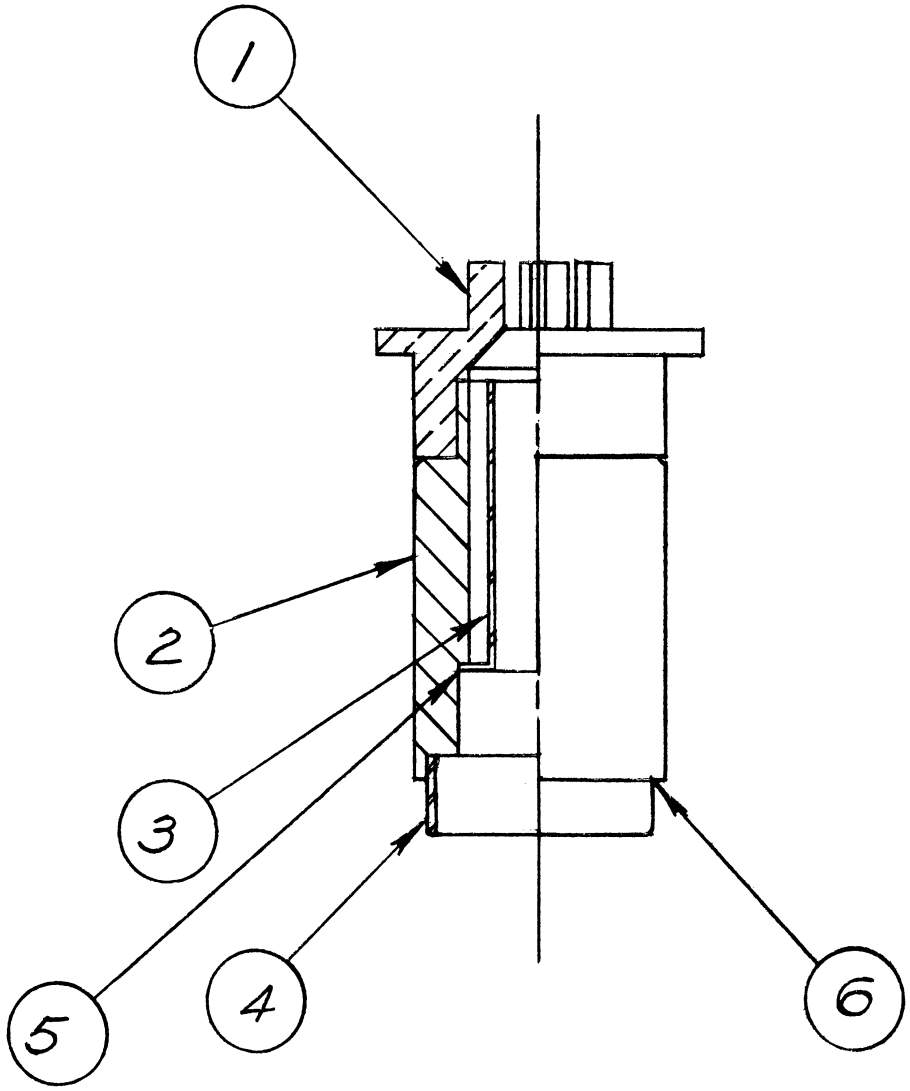

ALL DIMENSIONS UNLESS OTHERWISE SPECIFIED MUST BE HELD TO A TOLERANCE - FRACTIONAL ± 1/64," DECIMAL ± .005," ANGULAR ±

		DEPARTMENT OF ENGINEERING RESEARCH UNIVERSITY OF MICHIGAN ANN ARBOR MICHIGAN	DESIGNED BY J.R.B.	APPROVED BY H.W.W.
			DRAWN BY J.M.	SCALE FULL SIZE
			CHECKED BY R.S.B.	DATE 3/6/47
		PROJECT M-694	TITLE CATHODE POLE PIECE & ANOD ASSEMBLY	
1 ISSUE	3/6/47 DATE	CLASSIFICATION	DWG. NO.	A-10,003-1

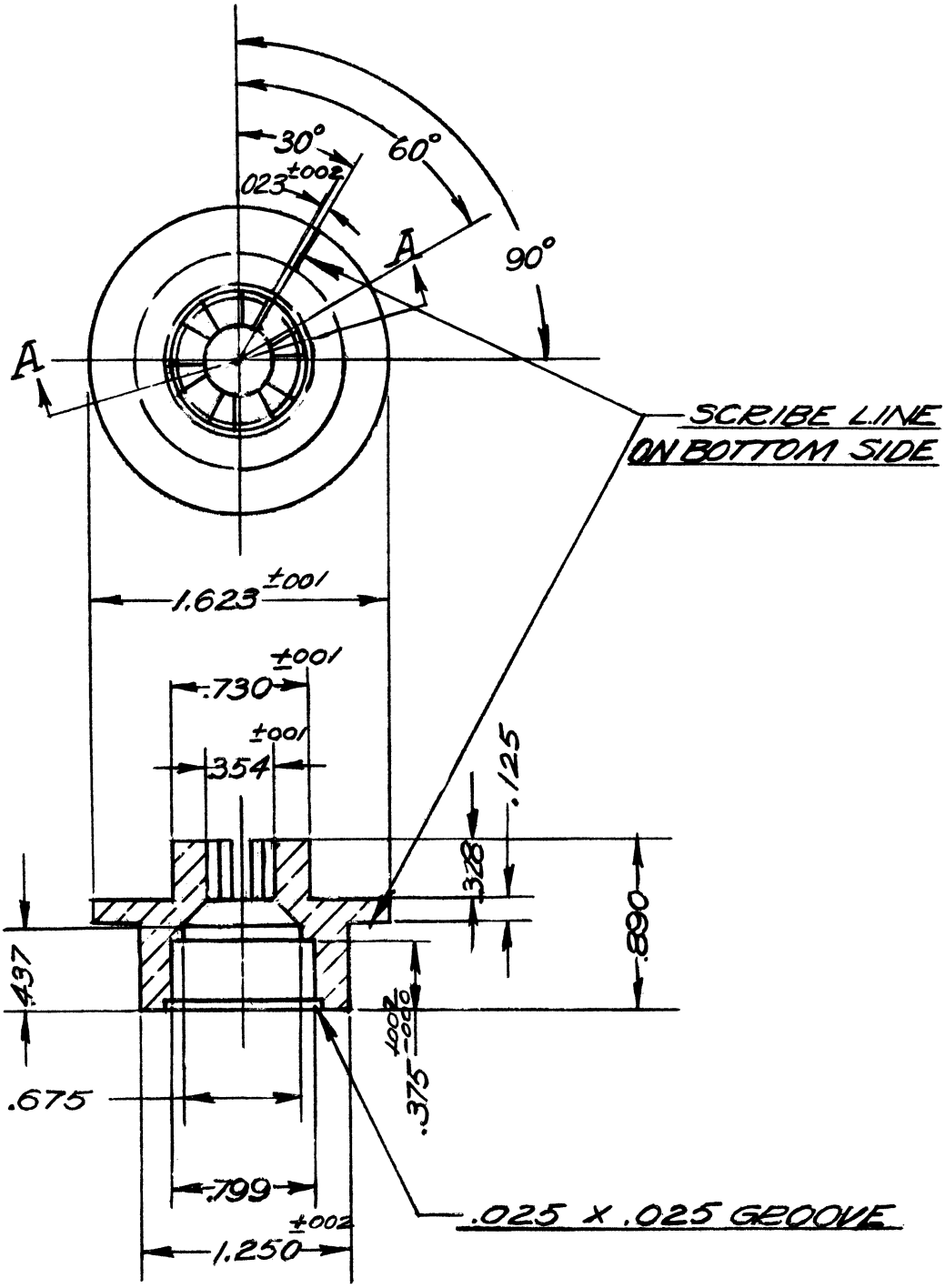

SECTION A-A

OFHC COPPER 1 REQ'D

ALL DIMENSIONS UNLESS OTHERWISE SPECIFIED MUST BE HELD TO A TOLERANCE - FRACTIONAL ± 1/64," DECIMAL ± .005," ANGULAR ± ½°

		DEPARTMENT OF ENGINEERING RESEARCH UNIVERSITY OF MICHIGAN ANN ARBOR MICHIGAN	DESIGNED BY J. W. W. / APPROVED BY
			DRAWN BY J. W. / SCALE FULL SIZE
			CHECKED BY R. S. B. / DATE
		PROJECT M-694	TITLE CAVITY ANODE
2	9/15/47	CLASSIFICATION	DWG. NO. A- 5004
1	5/15/47		
ISSUE	DATE		

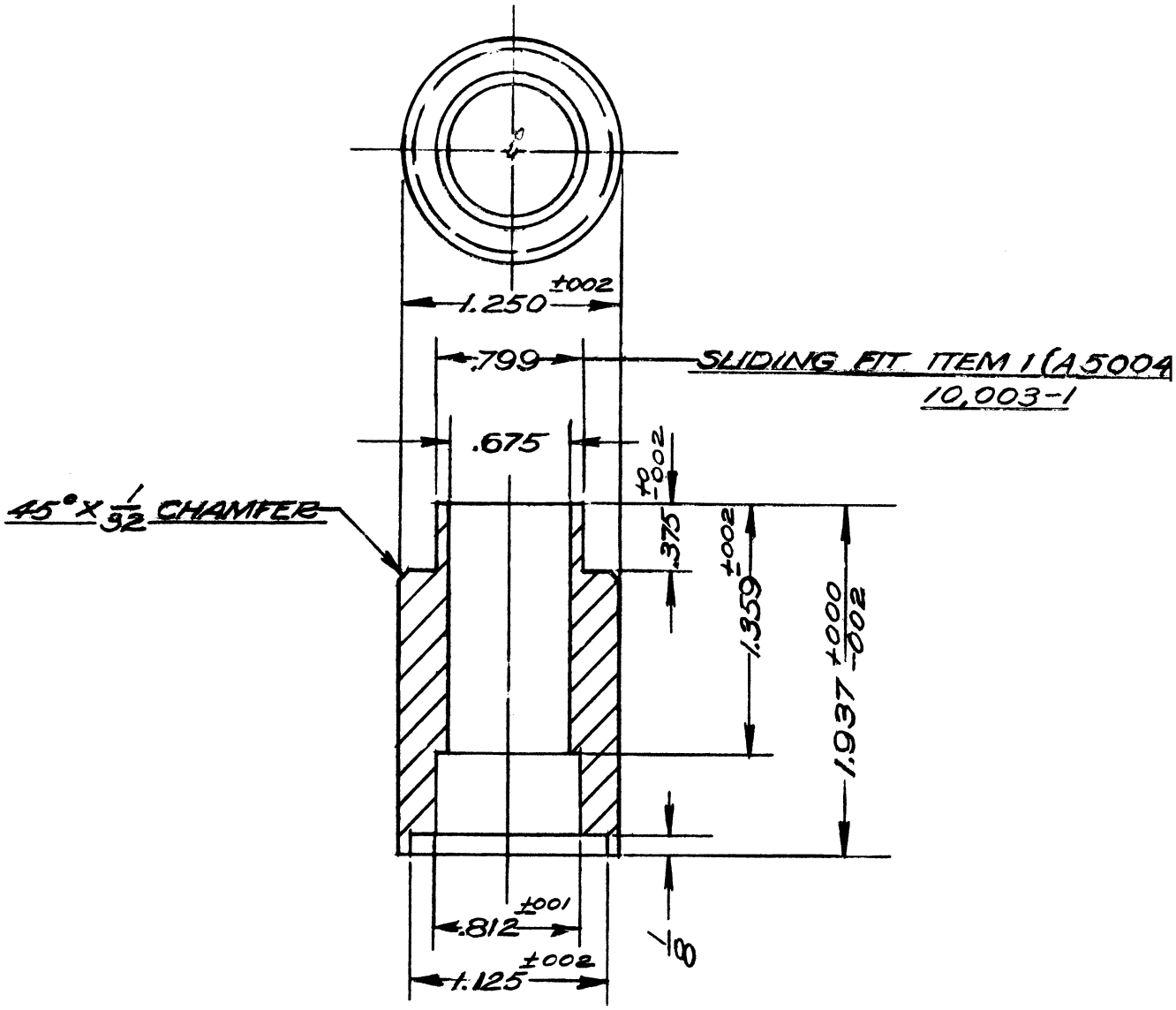

HRS 1 REQ'D

ALL DIMENSIONS UNLESS OTHERWISE SPECIFIED MUST BE HELD TO A TOLERANCE - FRACTIONAL ± 1/64," DECIMAL ± .005," ANGULAR ± 1/2°

ISSUE	DATE
3	1/22/46
2	8/4/47
1	5/1/47

DEPARTMENT OF ENGINEERING RESEARCH
UNIVERSITY OF MICHIGAN
ANN ARBOR MICHIGAN

PROJECT M-694

CLASSIFICATION

DESIGNED BY J. R. B.	APPROVED BY
DRAWN BY J. N.	SCALE FULL SIZE
CHECKED BY R. S. B.	DATE 5/1/47

TITLE
CATHODE POLE PIECE

DWG. NO. A-9007

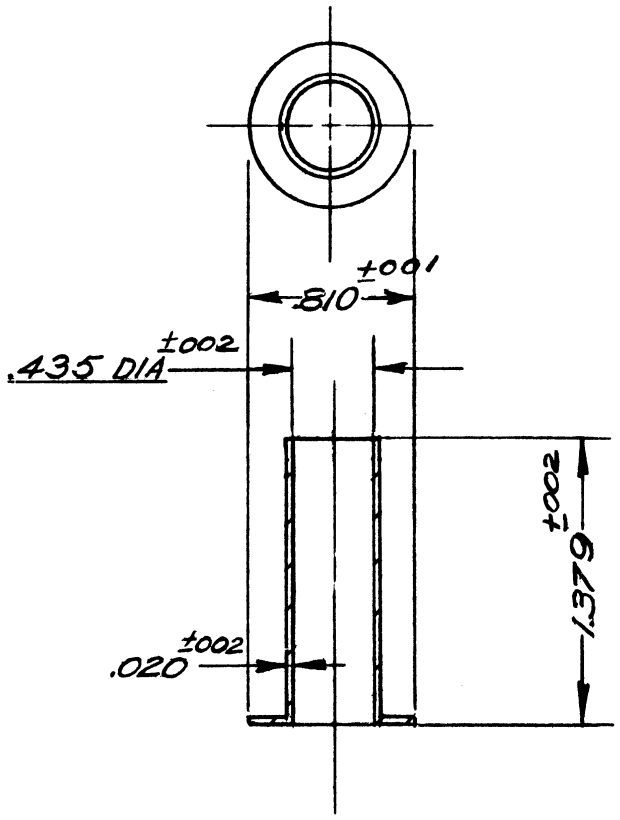

COPPER 1 REQ'D

ALL DIMENSIONS UNLESS OTHERWISE SPECIFIED MUST BE HELD TO A TOLERANCE - FRACTIONAL ± 1/64," DECIMAL ± .005," ANGULAR ± ½°

		DEPARTMENT OF ENGINEERING RESEARCH UNIVERSITY OF MICHIGAN ANN ARBOR MICHIGAN	DESIGNED BY J.R.B. / DRAWN BY J.M. / CHECKED BY R.S.B.
			APPROVED BY / SCALE FULL SIZE / DATE 5/2/47
		PROJECT M-694	TITLE CATHODE CHOKE
	5/2/47	CLASSIFICATION	DWG. NO. A-9,006
ISSUE	DATE		

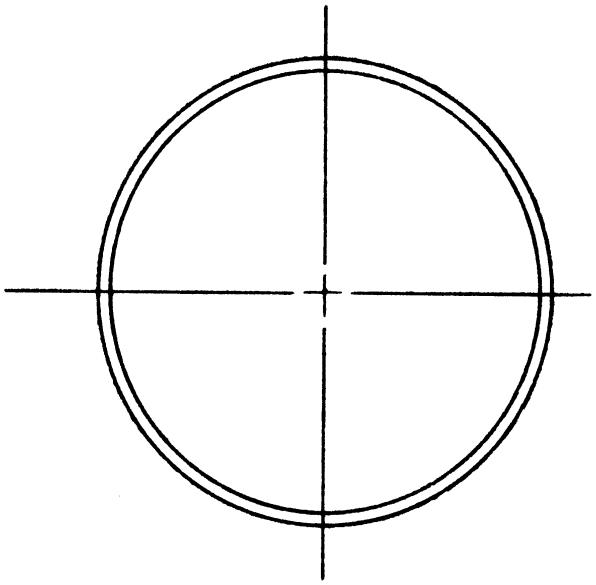

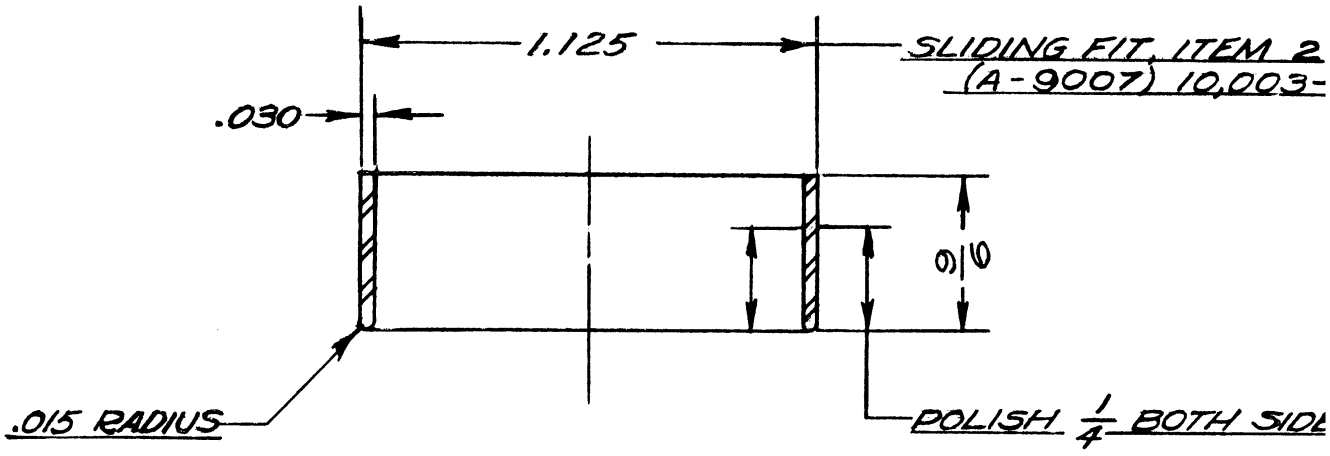

KOVAR 1 REQ'D

ALL DIMENSIONS UNLESS OTHERWISE SPECIFIED MUST BE HELD TO A TOLERANCE - FRACTIONAL ± 1/64," DECIMAL ± .005," ANGULAR ± 3

		DEPARTMENT OF ENGINEERING RESEARCH UNIVERSITY OF MICHIGAN ANN ARBOR MICHIGAN	DESIGNED BY J.R.B.	APPROVED BY
			DRAWN BY J.H.	SCALE DOUBLE SIZE
			CHECKED BY R.S.B	DATE 6/3/47
		PROJECT M-694	TITLE KOVAR SLEEVE	
1 ISSUE	6/3/47 DATE	CLASSIFICATION	DWG. NO. A-9015	

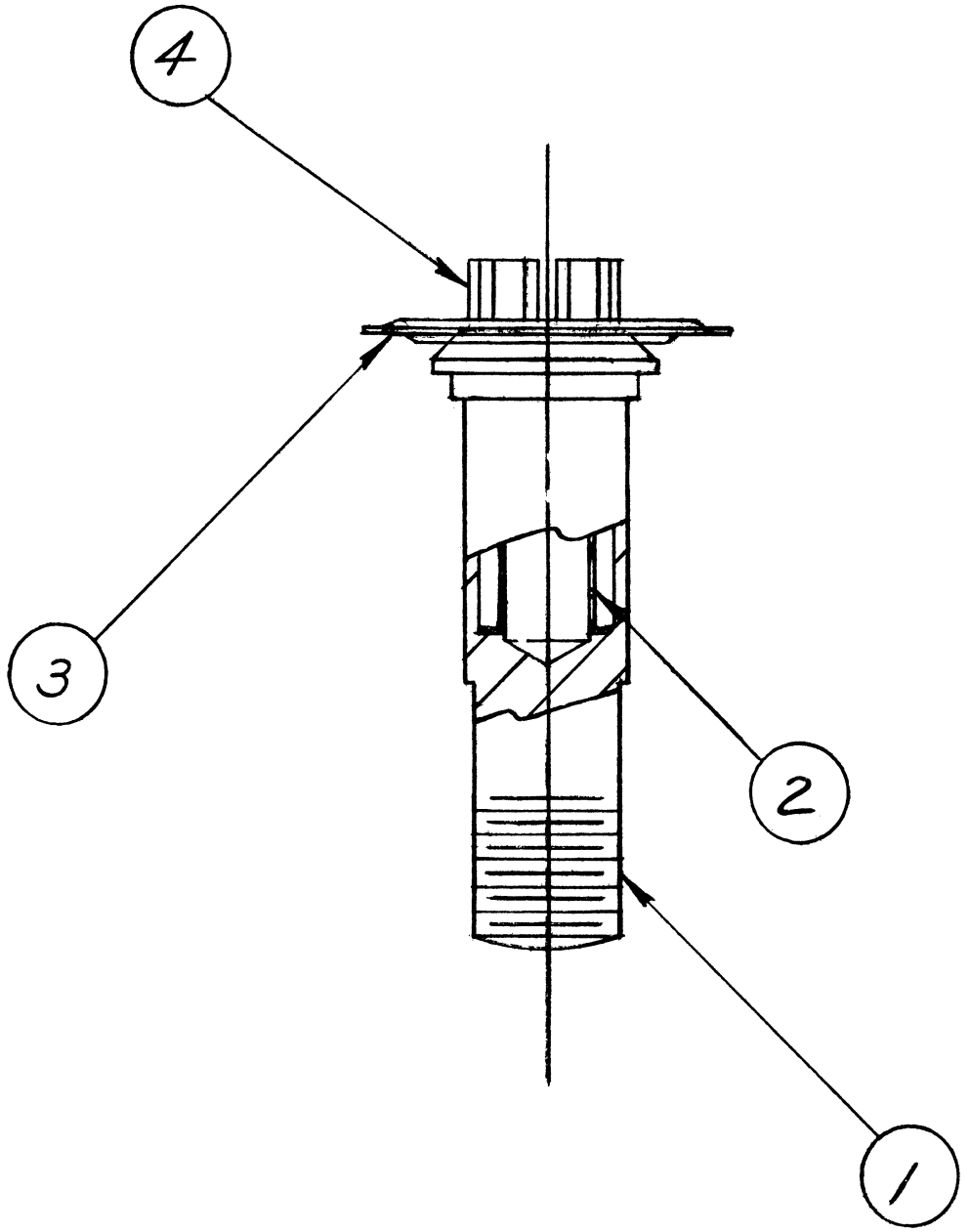

ALL DIMENSIONS UNLESS OTHERWISE SPECIFIED MUST BE HELD TO A TOLERANCE - FRACTIONAL ± 1/64," DECIMAL ± .005," ANGULAR ± ½°

		DEPARTMENT OF ENGINEERING RESEARCH UNIVERSITY OF MICHIGAN ANN ARBOR MICHIGAN	DESIGNED BY J.R.B. / DRAWN BY / CHECKED BY R.S.B.
			APPROVED BY / SCALE / DATE 5/27/47
		PROJECT M-694	TITLE TUNER SCREW & ANODE ASSEMBLY
	5/27/47	CLASSIFICATION	DWG. NO. A-10,003-2
ISSUE	DATE		

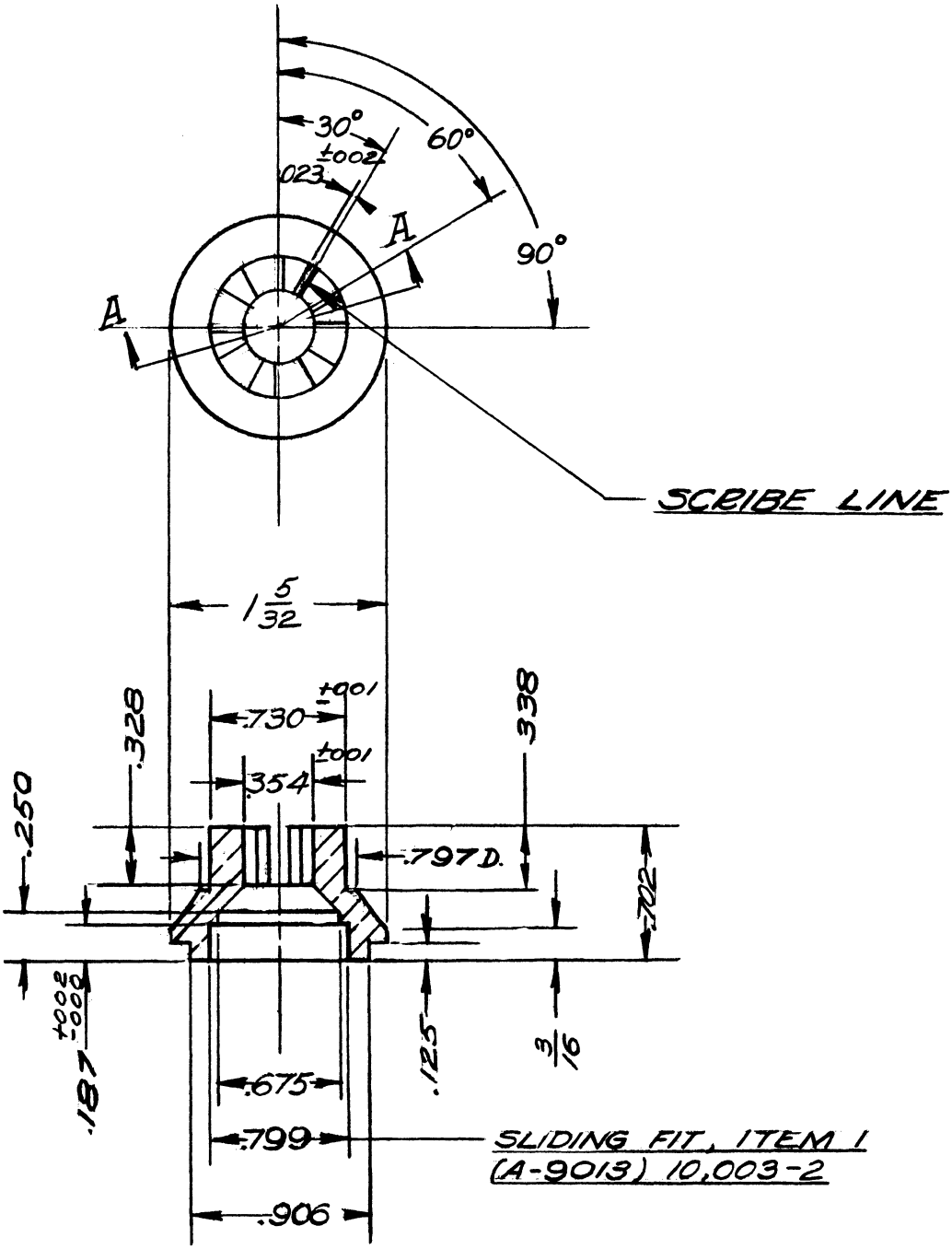

SECTION A-A

OFHC COPPER 1 REQ'D

ALL DIMENSIONS UNLESS OTHERWISE SPECIFIED MUST BE HELD TO A TOLERANCE - FRACTIONAL ± 1/64," DECIMAL ± .005," ANGULAR ±

ISSUE	DATE
2	9/15/47
1	5/15/47

DEPARTMENT OF ENGINEERING RESEARCH
UNIVERSITY OF MICHIGAN
ANN ARBOR MICHIGAN

PROJECT M-694

CLASSIFICATION

DESIGNED BY	J.R.B.
DRAWN BY	J.N.
CHECKED BY	R.S.B.
APPROVED BY	
SCALE	FULL SIZE
DATE	5/15/47

TITLE DIAPHRAM ANODE

DWG. NO. A-5003

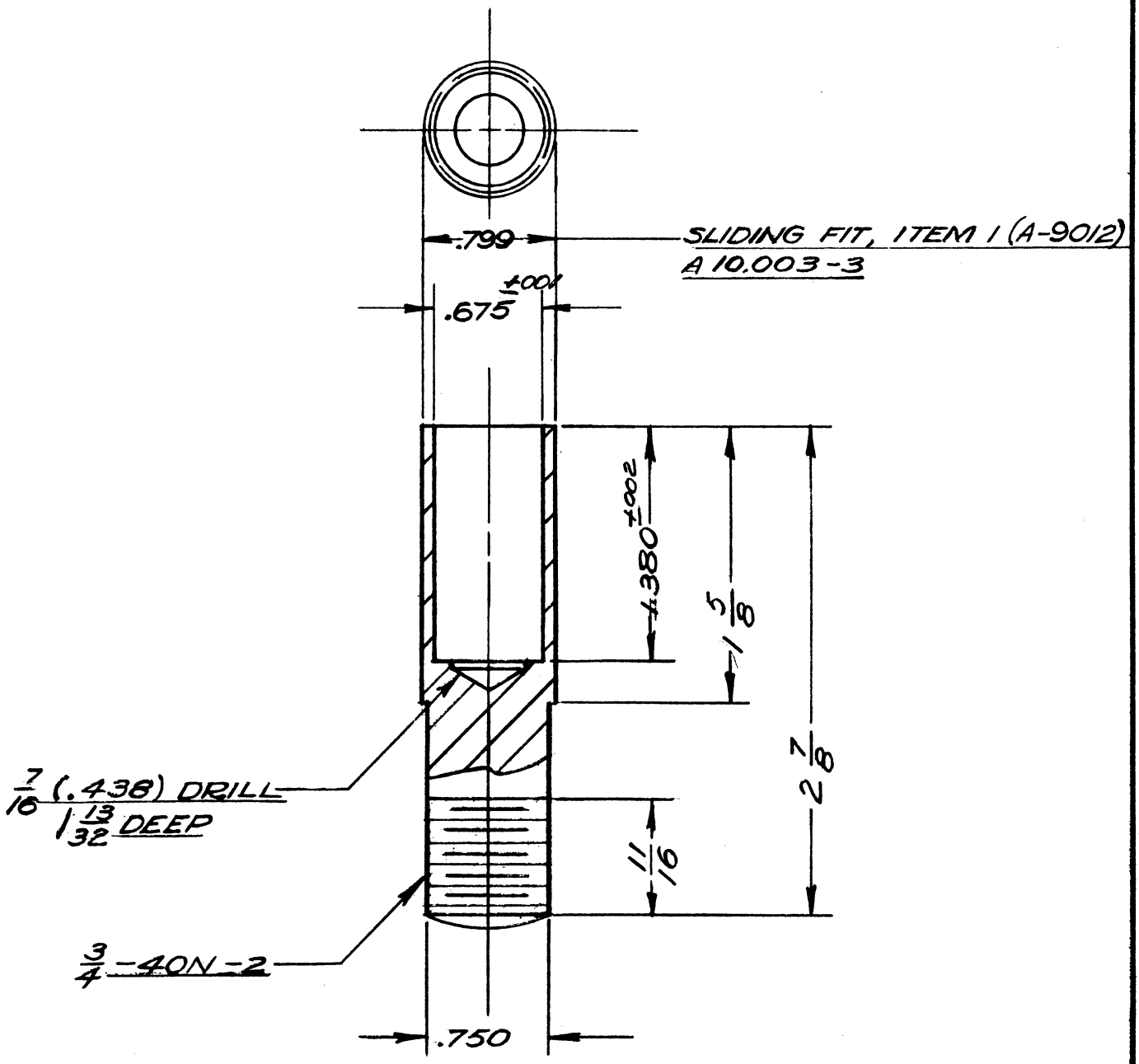

H.R.S. 1 REQ'D

ALL DIMENSIONS UNLESS OTHERWISE SPECIFIED MUST BE HELD TO A TOLERANCE - FRACTIONAL ± 1/64," DECIMAL ± .005," ANGULAR ± ½°

		DEPARTMENT OF ENGINEERING RESEARCH UNIVERSITY OF MICHIGAN ANN ARBOR MICHIGAN	DESIGNED BY J.R.B. / DRAWN BY J.H.W. / CHECKED BY K. Gwirtz
			APPROVED BY / SCALE FULL SIZE / DATE 5/21/47
		PROJECT M-694	TITLE TUNER SCREW
	5/21/47	CLASSIFICATION	DWG. NO. A-9013
ISSUE	DATE		

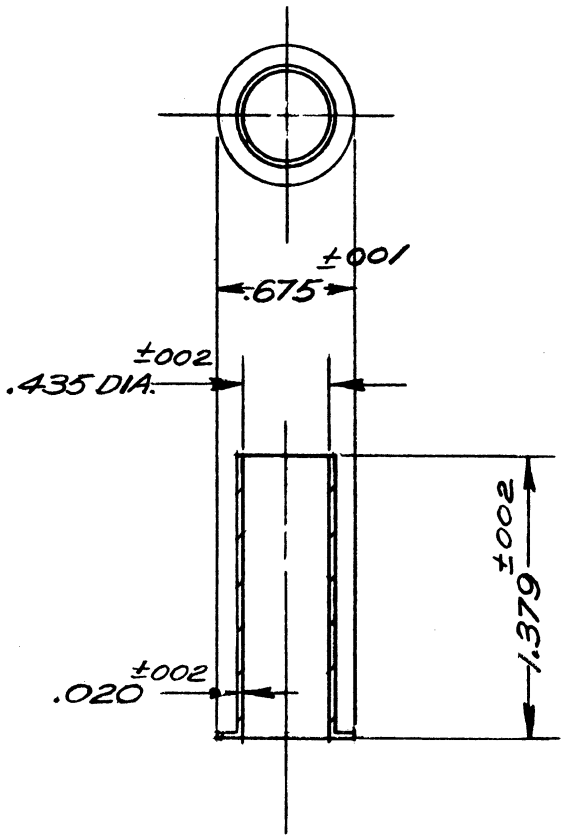

COPPER 1 REQ'D

ALL DIMENSIONS UNLESS OTHERWISE SPECIFIED MUST BE HELD TO A TOLERANCE - FRACTIONAL ± 1/64," DECIMAL ± .005," ANGULAR ± ½

		DEPARTMENT OF ENGINEERING RESEARCH UNIVERSITY OF MICHIGAN ANN ARBOR MICHIGAN	DESIGNED BY J. R. B.	APPROVED BY
			DRAWN BY J. M.	SCALE FULL SIZE
			CHECKED BY R. S. B.	DATE 6/4/47
		PROJECT M-694	TITLE TUNER CHOKE	
1	6/4/47	CLASSIFICATION	DWG. NO. A-9014	
ISSUE	DATE			

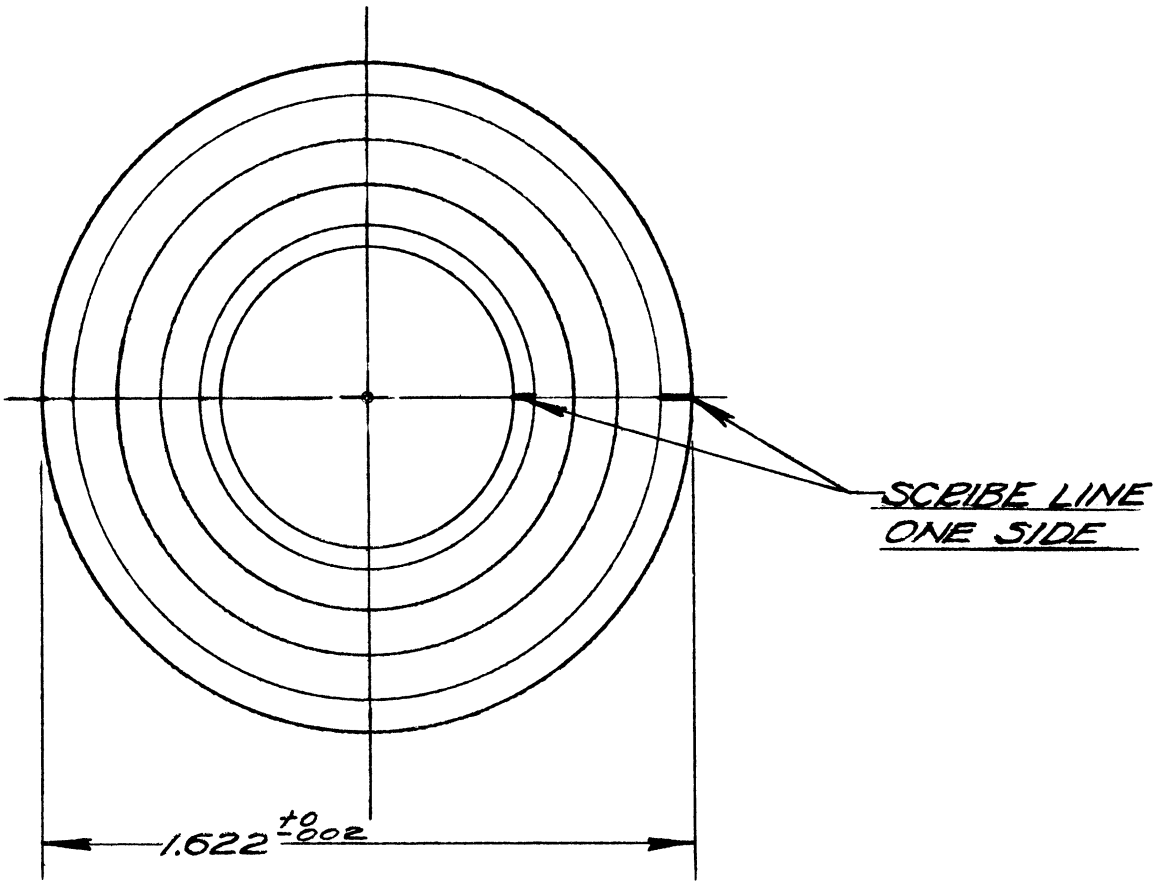

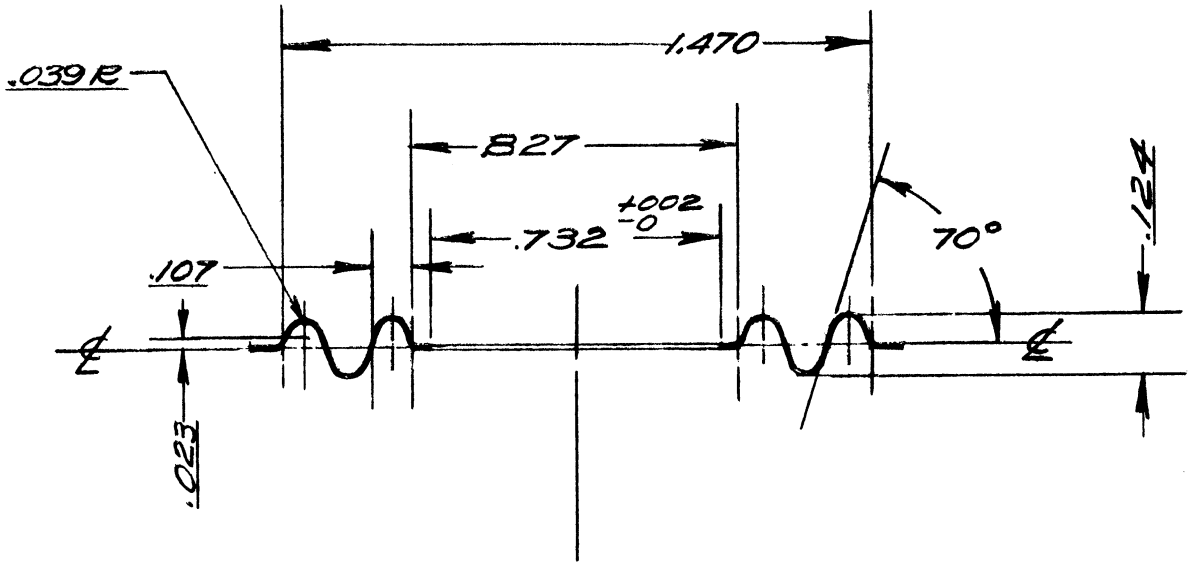

.007 MONEL 1 REQ'D

ALL DIMENSIONS UNLESS OTHERWISE SPECIFIED MUST BE HELD TO A TOLERANCE - FRACTIONAL ± 1/64," DECIMAL ± .005," ANGULAR ± 1/2°

ISSUE	DATE
2	9/15/47
1	7/31/47

DEPARTMENT OF ENGINEERING RESEARCH
UNIVERSITY OF MICHIGAN
ANN ARBOR MICHIGAN

PROJECT M-694

CLASSIFICATION

DESIGNED BY U.R.B.	APPROVED BY
DRAWN BY G.M.W.	SCALE DOUBLE SIZE
CHECKED BY R.B.	DATE 7/31/47

TITLE: DIAPHRAGM

DWG. NO. A-9016

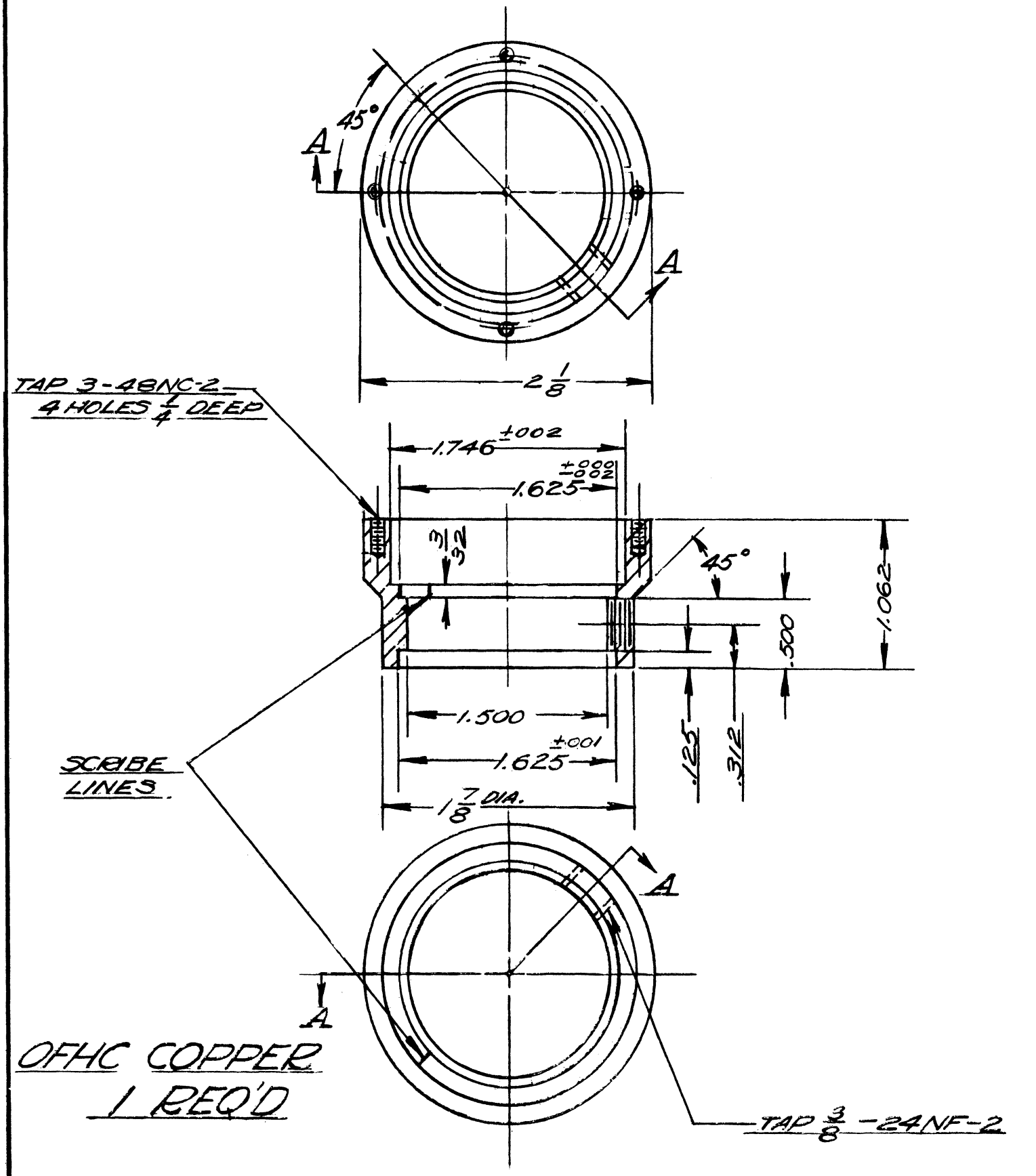

OFHC COPPER
1 REQ'D

ALL DIMENSIONS UNLESS OTHERWISE SPECIFIED MUST BE HELD TO A TOLERANCE - FRACTIONAL ± 1/64," DECIMAL ± .005," ANGULAR ± ½

ISSUE	DATE
2.	9/11/47
1	5/9/47

DEPARTMENT OF ENGINEERING RESEARCH
UNIVERSITY OF MICHIGAN
ANN ARBOR MICHIGAN

PROJECT M-694

CLASSIFICATION

DESIGNED BY J JR RB	APPROVED BY
DRAWN BY JW	SCALE FULL SIZE
CHECKED BY TB	DATE

TITLE CAVITY

DWG. NO. A-9010

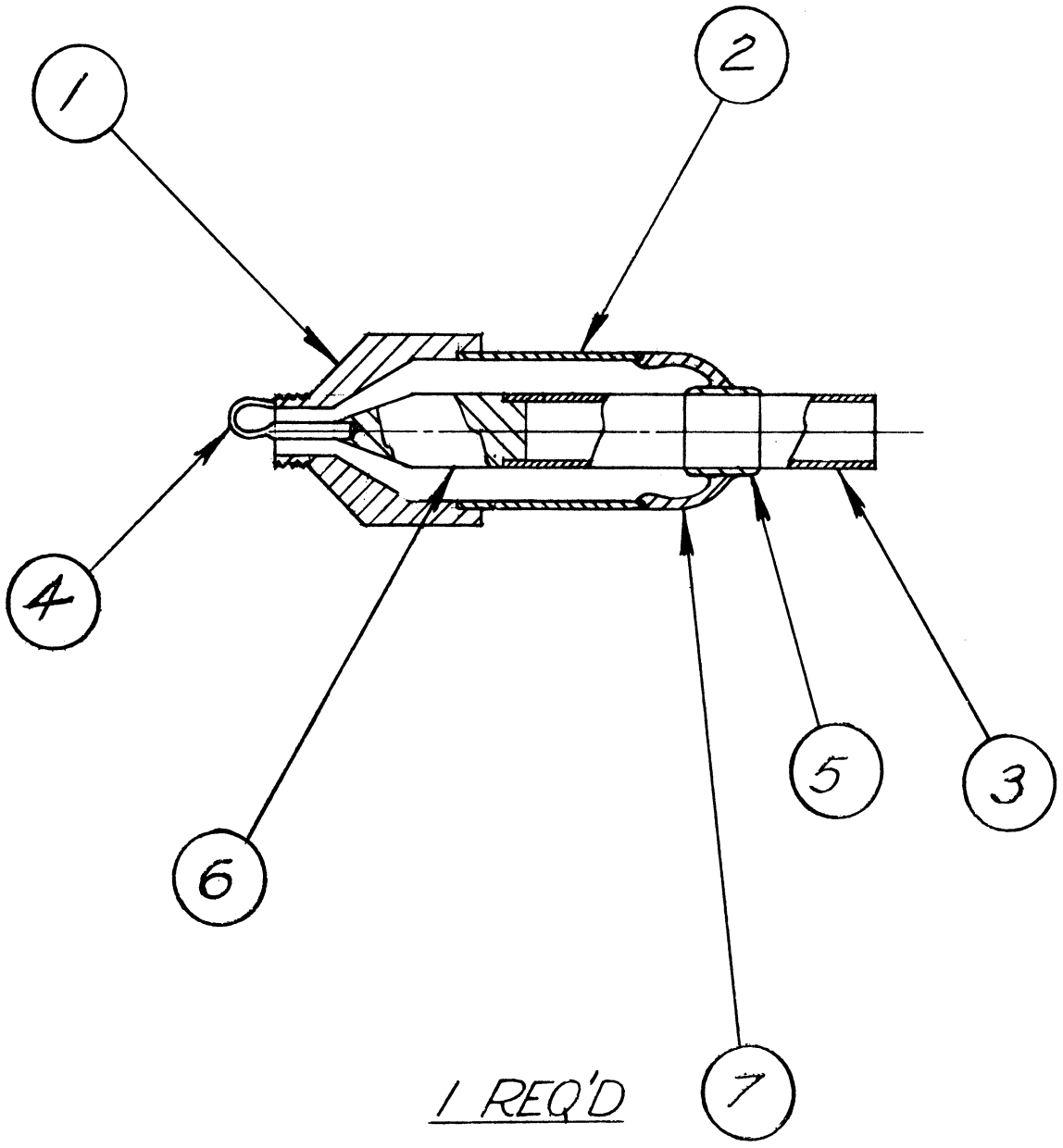

1 REQ'D

ALL DIMENSIONS UNLESS OTHERWISE SPECIFIED MUST BE HELD TO A TOLERANCE - FRACTIONAL ± 1/64," DECIMAL ± .005," ANGULAR ± ½°

ISSUE	DATE

DEPARTMENT OF ENGINEERING RESEARCH
UNIVERSITY OF MICHIGAN
ANN ARBOR MICHIGAN

PROJECT M-694

CLASSIFICATION

DESIGNED BY J.R.B.	APPROVED BY
DRAWN BY J.R.B.	SCALE FULL SIZE
CHECKED BY J.R.B.	DATE 1/8/47

TITLE OUTPUT ASSEMBLY

DWG. NO. A- 7001

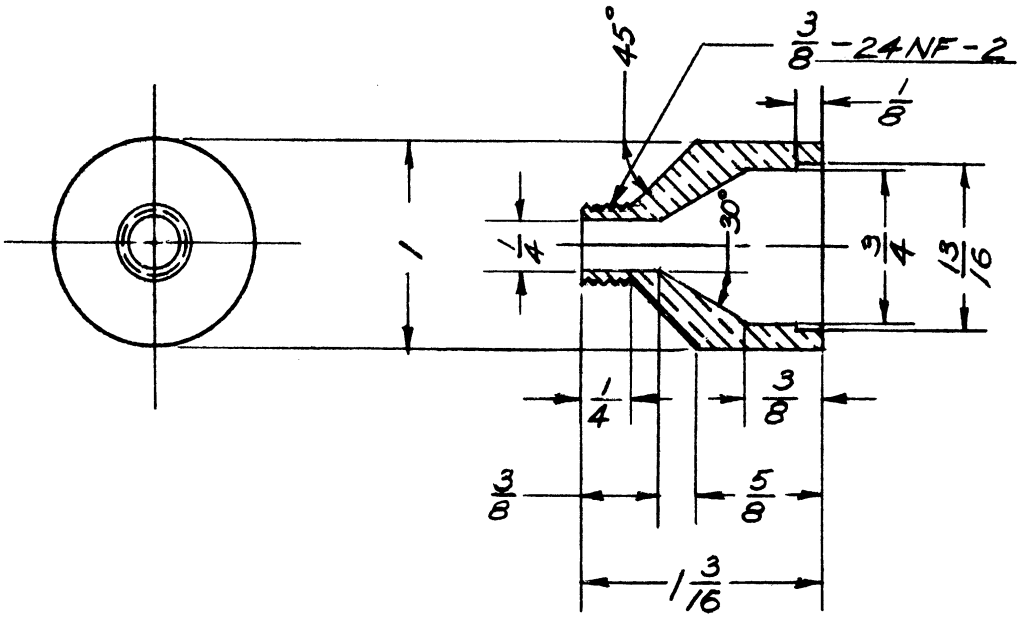

OFHC COPPER 1 REQ'D

ALL DIMENSIONS UNLESS OTHERWISE SPECIFIED MUST BE HELD TO A TOLERANCE - FRACTIONAL ± 1/64," DECIMAL ± .005," ANGULAR ±

		DEPARTMENT OF ENGINEERING RESEARCH UNIVERSITY OF MICHIGAN ANN ARBOR MICHIGAN	DESIGNED BY J.P.B DRAWN BY HM CHECKED BY J.P.B	APPROVED BY SCALE FULL SIZE DATE 2/13/47
		PROJECT M-694	TITLE OUTSIDE TAPER	
1 ISSUE	2/13/47 DATE	CLASSIFICATION	DWG. NO. A- 7001-1	

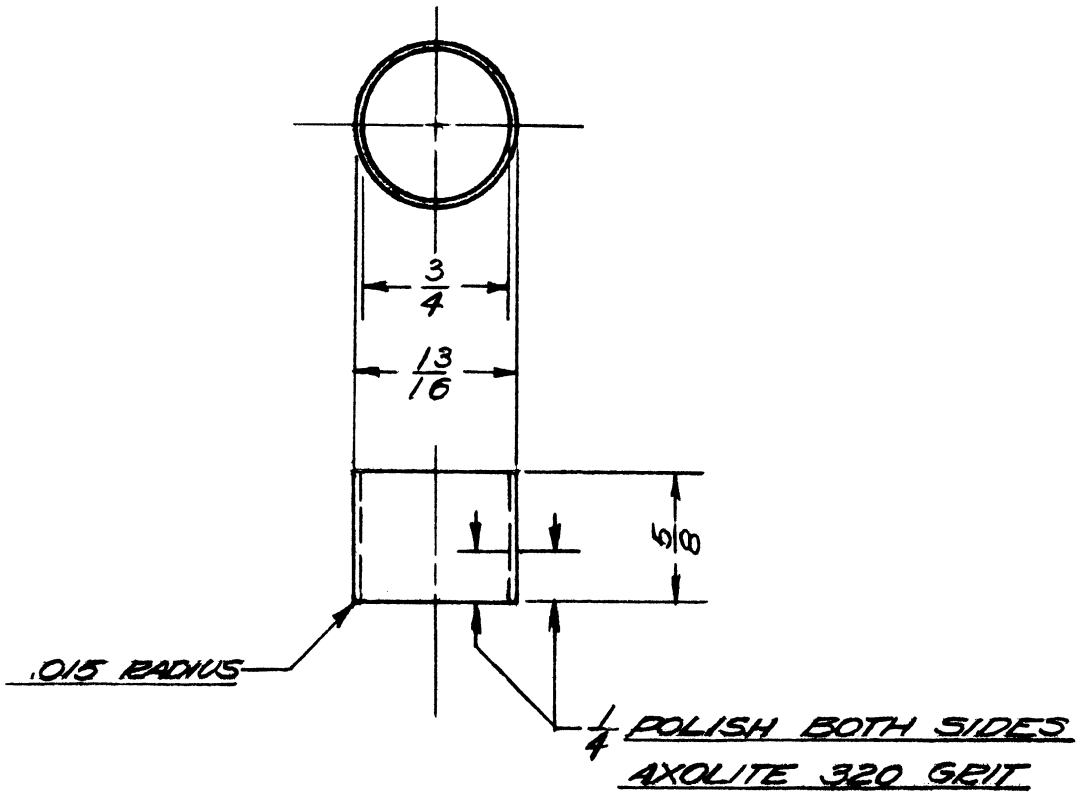

KOVAR 1 REQ'D

ALL DIMENSIONS UNLESS OTHERWISE SPECIFIED MUST BE HELD TO A TOLERANCE - FRACTIONAL ± 1/64," DECIMAL ± .005," ANGULAR ± 1/2°

		DEPARTMENT OF ENGINEERING RESEARCH UNIVERSITY OF MICHIGAN ANN ARBOR MICHIGAN	DESIGNED BY KVB
			DRAWN BY JM
			CHECKED BY J RB
		PROJECT M-694	TITLE OUTSIDE KOVAR
	2/13/47	CLASSIFICATION	DWG. NO. A- 7001-2
ISSUE	DATE		

APPROVED BY

SCALE FULL SIZE

DATE 2/13/47

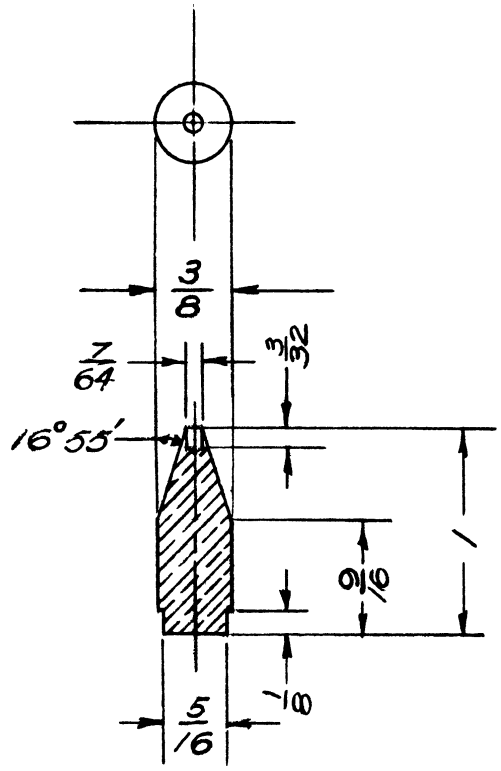

OFHC COPPER 1 REQ'D

ALL DIMENSIONS UNLESS OTHERWISE SPECIFIED MUST BE HELD TO A TOLERANCE - FRACTIONAL ± 1/64," DECIMAL ± .005," ANGULAR ±

		DEPARTMENT OF ENGINEERING RESEARCH UNIVERSITY OF MICHIGAN ANN ARBOR MICHIGAN	DESIGNED BY J. R. B.	APPROVED BY
			DRAWN BY JM	SCALE FULL SIZE
			CHECKED BY R. S. B.	DATE 2/14/47
		PROJECT M-694	TITLE INSIDE TAPER	
1	2/14/47	CLASSIFICATION	DWG. NO. A-7001-3	
ISSUE	DATE			

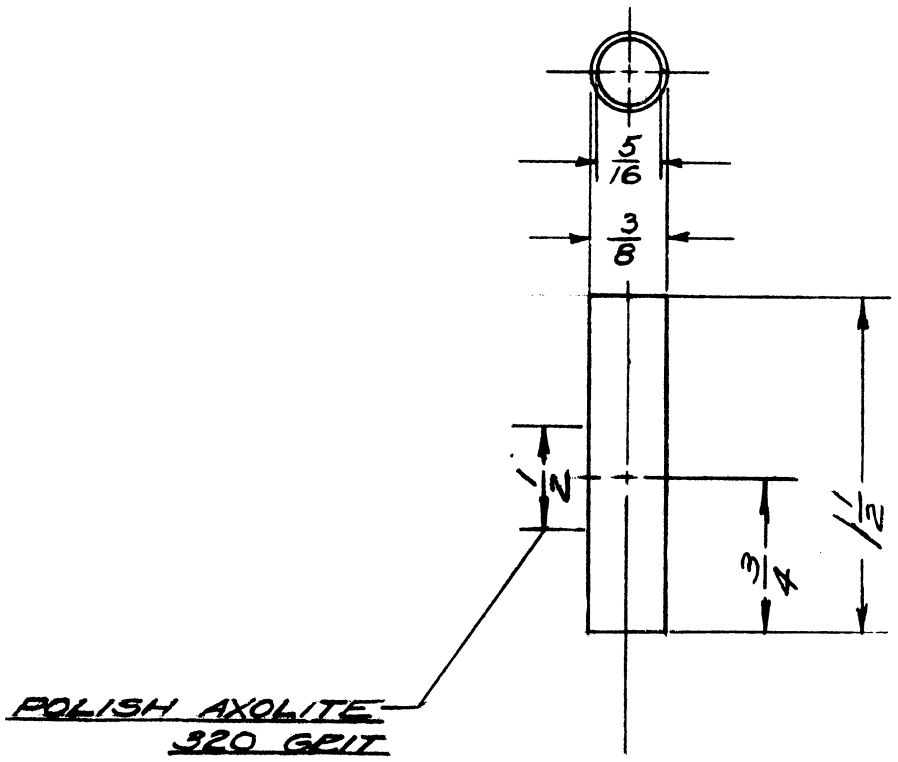

KOVAR 1 REQ'D

NOTE: MAKE FROM STUPAKOFF CATALOG NO 90375032

ALL DIMENSIONS UNLESS OTHERWISE SPECIFIED MUST BE HELD TO A TOLERANCE - FRACTIONAL ± 1/64," DECIMAL ± .005," ANGULAR ± ½°

		1/22/48	
		2/13/47	
ISSUE		DATE	

DEPARTMENT OF ENGINEERING RESEARCH
UNIVERSITY OF MICHIGAN
ANN ARBOR MICHIGAN

PROJECT M-694

CLASSIFICATION

DESIGNED BY JRB	APPROVED BY
DRAWN BY 9m	SCALE FULL SIZE
CHECKED BY JRB	DATE 2/13/47

TITLE INSIDE KOVAR

DWG. NO. A- 7001-4

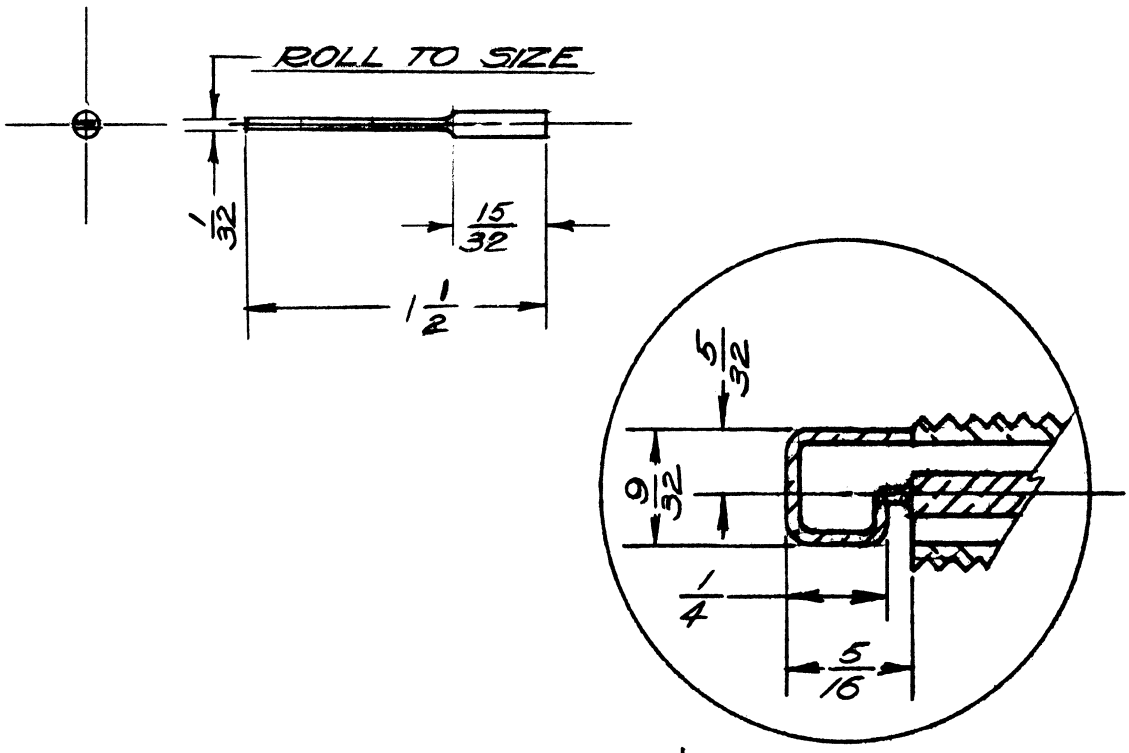

.108 DIA COPPER 1 REQ'D

ALL DIMENSIONS UNLESS OTHERWISE SPECIFIED MUST BE HELD TO A TOLERANCE - FRACTIONAL ± 1/64," DECIMAL ± .005," ANGULAR ± ½

		DEPARTMENT OF ENGINEERING RESEARCH UNIVERSITY OF MICHIGAN ANN ARBOR MICHIGAN	DESIGNED BY J. R. B. / APPROVED BY [illegible]
			DRAWN BY JM / SCALE FULL SIZE
			CHECKED BY J RB / DATE 2/25/47
		PROJECT M-694	TITLE COUPLING LOOP
1	2/25/47	CLASSIFICATION	DWG. NO. A-7001-5
ISSUE	DATE		

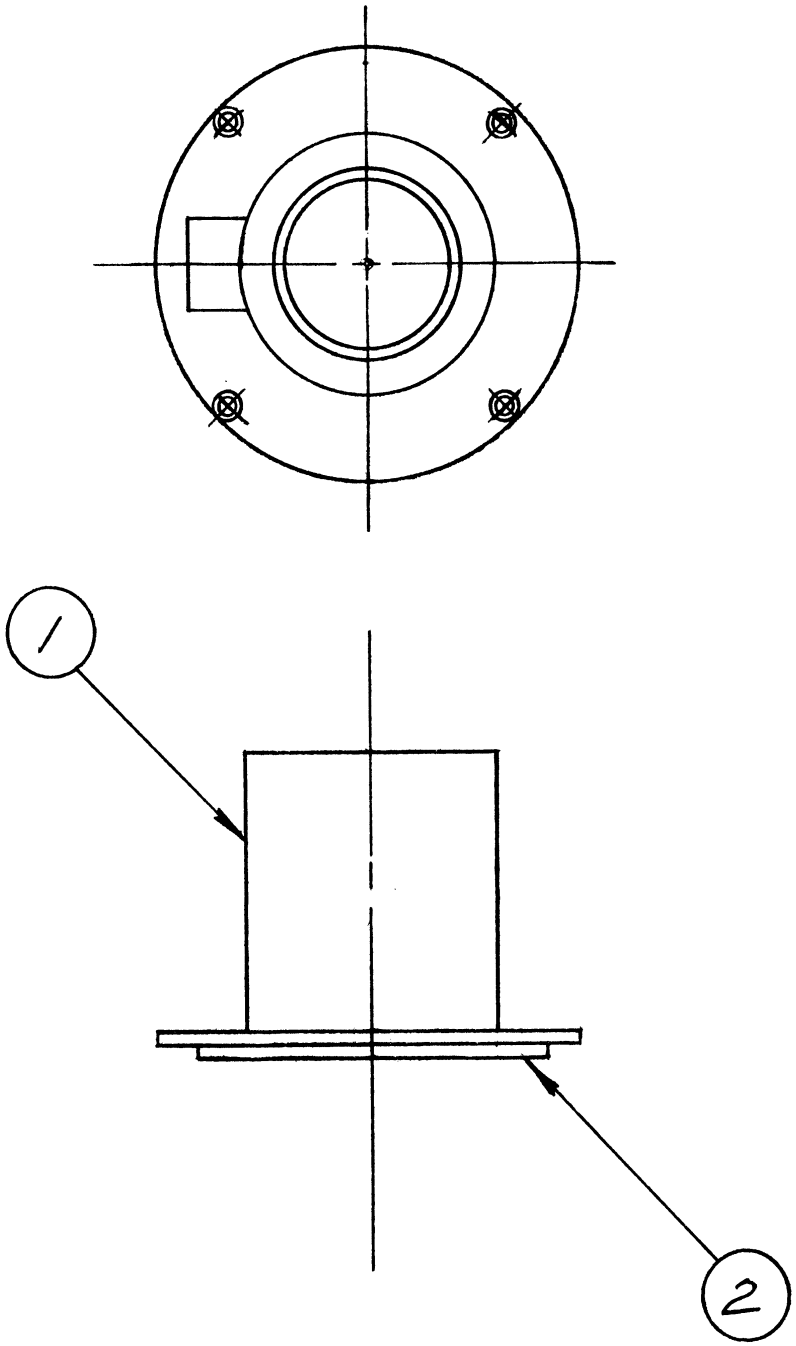

ALL DIMENSIONS UNLESS OTHERWISE SPECIFIED MUST BE HELD TO A TOLERANCE - FRACTIONAL ± 1/64," DECIMAL ± .005," ANGULAR ± 1/2°

		DEPARTMENT OF ENGINEERING RESEARCH UNIVERSITY OF MICHIGAN ANN ARBOR MICHIGAN	DESIGNED BY J.R.B. / DRAWN BY GW / CHECKED BY R.S.B.
			APPROVED BY / SCALE FULL SIZE / DATE 5/20/47
		PROJECT M-694	TITLE TUNER POLE PIECE ASSEMBLY
1	5/20/47	CLASSIFICATION	DWG. NO. A-10,003-3
ISSUE	DATE		

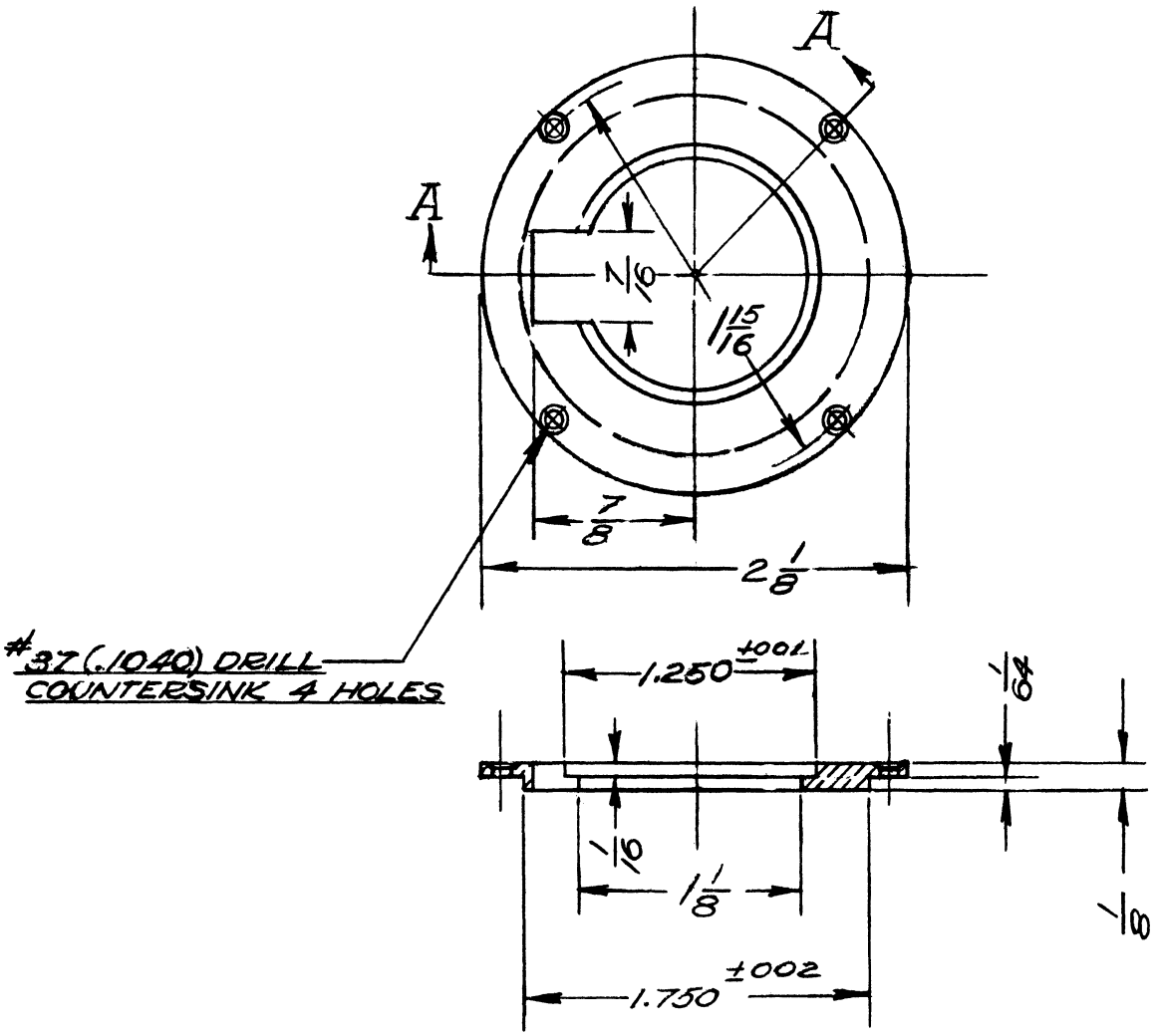

SECTION A-A

BRASS 1 REQ'D

ALL DIMENSIONS UNLESS OTHERWISE SPECIFIED MUST BE HELD TO A TOLERANCE - FRACTIONAL ± 1/64," DECIMAL ± .005," ANGULAR ± ½°

	DEPARTMENT OF ENGINEERING RESEARCH UNIVERSITY OF MICHIGAN ANN ARBOR MICHIGAN	DESIGNED BY J. K. B.	APPROVED BY
		DRAWN BY	SCALE FULL SIZE
		CHECKED BY R. S. B.	DATE 5/19/47
	PROJECT M-694	TITLE TUNER YOKE	
1 ISSUE	5/19/47 DATE	CLASSIFICATION	DWG. NO. A-9011

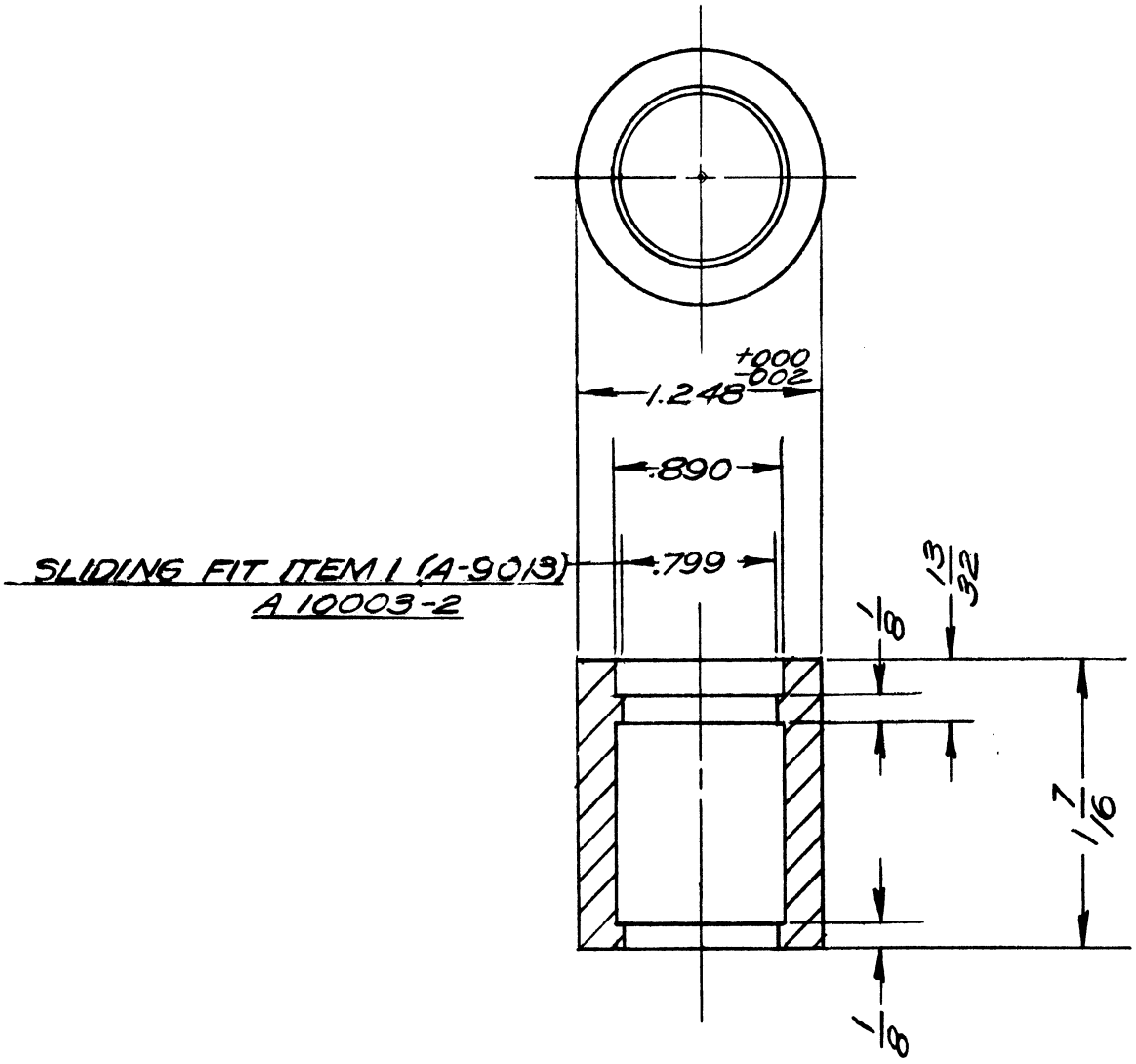

CRS 1 REQ'D

ALL DIMENSIONS UNLESS OTHERWISE SPECIFIED MUST BE HELD TO A TOLERANCE - FRACTIONAL ± 1/64," DECIMAL ± .005," ANGULAR ± ½°

		DEPARTMENT OF ENGINEERING RESEARCH UNIVERSITY OF MICHIGAN ANN ARBOR MICHIGAN	DESIGNED BY [illegible] DRAWN BY [illegible] CHECKED BY R. S. B.
		PROJECT M-694	APPROVED BY SCALE FULL SIZE DATE 5/21/47
			TITLE TUNER POLE PIECE
	5/21/47	CLASSIFICATION	DWG. NO. A-9012
ISSUE	DATE		

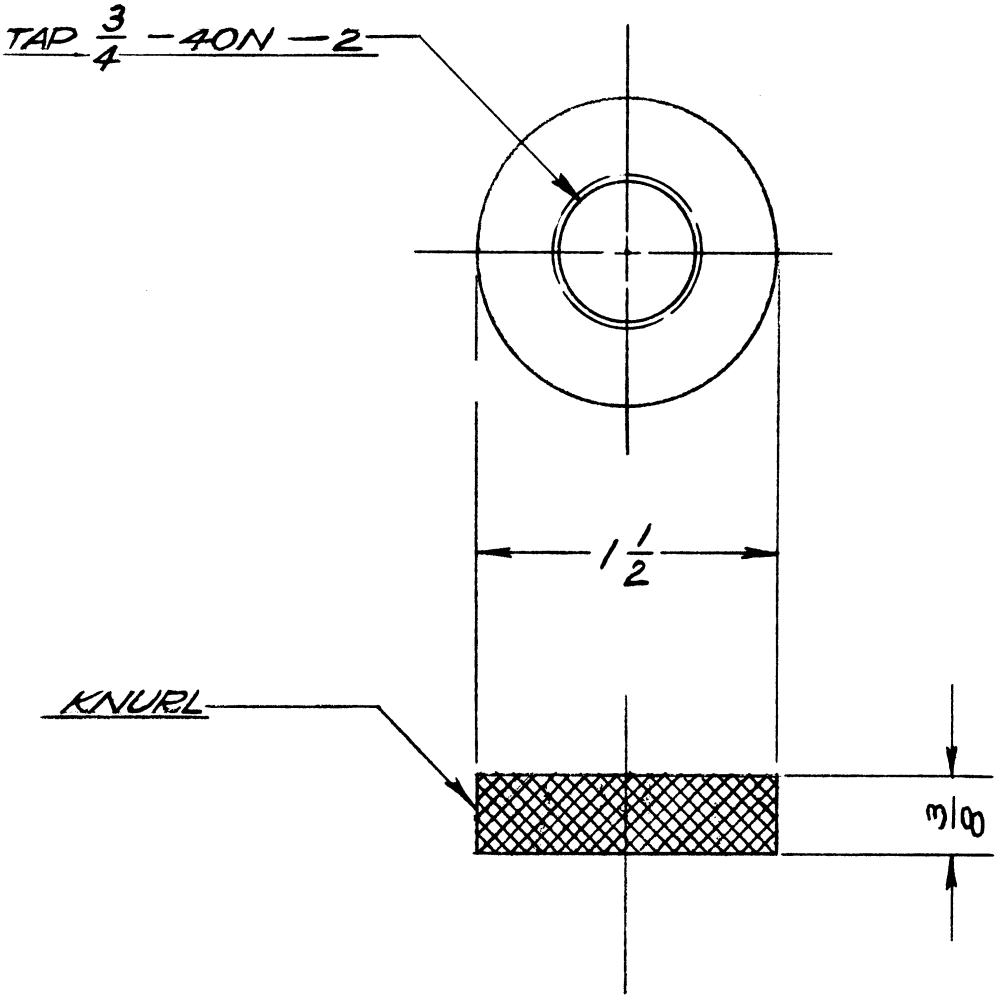

CRS 1 REQ'D

ALL DIMENSIONS UNLESS OTHERWISE SPECIFIED MUST BE HELD TO A TOLERANCE - FRACTIONAL ± 1/64," DECIMAL ± .005," ANGULAR ± ½°

		DEPARTMENT OF ENGINEERING RESEARCH UNIVERSITY OF MICHIGAN ANN ARBOR MICHIGAN	DESIGNED BY J. R. B. / APPROVED BY
			DRAWN BY JM / SCALE FULL SIZE
			CHECKED BY J R B / DATE 3/5/47
		PROJECT M-694	TITLE TUNING NUT
1	3/5/47	CLASSIFICATION	DWG. NO. A-9004
ISSUE	DATE		

APPENDIX E

Assembly and Parts for Model 4 Tungsten Cathode

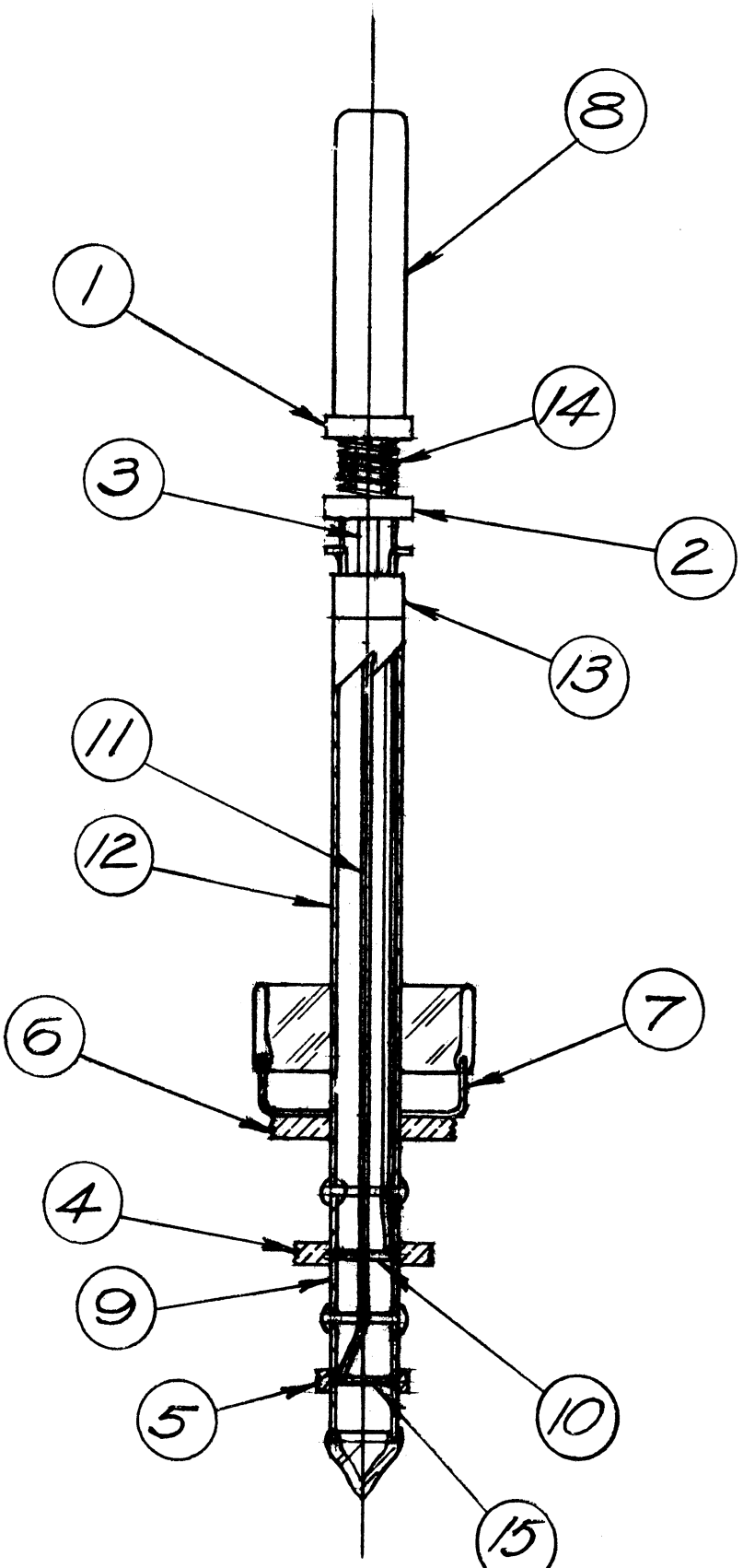

Fig.. 1

ALL DIMENSIONS UNLESS OTHERWISE SPECIFIED MUST BE HELD TO A TOLERANCE - FRACTIONAL ± 1/64," DECIMAL ± .005," ANGULAR ± 1/

DEPARTMENT OF ENGINEERING RESEARCH UNIVERSITY OF MICHIGAN ANN ARBOR MICHIGAN		DESIGNED BY JRB	APPROVED BY
		DRAWN BY JRB	SCALE FULL SIZE
		CHECKED BY HWW	DATE 6/4/48
PROJECT M-694		TITLE TUNGSTEN CATHODE MODEL #4	
1 ISSUE	6/4/48 DATE	CLASSIFICATION	DWG. NO. A-8003

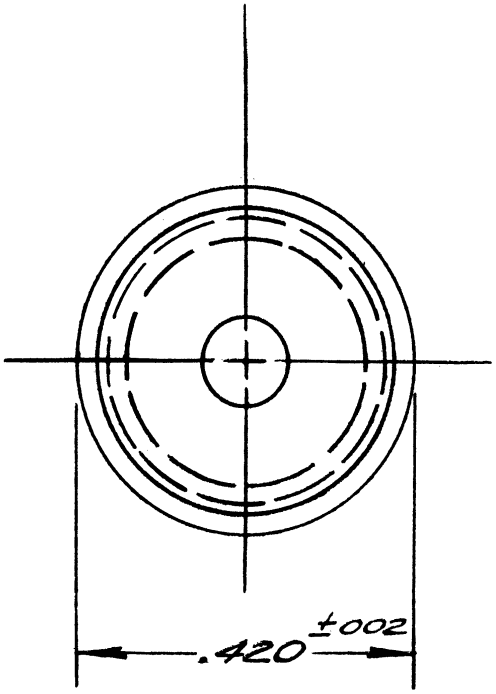

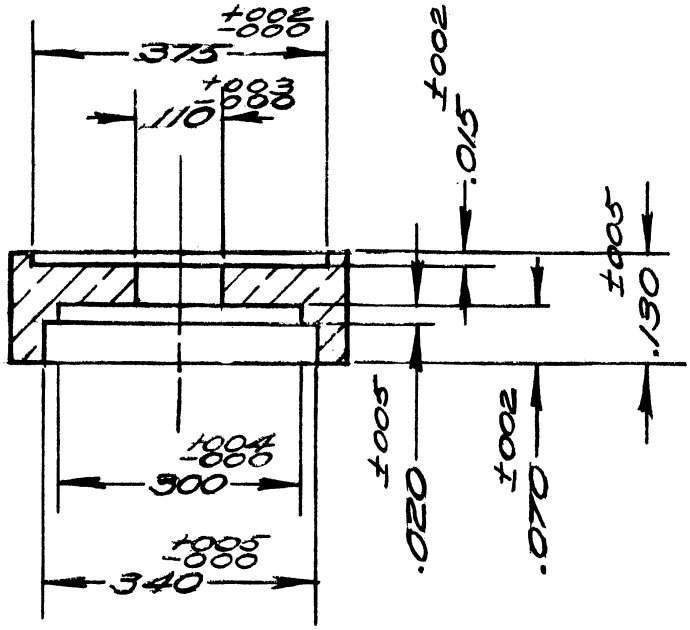

MOLYBDENUM 1 REQ'D

ALL DIMENSIONS UNLESS OTHERWISE SPECIFIED MUST BE HELD TO A TOLERANCE - FRACTIONAL ± 1/64," DECIMAL ± .005," ANGULAR ± ½°

ISSUE	DATE
2	8/11/48
1	5/26/48

CLASSIFICATION

DEPARTMENT OF ENGINEERING RESEARCH
UNIVERSITY OF MICHIGAN
ANN ARBOR MICHIGAN

PROJECT M-694

DESIGNED BY JRB	APPROVED BY
DRAWN BY [illegible]	SCALE X 4
CHECKED BY JRB	DATE 8/11/48

TITLE UPPER END HAT

DWG. NO. A-8003-1

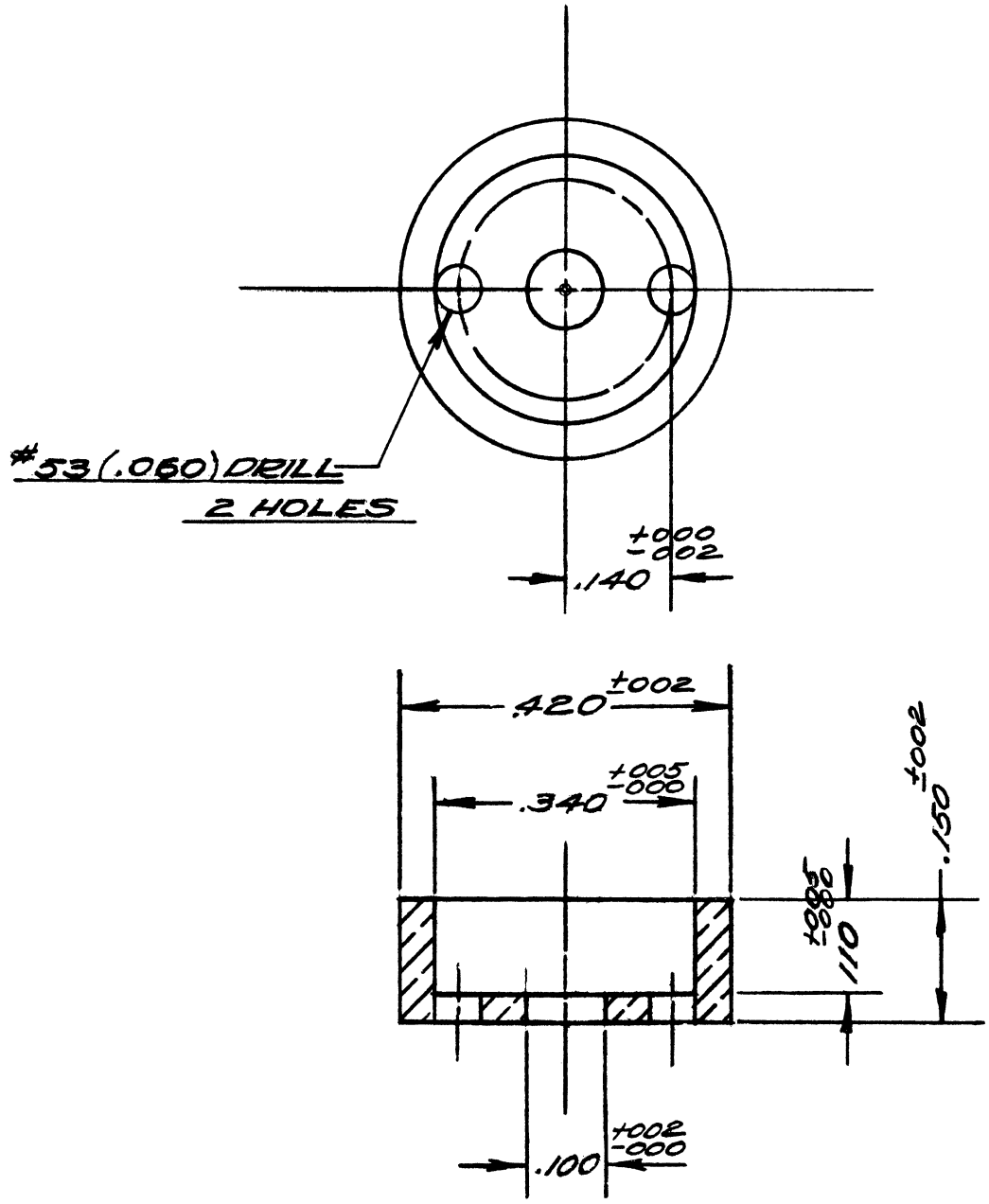

MOLYBDENUM 1 REQD

ALL DIMENSIONS UNLESS OTHERWISE SPECIFIED MUST BE HELD TO A TOLERANCE - FRACTIONAL ± 1/64," DECIMAL ± .005," ANGULAR ±

		DEPARTMENT OF ENGINEERING RESEARCH UNIVERSITY OF MICHIGAN ANN ARBOR MICHIGAN	DESIGNED BY J.R.B. DRAWN BY J.W. CHECKED BY H. Wiel	APPROVED BY SCALE X 4 DATE 2/5/48
		PROJECT M-694	TITLE LOWER END HAT	
1 ISSUE	2/2/48 DATE	CLASSIFICATION	DWG. NO. A-8003-2	

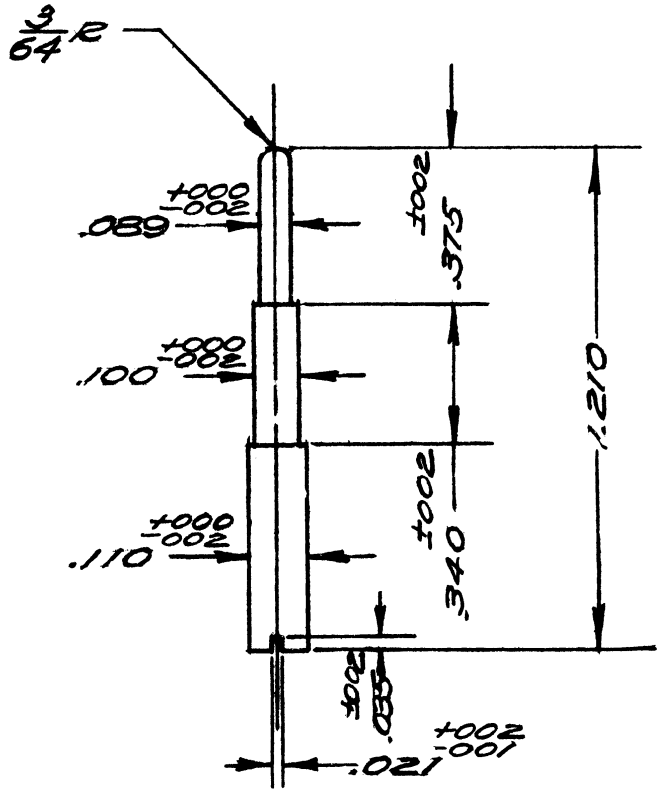

TUNGSTEN 1 REQ'D

ALL DIMENSIONS UNLESS OTHERWISE SPECIFIED MUST BE HELD TO A TOLERANCE - FRACTIONAL ± 1/64," DECIMAL ± .005," ANGULAR ± 1/2°

		DEPARTMENT OF ENGINEERING RESEARCH UNIVERSITY OF MICHIGAN ANN ARBOR MICHIGAN	DESIGNED BY JRB DRAWN BY JW CHECKED BY JRB APPROVED BY SCALE X 2 DATE 5/27/48
		PROJECT M-694	TITLE CENTER SUPPORT
1	5/27/48	CLASSIFICATION	DWG. NO. A-8003-3
ISSUE	DATE		

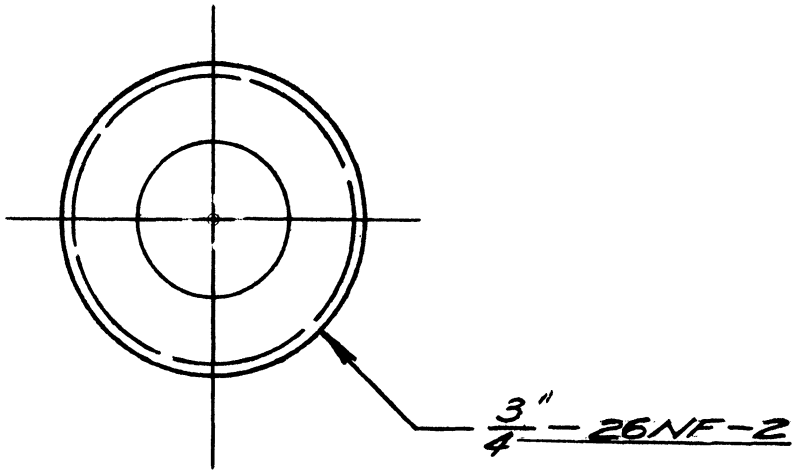

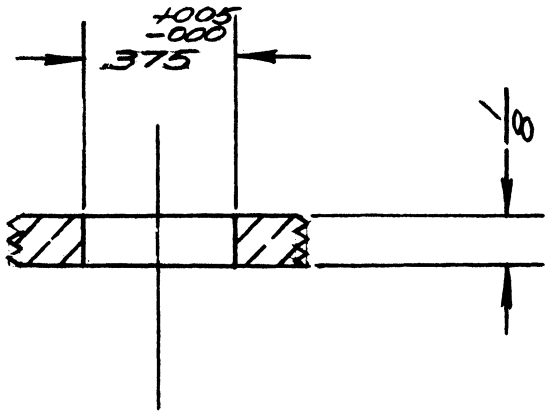

COPPER 1 REQ'D

ALL DIMENSIONS UNLESS OTHERWISE SPECIFIED MUST BE HELD TO A TOLERANCE - FRACTIONAL ± 1/64," DECIMAL ± .005," ANGULAR ± ½°

		DEPARTMENT OF ENGINEERING RESEARCH UNIVERSITY OF MICHIGAN ANN ARBOR MICHIGAN	DESIGNED BY J.R.B.	APPROVED BY
			DRAWN BY J.R.B.	SCALE X2
			CHECKED BY A.W.W.	DATE 2/12/48
		PROJECT M-694	TITLE MIDDLE CONNECTOR	
1 ISSUE	2/12/48 DATE	CLASSIFICATION	DWG. NO. A-8003-4	

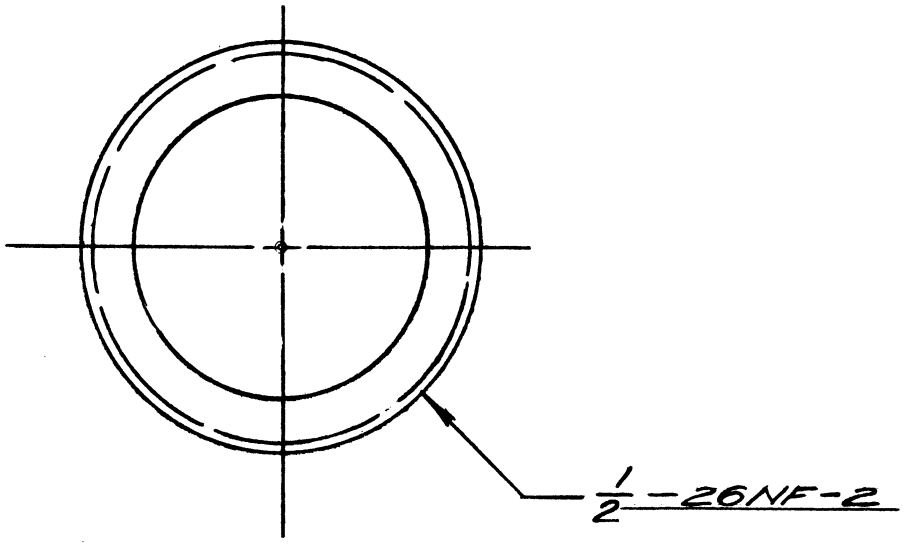

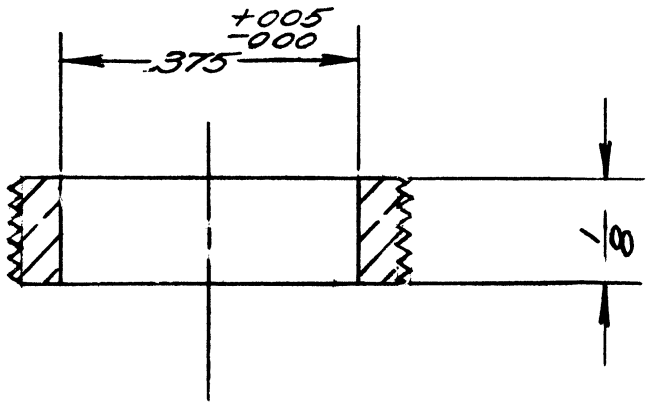

COPPER 1 REQ'D

ALL DIMENSIONS UNLESS OTHERWISE SPECIFIED MUST BE HELD TO A TOLERANCE - FRACTIONAL ± 1/64," DECIMAL ± .005," ANGULAR ± ½°

		DEPARTMENT OF ENGINEERING RESEARCH UNIVERSITY OF MICHIGAN ANN ARBOR MICHIGAN	DESIGNED BY JRB / DRAWN BY JRB / CHECKED BY KWW
			APPROVED BY / SCALE X 4 / DATE 2/12/48
		PROJECT M-694	TITLE LOWER CONNECTOR
1	2/12/48	CLASSIFICATION	DWG. NO. A-8003-5
ISSUE	DATE		

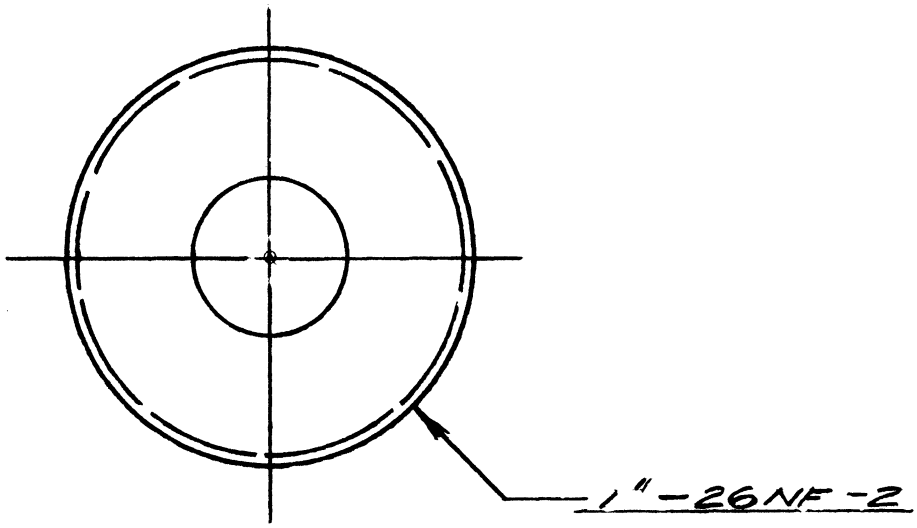

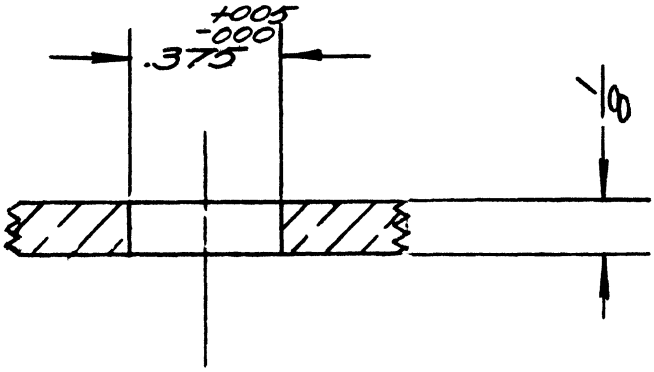

COPPER 1 REQ'D

ALL DIMENSIONS UNLESS OTHERWISE SPECIFIED MUST BE HELD TO A TOLERANCE - FRACTIONAL ± 1/64," DECIMAL ± .005," ANGULAR ± ½

		DEPARTMENT OF ENGINEERING RESEARCH UNIVERSITY OF MICHIGAN ANN ARBOR MICHIGAN	DESIGNED BY J. P. B.	APPROVED BY
			DRAWN BY	SCALE X2
			CHECKED BY	DATE 2/12/48
		PROJECT M-694	TITLE TOP CONNECTOR	
1	2/12/48	CLASSIFICATION	DWG. NO. A-8003-6	
ISSUE	DATE			

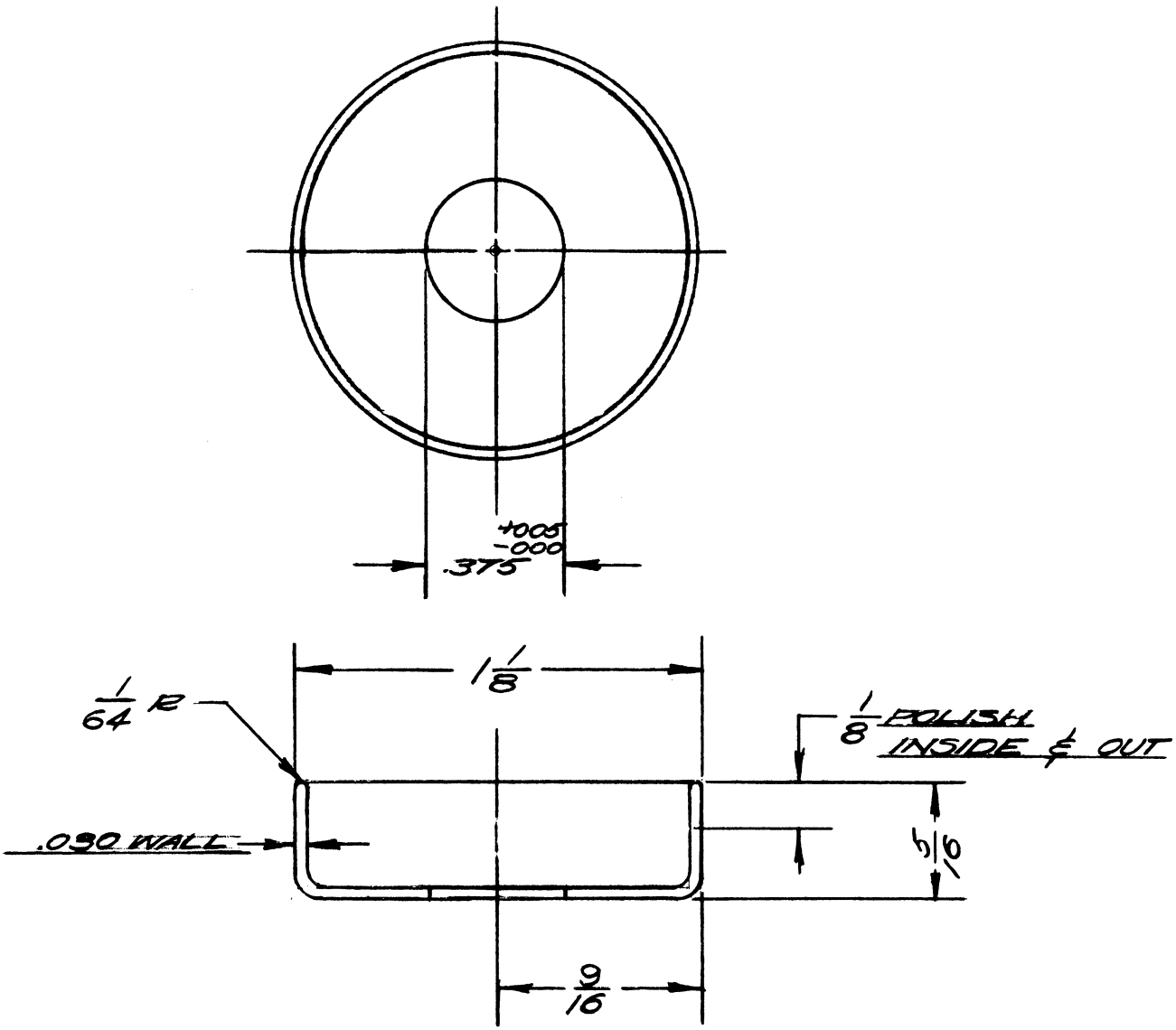

KOVAR 1 REQ'D

ALL DIMENSIONS UNLESS OTHERWISE SPECIFIED MUST BE HELD TO A TOLERANCE - FRACTIONAL ± 1/64," DECIMAL ± .005," ANGULAR ± ½°

		DEPARTMENT OF ENGINEERING RESEARCH UNIVERSITY OF MICHIGAN ANN ARBOR MICHIGAN	DESIGNED BY J.R.B.
			DRAWN BY J.R.B.
			CHECKED BY H.W.W.
		PROJECT M-694	TITLE CUP
	2/11/48	CLASSIFICATION	DWG. NO. A-8003-7
ISSUE	DATE		

APPROVED BY

SCALE X2

DATE 2/11/48

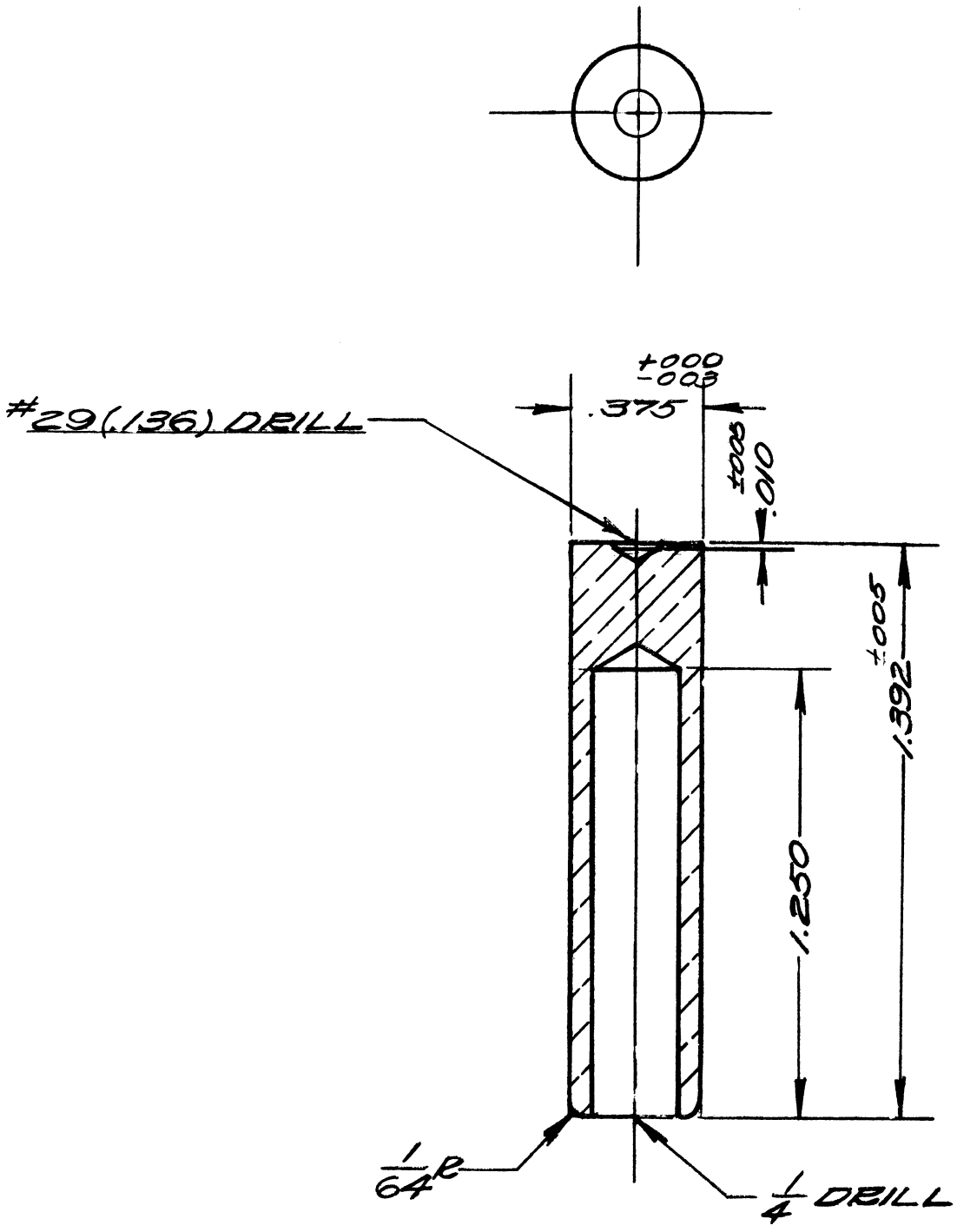

MOLYBDENUM 1 REQ'D

ALL DIMENSIONS UNLESS OTHERWISE SPECIFIED MUST BE HELD TO A TOLERANCE - FRACTIONAL ± 1/64," DECIMAL ± .005," ANGULAR ± ½

ISSUE	DATE
3	2/8/49
2	8/11/48
1	5/26/48

DEPARTMENT OF ENGINEERING RESEARCH
UNIVERSITY OF MICHIGAN
ANN ARBOR MICHIGAN

PROJECT M-694

CLASSIFICATION

DESIGNED BY JRB	APPROVED BY
DRAWN BY JM	SCALE X 2
CHECKED BY JRB	DATE 8/11/48

TITLE UPPER CATHODE

DWG. NO. A-8003-8

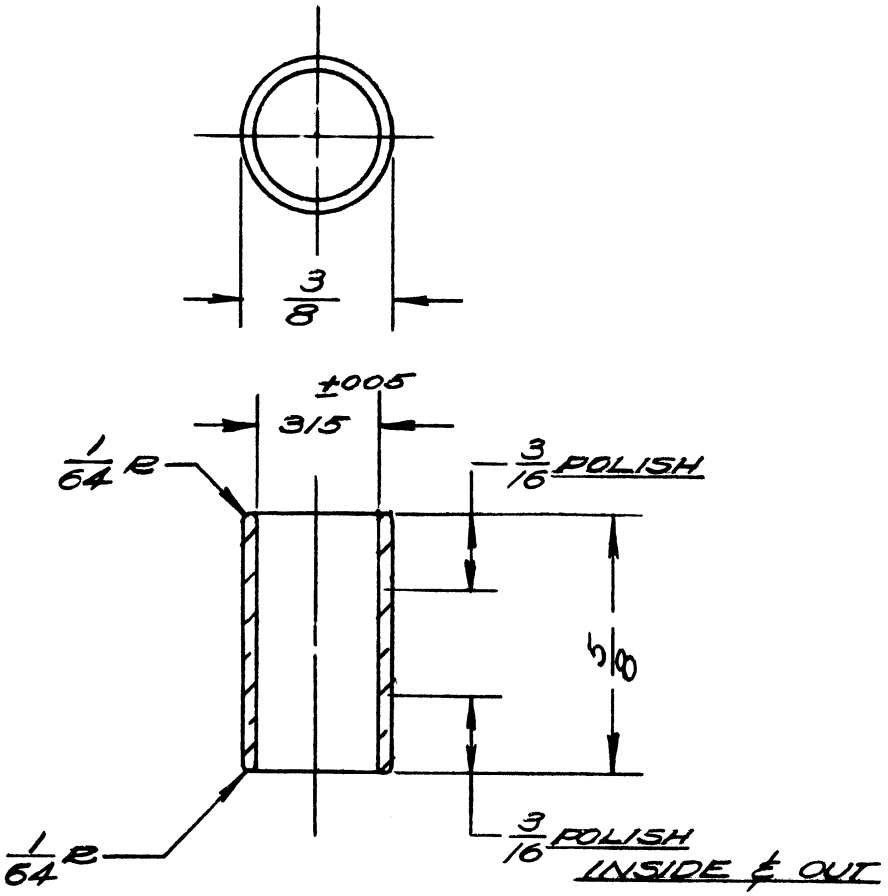

KOVAR 2 REQ'D

ALL DIMENSIONS UNLESS OTHERWISE SPECIFIED MUST BE HELD TO A TOLERANCE - FRACTIONAL ± 1/64," DECIMAL ± .005," ANGULAR ± 1/2°

		DEPARTMENT OF ENGINEERING RESEARCH UNIVERSITY OF MICHIGAN ANN ARBOR MICHIGAN	DESIGNED BY JRB
			DRAWN BY JRB
			CHECKED BY JRB
		PROJECT M-694	TITLE LUG
1	2/11/48	CLASSIFICATION	DWG. NO. A-8003-9
ISSUE	DATE		

APPROVED BY

SCALE X 2

DATE 2/11/48

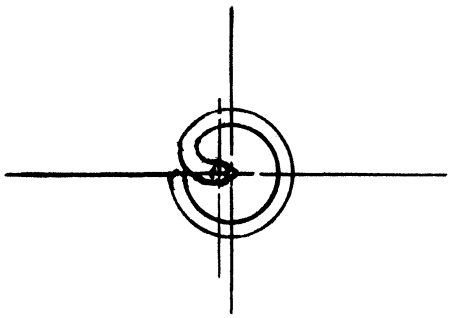

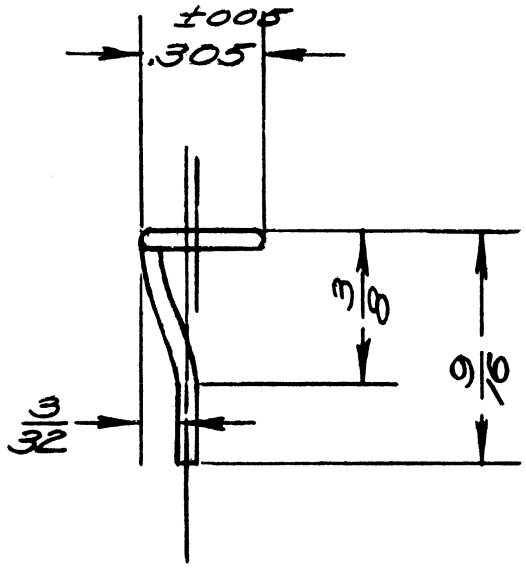

.050 NICKLE 1 REQ'D

ALL DIMENSIONS UNLESS OTHERWISE SPECIFIED MUST BE HELD TO A TOLERANCE - FRACTIONAL ± 1/64," DECIMAL ± .005," ANGULAR ±

		DEPARTMENT OF ENGINEERING RESEARCH UNIVERSITY OF MICHIGAN ANN ARBOR MICHIGAN	DESIGNED BY JRB DRAWN BY JRB CHECKED BY JRB
		PROJECT M-694	APPROVED BY SCALE X 2 DATE 6/22/42
			TITLE TOP LEAD
1	6/22/42	CLASSIFICATION	DWG. NO. A- 8003-10
ISSUE	DATE		

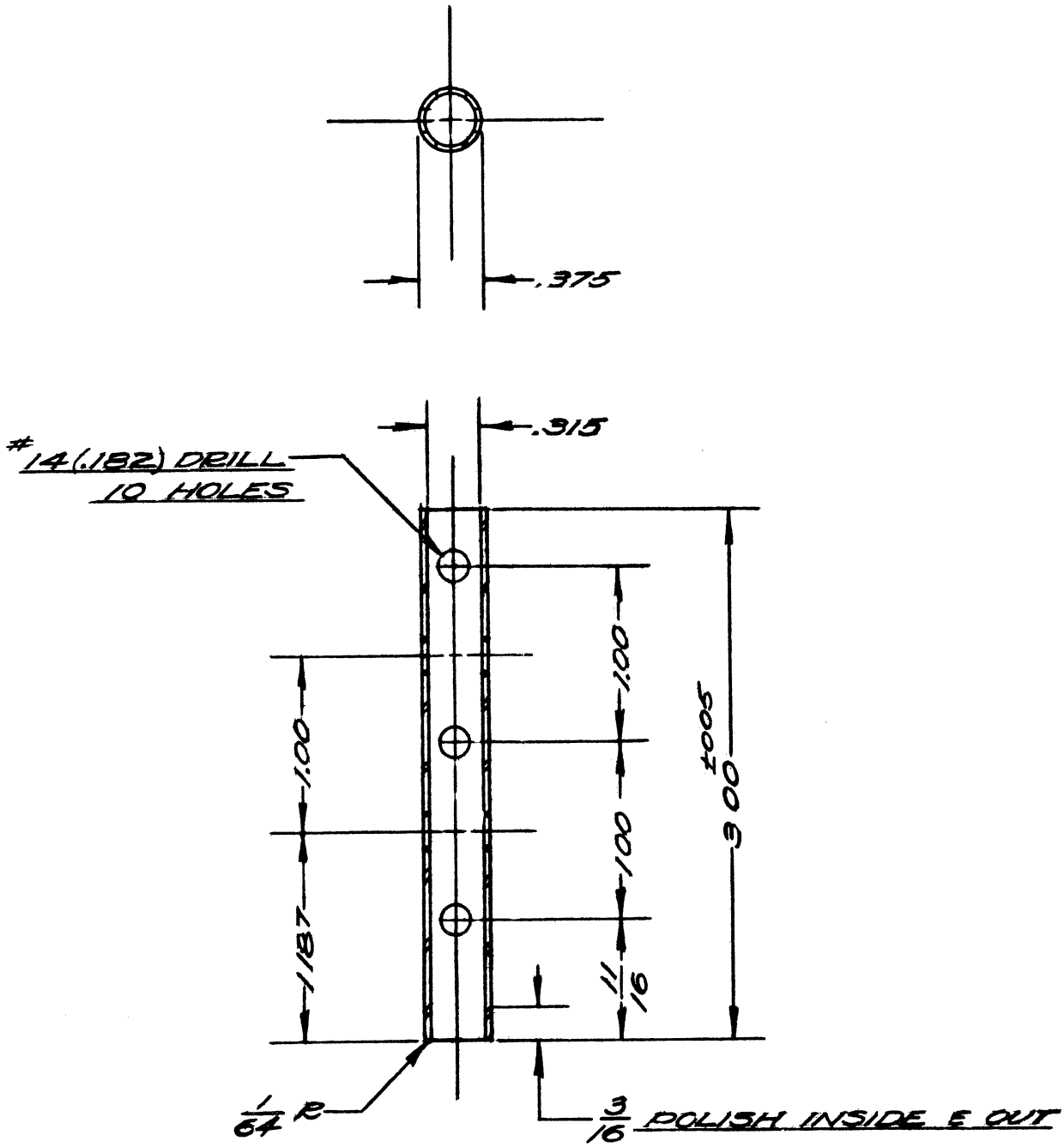

KOVAR REQ'D

ALL DIMENSIONS UNLESS OTHERWISE SPECIFIED MUST BE HELD TO A TOLERANCE - FRACTIONAL ± 1/64" DECIMAL ± .005, ANGULAR ± 1/2°

DEPARTMENT OF ENGINEERING RESEARCH UNIVERSITY OF MICHIGAN ANN ARBOR MICHIGAN		DESIGNED BY J R B DRAWN BY J R B SMN CHECKED BY J R B	APPROVED BY SCALE FULL SIZE DATE 2/11/48
PROJECT M-694		TITLE STEM	
CLASSIFICATION		DWG. NO. A-8003-12	

ISSUE	DATE
1	2/11/48

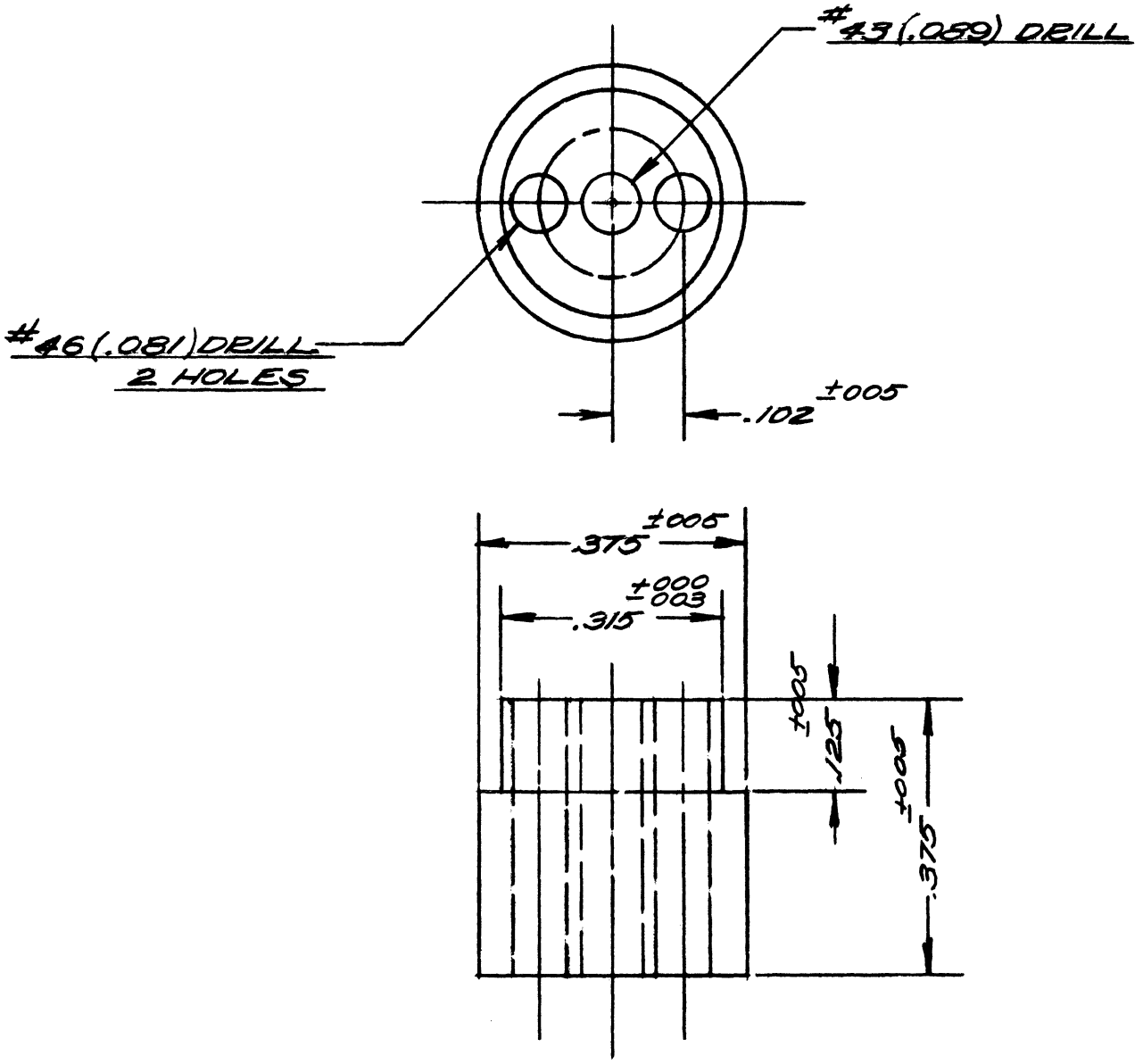

MONEL 1 REQ'D

ALL DIMENSIONS UNLESS OTHERWISE SPECIFIED MUST BE HELD TO A TOLERANCE - FRACTIONAL ± 1/64," DECIMAL ± .005," ANGULAR ± 1/2°

		DEPARTMENT OF ENGINEERING RESEARCH UNIVERSITY OF MICHIGAN ANN ARBOR MICHIGAN	DESIGNED BY J.R.B.	APPROVED BY
			DRAWN BY J.R.W.	SCALE X4
			CHECKED BY J.R.B.	DATE 2/11/48
		PROJECT M-694	TITLE SLUG	
1	2/11/48	CLASSIFICATION	DWG. NO. A-8003-13	
ISSUE	DATE			

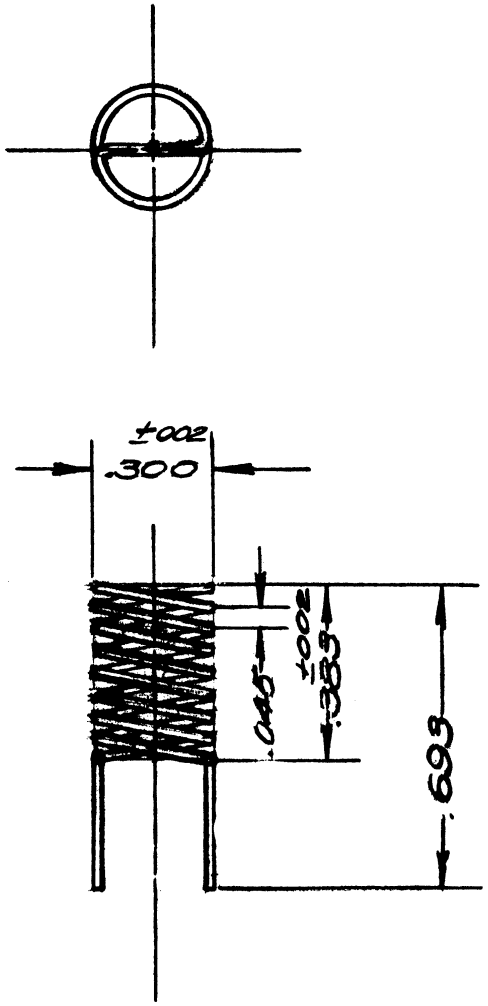

NOTE:
STRETCH .037 AT ASSEMBLY

.020 DIA. TUNGSTEN 1 REQ'D
MAKE 8 TURNS
11 THREADS/INCH = DOUBLE LEAD

ALL DIMENSIONS UNLESS OTHERWISE SPECIFIED MUST BE HELD TO A TOLERANCE - FRACTIONAL ± 1/64," DECIMAL ± .005," ANGULAR ± 1/2°

ISSUE	DATE
2	7/9/48
1	5/27/48

DEPARTMENT OF ENGINEERING RESEARCH
UNIVERSITY OF MICHIGAN
ANN ARBOR MICHIGAN

PROJECT: M-694

CLASSIFICATION:

DESIGNED BY JRB	APPROVED BY
DRAWN BY JSW	SCALE X 2
CHECKED BY JAB	DATE 5/27/48

TITLE: FILAMENT

DWG. NO. A-8003-14

Lithoprinted from copy supplied by author
by
Cushing-Malloy, Inc.
Ann Arbor, Michigan, U.S.A.